Comparative studies in the development of the nervous system in malacostracan crustaceans

D i s s e r t a t i o n

zur Erlangung des akademischen Grades

d o c t o r r e r u m n a t u r a l i u m

(Dr. rer. nat.)

im Fach Biologie

eingereicht an der

Lebenswissenschaftlichen Fakultät

der Humboldt-Universität zu Berlin

von

Dott.ssa in Scienze e Tecnologie per la Natura Caterina Biffis

Präsident der Humboldt-Universitat zu Berlin

Prof. Dr.-Ing. Dr. Sabine Kunst

Dekan der Lebenswissenschaftlichen Fakultät

Prof. Dr. Bernhard Grimm

Gutachter/innen: 1. Prof. Dr. Gerhard Scholtz

2. Prof. Dr. Steffen Harzsch

3. Prof. Dr. Alessandro Minelli

Tag der mündlichen Prüfung: 20. Juni 2017

"...καὶ τὸν περὶ φύσεως περὶ τῆς συνθέσεως καὶ τῆς ὅλης οὐσίας,
ἀλλὰ μὴ περὶ τούτων ἃ μὴ συμβαίνει χωριζόμενά ποτε τῆς οὐσίας αὐτῶν."
"...and who discusses about nature speaks about its composition and its overall essence, never speaks about each of its parts which are never separate from their own essence."

Aristoteles, "De partibus animalium" (Περί Ζώιων Μορίων) I, 5, 645 a

Table of contents

Table of contents v

List of figures vii

List of tables xi

List of abbreviations xiii

1. Introduction 1

1.1 The nervous system in Crustacea 1

1.2 The development of the nervous system in Crustacea 2

1.3 Aim and organization of the present study 5

2. Material and methods 8

2.1 Species collection and fixation 8

2.2 Scanning electron microscopy (SEM) 10

2.3 Fluorescence staining 10

2.4 Analysis of the stained specimens 13

2.5 3D image visualization 14

2.6 Notes on the applied methods 15

3. Results 17

3.1 *Meganyctiphanes norvegica* 20

3.1.1 Morphogenesis 21

3.1.2 Nervous system development 38

3.2 *Penaeus monodon* 78

3.2.1 Morphogenesis 79

3.2.2 Nervous system development 81

3.3 *Procambarus fallax* (Hagen, 1870) f. *virginalis* 118

3.3.1 Morphogenesis 118

3.3.2 Nervous system development 121

4. Discussion 150

4.1 The development of the Central Nervous System (CNS) 150

4.1.1 The development of the central nervous system in Crustacea: an overview 150
4.1.2 The development of the central nervous system in the naupliar region 151
4.1.3 The development of the central nervous system in the post-naupliar region 155
4.2 The development of the medulla terminalis: the anlage of a peripheral ganglion associated with an apical sensory organ 163
4.2.1 Subdivision of the protocerebrum in malacostracan crustaceans 163
4.2.2 The development of the medulla terminalis in Malacostraca 164
4.2.3 The development of the frontal organ in Malacostraca 169
4.2.4 Development and evolution of the frontal organ in Crustacea: an apical sensory organ associated with the medulla terminalis 173
4.3 The development of the Stomatogastric Nervous System (SNS) and its connection to the brain: new insights from a simple developmental pattern 185
4.3.1 The morphology of the stomatogastric nervous system of crustaceans 185
4.3.2 The developmental pattern of the stomatogastric nervous system in the three investigated species 187
4.3.3 Some clarification on the nomenclature and the identification of developmental units 190
4.3.4 The development of the inferior ventricular nerve in the ground pattern of crustaceans 195
4.3.5 The connection of the SNS to the brain 198
4.4 An overview of the basic scaffold of the nervous system: connectivity among different systems 201

Summaries 204

English summary 204

Deutsche Zusammenfassung 205

References 206

Acknowledgments 227

Selbstständigkeitserklärung 229

List of figures

Fig. 1 – Application of CONGO-red and combination with Sytox green stainings 11

Fig. 2 - Application of Imaris settings to the CLSM image stacks 15

Fig. 3 - Schematic representation of the body organization in the nauplius and in the egg-nauplius 19

Fig. 4 - External morphology in *M. norvegica*, embryonic stage 1 22

Fig. 5 - External morphology in *M. norvegica*, embryonic stage 2 24

Fig. 6 - External morphology in *M. norvegica*, nauplius stage 1 26

Fig. 7 - External morphology in *M. norvegica*, nauplius stage 2 29

Fig. 8 - External morphology in *M. norvegica*, metanauplius stage 33

Fig. 9 - External morphology in *M. norvegica*, calyptopis stage 36

Fig. 10 - *M. norvegica*, embryonic stage 1 38

Fig. 11 - Axogenesis in *M. norvegica*, embryonic stage 1 39

Fig. 12 - *M. norvegica*, embryonic stage 2 41

Fig. 13 - Axogenesis in *M. norvegica*, embryonic stage 2 42

Fig. 14 - *M. norvegica*, embryonic stage 2 45

Fig. 15 - Axogenesis in *M. norvegica*, nauplius stage 1 47

Fig. 16 - Axogenesis in *M. norvegica*, nauplius stage 1 49

Fig. 17 - Distribution of SL-ir structures in the nauplius stage 1 50

Fig. 18 - *M. norvegica*, embryonic stage 2 51

Fig. 19 - Axogenesis in *M. norvegica*, nauplius stage 2 53

Fig. 20 - The anlage of the stomatogastric nervous system and the innervation of the labrum in *M. norvegica*, nauplius stage 2 56

Fig. 21 - Distribution of SL-ir structures in *M. norvegica*, nauplius stage 2 58

Fig. 22 - *M. norvegica*, metanauplius stage 59

Fig. 23 – Axogenesis in the naupliar region of *M. norvegica*, metanauplius stage 60

Fig. 24 – Development of the nauplius eye complex in *M. norvegica*, metanauplius stage 62

Fig. 25 – Axogenesis in the ventral nerve cord of *M. norvegica*, metanauplius stage 64
Fig. 26 – Development of the stomatogastric nervous system in *M. norvegica*, metanauplius stage 66
Fig. 27 – Distribution of Sl-ir structures in the naupliar region of *M. norvegica*, metanauplius stage 67
Fig. 28 – Distribution of SL-ir structures in *M. norvegica*, late metanauplius stage 69
Fig. 29 - *M. norvegica*, calyptopis stage 1 70
Fig. 30 - Axogenesis in *M. norvegica*, calyptopis stage1 72
Fig. 31 - Distribution of SL-ir structures in *M. norvegica*, calyptopis stage 1 75
Fig. 32 - Morphogenesis in *P. monodon* 80
Fig. 33 - *P. monodon*, embryonic stage 81
Fig. 34 - Axogenesis in *P. monodon*, embryonic stage 83
Fig. 35 - *P. monodon*, nauplius stage 1-2 84
Fig. 36 - Axogenesis in *P. monodon*, early nauplius stage 1-2 86
Fig. 37 - Axogenesis in *P. monodon*, late nauplius stage 1-2 88
F8ig.38 - Distribution of SL-ir structures in the nauplius stage 1-2 89
Fig. 39 - *P. monodon*, nauplius stage 3-4 90
Fig. 40 - Axogenesis in the naupliar region of *P. monodon*, nauplius stage 3-4 92
Fig. 41 - Axogenesis in *P. monodon*, nauplius stage 3-4 93
Fig. 42 - Axogenesis of the stomatogastric nervous system in *P. monodon*, nauplius stage 3-4 94
Fig. 43 - Distribution of SL-ir structures in the nauplius stage 3-4 95
Fig. 44 - *P. monodon*, nauplius stage 5-6 (metanauplius) 96
Fig. 45 - Axogenesis of the naupliar region in *P. monodon*, nauplius stage 5-6 (metanauplius) 98
Fig. 46 – Axogenesis of the mandibular neuromere in *P. monodon*, nauplius stage 5-6 (metanauplius) 99
Fig. 47 – Axogenesis of the post-naupliar region in *P. monodon*, nauplius stage 5-6 (metanauplius) 101

Fig. 48 – Axogenesis of the stomatogastric nervous system in *P. monodon*, nauplius stage 5-6 (metanauplius) 102
Fig. 49 – SL-ir structure distribution in *P. monodon*, nauplius stage 5-6 (metanauplius) 104
Fig. 50 – *P. monodon*, protozoea stage 1 105
Fig. 51 – Axogenesis in *P. monodon*, protozoea stage 1 107
Fig. 52 – Axogenesis in *P. monodon*, protozoea stage 1 109
Fig. 53 – Distribution of SL-ir structures in *P. monodon*, protozoea stage 2 110
Fig. 54 – Distribution of SL-ir structures in the naupliar region in *P. monodon*, protozoea stage 2 112
Fig. 55 – Distribution of SL-ir structures in the VNC of *P. monodon*, protozoea stage 2 113
Fig. 56 – Architecture of the protocerebrum and of the nauplius eye complex in *P. monodon*, protozoea stage 3 114
Fig. 57 – Architecture of the protocerebrum in *P. monodon*, protozoea stage 3 ... 115
Fig. 58 – Morphogenesis in *P. fallax*, embryonic stages 3-7 120
Fig. 59 – Axogenesis of *P. fallax*, embryonic stage 3 121
Fig. 60 – Axogenesis of *P. fallax*, embryonic stage 3 123
Fig. 61 – Axogenesis of *P. fallax*, embryonic stage 4 124
Fig. 62 – Axogenesis in the naupliar region of *P. fallax*, embryonic stage 4 126
Fig. 63 – Axogenesis in the telson of *P. fallax*, embryonic stage 4 127
Fig. 64 – Axogenesis of *P. fallax*, embryonic stage 5 128
Fig. 65 – Axogenesis in the naupliar region of *P. fallax*, embryonic stage 5 130
Fig. 66 – Axogenesis of *P. fallax*, later phase of embryonic stage 5 131
Fig. 67 – Axogenesis of the stomatogastric nervous system of *P. fallax*, embryonic stage 5 133
Fig. 68 – Axogenesis of *P. fallax*, embryonic stage 6 134
Fig. 69 – Axogenesis in the naupliar region of *P. fallax*, embryonic stage 6 135
Fig. 70 – Axogenesis in the anterior portion of the ventral nerve cord of *P. fallax*, embryonic stage 6 (early phase) 137

Fig. 71 – Axogenesis in the ventral nerve cord of *P. fallax*, embryonic stage 6 (late phase) 139
Fig. 72 – Axogenesis of the stomatogastric nervous system of *P. fallax*, embryonic stage 6..... 141
Fig. 73 – Axogenesis of *P. fallax*, embryonic stage 7 142
Fig. 74 – Axogenesis in the naupliar region of *P. fallax*, embryonic stage 7..... 143
Fig. 75 – Axogenesis in the post-naupliar region of *P. fallax*, embryonic stage 7 145
Fig. 76 – Axogenesis in the stomatogastric nervous system of *P. fallax*, embryonic stage 7..... 146
Fig. 77 – Expression of SL immunoreactivity in the development of *P. fallax*, embryonic stage 8..... 148
Fig. 78 – Schematic representation of the developmental pattern of the naupliar brain..... 152
Fig. 79 – Schematic representation of the developmental pattern of the VNC 157
Fig. 80 – Correspondence of the SPX organ of *P. duorarum* to the frontal organ of *P. monodon* at corresponding developmental stage..... 166
Fig. 81 – Schematic representation of the development of the medulla terminalis and the optic lobe in Malacostraca 172
Fig. 82 – Comparison of developmental data on frontal filaments in cirripeds 175
Fig. 83 – Development of the frontal filaments in branchiopods..... 176
Fig. 84 – Comparison of the architecture of the medulla terminalis and its connections during development of malacostracans, cirripeds and branchiopods 178
Fig. 85 – Distribution of the characters associated with the medulla terminalis in Pancrustacea..... 181
Fig. 86 – Evolutionary scenarios based on the distribution of the structures associated with the medulla terminalis (simplified)..... 184
Fig. 87 – Schematic representation of the SNS developmental pattern and of the connection of the SNS to the brain..... 188
Fig. 88 – Comparison of SNS architecture in the marbled crayfish *P. fallax* stained with use of different techniques at a comparable developmental stage..... 192

Fig. 89 – The anlage of the SNS stained in a cephalocarid representative and in the marmorkrebs 199

Fig. 90 – Schematic representation of the anlage of the nervous system in malacostracans 202

List of tables

Table 1 - List of chemicals and solutions (in alphabetical order) 9

Table 2 - List of primary and secondary antibodies 13

Table 3 - Summary of the main developmental events in *M. norvegica* 76

Table 4 - Correspondence of the staging system used in the present study and the traditional staging system referred to Motoh (1981) 78

Table 5 – Formation and modification of the main external morphological characters during development of *P. monodon* 79

Table 6 (next page) 116

Table 7 - Summary of the main developmental events in *P. monodon* 117

Table 8 – Formation and modification of the main external morphological characters during development of *P. fallax* 119

Table 9 – (next page) - Summary of the main developmental events in *P. fallax*. 149

Table 10 – Comparison between the nomenclature adopted in the development of the SNS of *P. fallax* in the previous study by Vilpoux et al. (2006) and the present study 193

List of abbreviations

A	antenna	MXP	maxilliped
a	anterior	N	nerve
ce	cell cluster	n	neuromere
CNS	central nervous system	NEC	nauplius eye complex
CO	connective	OFG	olfactory glomeruli
COG	commissural ganglion	OL	optic lobe
CP	carapace	p	posterior
d	dorsal	PB	protocerebral bridge
DC	deutocerebrum	PC	protocerebrum
ECTB	ectoteloblasts	PE	pereiopod
ENS	enteric nervous system	pfc	peripheral cell cluster
EX	exopod	PG	paragnath
FO	frontal organ	PL	pleopod
FT	fiber tract	POC	post-oral commissure
INS	inter-segmental nerve	PR	proctodeum
ISN	intestinal nervous system	PRG	proctodeal ganglion
IVN	inferior ventricular nerve	PROC	pre-oral commissure
L	lateral	r	right
LA	lamina	SN	stomatogastric nerve
LB	labrum	SNS	stomatogastric nervous system
LBC	labral commissure	ST	stomodeum
LBG	labral ganglion	STC	stomodeal commissure
LO	lobula	TC	tritocerebrum
m	median	TE	telson
MD	mandible	TG	terminal ganglion
MDC	mandibular commissure	TH	thoracopod
MFT	median fiber tract	TSP	terminal spine
ME	medulla	v	ventral
MT	medulla terminalis	VNC	ventral nerve cord
MX	maxilla		

1. Introduction

1.1 The nervous system in Crustacea

Among arthropods, the Crustacea represents one of the most diverse taxon. With their variety of forms, reflecting the manifold life histories of these animals, they have interested biologists for centuries. Studies on the nervous system of crustaceans date back to the late 17th century, and have attracted the increased interest of neurobiologists since the late 19th century. Some of the more well-known studies on the anatomy and physiology of the nervous system in the past century include the pioneering works of Sigmund Freud (1856-1939), Charles Richet (1850-1935), Wilhelm Biedermann (1852-1929), and Albert Bethe (1872-1954) and the works on comparative anatomy reviewed in the text books of Hanström (1928) and Bullock and Horridge (1965). More recently, the application of immunohistochemical techniques has added a large amount of new data to neuroanatomy. This has been used to, among other applications, better define neural architectures and to provide information about ground patterns, support phylogenetic hypothesis, and reconstruct the evolution of the nervous system and evolution in general under the name of a new discipline called "*neurophylogeny*" (Harzsch 2006; Richter et al. 2010; Loesel 2011; Strausfeld and Andrew 2011; Strausfeld 2012).

The nervous system of crustaceans, as of arthropods in general, is a system of neurons making up both the central nervous system and the peripheral nervous system. Although the distinction between a central and a peripheral nervous system has been discouraged (Richter et al. 2010), the current studies, including the present, maintain this distinction to simplify descriptions.

The central nervous system

The central nervous system of crustaceans is composed of a set of neurons metamerically organized along the antero-posterior axis of the animal, which form the brain and the ventral nerve cord. The brain of crustaceans is a tripartite brain (Lichtneckert and Reichert 2005) also referred to as a syncerebrum (Richter et al. 2010; Richter et al. 2013) formed during development through a process of condensation of three segmental cephalic neuromeres: the proto-, the deuto- and the tritocerebrum. These identify three morphological regions: the protocerebral region, associated with the compound eyes (called the ocular/protocerebral region following Scholtz 1995a), the deutocerebral region, associated with the first antenna

(antennular region), and the tritocerebral region, associated with the second antenna (antennal region) (Scholtz and Edgecombe 2006; Bitsch and Bitsch 2007, 2010; Richter et al. 2013). The ventral nerve cord is composed, from anterior to posterior, by the mandibular, maxillular and maxillary ganglia, a chain of thoracic and of pleonic ganglia in a varying number among species. Each ganglion of the ventral nerve cord is a bilaterally symmetrical structure which develops from a pair of embryonic neuromeres and, with the exception of the terminal pleonic ganglia, is associated with a pair of appendages.

The peripheral nervous system

The peripheral nervous system includes the peripheral neuromuscular synapses, the somatosensory nervous system and the stomatogastric nervous system. The somatosensory nervous system includes the more complex visual organs, such as the compound eyes and the ocelli, and any kind of simpler photo-sensitive receptor organs, the olfactory organs, which can become highly complex systems in some species, and simple sensory organs which include mechano-, chemo-, and proprio-receptor organs (e.g. Bate 1978; Laverack 1968, 1987; Nilsson and Osorio1998). The stomatogastric nervous system (SNS) is one of the most investigated motor systems in crustaceans (e.g. Maynard and Dando 1974; Harris-Warrick 1992; Selverston and Moulins 2012; for a review see also Harzsch et al. 2012). It is composed of a relatively small number of neurons that form a complex neural network which is responsible for the innervation of the labrum, the oral cavity and the esophagus and regulates the rhythmic movement of the digestive tract (e.g. Selverston and Moulins 2012).

Thanks to the growth of new methods for morphological research, the amount of data on the nervous system has exponentially increased in the last years, including detailed descriptions of fine neural architectures (e.g. Kirsch and Richter 2007; Brenneis and Richter 2010; Stegner et al. 2014). The comparison of characters at a high level of resolution have contributed to crucial evolutionary discussions on topics such as brain architecture and head segmentation (e.g. Fanenbruck et al. 2004; Fanenbruck and Harzsch 2005; Stegner and Richter 2011; Kenning et al. 2013).

1.2 The development of the nervous system in Crustacea

In this context, understanding neurogenesis and the mechanisms guiding the neural development becomes indispensable in order to maximize the efficiency of comparative studies and unravel evolutionary relationships among taxa. Given the extreme manifold life

histories of crustaceans reflected in their variety of patterns of embryonic and larval development, the potential provided by a comprehensive knowledge of neurogenesis in these animals becomes obvious.

Short review of past studies on the development of the nervous system in crustaceans

Research on the development of the nervous system in crustaceans has been mainly focused on malacostracans in the past. The first studies to reveal the structure of the embryonic central nervous system have been performed by means of classical histology (e.g. Scholtz 1992; Harzsch and Dawirs 1993, 1996a; Helluy et al. 1993, 1995, 1996; Rotllant et al. 1995) and with the use of neuron-specific antibodies (e.g. Meier and Reichert 1990; Garzino and Reichert 1994). Neurogenesis has been studied by in-vitro incorporation of BrdU in larvae (e.g. Harzsch and Dawirs 1994, 1996c) by rhodamine phalloidin staining (e.g. Whitington el al. 1993; Scholtz 1995a), and the neuronal expression of the gene *engrailed* has been detected in embryos (e.g. Patel et al. 1989; Scholtz 1995a, b; Sintoni et al. 2007; Vilpoux et al. 2008). Moreover, intracellular tracing techniques (e.g. Whitington el al. 1993) and, more recently, in vivo labelling of single neural precursor cells in the neuroectoderm (e.g. Gerberding and Scholtz 2001; Ungerer and Scholtz 2008) have contributed considerably to the understanding of neurogenesis in malacostracan crustaceans. Furthermore, with the introduction of immunohistochemical techniques it has been possible to visualize the ontogeny and maturation of neurotransmitters and neuroendocrine systems (e.g. Beltz et al. 1990, 1992; Webster and Dircksen 1991; Helluy et al. 1993; Rotllant et al. 1993; Cournil et al. 1995; Harzsch and Dawirs 1995, 1996b; Schneider et al. 1996; Rieger and Harzsch 2008). More recently, the immunohistochemical detection of acetylated α-tubulin and of antibodies against specific neurotransmitters (e.g. serotonin, FMRF-amide, histamine) in combination with the use of laser scanning confocal microscopy and 3D reconstruction have allowed the tracing of the early spatio-temporal developmental pattern of the nervous system's main axonal pathways not only in malacostracan species (e.g. Decapoda: Harzsch et al. 1997, 1998; Stomatopoda: Fischer and Scholtz 2010; Peracarida: Ungerer et al. 2011), but also in several non-malacostrcans (e.g. Branchiopoda: Harzsch and Glötzner 2002; Fritsch and Richter 2010; Frase and Richter 2016; Cirripedia: Semmler et al. 2008; Cephalocarida: Stegner and Richter 2015). Collectively, these studies have created a solid foundation of data suitable for comparative analyses and evolutionary interpretations.

Main topics and open questions

The development of the central axonal pathways of crustaceans shares a general common pattern with all arthropods. The brain develops in the shape of a neuropil ring that surrounds the stomodeum, the so called circumesophageal nerve ring delimited anteriorly by a pre-oral commissure and posteriorly by a post-oral commissure. The segmental axonal scaffold of the ventral nerve cord develops in a defined gradual antero-posterior developmental pattern resulting in a ladder-like chain of neuromeres. Each neuromere is composed of lateral longitudinal connectives, transversal commissures and a median unpaired longitudinal nerve, generally called the median fiber tract. However, fundamental differences have been revealed among different species in the axonal architectures of the forming central neuropils at specific developmental stages, as well as in the relative timing of formation of certain neural elements, and sometimes, in the mechanisms guiding neural development. These differences have in turn generated different evolutionary evaluations (e.g. Harzsch et al. 1998; Harzsch and Glötzner 2002; Vilpoux et al. 2006; Fischer and Scholtz 2010; Ungerer et al. 2011; Fritsch and Richter 2012; Stegner and Richter 2015). Particular attention has been directed also to the development of some peripheral systems especially in the head region, such as the development of the visual system (e.g. Harzsch et al. 1997; Harzsch and Waloszek 2001; Frase and Richter 2016) and, more recently, the development of apical sensory organs (Semmler et al. 2008; Fritsch and Richter 2010; Fritsch et al. 2013b; Frase and Richter 2016). Some data on the development of the stomatogastric nervous system and of the innervation of the labrum have been discussed (Harzsch and Glötzner 2002; Fritsch and Richter 2010). New insights have been gained on our comprehension of neurogenesis in crustaceans, and new perspectives on some of the most compelling evolutionary issues have been addressed, including the definition of the segmental boundaries of the brain, and the long-standing debate on the head segmentation in arthropods (e.g. Scholtz and Edgecombe 2006; Frase and Richter 2013; 2016; Richter 2013).

Nonetheless, the amount of data offering a comprehensive description of the development of the nervous system in a consistent temporal sequence is still scarce and, surprisingly, data is particularly lacking in this area for malacostracans. Moreover, a consistent lack of data on the very early stages of axogenesis is a general feature in those studies. In particular, most studies on anamorphic species have mainly addressed their attention to larval development and only limited data is available on the embryonic stages. Research on embryos with different developmental modes has focused on very few stages with the exception of the study on the

development of the nervous system of the amphipod *Orchestia cavimana* (Ungerer et al. 2011). Likewise, only scarce interest has been given to the development of peripheral sensory structures other than the eyes and the olfactory receptors (i.e. the somatosensory nervous system). We have some scattered data for different species (e.g. Harzsch and Glötzner 2002; Ungerer et al. 2011; Fritsch et al. 2013b), but there are no systematic studies on the development of the peripheral nervous system as a whole.

1.3 Aim and organization of the present study

The present study offers a comprehensive description of the nervous system development of three malacostracan species by means of immunohistochemical methods, combined with confocal-laser scanning microscopy and 3D reconstruction. The development of the main axonal pathways of the euphausiid *Meganyctiphanes norvegica* and of the two decapods *Penaeus monodon* and *Procambarus fallax* f. *virginalis* is described from the very early stages of axogenesis, in a consistent temporal sequence of development for the first time. The data have been analyzed with a comparative approach and discussed in an evolutionary context. The development of the axonal scaffold of the central nervous system of the three species is illustrated in detail and its fundamental architecture in relation to the segmental boundaries of the forming body is discussed. Particular attention is also given to the development of the peripheral nervous system and to its contribution to the formation of the axonal scaffold. In this respect the development of the somato-sensory nervous system is illustrated. Special attention has been directed towards the ontogeny of the apical sensory organs in the protocerebral region, especially those connected to the medulla terminalis (i.e. frontal organs and compound eyes). Likewise, the development of sensory elements in the terminal regions of the animals' bodies (i.e. the appendages, the labrum and the telson) is detected and discussed in an overall context. Moreover, the present study provides a comprehensive description of the ontogeny of the stomatogastric nervous system, in addition to some observations on the development of the intestinal nervous system, and offers for the first time an overview on the development of the enteric nervous system as a whole.

Significance of the investigated species

M. norvegica as representative of Euphausiacea, and the two decapods *P. monodon* as representative of Dendrobranchiata, and *P. fallax* as representative of Astacida are species of particular interest in evolutionary-developmental studies (e.g. Alwes and Scholtz 2004, 2006;

Biffis et al. 2009). According to the most recent phylogenetic analyses, within the Malacostraca, the Euphausiacea are closer related to the Peracarida (and Pancarida) (Jarman 2001; Richter and Scholtz 2001). This interpretation is in contradiction with the more traditional view in which the Euphausiacea are regarded as the sister group of the Decapoda (Siewing 1963; Schram and Hof 1998). Decapoda split into the Dendrobranchiata, which include the penaeoidean and sergestoidean shrimps, and the Pleocyemata, which include caridean shrimps, lobsters and crabs. The Dendrobranchiata show many supposedly plesiomorphic characters (Hertzler 2015). Dendrobranchiata and Euphausiacea are the only two groups among the Malacostraca which go through a true anamorphic development, with a free-living nauplius stage during development. The nauplius larva is traditionally considered the ancestral form of development of the Crustacea (Müller 1864); however, the nauplius forms of euphausiids and dendrobranchiates are claimed to have evolved independently twice within malacostracans, while the apomorphic condition of this taxon is a developmental stage which resembles an embryonized nauplius, the so called "*egg-nauplius*" (Scholtz 2000; and see for further discussion Jirikowski et al. 2013, 2015).

Systematic studies on the development of the nervous system of anamorphic species of non-malacostrcans have (surprisingly) grown with particular intensity in recent years (e.g. Fritsch and Richter 2010; Fritsch et al. 2013a, b; Stegner and Richter 2015; Frase and Richter 2016) while no nauplius larva of any malacostracan species has been investigated so far. Despite some focused studies in this area (e.g. Elofsson 1969), the lack of comprehensive data on the neurogenesis on both eupahusiaceans and dendrobranchiates is manifest.

Among the Pleocyemata, the Astacida is one of the most investigated clade. In particular, the parthenogenetic marbled crayfish, also known as Marmorkrebs and recently identified with the name *Procambarus fallax* f. *virginalis* (Martin et al. 2010), has been proposed as a model organism for embryological research (e.g. Jimenez and Faulkes 2010; Vogt et al. 2004; Vogt 2008, 2011; Harzsch et al. 2015) and its development has been especially well characterized (e.g. Vogt et al. 2004; Alwes and Scholtz 2006). Although we have some studies on different aspects of the development of the nervous system of crayfish in general (e.g. Sandeman and Sandeman 1990; Scholtz 1992; Sullivan and Macmillan 2001; Sandeman and Sandeman 2003; Vilpoux et al. 2006; Rieger and Harzsch 2008; Zieger et al. 2013), we do not however have an overall comprehensive investigation of the development of the nervous system in those animals using consistent techniques.

Choice of methods

In order to fill in this gap in our knowledge, the development of the nervous system in the three species has been consistently studied with the use of acetylated α-tubulin and serotonin antibody stainings. Each specimen was fixed at monitored regular developmental intervals and immune-labelled. A continuous sequence of development is provided, comprehensive of the earliest stages of formation of detectable neural structures until the formation of the main axonal scaffold. Each investigated stage has been characterized and visualized with fluorescent nucleic dyes, and in addition, the nauplius larvae have been processed by the use of scanning electron microscopy (SEM). The immunohistochemical detection of acetylated α-tubulin has emerged as one of the most successful methods for investigating neurogenesis in crustaceans, and is becoming one of the most widespread for the visualization of the general morphology of the developing nervous system in this taxon. In fact, the immuno-labelling with the antibody against acetylated α-tubulin allows not only the detection of the axonal projections but also, in some cases, of the somata of developing neurons (e.g. Ungerer et al. 2011). Likewise, the identification of serotonin-like immunoreactivity is a common and powerful tool for seeking out homologous neural structures not only among crustaceans, but among all arthropods, and also provides characters used for phylogenetic inference (e.g. Harzsch and Waloszek 2000; Beltz and Kravitz 2002; Harzsch 2003a). Moreover, the description of the appearance of serotonin-immunoreactive structures during development has been used in a comparative context (e.g. Beltz et al. 1990; Helluy et al. 1993; Harzsch and Dawirs 1995; Stegner and Richter 2015), as serotonin is the only neurotransmitter which can be detected immunohistochemically during ontogeny.

In summary, the present study offers a solid background for comparison with existing data and promotes future systematic research on the development of both the central and the peripheral nervous system in a comprehensive perspective. Moreover, the present study increases and solidifies our knowledge on developmental neuroanatomy, thus providing new characters for phylogenetic discussions and contributing towards answering the most fundamental evolutionary questions.

2. Material and methods

2.1 Species collection and fixation

The Northern krill *Meganyctiphanes norvegica* (M. Sars 1856) was collected in the Gullmarsfjord of Fiskebäckskil in Sweden (58° 19.9' N, 11° 33.8' E) in the summers of 2008 and 2009 (July-August). In this region adult krill reside in the deepest region of the fjord were they aggregate between -80 and -110 m during the day and disperse at night in the upper layers to feed and spawn (Tarling et al. 1999; Thomasson 2003; Cuzin-Roudy et al. 2004). Copulation starts in January, and fully developed spermatophores are present in males for at least 9 months. Spawning starts in April and continues until October with a marked peak in July (Boysen and Buchholz 1984). The animals were collected using an Isaacs-Kidd mid-water trawl with a mesh size of 2 mm connected to an echo sound-system (120 kHz) on board which detected the position of the krill swarms at a depth of -80 to -120 m. The animals were maintained in deep-sea seawater at the Kristineberg Marine Research Station in an aquarium with 1 m3 seawater flowing through (as recommended by Komaki 1966), in a dark and temperature-controlled room (6°C). They were fed regularly with a special mixture of phytoplankton and copepods (Lass et al. 2001). Gravid females, which carry the two male spermatophores between the coxae of the sixth thoracopods, were isolated for spawning in 1 l jars. The deep-sea sea water in the jars was daily checked passing through a millimeter grid and renovated. After spawning, the embryos were transferred into glass-Petri dishes and their development monitored under a light microscope. Hatching occurs after 24-38 hours post-spawning and the molts follow with a time interval which varies from 1 to 3 days depending on the brood-stocks and the naupliar stage. Around 10 samples per stage in each brood-stock were selected and fixed in 4 % PFA in deep-sea sea water at room temperature for 20 to 30 min then carefully washed in deep-sea sea water and stored in 1% NaNO3 diluted in deep-sea sea water at 4°C. For performing SEM some larval samples were stored in 4% PFA.

The samples of the giant tiger prawn *Penaeus monodon* (Fabricius, 1798) were collected at the CSIRO Marine and Atmospheric Research station (CMAR) in Queensland, Australia, in late summer 2008 (August-September). Here, second generation stocks of P. monodon were reared in 10000 l sand-substrate tanks (Coman et al. 2006) and gravid females transferred to circular spawning tanks (water temperature 29°C) fitted with an automated spawning detection and alarm system (Coman et al. 2003). Immediately after spawning detection, the water was removed from the spawning tanks and collected in ventilated jars. Embryos were

collected after passing a millimeter grid at the bottom of the jars and controlled under a light microscope. Relevant stages were fixed in 4% PFA in 1x PBS at room temperature for 20 to 30 min than washed in PBS and stored at 4°C. Some samples were transferred into absolute methanol and stored at -8°C. Some larval samples were kept in 4% PFA for performing SEM.

NAME	CHEMICAL COMPOSITION
CONGO-red	CONGO-red (Sigma-Aldrich, Steinheim, Germany) 1,5mg/ml distilled water
DABCO-Glycerol	2,5g DABCO (1,4-Diazabicyclo-[2,2,2]-octan) in 10ml PBS and 90ml Glycerol
Et-OH	100% Ethanol (C_2H_6O)
Hoechst	H33258, bisbenzimide ($C_{25}H_{24}N_6O$)(Molecular probes) 1µg/ml (1:1000 dilution in PBS of 1mg/ml stem solution)
PBS	Phosphate Buffered Saline 1,86mM NaH_2PO_4, 8,41mM Na_2HPO_4, 175mM NaCl in dH_2O; pH 7,4
PBT	PBS containing 0,5% BSA, 0,3%Triton X-100, and 1,5% DMSO (dymethyl-sulfoxide, Heranaeus)
PBT+N	PBT containing 5% Normal Goat Serum
PFA	5% Paraformaldehyde in PBS
Sytox	Sytox®Green Nucleic Acid Stain (Molecular Probes) 5nmol/ml (1:1000dilution in TBS of 5µmol/ml stem solution)
TBS	TRIS-HCl buffered saline 0,9% NaCl and 10mM TRIS-HCl; pH 7,5
Vectashield	Vectashield® Mounting Medium (Vector Laboratories, Inc.)

Table 1 - List of chemicals and solutions (in alphabetical order)

Specimens of the marbled crayfish *Procambarus fallax* (Hagen, 1870) f. *virginalis* were reared and collected at the Institute of Biology (Comparative Zoology) of the Humboldt

University Berlin, Germany. Single females were maintained in an aquarium system formed by natural gravel-substrate tanks (2 batteries x 7 serial tanks) connected to each other and to a special filter for fresh water aquaria, each tank was separately ventilated (water volume per tank: 13,5 l; water flow rate ca. 70 l hr-1). Environmental conditions were maintained constant and the water temperature at 20°C with a photoperiod of 13 hours. Each tank was provided by half of a flower pot as shelter for the animals. The animals were fed every two days with commercial crab food chips (NovoCrabs, JBL GmbH & Co. KG, Germany) (Martin and Scholtz 2012). Gravid females were not fed and monitored daily taking off some eggs from the brood and the morphology of the embryos was checked under a light microscope to pick up the relevant stages. Fixation was performed using 4% PFA in 1xPBS at room temperature for 20 to 30 min. While in the fixative solution, the eggs were manually dissected under the light microscope and the chorion removed with the use of the tip of micro syringes as scalpels. Embryos were then washed in PBS and the yolk carefully removed. The specimens were stored in 1xPBS at 4°C.

2.2 Scanning electron microscopy (SEM)

Best preserved larvae of *M. norvegica* and *P. monodon* were selected for SEM and carefully put through a graded ethanol (Et-OH) series. To avoid shrinkage the first steps of the series (alcohol 15% and 30%) were added gradually and the incubation time prolonged to 20 min instead of 10 min spent for the following series. The critical point-drying was performed in a BALTEC CPD 030 using ethanol (surface tension: 23 Dynes/cm) as intermediate fluid and carbon dioxide (CO2 critical constant: +31,1°C; 1072 psi) as transitional medium. The dry specimens were mounted on SEM stubs and in some samples the cuticle was removed manually with the use of sharpened tungsten needles. The stubs were sputter-coated with gold following standard procedures using a BALTEC SCD 005. A Zeiss Leo 1450VP scanning electron microscope was used for observations and digital photography.

2.3 Fluorescence staining

Nuclear stainings

Nuclear stainings were performed with the use of Sytox®Green or alternatively Hoechst nucleic acid stains. Sytox is a fluorescent dye (excitation maximum: 523 nm) which has a high affinity to nucleic acids in general (i.e. DNA and RNA). The specimens were washed in TBS (2x5 min, 4x30 min) before incubation in Sytox solution for 3 hours at room temperature

in the dark. They were then rinsed in TBS (5x10 min, 2x30 min) and stored in the fridge at 4°C covered by aluminum foil to protect the stained objects from light. Hoechst is a relatively small molecule with a high binding affinity to AT-rich regions of the DNA and therefore used as fluorescent marker for cell nuclei (excitation maximum: 352 nm). Hoechst was preferred to Sytox double stainings e.g. with antibody-stainings to avoid possible overlapping of emission wave lengths and production of unspecific signal. The staining protocol was the same used for Sytox with the difference of using PBS as washing solution and the incubation time in Hoechst solution being reduced to 10 min.

Note on the use of CONGO-red as fluorescence marker

Following the procedure of Michels and Büntzow (2010) some samples of *M. norvegica* and *P. monodon* were successfully stained by CONGO-red (Fig. 1A, A'). The obtained samples were used for better stages distinction and for checking details not visible with bright field microscopy. Moreover, some of the stained specimens where additionally stained by Sytox green (Fig. 1B) following the same procedure described in the previous paragraph. The resulting combination of the stainings offers an excellent detection of the nuclei of the external cell layers with significant reduction of background artifacts (Fig. 1B).

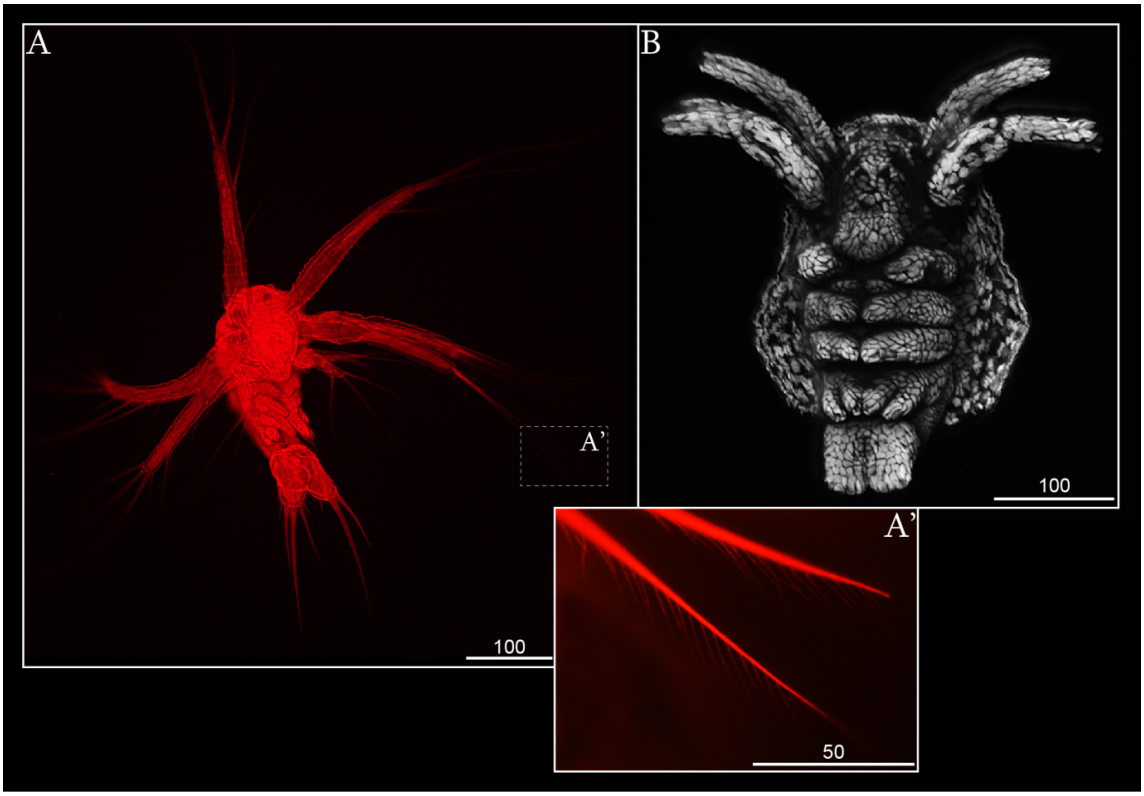

Fig. 1 – Application of CONGO-red and combination with Sytox green stainings

A, A' - Metanauplius of *P. monodon* stained by CONGO-red (ventro-lateral view). Fluorescence microscope image. **A -** General overview. **A' -** Detail of the distal setae at tips of antenna 2. The presence of additional tiny setulae is highlighted by the dye.

B - Metanauplius of *M. norvegica* stained by CONGO-red in combination with Sytox green (ventral view). Fluorescence microscope image. Volume rendering of the entire larva. The distribution of cell nuclei at the surface of the sample is visualized at a high resolution. **Scale bars** are as indicated in each image in micrometer (µm).

Immunohistochemical staining

A list of the antibodies used for immunohistochemical labeling and the dilution of the antibody stem solution is given in Table 2.

Alpha-tubulin is an essential component of the microtubules of eukaryotic cell's cytoskeleton and its acetylated isoform is a common post-translational modification found in particular in nerve cell axons of invertebrates (Harzsch et al. 1997). In this way it is possible to obtain a general overview of the main axonal scaffold of the nervous system. Before starting the immunohistochemical procedure the specimens were rinsed in PBS (5x10 min), washed in PBT (3x10 min, 4x30 min) and transferred to PBT+N (2x30 min) to block unspecific binding sites. A murine monoclonal antibody (clone 6-11 B-1) was chosen as primary antibody and diluted in PBT+N. The specimens were incubated in this solution overnight at room temperature on the shaker. During incubation all the larval specimens were ultrasonicated (3 pulses x 3 sec) to make their cuticle more easily penetrable. The subsequent washing was performed in PBT on the shaker at room temperature (3x10 min, 4x30 min). Then the specimens were again transferred to PBT+N (2x30 min). A secondary antibody conjugated with the fluorochrome CyTM3 (emission maxima: 568 nm) was used. The specimens were incubated in the secondary antibody diluted in PBT+N overnight on the shaker at room temperature in the dark. The third day the secondary antibody was rinsed in several changes of PBS (5x10 min, 2x30 min) and stored in the buffer in the fridge at 4°C covered by aluminum foil to protect the stained objects from light.

Serotonin (5-hydroxytryptamine, 5-HT) is a biogenic monoamine neurotransmitter in the central nervous system which may be found in synapses, axons and cell somata. Labeling against serotonin was performed using a primary polyclonal rabbit antiserum and a secondary antibody coupled to the green-fluorescing Alexa Fluor® 488 (emission maxima: 520nm). The used procedure for the staining generally followed the same protocol as used for the anti-acetylated-α-tubulin staining.

ANTIBODY	DILUTION
PRIMARY	
Anti-acetylated-α-tubulin (IgG 2b Isotype) mouse monoclonal (6-11 B-1, Sigma T6793)	1:100 dilution in PBT+N
Anti-serotonin (5HT) polyclonal (Immunostar)	1:100 dilution in PBT+N
SECONDARY	
Goat anti-mouse IgG (H+L) affini pure Cy™3 (Jackson/Dianova)	1:200 dilution in PBT+N
Goat anti-rabbit IgG (H+L) Alexa Fluor® 488 (Molecular Probes)	1:500 dilution in PBT+N

Table 2 - List of primary and secondary antibodies

Stained embryos and larvae were mounted in 2,5% DABCO-Glycerol or Vectashield. Both media protect the stains from rapid bleaching and the latter preserves the intensity of the fluorescence signal longer than the first one. Cover slips were used and small pieces of plasticine were fixed at their corners to prevent crushing of the mounted specimens.

2.4 Analysis of the stained specimens

Epifluorescence Microscopy

To analyze specimens before and after staining and to select the stained samples worth to be scanned by CLSM a fluorescence microscope (Axioskop 2 Plus, Zeiss) and a fluorescence stereomicroscope (Lumar V12, Zeiss) were used. Relevant samples were documented by images produced by digital cameras (AxioCamHRc) and processed by the associated software (AxioVision).

Confocal Laser Scanning Microscopy (CLSM)

Selected stained objects were scanned with a confocal laser-scanning microscope (Leica DM IRE2) equipped with a laser-scanning unit (Leica TCS SP2 AOBS). Step sizes of 0,5 µm to 0,8 µm between successive images were chosen, depending on species and structure. According to the optimal excitation of wavelength of the fluorochromes labeling the objects lasers of different wavelengths were chosen: a UV-laser (405 nm wavelength) for Hoechst, an argon laser (488 nm wavelength) for Sytox and anti-Serotonin and the helium-neon laser (543 nm) for anti-acetylated α-tubulin. In case of double (e.g. Hoechst and anti-serotonin) or triple

(e.g. Hoechst, anti-serotonin and anti- acetylated α-tubulin) labeling the channels were recorded consecutively to avoid overlapping of signals.

The advantage of scanning with a confocal laser-scanning microscope lies in its ability to create an image collecting the light emitted from the x-y focal planes only, and excluding the signal coming from sources on different planes along the z-axis. The successive z-sections of the scanned objects are rendered in a 3D high-resolution volume after digital compilation of image stacks.

2.5 3D image visualization

The digital data obtained with the CLSM were analyzed with the 3D-reconstruction program Imaris 7.4.2. (Bitplane AG, Zürich, Switzerland) which includes various settings for visualization and analysis of the image stacks.

The 'surpass volume mode' offers a 3D representation of the object arranging all the images of a scan in a virtual stack. The resulting 3D volume can be rotated and turned in every spatial dimension and magnified as convenient. The intensity of the channels can be regulated and the function 'Blend' or 'Shadows projection' can be activated to obtain a clearer image of surfaces. Several 'clipping planes', with any chosen rotation, can be added simultaneously in the volume to analyze the internal structures of the image stack. Each plane truncates the image along a given plane in 3D space by cutting away objects on one side of the plane (Fig.2A).

The 'surpass oblique slicer' represents a plane that can be freely moved and rotated within the data set showing only the selected objects comprised in the chosen section. With the combination of two planes the internal view of a given region of the object is visualized by two separate planes with a different spatial orientation (Fig.2B).

The 'section mode' shows all the three section plane simultaneously centered in one spot within the image stack. Cross-lines can be moved to any point of one section with the other two section plane images moving accordingly. By activation of the function 'extended' several slices of the stack are included in the section plane and enable to analyze substructures in detail (e.g. the position of a given cell soma or the path of an axon).

With the feature 'Snapshot' the processed image stack is captured as 2D image of the 3D image data as it currently appears in the viewing area. A new file containing the digital image

is created which includes all scale information and measurement data displayed. All images were performed with predefined dimensions and a resolution of 300 dpi.

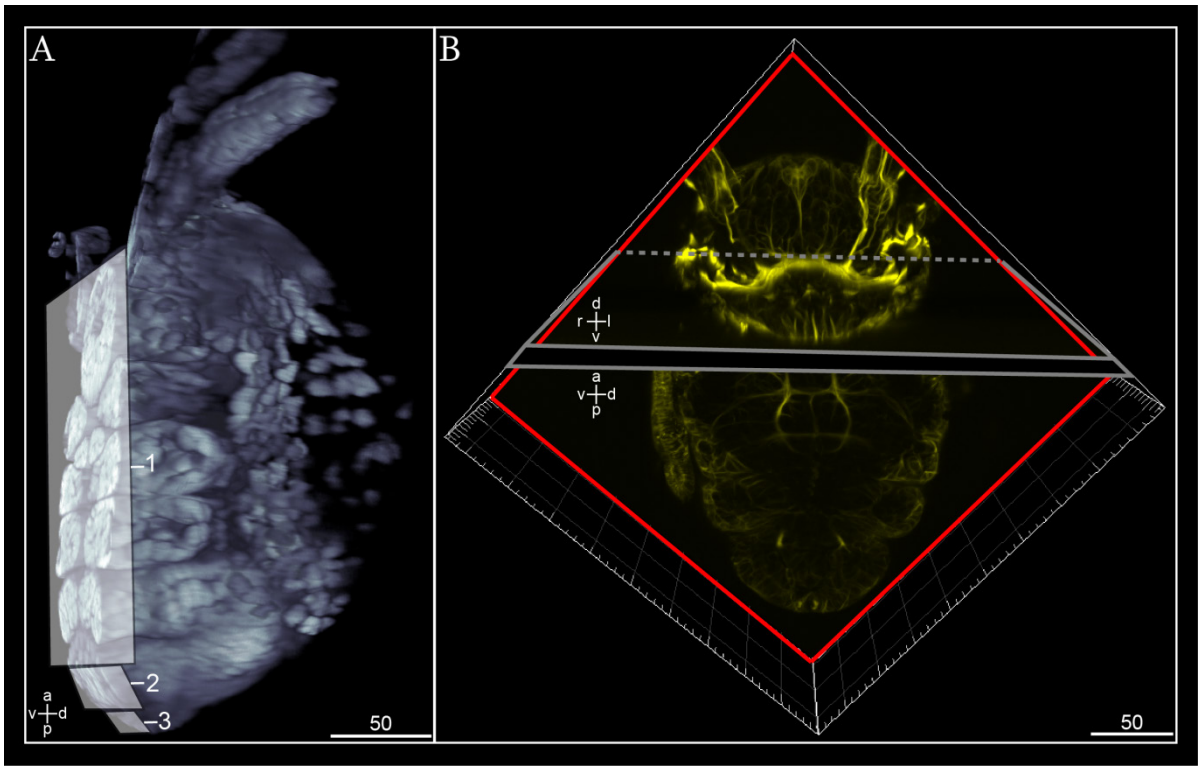

Fig. 2 - Application of Imaris settings to the CLSM image stacks

A - Example of the use of clipping plane in the 'surpass volume mode'. *M. norvegica*, metanauplius stage (lateral view). Sytox staining. Transparent rectangles (1-3) mark the three different planes in which the clipping planes have been applied. The internal cell nuclei of the object are visible on the surfaces of the cut object. **B -** Example of the use of of the 'surpass oblique slicer'. *M. norvegica*, metanauplius stage (ventral view). Anti-acetylated α-tubulin staining. The white grid represents the frame of the total volume occupied by the object. The red line marks the border of one oblique slice applied perpendicular to the z-axis. The grey lines mark the position of a second oblique slice which intersects the first one at the level indicated by the stippled grey line. **Scale bars** are as indicated in each image in micrometer (µm).

All the pictures shown in this study (i.e. SEM micrographs and fluorescence digital images) were processed and labelled with the use of 'Adobe Photoshop' (Version CS5.1) and 'Adobe Illustrator' (Version CS5.1).

2.6 Notes on the applied methods

As already observed in previous studies (e.g. Ungerer et al. 2011), the use of anti-acetylated α-tubulin as primary antibody also reveals structures other than axons such as cell somata or muscle fibers. This is due to the high binding affinity of the antibody to the cortical cytoskeleton of most of cell somata, especially during development, with a high level of cell activity (e.g. cell division, cell movement). Nevertheless specific neural labeling is indicated

by (1) stronger binding to the antibody and thus more intense signal of the growing neurites associated with their neurons than the one on cytoskeleton of surrounding cells; (2) shape of cell somata and size; (3) location related to neurogenesis in the following stages; (4) time of expression. These parameters have been carefully evaluated under the light of previous investigations. Moreover, the terminal spines of the limb buds and of the telson show high signal intensity. At least in part this staining is likely to relate to a binding of the α-tubulin antibody to non-neural structures. Therefore, unequivocal distinction of developing neural structures in the spines was not always possible with the applied methods.

The use of polyclonal antisera against serotonin does not rule out the labeling of related neuro-reactive substances so that the terms serotonin-like immuno-reactive (SL-ir) structures and serotonin-like immunoreactivity (SLI) are used to these structures. With the applied methods, identification of the origin of neurites contributing to a given bundle cannot be unambiguously resolved in every case. With some exceptions, no definite statements can be made concerning the direction of growth of nerve fibers.

The description of the neural structures will proceed along the anterior-posterior axis and will begin with the central parts and proceed to the periphery. Moreover, since most of the structures are arranged in a bilaterally symmetric pattern, the descriptions will be limited to one body half, the contra lateral counterpart being its mirror image. Unpaired structures will be explicitly remarked. The nomenclature used for describing the development of the nervous system follows the neuroanatomical glossary proposed by Richter et al. (2010).

3. Results

General remarks and nomenclature

This part of the thesis is subdivided into three chapters, each devoted to the description of the development of a particular species. The order is as follows: *Meganyctiphanes norvegica*, *Penaeus monodon* and *Procambarus fallax* f. *virginalis*. Each chapter includes observations on the changes of the external morphology, in the section "Morphogenesis", and of the main axonal pathways in the central and in the peripheral nervous system, in the section "Nervous system development". In this last section, the descriptions of the general axogenesis, of the stomatogastric nervous system (SNS) development, and of the serotonergic-like (SL) expression pattern are each treated in separate sub-sections.

The staging system is based on intervals between main neural differentiation events in combination with external morphological changes. Specific indications for the staging nomenclature for each species are illustrated at the beginning of each chapter. Additionally, a summarizing table of the main developmental characters throughout the investigated stages is provided at the end of each chapter.

The development of both *M. norvegica* and *P. monodon*'s nauplius larvae and of *P. fallax*' egg-nauplius of follows the common plan summarized in Fig. 3. Two main compartments can be distinguished in terms of space and time called the **naupliar region** and the **post-naupliar region** (e.g. Whitington 2004). The naupliar region includes the brain neuromeres and the mandibular neuromere, while the post-naupliar region houses the neuromeres developing posterior to the mandibular segment and includes the telson.

The **brain** is formed by the protocerebrum which is associated with the compound eyes, the deutocerebrum which targets the segment of antenna 1, and the tritocerebrum which targets the segment of antenna 2. The neural connections spanned among the brain neuromeres form a ring around the prospective digestive tube which is called the circumesophageal nerve ring. This is formed by the **pre-oral commissure** in the protocerebral region, developing anterior to the stomodeum, and by the **post-oral commissure** in the tritocerebral region, developing posterior to the stomodeum.

The neurite bundle which develops between the protocerebrum and the various components of the medulla terminalis is called the **frontal tract**, which substitute the former term "*optic fiber tract*", "*optic tract*" or "*optic nerve*" (see Discussion).

The term **optic lobe** describes a morphological region observed during development that is the lobe in which the compound eye develops (see also e.g. eye chamber in Kauri 1962). It can correspond to the eye stalk with the inclusion of the medulla terminalis additionally as it is the case for the three species investigated in the present study.

The term **visual neuropils** is here adopted to indicate all the neuropils which process the visual information and thus (from more proximal to distal): the medulla terminalis, the lobula, derived from the previous one, the medulla and the lamina. Since these last two neuropils share a common anlage, sometimes they are referred as 'medulla+lamina' as a unit.

The presence of apical sensory organs connected to the medulla terminalis is for the first time documented in the nauplius larvae of *M. norvegica* and *P. monodon*, and are called the **frontal organs**, which substitute the term of "*frontal filaments*" used in other crustacean species (see Discussion for homology of these organs).

The **mandibular neuromere** is the last posterior segment of the naupliar region and also the anterior-most neuromere of the ventral nerve cord being connected to the anterior end of the median fiber tract and of the longitudinal connective (Fig. 3).

The **ventral nerve cord** eventually includes the mandibular neuromere, the post-naupliar neuromeres (i.e. maxillar, thoracic and pleonal neuromeres), the median fiber tract and the longitudinal connective, these two last ending posteriorly in the **telson** (Fig. 3). Each neuromere of the ventral nerve cord develops commissural neurites and targets one of the developing segments.

In adult decapods, in the post-naupliar region, the first three thoracic appendages posterior to the two maxillae are commonly named **maxillipeds** to indicate their differentiation in feeding organs and to distinguish them from the following thoracic locomotory appendages (pereiopods). This nomenclature is maintained in the description of the embryonic development of *P. fallax* whereas in the description of development of the larval stages of *P. monodon* I preferred to apply the generic term **thoracopods** to all the thoracic limbs to facilitate the comparison with *M. norvegica* which does not differentiate maxillipeds in the course of development.

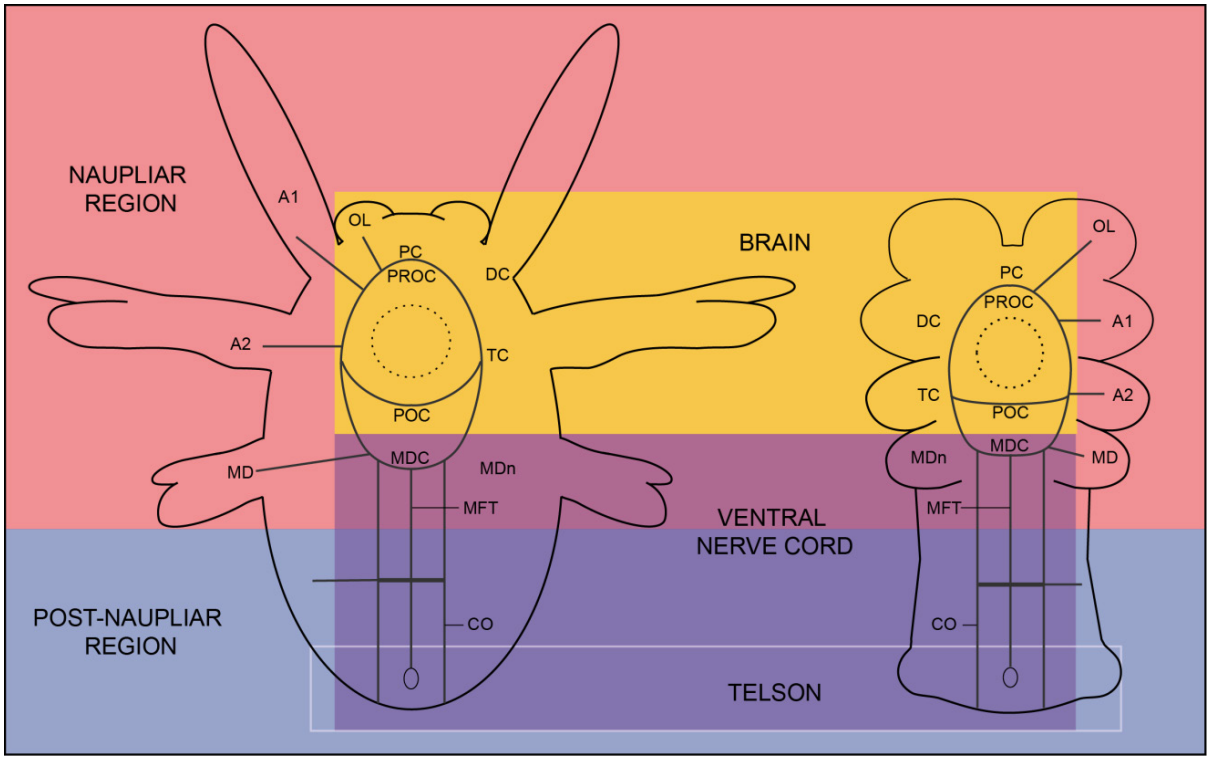

Fig. 3 - Schematic representation of the body organization in the nauplius and in the egg-nauplius

Comparative view of the nauplius (on the left image) and of the egg-nauplius (on the right image) (ventral view). The naupliar region (red background) includes the brain (yellow background) and the mandibular neuromere (purple background). Each nerve of the naupliar region is represented by a black line. These are from anterior to posterior: the frontal tract, the antenna 1 and 2 nerves and the mandibular nerve. The post-naupliar region (blue background) includes the ventral nerve cord posterior to the mandible up to the telson. The architecture of each post-naupliar segment is represented by one commissure and one associated segmental nerve. The region of the telson is marked by the white frame. A stippled circle marks the position of the stomodeum. A small oval marks the position of the proctodeum.

A1: antenna 1; A2: antenna 2; CO: connective; DC: deutocerebrum; MD: mandible; MDn: mandibular neuromere; MDC: mandibular commissure; MFT: median fiber tract; OL: optic lobe; PC: protocerebrum; POC: post-oral commissure; PROC: pre-oral commissure; TC: tritocerebrum.

3.1 Meganyctiphanes norvegica

General remarks on the used staging

In addition to the naupliar development this study includes observations on the late embryonic stages and on the first post-naupliar stage: the calyptopis 1 stage. The distinction between embryonic stage 1 and 2 is based on main external morphological changes and differences in the degree of nervous system differentiation. Embryonic stage 1 refers to the first stage in which the first appearance of neural structure differentiation has been detected with the use of the applied techniques. The staging system nomenclature of the larval development follows Alwes (2008) and identifies two nauplius stages (N1 and N2) and one meta-nauplius (META) before the first calyptopis (CALY). The distinction between an early and a late time of development within each larval stage is supported by evidences on changes of external morphology, cellular differentiation and features of neural development. In addition to the description of external morphological features, some observations on the arrangement of the external ectodermal cells are provided. Any implication on cell-linage tracing is beyond the scope of the present work which only points at regions of interest for further studies in this field.

Notes on larval development

Between 24 and 48 hours post-spawning, the embryo hatches out of the eggshell as a free-living nauplius. The three naupliar appendages flap laterally. Antennae 1 and 2 and mandibles start to move synchronously and the nauplius begins swimming, at first mainly in the horizontal plane and later, before the first molt, along the vertical plane. Recurrently, the nauplius pushes upwards by actively moving the appendages and jerkily falls down when suspending that movement. The larva undergoes two molts, which lead to the second nauplius and a metanauplius. The metanauplius swims with the use of the antennae 1 and 2 alone, while its mandibles, reduced in size, lose their swimming function and become part of the prospective feeding apparatus together with the labrum and the paragnaths. The first three post-naupliar appendage anlagen (maxilla 1 and 2 and thoracopod 1) have grown out but are not functional at this stage. The caudal papilla has also grown and maintains its position flexed towards the ventral body surface. At the third molt the larva hatches as a calyptopis, which starts to feed. The locomotion involves the post-naupliar appendages and the caudal papilla, which is released from the bent position at the metanauplius stage.

3.1.1 Morphogenesis

3.1.1.1 Embryonic stage 1

The embryo has a spherical shape (Fig. 4) and is dominated by the presence of the naupliar limb anlagen. These insert equidistantly at the ventro-lateral side of the body and cover its entire length from anterior to posterior (Fig. 4A). They are tightly pressed to the lateral side of the body and embrace the embryo dorsally (Fig. 4A, B). The anlagen of the uniramous antenna 1 and of the biramous antenna 2 and mandible have a distinct shape and bear terminal short spines (Fig. 4A, B). The anlage of antenna 2 shows a subdivision into a longer exopod and a shorter endopod, while the future biramous character of the mandible anlage is as yet only weakly developed, the exopod being slightly longer than the endopod (Fig. 4B).

Ectodermal cell arrangement

At the anterior pole of the embryo, in the region anterior to the insertion of the antenna 1 anlage, regular longitudinal rows of cells are observed (asterisks in Fig. 4C, D). An unpaired median row of cells with small nuclei (filled arrowhead in Fig. 4D) is distinguishable from a lateral row comprising three cells with conspicuous large nuclei (asterisks in Fig. 4D). Lateral to these, the adjacent cells maintain a regular bilateral pattern and are located in a somewhat more basal layer than the surrounding cells (open arrowheads in Fig. 4D, D'). At this level, divisions in the transversal plane with a bilaterally symmetric distribution are observed frequently (e.g. short lines in Fig. 4D'). Furthermore, also in the region enclosed by the insertions of the antenna 1 and 2 anlagen a bilaterally symmetric distribution of cells can be recognized (asterisks in Fig. 4C and E), while in median position unpaired cells lay at the level of the mandible anlage (small ovals in Fig. 4C and E).

The region posterior to the mandible anlage insertion is dominated by the presence of six enlarged cells symmetrically distributed at each side, anterior to the blastopore region (stars in Fig. 4C and E, E'). These cells correspond to the ectoderm precursor cells described by Alwes (2008). They are medially separated by a small number of cells of different size (Fig. 4E). More posterior, immediately anterior to the blastopore region (open arrowhead in Fig. 4E'), an oblique row of four cells (asterisks in Fig. 4E') points to a symmetry of the ectodermal layer, which is preserved also at the lateral side of the blastopore region (e.g. median cell (small ovals) and bilaterally symmetric cell division (short lines) in Fig. 4E').

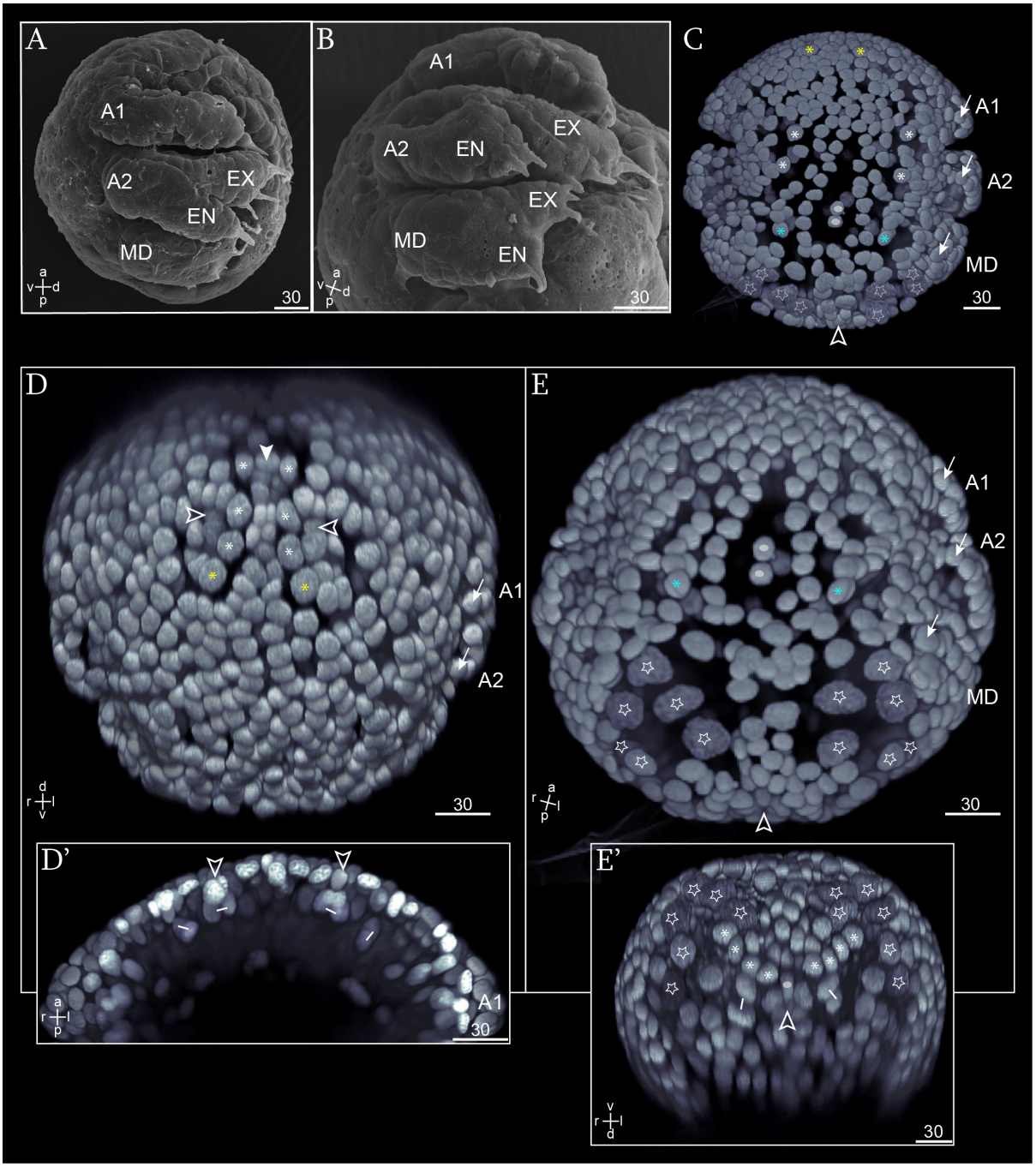

Fig. 4 - External morphology in *M. norvegica*, embryonic stage 1

A, **B -** SEM micrographs. **A -** General overview of the embryo (lateral view). All three naupliar appendages insert equidistantly at the ventro-lateral side of the body. Their distal ends point at the dorsal of the embryo and bear terminal spines. **B -** Detail of the anlage of antenna 2 and mandible (postero-lateral view); the posterior margin of antenna 1 is also included in the picture. The exopod and endopod of antenna 2 anlage are prominently developed while they are only slightly differentiated in the mandible anlage. Terminal spines at the distal end of each ramus are visible.

C-**E' -** Sytox-green staining. Imaris surpass mode: volume (blend); clipping plane in **D'**. Arrows mark the posterior margin of each limb bud. Asterisks mark cell nuclei symmetrically distributed in each body half. Stars mark each of the EPC cell nuclei. Small ovals mark unpaired cell nuclei in the median axis. **C -** General overview of the embryo (ventral view). The proximal portion of the naupliar limb anlagen protrudes at the lateral side of the embryo. The distribution of cells in the ventral ectoderm shows a regular arrangement. The upper-most marked cell nuclei (yellow asterisks) correspond to the posterior-most pair

of the apical longitudinal rows (compare with **D**). The cell nuclei marked by light blue asterisks correspond to the ones in **E**. Open arrowhead points at the region of the blastopore. **D -** View of the apical pole of the embryo (antero-ventral view). Asterisks mark big cell nuclei forming the apical longitudinal rows while the filled arrowhead points at the median row of smaller cells. Open arrows point at cell nuclei located in a lower position than the apical ectodermal layer (compare with **D'**). **D' -** Detail of the ectodermal layers at the apical pole of the embryo (ventral view). The clipping plane is perpendicular to the horizontal plane. The position of the open arrows corresponds to the ones in **D**. Short lines connect sister cells in division with bilateral symmetric distribution. **E -** View of the side of the embryo (postero-ventral view). The upper most marked pair of cell nuclei (light blue asterisks) corresponds to the one in **C** at the same level. Open arrowhead points at the region of the blastopore. **E' -** View of the posterior pole of the embryo (posterior view). Anterior to the blastopore region (open arrowhead) bilaterally symmetric oblique rows of four cells are marked by asterisks. Short lines connect sister cells symmetrically distributed at the lateral side of the blastopore region. **Scale bars** are as indicated in each image in micrometer (μm).

A1: antenna 1; A2: antenna 2; EN: endopod; EX: exopod; MD: mandible.

3.1.1.2 Embryonic stage 2

The late embryonic stage, called the embryonic stage 2, is still characterized by a spherical shape (Fig. 5A). The embryo can be subdivided into two main regions: the naupliar region which comprises the anterior pole and the three naupliar segment anlagen (i.e. antenna 1, 2 and mandibular segments), and the post-naupliar region which extends posterior to the naupliar region until the region of the proctodeum. The naupliar limbs have grown in length and still adhere to the body pointing to the posterior towards the median body axis (Fig. 5A, B). Their terminal spines have elongated (data not shown). The insertion of antenna 1 and antenna 2 are close to each other (open arrowheads in Fig. 5A, B) while the mandible insertion is located more posterior, quite detached from antenna 2 (Fig. 5A, B). The mandible remains tightly pressed to the body, covering part of the lateral portion of the post-naupliar region (Fig. 5C). They still preserve a primordial shape with no elongation of the two rami.

Ectodermal cell arrangement

In the naupliar region, at the anterior pole of the embryo, a single unpaired median row of cells (small ovals in Fig. 5A, B) extends beyond the level of the antenna 1 insertion and terminates ventrally in the region anterior to the mandible insertion (Fig. 5A). At its lateral sides a symmetrical distribution of cells is also recognizable (e.g. asterisks in Fig. 5A, B). Anterior to the insertion of the mandible a region with a lesser concentration of cell nuclei (stippled circle in Fig. 5A) signs the border between the naupliar and the post-naupliar region. These cells have probably a higher amount of cytoplasm then the surrounding ones.

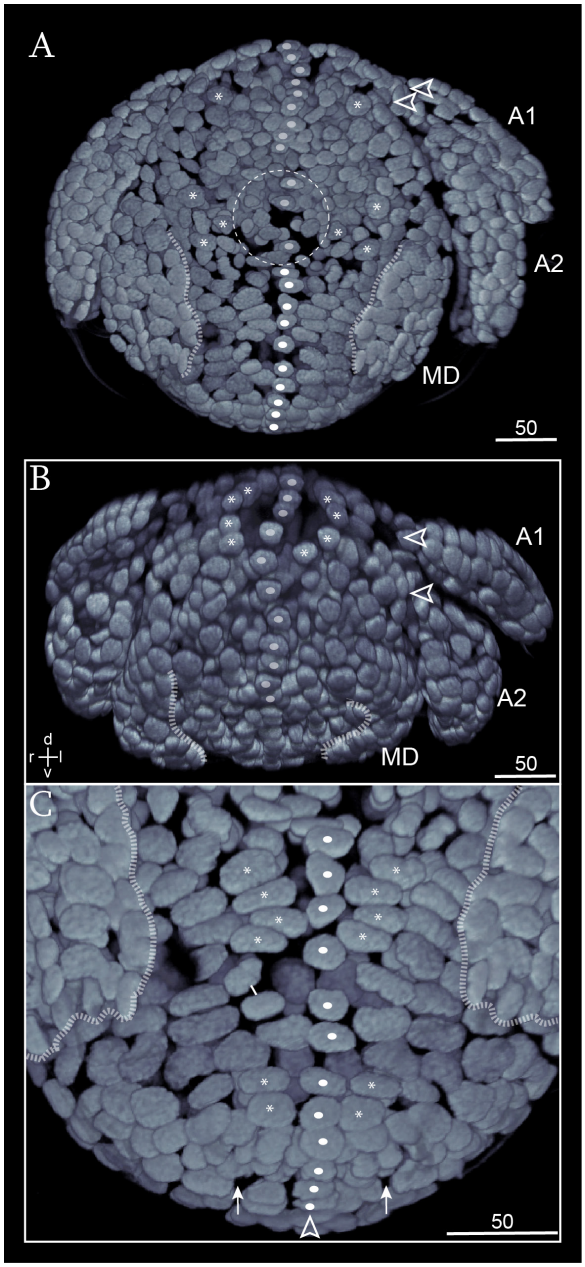

Fig. 5 - External morphology in *M. norvegica*, embryonic stage 2

Sytox-green staining. CLSM image stack. Imaris surpass mode: volume (blend). Open arrowheads point at the insertion of antenna 1 and 2. Asterisks mark bilaterally symmetric cell nuclei. Small ovals point at unpaired cell nuclei in the median axis. White small ovals mark the cell nuclei of the post-naupliar midline. **A -** General overview of the embryo (ventral view). The anlagen of the naupliar appendages point posteriorly. Stippled lines mark the medial border of the mandible anlagen. They cover part of the ventro-lateral post-naupliar region of the embryo. A stippled circle marks the median region with a low density of cells anterior to the posterior midline. **B -** View of the apical pole of the embryo (antero-ventral view). A distinct median row of cell nuclei extends from the level of the antenna 1 insertion ventrally, up to the anterior level of the insertion of the mandible anlage. Stippled lines mark the median border of the mandible anlagen. **C -** Detail of the distribution of the ventral ectoderm in the post-naupliar region (ventral view). The short line connects sister cells symmetrically distributed at the lateral side of the midline. Open arrowhead marks the position of the proctodeum. Arrows point to cell nuclei located somewhat deeper to the external ectodermal layer. Stippled lines mark the median and posterior borders of the mandible anlagen. **Scale bars** are as indicated in each image in micrometer (µm).

A1: antenna 1; A2: antenna 2; MD: mandible.

In the post-naupliar region the cells of the ventral ectoderm are arranged in a bilateral symmetrical pattern (Fig. 5A and C). An unpaired longitudinal median row of cell nuclei (white small ovals in Fig. 5A and C) extends until the prospective region of the proctodeum (open arrowhead in Fig. 5C). At each side of the midline at least two longitudinal parallel rows of cells are regularly distributed in each body half (e.g. asterisks in Fig. 5C). Numerous divisions of these cells are observed (e.g. the short line in Fig. 5C). They all divide along the longitudinal axis. At the very posterior pole of the embryo small cells surround the proctodeum. Cell nuclei located somewhat deeper than the external ectodermal layer are observable in this region (arrows in Fig. 5C).

3.1.1.3 Nauplius stage 1

In the early phase as a free-living larva the nauplius maintains a spherical body, slightly elongated along the longitudinal axis (Fig. 6A). The surface of the ventral body is homogeneous with no protuberances nor invaginations (Fig. 6A). The naupliar appendages maintain a vestigial shape but they are all spread at the lateral side of the body and point laterally, slightly flexed to the posterior. The endopod and exopod of the mandible are protruded; the endopod is somewhat thicker than the exopod but equal in length (Fig. 6A).

In the later phase of the first larval stage, the nauplius has an oval shape, elongated along the longitudinal axis (Fig. 6B). The surface of the ventral body is still homogeneous except for one pair of short terminal spines which protrude under the cuticle at the posterior tip of the nauplius (arrowheads in Fig. 6B'). At the dorsal side the anlage of the carapace bulges out posterior to the insertion of the mandibles (arrow in Fig. 6B). The naupliar appendages have an elongated tubular shape and their distal spines have elongated (compare Fig. 6A with B). Antenna 2 has a thick and homogeneous proximal attachment and the exopod is longer and thinner than the endopod (Fig. 6B, C). The mandible is the shortest of the naupliar limbs; its exopod is thinner and shorter than its endopod (Fig. 6B, C and C'). The insertions of antenna 1 and 2 have an antero-lateral position and lie quite close to each other. The insertion of the mandible takes a postero-lateral location quite distant from the one of the antenna 2 (Fig. 6B, C and D).

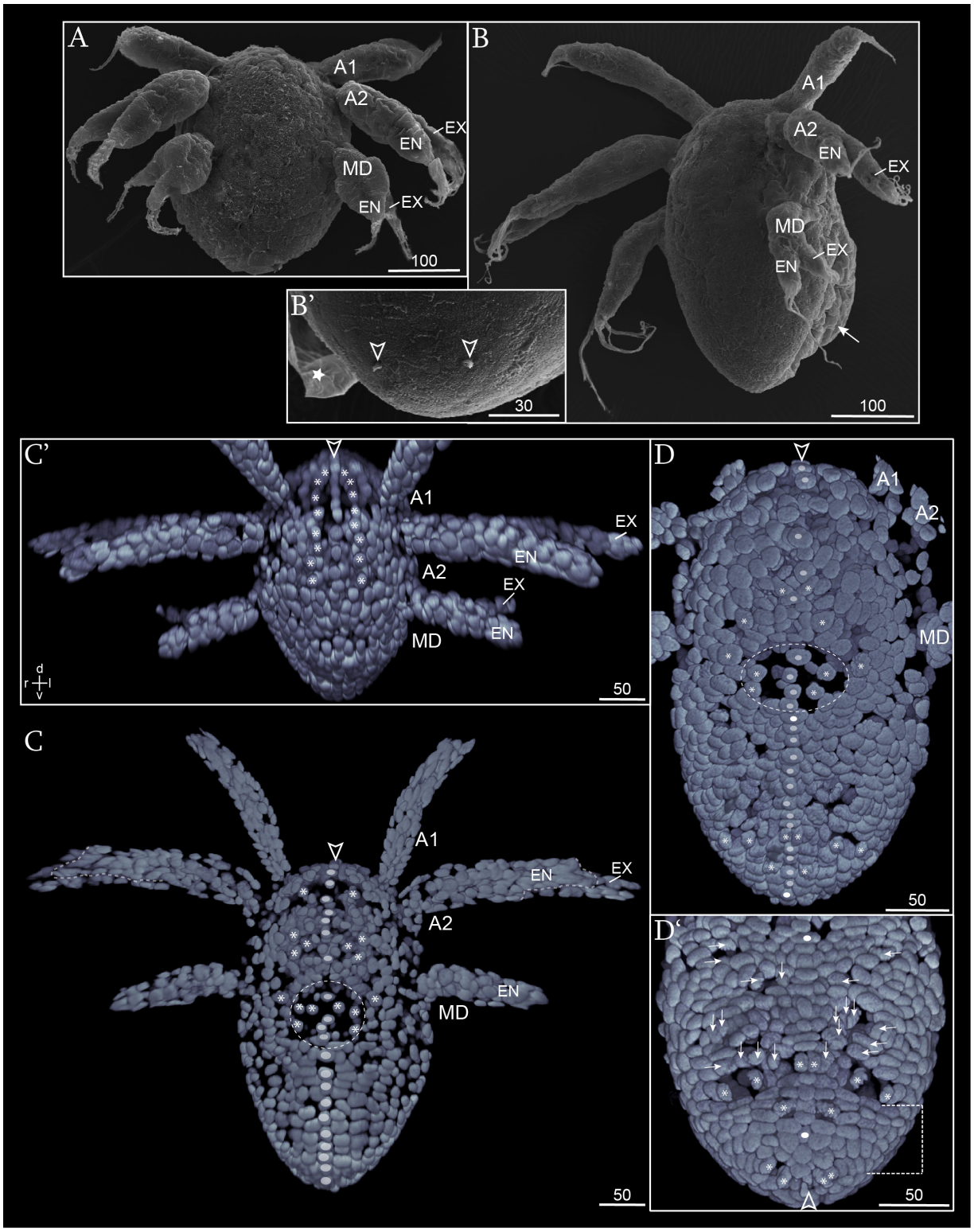

Fig. 6 - External morphology in *M. norvegica*, nauplius stage 1

A-**B' -** SEM micrographs. **A -** General overview of the early nauplius stage 1. The body has slightly elongated and the naupliar appendages have a vestigial shape. **B -** General overview of the late nauplius stage 1 (ventro-lateral view). The naupliar appendages have an elongated tubular shape. The arrow points to the posterior portion of the forming carapace at the dorsal side of the nauplius. **B' -** Detail of the posterior pole of the nauplius (ventral view). Open arrowheads mark one pair of short spines visible under the cuticle (this last marked by a star). The cuticle has been manually removed.

C-D' - Sytox-green staining: Imaris surpass mode: volume (blend). Asterisks mark cell nuclei symmetrically distributed in each body half. Small ovals mark unpaired cell nuclei in the median axis. **C -** General overview of the nauplius (ventral view). Open arrowhead points at the anterior end of the naupliar midline. A stippled circle marks the median region with a low density of cells anterior to the post-naupliar midline. Stippled lines mark the terminal border of the endopod in antenna 1. **C' -** View of the anterior pole of the nauplius (antero-ventral view). The distal portion of antenna 1 has been cut out of the image. Open arrowhead points at the anterior end of the naupliar midline. **D**, **D' -** View of the ventral side of a nauplius at the latest phase of the stage. White small ovals mark the anterior-most and the posterior-most cell nuclei of the post-naupliar midline. **D -** General overview (ventral view). The naupliar appendages have been cut out of the image; only their proximal insertions are visible. Open arrowhead points to the anterior-most portion of the naupliar midline. **D' -** Detail of the post-naupliar region (postero-ventral view). Arrows point at some example of cell nuclei in mitotic activity in the region lateral to the midline. The stippled square bracket marks the region with regular transversal rows arrangement anterior to the proctodeum (open arrowhead). **Scale bars** are as indicated in each image in micrometer (μm).

A1: antenna 1; A2: antenna 2; EN: endopod; EX: exopod; MD: mandible.

Ectodermal cell arrangement

At the anterior pole of the nauplius an increasing number of cell nuclei is visible dorsal to the insertion of antenna 1 (Fig. 6C, C'). From this region a median row of cell nuclei is visible, which extends ventrally, posterior to the region of the antenna 2 insertion (Fig. 6C). One lateral row of cell nuclei runs parallel to the median row at each side with a bilateral symmetrical distribution (asterisks in Fig. 6C'). Posterior to the mandible insertion a region with less concentrated nuclei is still observable signing the border to the post-naupliar region (stippled circle in Fig. 6C, D). Interestingly, these cells are also arranged in a bilaterally symmetric pattern (Fig. 6C, D). The median row of cells in the post-naupliar region has elongated (Fig. 6C). At least four lateral rows at the midline sides run parallel to each other and maintain a highly regular distribution of cell nuclei, some of them are visibly dividing along the longitudinal axis (Fig. 6C).

At the latest phase of the stage in the post-naupliar region the cells of the midline increase up to 16 (Fig. 6D, D'). Tangential cells divisions in medio-lateral direction are observable in the midline and lateral to this (e.g. asterisks in Fig. 6D, D'). At the lateral sides regular longitudinal rows cannot be easily followed any longer, being interrupted by scattered cell divisions (arrows in Fig. 6D'). This remarkable cell activity probably corresponds to the first differentiation of the first post-naupliar segments. At the posterior pole, symmetry is maintained and, anterior to the proctodeum (open arrowhead in Fig. 6D'), about six transversal rows with a regular bilateral distribution of cells are observable (stippled square bracket in Fig. 6D').

3.1.1.4 Nauplius stage 2

The body of the second nauplius has enlarged (Fig. 7A, B). The anterior pole has bulged and protrudes dorsally, while the posterior pole has squared and brings the terminal spines which have tilted out and point at the posterior (Fig. 7A-B'). The ventral surface is ploughed by transversal furrows which mark, from anterior to posterior, the anlagen of the labrum, of the paragnaths and of the first three post-naupliar limb pairs, i.e. maxillae 1 and 2 and thoracopods 1 (Fig. 7B, C and E). The carapace has grown and extends to the anterior covering part of the dorsal surface behind the antenna 1 insertion (filled arrowhead in Fig. 7A, B). The proximal portion of antenna 1 and 2 has become thicker. The endopod and the exopod of antenna 2 have elongated and become more robust, the exopod is still longer than the endopod (Fig. 7A, B). Noticeably, the mandible has not grown further.

At the latest phase of the stage the nauplius has elongated and broadened and the cuticle does not adhere tightly to the entire body surface (Fig. 7B). The anlage of the labrum, of the paragnaths and of the post-naupliar limbs can be recognized ventrally bulged under the cuticle (Fig. 7B). The telson anlage is defined in a bi-lobed shape and, at its terminal portion, the long median spine is flanked by additional short lateral ones (arrows in Fig. 7B'). The carapace extends to the anterior, encloses the lateral side of the nauplius and covers its dorsal surface until the posterior margin of the thoracopod 1 anlage, leaving the telson anlage bare at the posterior pole (Fig. 7B, B'). The proximal portion of antenna 2 is marked by two annular furrows plugged by tiny teeth (arrows in Fig. 7B). The more distal of the two furrows signs the border with the two distal rami. The distal portion of the mandible is reduced, its endopod and exopod have become thinner and cannot be distinguished any longer (Fig. 7B).

Ectodermal cell arrangement

In the earliest phase of the stage the anterior median row of cell nuclei still extends ventrally until the region posterior to the insertion of antenna 2 (comprised between the two filled arrowheads in Fig. 7C). Dorsally, at the level of antenna 1 insertions a transversal row of four elongated cell nuclei interrupts the extension of the median row (stars in Fig. 7D). Laterally, at the same height, cell divisions occur in a more basal ectodermal layer (short lines in Fig. 7D). In the surrounding, a regular distribution of median cell nuclei and bilaterally symmetrical ones is preserved (Fig. 7D). The median region with less crowded nuclei is still observable at the level of the mandible insertion and maintains a symmetric arrangement of cell nuclei (stippled circle in Fig. 7C).

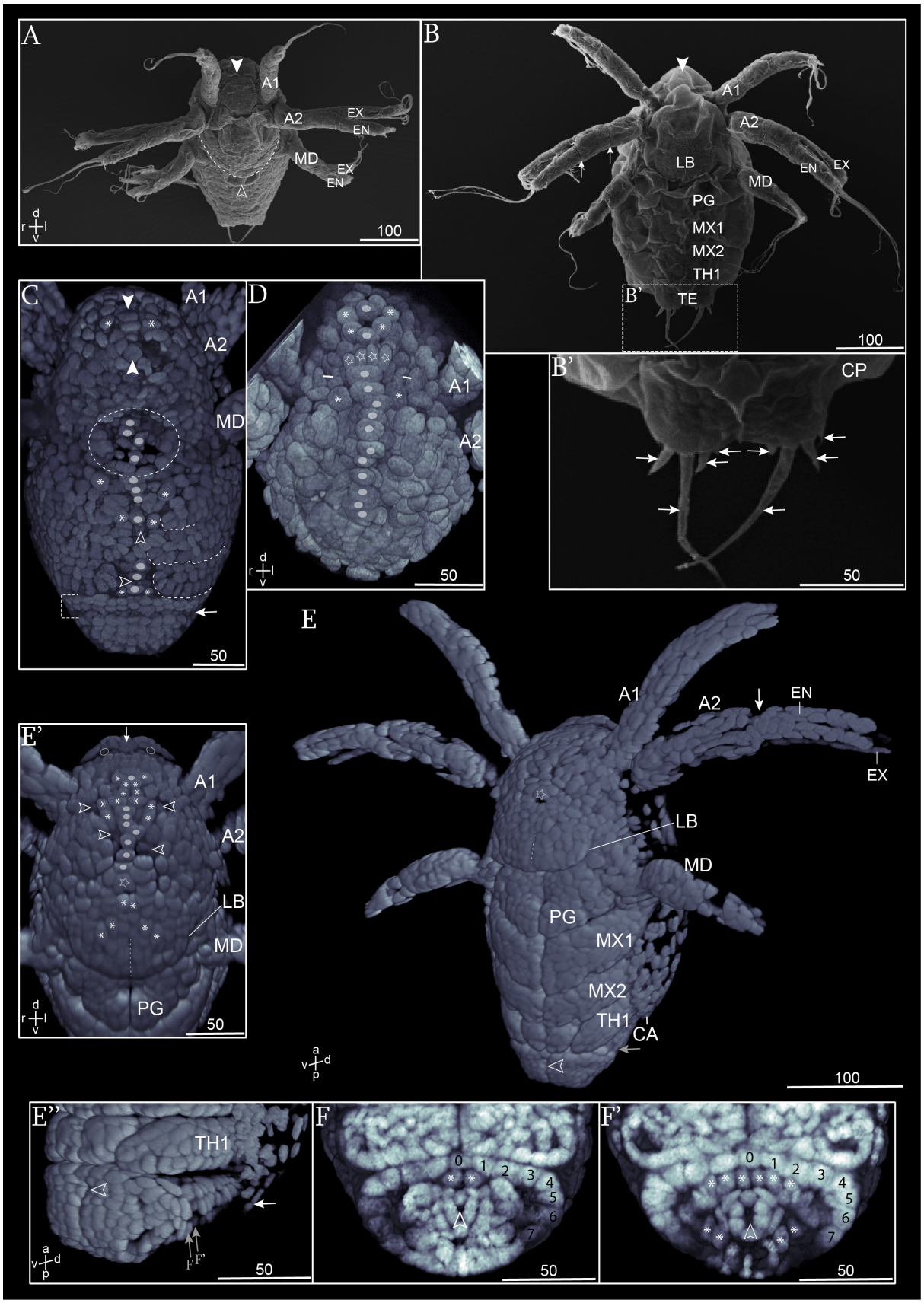

Fig. 7 - External morphology in *M. norvegica*, nauplius stage 2

A-**B' -** SEM micrographs. The filled arrowhead points at the anterior end of the carapace anlage. **A -** General overview of the early nauplius stage 2 (antero-ventral view). The open arrowhead points at the bud of the paragnaths anlage. A stippled line marks the posterior margin of the labrum anlage. **B -** General overview of the late nauplius stage 2 (ventral view). Arrows point at the annular rows of small dents in the proximal portion of antenna 2. **B' -** Detail of the telson anlage (ventral view). Arrows point at the terminal spines.

C-**F' -** Sytox-green staining. Imaris surpass mode: volume (blend), clipping plane in **D**, **F** and **F'** Asterisks mark cell nuclei symmetrically distributed in each body half. Ovals mark unpaired cell nuclei in the median axis. Short lines connect sister cells. **C -** General overview of the early nauplius stage 2 (ventral view). Filled arrowheads point at the anterior and posterior ends of the naupliar midline. Open arrowheads point to cell nuclei which lie in a more basal layer along the post-naupliar midline. Arrow points at the position of the ectoteloblasts' row. The stippled circle marks the median region comprised between the mandibles with a low density of cells. Stippled lines mark the postero-median borders of the post-naupliar limb anlagen. The stippled square bracket includes the three rows of cell nuclei (i.e. ectoteloblasts) anterior to the telson anlage. **D -** Detail of the apical pole of the early nauplius stage 2 (antero-ventral view). The extension of the antennae has been cut out from the picture, only their proximal attachments are viewed. Stars mark the transversal row of four cell nuclei which interrupt the anterior end of the naupliar midline. The cell nuclei marked as sister-cells lie in a more basal layer of the ectoderm. **E**-**E" -** View of the late nauplius stage 2. Star marks the median unpaired big cell nucleus at the posterior end of the naupliar midline. Stippled line marks a median furrow in the labrum. **E -** General overview (ventro-lateral view). A stippled line marks the median longitudinal furrow in the labrum. The white arrow points at the border between the proximal portion of A2 and its distal rami. The distal portion of the mandible has visibly reduced. The grey arrow marks the position of the ectoteloblasts row. Open arrowhead points at the opening of the proctodeum. **E' -** Detail of the apical pole (antero-ventral view). Arrow points at the antero-ventral margin of the carapace anlage. Small circles mark the position of the frontal organ anlagen. Open arrowheads point at cell nuclei located in a basal layer. A stippled line marks the median longitudinal furrow in the labrum. **E" -** Detail of the posterior pole (ventro-lateral view). Open arrowhead points at the opening of the proctodeum. White arrow points at the posterior end of the carapace. Grey arrows indicate the level of the applied clipping planes in **F** and **F'**. **F**, **F' -** Detail of the ectoteloblasts anlage (ventral view). The clipping plane has been applied transversally through the telson. **F** shows a more ventral plane then **F'**. Seven ectoteloblasts per each side (1-7) plus one median (0) are arranged in a semicircle in a bilateral symmetrical pattern. Open arrowhead points to the proctodeum. **Scale bars** as indicated in each image in micrometer (μm).

A1: antenna 1; A2: antenna 2; CA: carapace; EN: endopod; EX: exopod; LB: labrum; MD: mandible; MX1: maxilla 1; MX2: maxilla2; PG: paragnaths; TE: telson; TH1: thoracopod 1.

In the post-naupliar region, the midline is still visible but is not continuous any longer being interrupted by "holes" in which cell nuclei lie in a more basal layer (e.g. open arrowheads in Fig. 7C). The lateral side of the body is crossed by transversal rows of regularly distributed cells which prefigure the anlagen of the first three post-naupliar limbs (i.e. maxilla 1 and 2, and thoracopod 1). Their distal portion can be already distinguished adjoining the midline (stippled lines at the right side of Fig. 7C). Posterior to the anlage of thoracopod 1 three transversal rows of cell nuclei occur in a regular bilaterally symmetric pattern (stippled square bracket in Fig. 7C). From anterior, the nuclei of the third row are not clearly visible since they lay somewhat in a more basal layer (arrow in Fig. 7C). They probably represent the anlage of the ectoteloblasts and mark the border with the telson.

In a later phase of the stage the number of nuclei has noticeably increased (Fig. 7E). At the dorsal side the cell nuclei of the carapace show flattened and irregular shapes (Fig. 7E and E”). At the anterior pole, immediately ventrally to the carapace fold, the frontal organs pop out as a pair of small cylindrical lateral structures (small circles in Fig. 7E’). The ventral region comprised between antenna 1 and 2 insertions maintains a regular distribution of cell nuclei in a bilaterally symmetric distribution (Fig. 7E’). Some of the lateral cell nuclei have a more basal position in the ectodermal layer (e.g. open arrowheads in Fig. 7E’). Moreover one big nucleus marks the posterior end of the naupliar midline (star in Fig. 7E, E’). Posteriorly the anlage of the labrum has differentiated (Fig. E, E’). This is constituted by a group of small nuclei closely packed together in a symmetric arrangement and is defined at its posterior margin by a transversal furrow anterior to the level of the mandible insertion (Fig. 7E, E’). Medially the symmetric arrangement of the cell nuclei defines a median longitudinal furrow (stippled line in Fig. 7E, E’). Posterior to the labrum anlage the stomodeum is recognizable (data not shown). The paragnaths buds have protruded posterior to the mandibular sternal region (Fig. 7E, E’). Their tips meet at the median axis and point at the posterior (Fig. 7E, E’).

In the post-naupliar region, the ventral midline is not visible any longer, being covered by the anlagen of the post-naupliar limbs which protrude to the ventral, point to the posterior and meet their contra-lateral counterparts along the median axis (Fig. 7E). Posterior to the thoracopod 1, the telson is crossed by a longitudinal furrow which signs at its anterior end the opening of the proctodeum (open arrowhead in Fig. 7E, E”). Antero-dorsally to the telson anlage, covered by the extension of the thoracopod 1, a row of big cell nuclei surrounding the proctodeum is distinguishable (grey arrow in Fig. 7E and Fig. 7E”-F’). This represents the anlage of the ectoteloblasts ring which is constituted at this stage by ca. seven cells per side arranged in a semi-circle (n° 0-7 in Fig. 7F, F’). In some specimens, divisions of the ectoteloblasts have been observed along the transversal plane (data not shown). In the corresponding basal layer a regular distribution of mesodermal cell nuclei is observable (asterisks in Fig. 7F, F’). The ring of the teloblasts separates the telson from the anterior portion of the forming caudal papilla which extends further in an oblique plane postero-dorsally to the thoracomere 1 anlage, its dorsal end covered by the posterior fold of the carapace (white arrow in Fig. 7E”).

3.1.1.5 Metanauplius stage

The early phase of the metanauplius stage is characterized by a general increase in body size (Fig. 8A). The ventral side of the naupliar region is dominated by the presence of the labrum which protrudes to the ventral and points to the posterior (Fig. 8A). While antenna 1 and 2 have elongated, the mandible has reduced in length and retracted towards the median axis posterior to the labrum; its terminal portion has reduced to a short process which points to the lateral (asterisks in Fig. 8A). The paragnaths protrude as a median paired structure partially covered in its lateral portion by the mandible (Fig. 8A). The carapace has extended to the lateral sides of the larva (filled arrowheads in Fig. 8A) and taken a saddle-like shape. Short spines are visible at its anterior edge (stippled square in Fig. 8A). They have a bilateral symmetrical distribution. Posteriorly the carapace inserts dorsal to the attachment of thoracopod 1 (arrow in Fig. 8A).

In the post-naupliar region maxilla 1 and 2 and thoracopod 1 have elongated and protrude towards the postero-ventral side (Fig. 8A). Their contra-lateral tips still meet along the median axis while their proximal insertions are visibly elevated at the lateral side of the body (open arrowheads in Fig.7A). Thoracopod 1 is biramous with the endopod and the exopod being equal in length. At the posterior pole the anlage of the caudal papilla develops along the antero-posterior axis in an oblique dorso-ventral extension (square bracket in Fig. 8A). It is covered by the thoracopod 1 at its antero-ventral surface except for the telson which develops bare posterior to thoracopod 1 along the antero-posterior axis (Fig. 8A). The furcal spines have elongated (Fig. 8A).

In a later phase, the metanauplius has further increased in size (compare Fig. 8A and B). At the anterior pole dorsal to the insertion of antenna 1 the frontal organs have protruded (stippled circles in Fig. 8B) and bulge out ventrally to rim of the carapace (open arrowheads in Fig. 8C). The labrum has grown towards the postero-ventral side partially covering the mandibular sternite (Fig. 8B). The mandible has further reduced; its terminal tips point to the median axis (asterisks in Fig. 8B, C). The carapace has extended further and wraps the larva as a mantel (Fig. 8B). The spines at the top of the edge have elongated (open arrowheads in Fig. 8B). Additional short spines have grown all along its edge. All the three post-naupliar limbs have elongated further (Fig. 8B). The telson has also elongated and bears short additional lateral spines (open arrowheads in Fig. 8B').

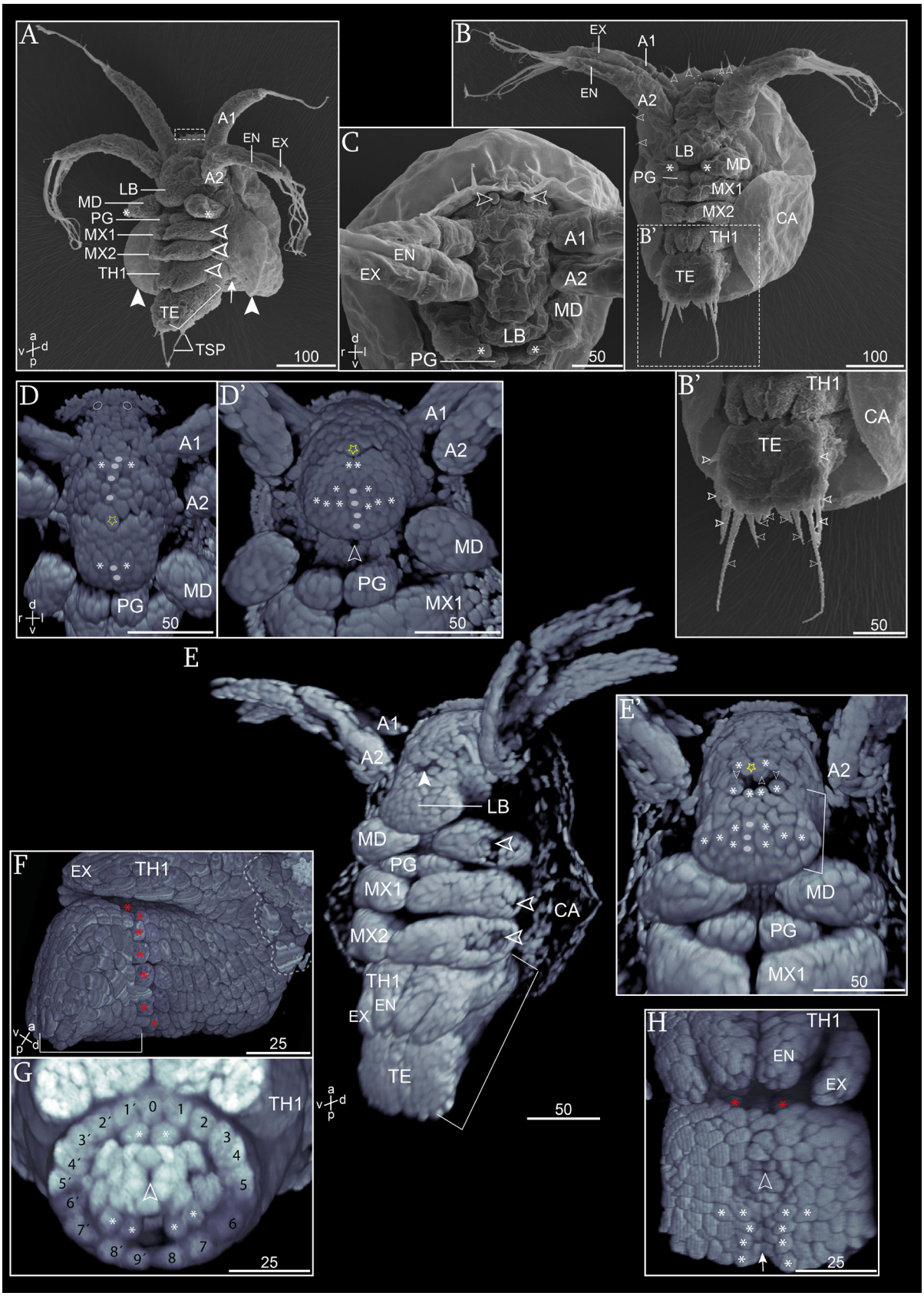

Fig. 8 - External morphology in *M. norvegica*, metanauplius stage

A-C - SEM micrographs. **A -** General overview of the early metanauplius stage (ventro-lateral view). Stippled square encloses the anterior short spines at the edge of the carapace. The mandibles are reduced;

their terminal tips (asterisks) point at the lateral. Arrow points to the posterior insertion of the carapace anlage. Filled arrowheads point at the lateral extension of the carapace. The caudal papilla (square bracket) extends obliquely partially covered by thoracopods 1. **B -** General overview of the late metanauplius stage (ventro-lateral view). Asterisks mark the distal tips of the mandibles. Open arrowheads point at the elongated spines at the anterior edge of the carapace. **B' -** Detail of the posterior pole of the late metanauplius (ventro-lateral view). Open arrowheads point at the furcal spines. **C -** View of the anterior pole of the late metanauplius (antero-ventral view). Open arrowheads point at the frontal organs. Asterisks mark the tip of the mandibles.

D-**H -** Sytox-green staining. Imaris surpass mode: volume (blend), clipping plane in **G**. Asterisks mark cell nuclei symmetrically distributed in each body half. Small ovals point at unpaired cell nuclei in the median axis. **D**, **D' -** View of the naupliar region of the early metanauplius (antero-ventral view in **D**; ventral view in **D'**). The yellow star marks the posterior-most cell nucleus at the posterior end of the naupliar midline, anterior to the labrum. **D -** Small circles mark the position of the frontal organs. **D' -** Open arrowhead points to a median hole anteriorly in the mandibular sternite. **E -** General overview of the late metanauplius stage (ventro-lateral view). A filled arrowhead points at the region anterior to the labrum. Open arrowheads point at the regions with a less dense concentration of cell nuclei at the lateral side of the mandible, maxilla 1 and maxilla 2. A square bracket marks the extension of the caudal papilla. **E' -** Detail of the naupliar region of the late metanauplius (ventral view). The yellow star marks a median big cell nucleus anterior to the labrum. Open arrowheads point at cell nuclei located in a more basal layer. Square bracket marks the extension of the labrum. **F -** Detail of the posterior pole of the late metanauplius (lateral view). The red asterisks mark the lateral extension of the ectoteloblasts ring. Stippled line marks the postero-lateral end of the carapace. **G -** Detail of the distribution of the ectoteloblasts (0-9/9´) (ventral view). Note they have not yet reached their final number and the y do not have a symmetrical distribution (i.e. in number of nine (9`) on the right and of eight (8) on the left side of the animal). Open arrowhead points to the lumen of the hindgut anlage. **H -** Detail of the ventral extension of the telson (ventral view). Open arrowhead points to the opening of the proctodeum. Arrow points at the posterior end of the median groove. The two red asterisks mark the position of the two first pair of ectoteloblasts. **Scale bars** as indicated in each image in micrometer (µm).

A1: antenna 1; A2: antenna 2; CA: carapace; EN: endopod; EX: exopod; LB: labrum; MD: mandible; MX1: maxilla 1; MX2: maxilla2; PG: paragnaths; TE: telson; TH1: thoracopod 1; TSP: terminal spine.

Ectodermal cell arrangement

At the anterior pole a regular bilaterally symmetric distribution of cell nuclei is maintained. A longitudinal median row of cell nuclei extends posterior to the insertion of antenna 1 and one big median cell nucleus marks its posterior end anterior to the labrum (yellow star in Fig. 8D, D' and E'). The number of cells of the labrum has increased and a regular distribution of cell nuclei occurs at its posterior pole where a longitudinal row is flanked by lateral symmetrical ones (Fig. 8D, D'). Posterior to the labrum, set between the mandibles and anterior to the paragnaths, the cell nuclei constituting the mandibular sternite also show a regular distribution. Right at their border with the labrum arrangement (open arrowhead in Fig. 8D').

In a later phase of development the presence of a median area with a lower concentration of cell nuclei which resembles a hole characterizes the region comprised between the antenna 2 insertions, right anterior to the labrum anlage (filled arrowhead in Fig. 8E). Cell nuclei in its surrounding are distributed in a symmetrical arrangement and big cell nuclei are visible in a more basal layer (open arrowheads in Fig. 8E'). The labrum has elongated and broadened

maintaining a regular distribution of cell nuclei (Fig. 8E'). The lateral side of the mandible and of both the maxillae 1 and 2 is characterized by a region with nuclei distributed with lower density, suggesting a "hole" (open arrowheads in Fig. 8E). While in the mandible this is located in a median position between its insertion and its distal tips, in maxilla 1 and 2 this takes a more proximal position. Posteriorly and partly dorsally to thoracopod 1 the caudal papilla has elongated (square bracket in Fig. 8E and Fig. 8F). The number of ectoteloblasts has increased and now these cells form a complete ring around the forming hindgut (red asterisks in Fig. 8F and H and Fig. 8G). The ectoteloblast ring separates the anterior prospective which provides material for the left-over post-naupliar segments, from the terminal telson anlage (square bracket in Fig. 8F). Active divisions of the ectoteloblasts are observable along the tangential plane which brings the ectoteloblast ring to a final number of nine cells per side plus the antero-ventral unpaired median one (Fig. 8G). The divisions happen in a bilaterally symmetrical pattern but at slightly asynchronous intervals (data not shown).

The telson has enlarged and elongated (square bracket in Fig. 8F). In its ventral extension the longitudinal median furrow has enlarged to a groove (arrow in Fig. 8H) and is now flanked by longitudinal rows of cell nuclei symmetrically distributed at its sides (asterisks in Fig. 8H). The opening of the proctodeum lies at the anterior end of the groove (open arrowhead in Fig. 8H).

3.1.1.6 Calyptopis stage

A general increase in body size is noticeable at this stage (Fig. 9A). The antennae have elongated and proximally become more robust (Fig. 9A, B). The mandible and the paragnath have differentiated and together enclose the posterior margin of the labrum (Fig. 9A, B). The labrum has grown further and enlarged at its posterior margin. The frontal organs have protruded further taking a cylindrical shape (filled arrowheads in Fig. 9A). The carapace has enlarged, and its edge at the apical pole partially covers the frontal organs (Fig. 9A). The maxilla 1 and 2 and the thoracopod 1 have elongated and detached from the midline, and point (Fig. 9A, B). They all have become segmented (Fig. A, B), each segment bearing several setae (Fig. 9A). The caudal papilla has also become longer and the anlage of the anus has formed at the ventral surface of the telson (open arrowhead in Fig. 9A).

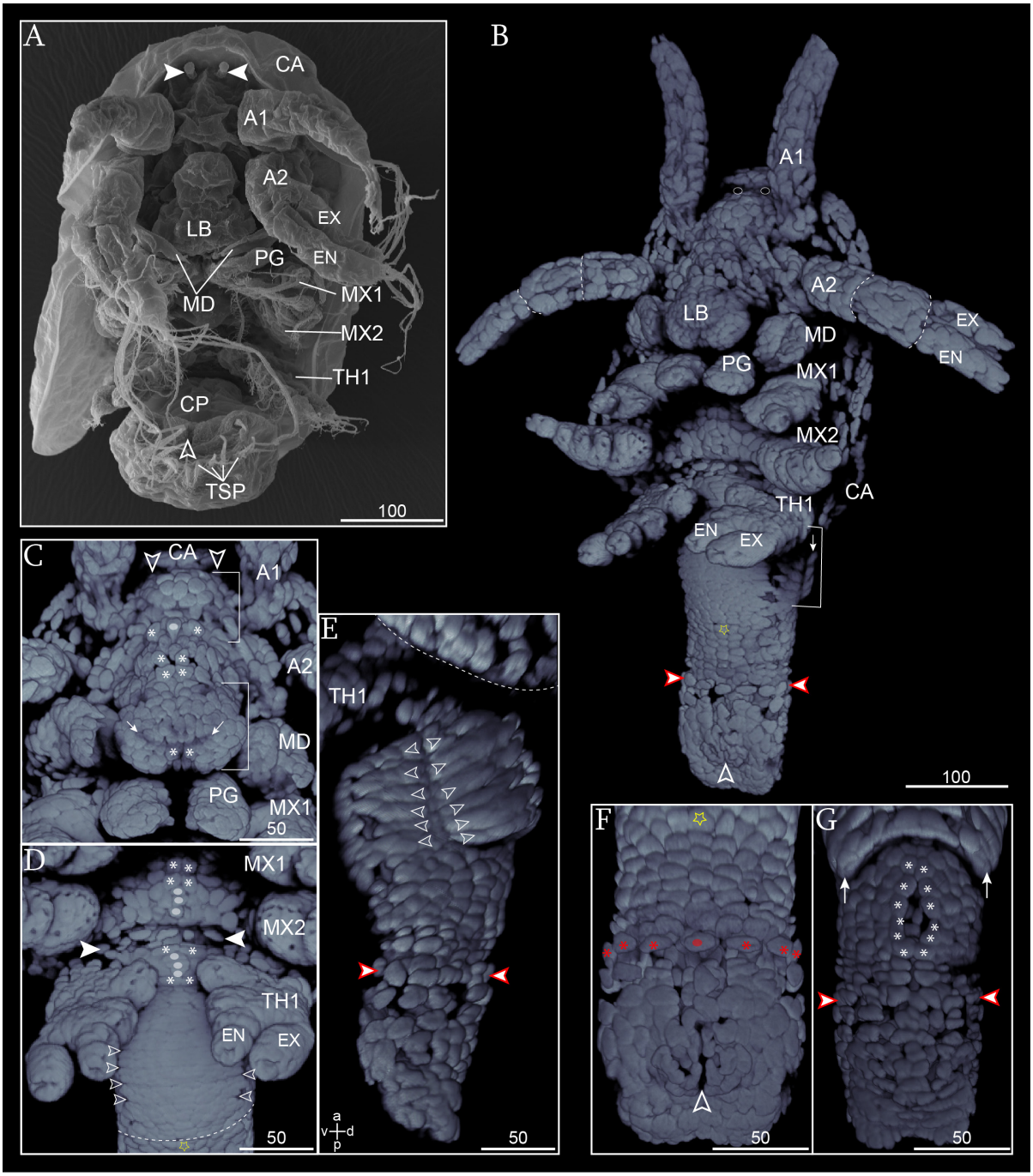

Fig. 9 - External morphology in *M. norvegica*, calyptopis stage

A - SEM micrograph. General overview of the larva (ventral view). Filled arrowheads point at the frontal organs. Open arrowhead points at opening of the proctodeum.

B-**G -** Sytox-green staining. Imaris surpass mode: volume (blend). Asterisks mark cell nuclei symmetrically distributed in each body half. Small ovals point at unpaired cell nuclei in the median axis. The median yellow star in **B**, **D** and **F** labels one median cell nucleus taken as a marker of the posterior region of the growth zone. The red framed arrowheads in **B**, **E** and **G** indicate the level of the ectoteloblast ring. **B -** General overview of the calyptopis 1 stage (ventro-lateral view). Small circles mark the position of the frontal organs. Stippled lines in antenna 2 mark the segmental borders. The square bracket marks the extension of the anterior region of the growth zone. Arrow marks the fold of the corresponding tergal plate. Open arrowhead marks the position of the opening of the proctodeum. **C -** Detail of the naupliar region (ventral view). Open arrowheads point at the position of the frontal organs. Arrows point at the lateral sides of the transversal furrow at the postero-ventral side of the labrum. The upper square bracket

includes the anterior-most portion of the naupliar region while the lower one includes the tip of the labrum. **D -** Detail of the sternal surface posterior to maxilla 1 segment and of the anterior region of the growth zone (ventral view). Filled arrowheads point at the side of the transversal row of yolk-rich cells posterior to the maxilla 2 insertion. Open arrowheads point at the lateral ends of forming furrows between cell rows in the anterior region of the growth zone. The transversal stippled line marks the posterior border of the anterior region of the growth zone. **E -** View of the caudal papilla (lateral view). Open arrowheads mark the position of the putative segment anlagen. Note the tergal plate at this level is posteriorly lifted. Stippled line marks the posterior border of the carapace. **F -** View of the posterior region of the growth zone and of the telson (ventral view). The cell nuclei forming the ring of the ectoteloblasts are marked in red. Open arrowhead points at the aperture of the proctodeum. **G -** View of the posterior region of the growth zone and of the telson (dorsal view). Arrows point laterally at the posterior fold of the tergal plate. Asterisks mark single cell nuclei surrounding a dorsal hole. **Scale bar** are as indicated in the image in micrometer (µm).

A1: antenna 1; A2: antenna; CA: carapace; EN: endopod; EX: exopod; LB: labrum; MD: mandible; MX1: maxilla 1; MX2: maxilla2; PG: paragnaths; TH1: thoracopod 1; TSP: terminal spine.

Ectodermal cell arrangement

In the naupliar region a regular distribution of cell nuclei is maintained (Fig. 9C). Here three main regions can be distinguished: one apical comprised in between the insertions of the antennae 1, which is constituted by big roundish cell nuclei forming a median bulge (upper square bracket in Fig. 9C); one medial comprised between the insertions of the antennae 2, which is formed by smaller cell nuclei (e.g. asterisks in Fig. 9C); one postero-ventral, which covers the labrum (lower square bracket in Fig. 9C). This last extends posteriorly partially covering the paragnaths (Fig. 9B, C). At its posterior end the labrum is carved by a transversal furrow (pointed by the two arrows in Fig. 9C) marking the border with a bi-lobed distal most tip (Fig. 9C).

In the post-naupliar region the prospective sternal region comprised between the attachments of the post-naupliar limbs shows a regular distribution of cell nuclei (Fig. 9D). Posterior to the level of maxilla 2 one transversal row can be distinguished for its composition of elongated cell nuclei distributed at a lesser concentration than the surrounding ones (comprised between the two filled arrowheads in Fig. 9D). This is probably due to a higher amount of cytoplasm in these cells than in the surrounding ones. In the caudal papilla, the region comprised between the ectoteloblasts and the posterior border of thoracomere 1 can be subdivided into two parts (Fig. 9B and D, E). The anterior one is formed by transversal cell rows closely packed together (square bracket in Fig. 9B and anterior to the stippled line in Fig. 9D). Transversal furrows start to form here signing the beginning of differentiation of the posterior segment anlagen (open arrowheads in Fig. 9D, E). This ventral region corresponds dorsally to a segmented tergal plate anlage (arrow in Fig. 9B and open arrowheads in Fig. 9E). The more posterior region is formed by cell nuclei in a lesser amount and regularly distributed (Fig. 9B

and F, G). This regularity is preserved at the dorsal side except for a median "hole" separating the dorsal-most cell nuclei (asterisks in Fig. 9G). The ectoteloblasts' ring (Fig. 9B, E-G) is composed of 19 cells (i.e. 9 per side +1 median at the ventral side). In the telson the opening of the proctodeum is signed by a median longitudinal aperture (open arrowhead in Fig. 9B and F). This is surrounded by cell nuclei with an irregular shape which form a small bulge anterior to the distal most tip of the telson and represent the anlage of the anus (Fig. 9B and F).

3.1.2 Nervous system development

3.1.2.1 Embryonic stage 1

Axogenesis

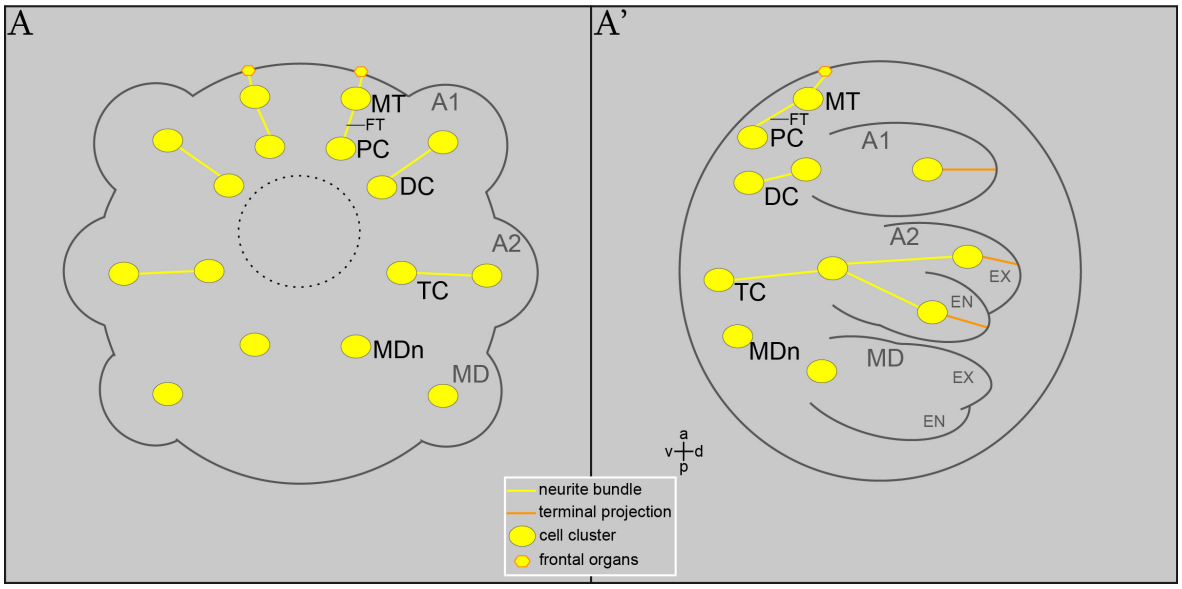

Fig. 10 - *M. norvegica*, embryonic stage 1

Schematic illustration of the distribution of differentiated neural structures (ventral view in **A**; lateral view in **A'**). The region of the stomodeum is marked by black circular line.

A1: antenna 1; A2: antenna 2; DC: deutocerebrum; EN: endopod; EX: exopod; FT: frontal tract; MD: mandible; MDn: mandibular neuromere; MT: medulla terminalis; PC: protocerebrum; TC: tritocerebrum.

The first positive α-tubulin signal specifically labelling differentiating neural structures has been detected in embryonic stage 1. Because of the weak signal and profuse unspecific background staining, no CLSM documentation was performed, therefore the analysis is based on epifluorescence data alone (Fig. 11). Positive specific α-tubulin signal is detected in the naupliar region, while in the post-naupliar region no specific signal is observable (Fig. 11A).

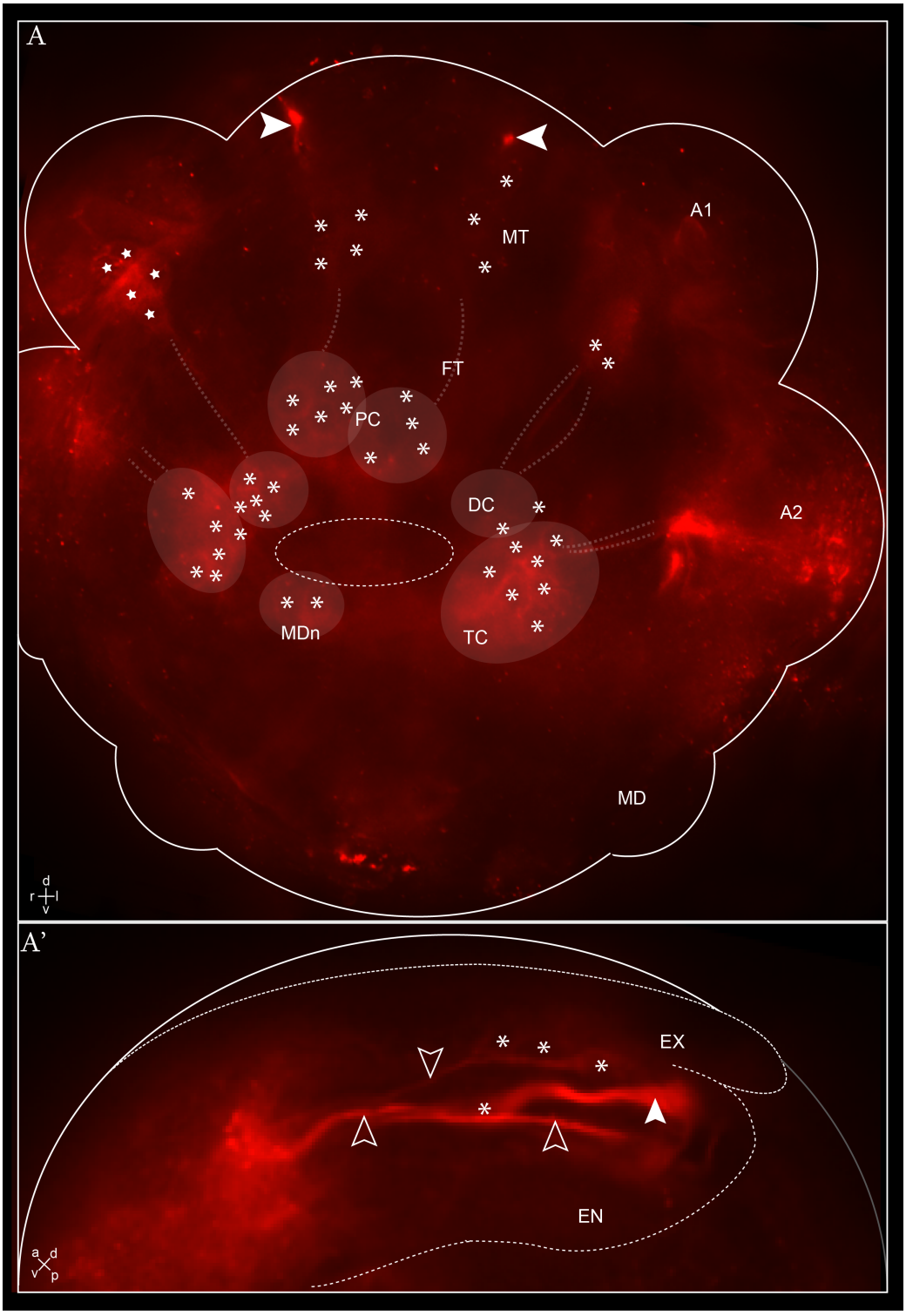

Fig. 11 - Axogenesis in *M. norvegica*, embryonic stage 1

Anti-ac-α-tub labelling. Epifluorescence microscopic image. Asterisks point at single cell bodies. **A -** General overview of the embryo (antero-ventral view). The stippled oval marks the region of the stomodeum. Filled arrowheads point at the frontal organ anlagen. The cell clusters of the naupliar neuromeres are marked by transparent oval areas. The axons spanned between the central neuromeres and the periphery are underlined by stippled transparent lines. **A' –** View of the antenna 2 anlage (postero-lateral view). (The border of the antenna is marked by a stippled line. At the distal tip of the limb bud bipolar neurons are visibly stained. Open arrowheads point at axons forming the antennal nerve. The filled arrowhead points at a terminal spine.

A1: antenna 1; A2: antenna 2; DC: deutocerebrum; EN: endopod; EX: exopod; FT: frontal tract; MD: mandible; MDn: mandibular neuromere; MT: medulla terminalis; PC: protocerebrum; TC: tritocerebrum.

Clusters of cell somata surround the area of the stomodeum (transparent oval areas in Fig. 11A). They represent the anlagen of the brain ganglia; from anterior to posterior: the protocerebrum, the deutocerebrum, the tritocerebrum and the mandibular neuromere anlagen.

In the protocerebral region two paired cell clusters are distinguishable: one posterior which represents the anlage of the protocerebrum, and one anterior in a more dorsal position than the protocerebrum, which represents the anlage of the medulla terminalis (Fig. 11A). These two cell clusters are connected to each other via a feeble neurite bundle which represents the anlage of the frontal tract (Fig. 11A). At the anterior pole of the embryo, an intensely stained paired structure connected to the medulla terminalis anlage is visible and corresponds to the anlage of the frontal organ (filled arrowheads in Fig. 11A).

Antero-laterally to the stomodeum at the level of the antenna 1 bud insertion, a small cluster of labelled cells represents the deutocerebrum anlage. Two neurite bundles extend from this region antero-laterally into the antenna 1 anlage forming the segmental nerve anlage (Fig. 11A'). Slightly posterior, lateral to the stomodeum the tritocerebrum anlage is represented by another cell cluster, and a thin neurite bundle forms the anlage of the segmental nerve running laterally into the antenna 2 bud (Fig. 11). At the level of the insertion of antenna 1 and 2 intense signal of α-tubulin is detected and can be assigned in some cases to clusters of cell somata (e.g. asterisks in Fig. 11A'). A specific high signal of α-tubulin is visible within antenna 2 anlage in its distal portion (Fig. 11A'). Here two to three neurites run into each of the two rami and reach their terminal tips (open arrowheads in Fig. 11A'). Cell somata intercalated along the neurites extension (bipolar neurons) are observable (asterisks in Fig. 11A'), some of which are distally connected with the limb terminal sensory spine. At the posterior end of the stomodeum in the region enclosed between the mandible bud insertions, some cell somata are stained and indicate the presence of the anlage of the mandibular neuromere (Fig. 11A). No neurite bundle is detectable in this region.

Serotonin-like expression pattern

No data on SL-ir structures have been successfully performed for this stage.

3.1.2.2 Embryonic stage 2

Axogenesis

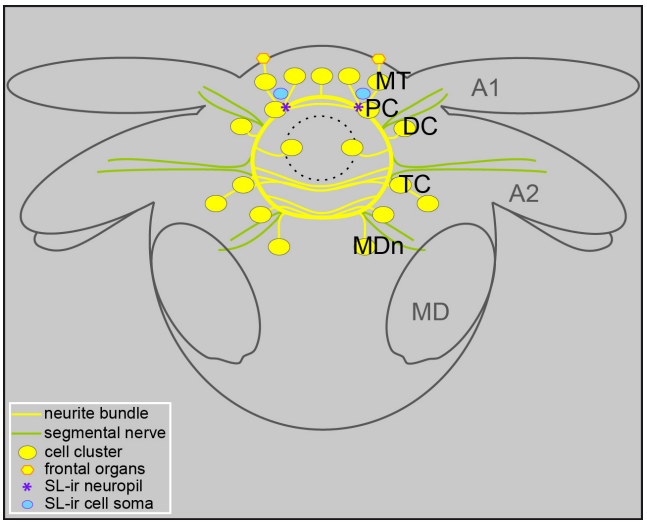

Fig. 12 - *M. norvegica*, embryonic stage 2

Schematic illustration of the distribution of differentiated neural structures (ventral view). The region of the stomodeum is marked by a black stippled circle.

A1: antenna 1; A2: antenna 2; DC: deutocerebrum; MD: mandible; MDn: mandibular neuromere; MT: medulla terminalis; PC: protocerebrum; TC: tritocerebrum.

In the naupliar region the nervous system has further differentiated (Fig. 13). Here the primordial scaffold of the brain is visibly stained (Fig. 13A, B). The proto-, deuto- and tritocerebrum anlagen are connected to each other and to the more posterior mandibular neuromere anlage by several neurite bundles and the circumesophageal nerve ring has formed (Fig. 13A, B). In the protocerebral region the anlage of the frontal tract has thickened (Fig. 13A, B). The medulla terminalis has increased in volume (stippled circles in Fig. 13A). The frontal organ anlage (filled arrowheads in Fig. 13A) is connected to a group of bipolar neurons in the medulla terminalis which identify the frontal organ center (see Discussion). These connect, on the one hand, the frontal organ via the frontal organ nerve, and, on the other hand, the protocerebrum contributing to the frontal tract anlage (see below). At the level of the protocerebrum the pre-oral commissure has formed, constituting the anterior transverse connection of the circumesophageal nerve ring (Fig. 13A-C). Its architecture can be further resolved. It consists of one anterior thicker and one posterior thinner neurite bundle (Fig. 13A, B).

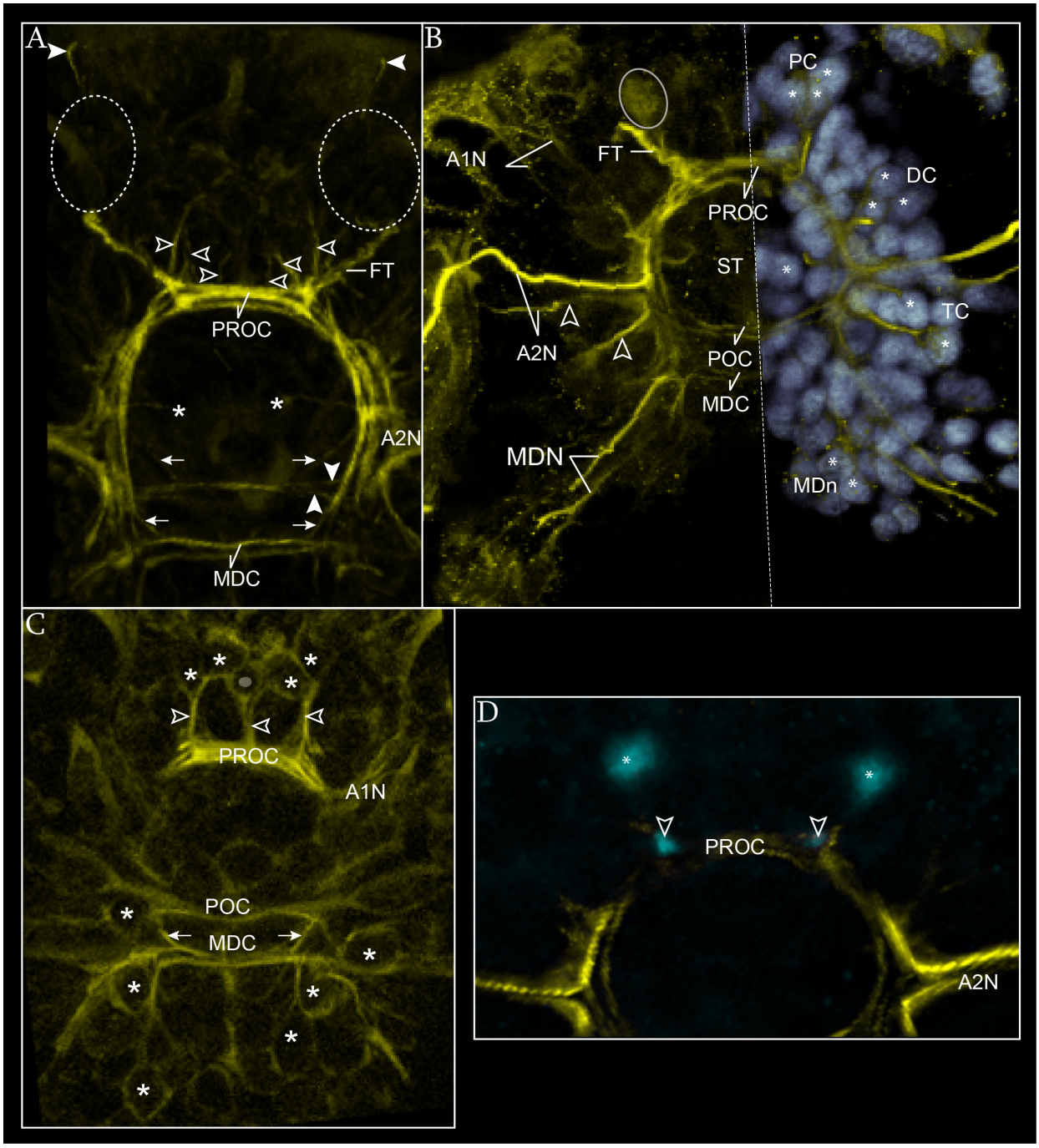

Fig. 13 - Axogenesis in *M. norvegica*, embryonic stage 2

Anti-ac-α-tubulin labelling in yellow. Hoechst staining in grey. Anti-serotonin-like labelling in light blue. CLSM image stack. Imaris surpass mode: volume; clipping plane. **A -** View of the nervous system in the naupliar region (ventral view). Filled arrowheads point at the frontal organs anlage. Stippled circles mark the position of the medulla terminalis. Open arrowheads point at neurites which connect anterior lateral clusters of the protocerebrum to the pre-oral commissure. Asterisks mark single cell somata located medially within the nerve ring and connected with the nerve ring in the region between the deutocerebral and tritocerebral regions. Arrows point to anterior neurites contributing to the formation of the post-oral commissure (upper) and to the mandibular commissure (lower). Filled arrowheads point at the two separate neurite bundles of the post-oral commissure. **B -** View of the nervous system in the naupliar region (ventral view). The image represents a combination of two different snapshots of the same object; the stippled line marks the border between the two. **Left image -** The channel for the nucleic staining is turned off. The circle marks the SL-ir positive cell soma in the protocerebral region (compare with **D**).

Open arrowheads mark the path of the posterior neurite bundle forming the segmental nerve of antenna 2. **Right image -** Asterisks point at single cell nuclei connected to the central axonal scaffold of the naupliar region. **C -** Detail of the dorsal components of the naupliar commissures (ventral view). Asterisks mark paired cell somata connected with the commissural anlagen. The small oval points at an unpaired median cell soma. Open arrowheads point at neurite bundles which connect clustered cell somata to the commissural anlagen. Arrows point at the anterior component of the mandibular commissure anlage. **D -** Distribution of SL-ir structures (ventral view). Asterisks mark the two anterior SL-ir cell somata. Open arrowheads point at SL-ir forming neuropil at the lateral side of the pre-oral commissure.

A1: antenna 1; A2: antenna 2; A1N: antenna 1 nerve; A2N: antenna 2 nerve; DC: deutocerebrum; FT: frontal tract; MD: mandible; MDC: mandibular commissure; MDN: mandibular nerve; MDn: mandibular neuromere; PC: protocerebrum; POC: post-oral commissure; PROC: pre-oral commissure; ST: stomodeum; TC: tritocerebrum.

Anterior to the pre-oral commissure a medio-ventral cell cluster is visible (Fig. 13B, C). This is composed of two distinct groups of cells: one paired lateral and one unpaired median, each constituted by one or two neurons connected to the commissural anlage via a single short neurite (open arrowheads in Fig. 13 A and C). Longitudinal axonal connections between the protocerebrum to the more posterior neuromere anlagen form the connectives of the circumesophageal nerve ring (Fig. 13A, B). Also in the region of the deutocerebrum one separate cell cluster can be distinguished (right image in Fig. 13B) connected via short neurites to the nerve ring. The anlage of the segmental nerve of antenna 1 is composed of two weakly α-tubulin-stained neurite bundles which run from the dorsal margin of the connective to the insertion of antenna 1 (left image in Fig. 13B). Proximally, they lie very close together but then they separate to describe a loop before meeting again further distally to enter the antenna 1 together (left image in Fig. 13B). Slightly more posterior along the connective, at the border of the deutocerebral and the tritocerebral neuromeres a single soma located at the medio-ventral side of the nerve ring sends a thin neurite laterally into the ring (asterisks in Fig. 13A).

The root of the segmental nerve anlage of antenna 2 is located anterior to the level of the post-oral commissure (Fig. 13A, B). The segmental nerve anlage is composed of two main neurite bundles. The anterior-most is thicker and is connected with the anterior regions of the nerve ring (Fig. 13B). The posterior-most is thinner and is connected with a distinct cluster of cell somata located posterior to the segmental nerve anlage (right image in Fig. 13B). One neurite bundle runs from this posterior cluster antero-medially into the nerve ring where it flexes and enters the antenna 2 anlage contributing the formation of the posterior portion of the segmental nerve (open arrowheads in the left image in Fig. 13B). The post-oral commissure of the nerve ring has been established (Fig. 13A-C). This is composed of feebly stained neurites grouped into two neurite bundles (Fig. 13A, B). The anterior neurite bundle receives

neurites from the more anterior regions of the brain (upper arrows in Fig. 13A) while the posterior one is formed by neurites (filled arrowheads in Fig. 13A) spanned between two distinct tritocerebral cell clusters at the dorso-lateral side of each hemi-neuromere (Fig. 13C). The connectives of the nerve ring run more posteriorly in the region of the mandibular neuromere (Fig. 13A, B). At this level the mandibular commissure anlage has formed (Fig. 13A-C) and is constituted by two transversal neurite bundles. The anterior neurite bundle collects also fibers from the more anterior neuromeres (lower arrows in Fig. 13A) while the posterior is formed exclusively by neurites spanning between the two hemi-neuromeres (Fig. 13C). Distinct clustered somata connected to the commissure anlage are located directly at its lateral side in dorsal position and more posteriorly median to the anlage of the segmental nerve (Fig. 13C). The mandibular nerve anlage consists of two distinct neurite bundles that run postero-laterally from the lateral ends of the mandibular commissure and enter the mandible anlage (left image in Fig. 13B).

At the post-naupliar region no neural differentiation has occurred yet.

Serotonin-like expression pattern

The first evidence of SL-ir structures has been observed at this stage of development. One paired cell soma in the protocerebral region is stained (asterisks in Fig. 13D). This is located dorsal to the anterior cluster of the protocerebrum anlage and it is connected to the frontal tract anlage slightly dorsal to the level of its connection with the pre-oral commissure anlage (circle in Fig. 13D). Positive signal is also detected right at the lateral side of the pre-oral commissure anlage defining the beginning of the formation of a neuropilar layer (open arrowheads in Fig. 13D).

3.1.2.3 Nauplius stage 1

Axogenesis

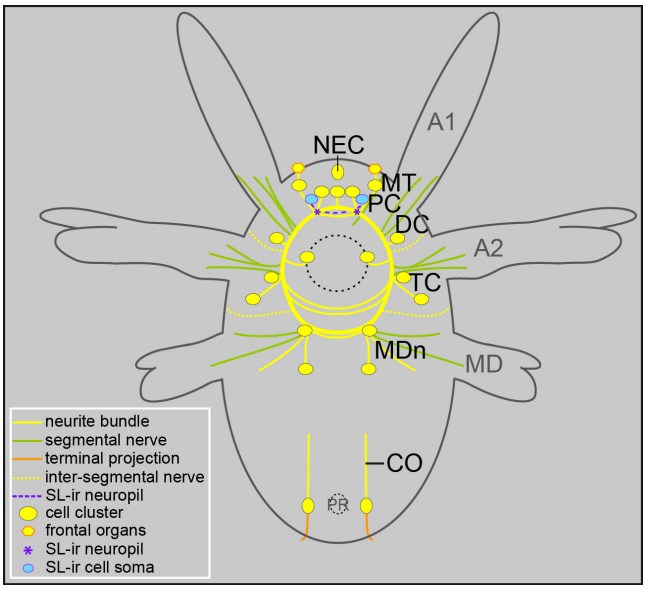

Fig. 14 - *M. norvegica*, embryonic stage 2

Schematic illustration of the distribution of differentiated neural structures (ventral view). The region of the stomodeum is marked by a black stippled circle.

A1: antenna 1; A2: antenna 2; CO: connective; DC: deutocerebrum; MD: mandible; MDn: mandibular neuromere; MT: medulla terminalis; NEC: nauplius eye complex; PC: protocerebrum; PR: proctodeum; TC: tritocerebrum.

The first nauplius stage is characterized by a general increase of the size of the brain neuromeres and the growth of the diameter of the neurite bundles forming the circumesophageal nerve ring (Fig. 15A). Single cell somata connected with the nerve ring are still observable in the same position as in the previous stage (asterisks in Fig. 15A). In the protocerebral region at the anterior pole of the nauplius the medulla terminalis has increased its volume extending more into the region dorsal to the antenna 1 insertion (Fig. 15B). The frontal organ maintains a rudimental shape and the frontal organ nerve has become a neurite bundle thicker than in the previous stage (filled arrowheads in Fig. 15B). Dorsally to the protocerebral medio-ventral cell cluster, in correspondence with the ectodermal midline cell row (see the ectodermal cell arrangement of nauplius stage 1 in the previous section) but in a more basal layer, the anlage of the nauplius eye complex appears as a median cluster of four cell somata (small circles in Fig. 15C). These cells show a diffuse α-tubulin-positive signal but no distinct neurites are observable connecting the central protocerebral neuropil. A regular distribution of the cells anterior and lateral to the mentioned anlage is observable (e.g.

asterisks in Fig. 15C). Both neurite bundles forming the pre-oral commissure have become thicker (Fig. 15A, B). The anterior neurite bundle now takes a more dorsal position and keeps the connection with the frontal tract anlage (Fig. 15B). In the deutocerebral region the anlage of the segmental nerve of antenna 1 is formed by two neurite bundles (Fig. 15A and D). The anterior one is sub-divided into two branches which run closely together in their proximal path and bifurcate before entering antenna 1 (Fig. 15A). The posterior component runs in parallel to the previous and enters antenna 1 at its posterior margin. Intercalated between the anlagen of antenna 1 and 2 segmental nerves the anlage of inter-segmental nerve 1 has formed (arrow in Fig. 15D). It runs in antero-lateral direction to the lateral shield comprised between the two antennae. In the tritocerebral region one additional anterior neurite bundle has formed in antenna 1 nerve (open arrowhead in Fig. 15D).

The neurites of the post-oral and of the mandibular commissures are still distributed into two separate neurite bundles, each has increased its diameter (Fig. 15A). Postero-dorsally to the mandibular commissure one median big cell soma has formed (lower small oval in Fig. 15A). The mandibular nerve anlage is formed by three distinct thin neurite bundles (Fig. 15A and D). The most anterior one runs to the ventro-lateral side of the mandible insertion (Fig. 15A and D). The most posterior bundle runs parallel to the previous and extends into an elongated brightly stained oblique structure which embraces the posterior margin of the mandible at its insertion (encircled by a stippled line in Fig. 15D). This last may represent the anlage of a muscle. The intermediate bundle runs straight to the lateral from the commissural anlage to the antero-dorsal margin of the mandible (Fig. 15A and D). Brightly stained structures are visible at the level of the insertion of each of the naupliar limbs, at their anterior and posterior margin (filled arrowheads in Fig. 15D). They probably represent the anlagen of muscle attachment sites e.g. tendons.

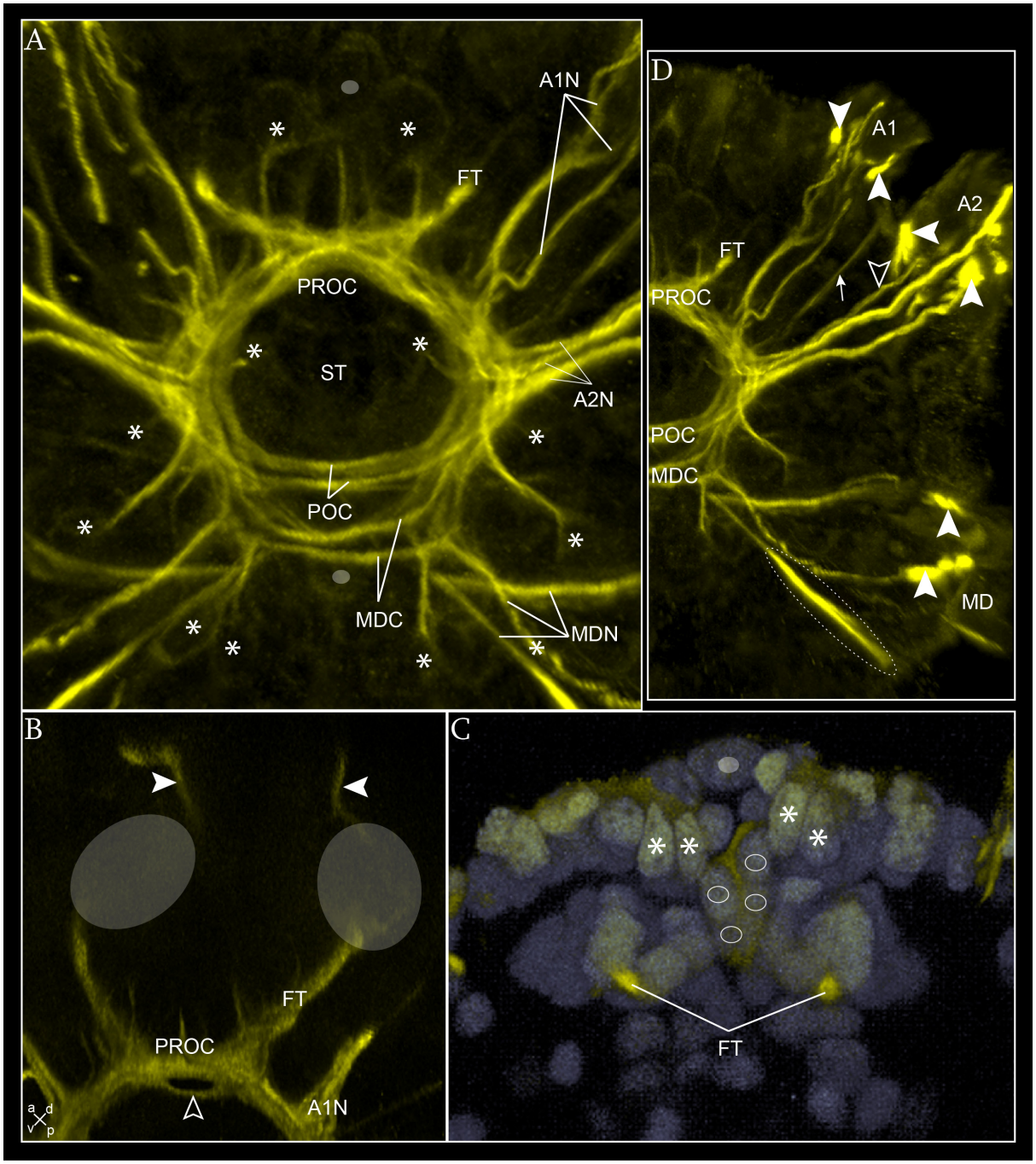

Fig. 15 - Axogenesis in *M. norvegica*, nauplius stage 1

Anti-ac-α-tubulin labelling in yellow. Sytox-green staining in grey. CLSM image stack. Imaris surpass mode: volume (blend in **B**), clipping plane in **B** and **D**, section mode in **C**. **A -** View of circumesophageal nerve ring anlage (ventral view). Asterisks point at single cell somata within a cluster connected to the circumesophageal nerve ring. Small ovals mark median unpaired cell somata. **B -** Detail of the neural structures in the protocerebral region (antero-ventral view). The frontal organs (filled arrowheads) are connected to the medulla terminalis (transparent ovals) via the frontal organ nerve. The pre-oral commissure anlage is formed by a thick antero-dorsal neurite bundle and a thin postero-ventral one (open arrowhead). **C -** Detail of the nauplius eye complex anlage (ventral view). The section includes the plane dorsal to antenna 1 insertion. Small oval marks unpaired median cell nucleus part of the naupliar midline (described in the previous section). Circles mark median cell nuclei representing the anlage of the nauplius eye complex. Asterisks mark single cell nuclei symmetrically distributed at the antero-lateral side of the nauplius eye complex anlage. **D -** View of the left half of the naupliar region (ventral view). The

open arrowhead points at the anterior-most neurite bundle forming the segmental nerve of antenna 2. Arrow points at the anlage of inter-segmental nerve 1. Filled arrowheads point at putative tendons at the level of the insertion of antenna 1, 2 and mandible. A stippled circle marks a putative muscle anlage at the posterior margin of the mandible insertion.

A1: antenna 1; A1N: antenna 1nerve; A2: antenna 2; A2N: antenna 2 nerve; FT: frontal tract; MD: mandible; MDC: mandibular commissure; MDN: mandibular nerve; POC: post-oral commissure; PROC: pre-oral commissure; ST: stomodeum.

At the latest phase of the stage, the general architecture of the brain has become more compact (Fig. 16A). Moreover the shape of the nerve ring has elongated along the longitudinal axis so that the distance between the pre- and the post-oral commissures has increased. Also the two antennal nerve roots result more separate and the root of antenna 2 results noticeably detached from the post-oral commissure keeping a defined para-oral position (Fig. 16A). The anlage of the inter-segmental nerve 2 has formed (Fig. 16A). It runs from the nerve ring connective comprised between the post-oral and the mandibular commissure to the dorso-lateral side of the nauplius.

In the post-naupliar region the first signal of neural differentiation occurs in the earliest phase of the stage (Fig. 16B). At the lateral side of the proctodeum a paired cluster of somata shows a diffuse signal (asterisks in Fig. 16B). A slender projection extends posteriorly and enters the terminal spine anlage (arrows in Fig. 16C). One additional longitudinal neurite bundle starts to extend from each cluster to the anterior (open arrowhead in Fig. 16B). Later, these two neurite bundles elongate and become thicker forming the anlage of the connective of the prospective ventral nerve cord (Fig. 16C). They do not connect the anterior brain anlage, yet, but connect some intermediate cell clusters (interneurons) along their path (data not shown). In this respect, the telsonic cell cluster lateral to the proctodeum contains the pioneer neurons of the connective of the ventral nerve cord.

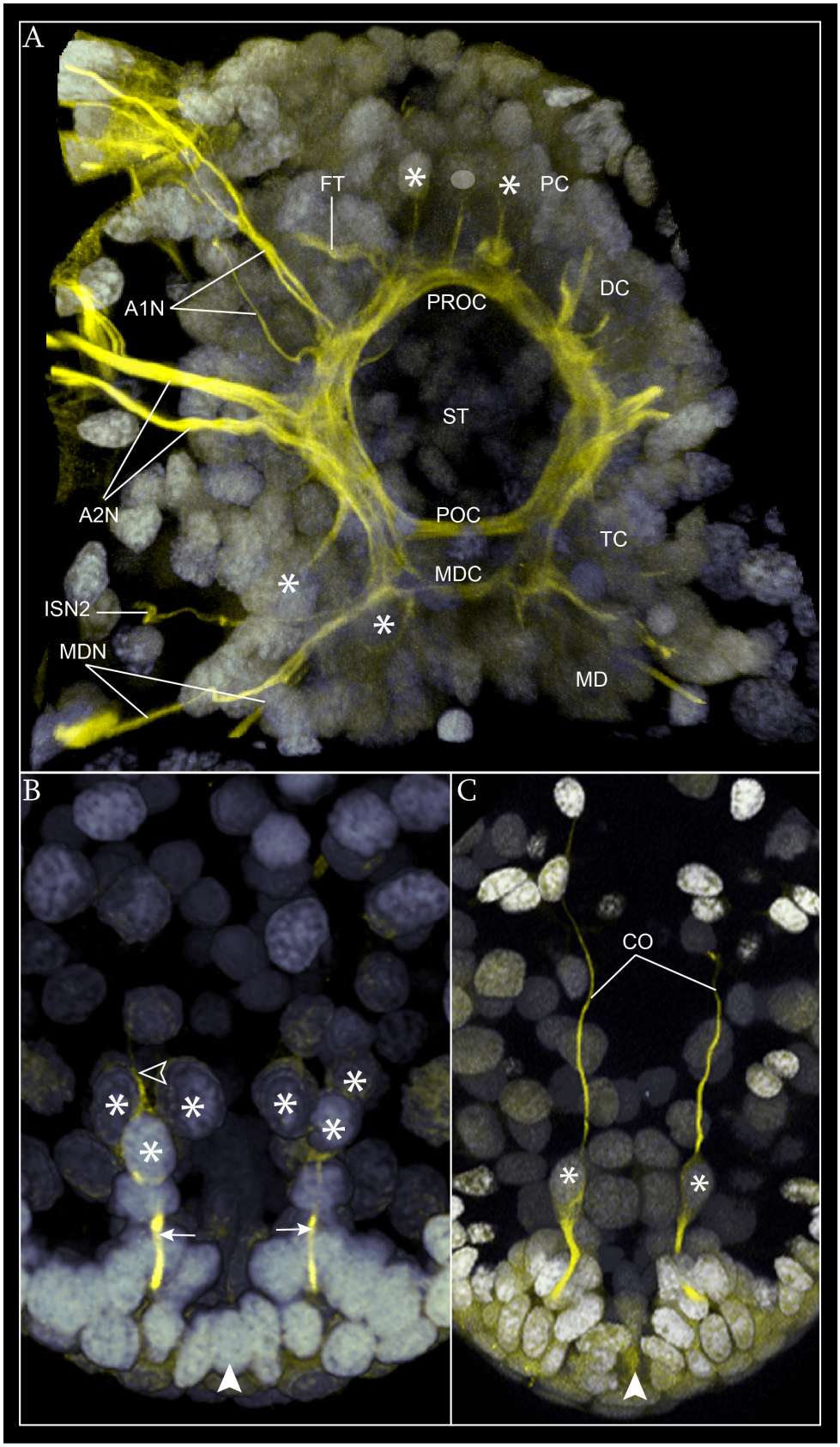

Fig. 16 - Axogenesis in *M. norvegica*, nauplius stage 1

Anti-ac-α-tubulin labelling in yellow. Sytox-green staining in grey. CLSM image stack. Imaris: surpass mode: volume, clipping plane. **A –** View of part of the naupliar region in the late nauplius stage 1 (ventral

view). The right most side of the nauplius has been cut out from the image. Asterisks mark lateral single cell nuclei connected to the pre-oral commissure. Small oval marks median unpaired cell nucleus connected with the pre-oral commissure. **B -** View of the posterior pole of the early nauplius stage 1 (ventral view). Asterisks mark single cell nuclei within a symmetrical cluster at the antero-lateral side of the proctodeum (filled arrowhead). Open arrowhead points at the left anlage of the connective. **C -** View of the posterior pole of the late nauplius stage 1 (ventral view). Asterisks mark the putative pioneer neurons of the connective. The filled arrowhead points at the position of the proctodeum.

A1N: antenna 1nerve; A2N: antenna 2 nerve; CO: connectives; DC: deutocerebrum; ISN2: inter-segmental nerve 2; MD: mandible; MDC: mandibular commissure; MDN: mandibular nerve; MDn: mandibular neuromere; FT: frontal tract; PC: protocerebrum; POC: post-oral commissure; PROC: pre-oral commissure; ST: stomodeum; TC: tritocerebrum.

Serotonin-like expression pattern

The same pair of SL-ir neuronal somata in the same position as observed in the previous embryonic stage is more intensely stained at this stage (asterisks in Fig. 17). Moreover, an intense signal occurs within the antero-dorsal component of the pre-oral commissure connected to the SL-ir neurons. This marks the beginning of differentiation and arborisation of the protocerebral neuropilar layer (open arrowheads in Fig. 17).

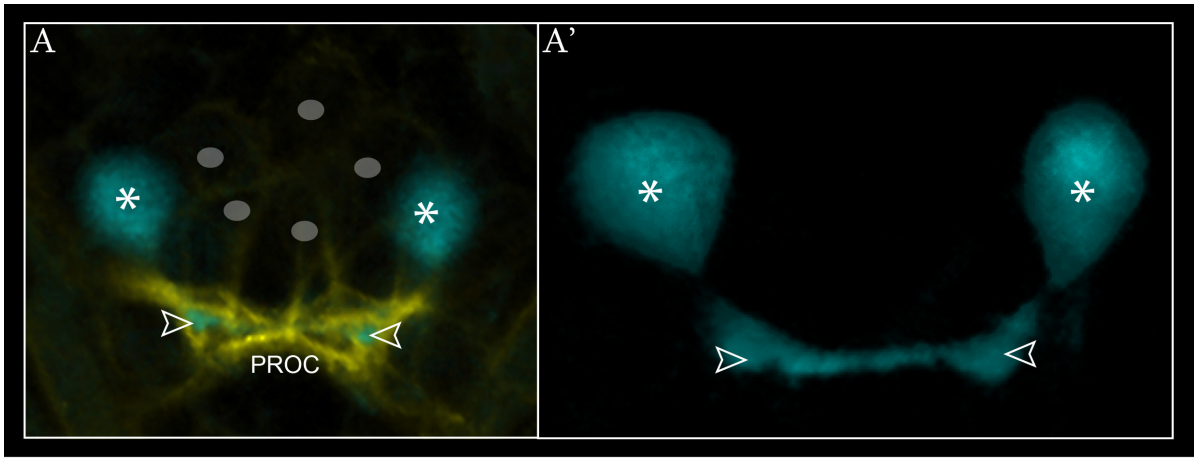

Fig. 17 - Distribution of SL-ir structures in the nauplius stage 1

Anti-ac-α-tubulin labelling in yellow. Anti-serotonin-like labelling in light blue. CLSM image stack. Imaris surpass mode: volume (blend in **A'**), clipping plane. View of the antero-ventral protocerebral region (ventral view). Asterisks mark each of the SL-ir cell neurons. Open arrowheads point at the SL-ir differentiating neuropil in the antero-dorsal component of the pre-oral commissure; small grey ovals in **A** mark single median neurons in the anterior protocerebral region.

PROC: pre-oral commissure.

3.1.2.4 Nauplius stage 2

Axogenesis

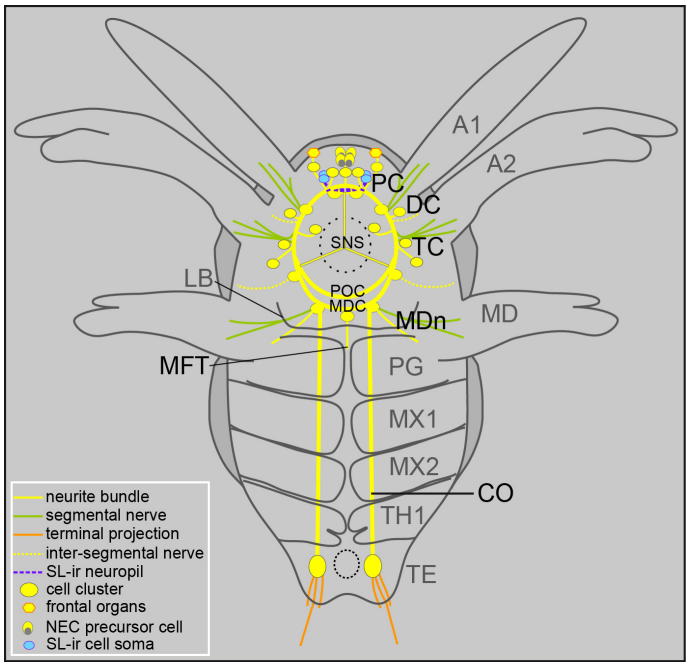

Fig. 18 - *M. norvegica*, embryonic stage 2

Schematic illustration of the distribution of differentiated neural structures (ventral view). The carapace edge is represented by the dark grey frame around the body shape. Only the ventral portion of the SNS is represented. The region of the stomodeum is marked by black circular stippled line. The small stippled circle in the telson represents the proctodeum.

A1: antenna 1; A2: antenna 2; CO: connective; DC: deutocerebrum; LB: labrum; MD: mandible; MDC: mandibular commissure; MDn: mandibular neuromere; MFT: median fiber tract; MX1: maxilla 1; MX2: maxilla 2; PC: protocerebrum; PG: paragnaths; POC: post-oral commissure; SNS: stomatogastric nervous system; TC: tritocerebrum; TE: telson; TH1: thoracopod 1.

In the naupliar region the number of neurites and neuronal somata has increased further and the brain anlage assumes a more compact structure (Fig. 19A). At the anterior pole the frontal organ pops out, and is connected to the medulla terminalis by two slender neurite bundles connecting the lateral sides of the organ (arrows in Fig. 19B). The medulla terminalis has increased the number of constituting cells and, thus, increased its volume (grey area in Fig. 19B). The anlage of the nauplius eye complex appears as a cluster of cells medially connected to the protocerebrum (Fig. 19B-D). Four distinct median cell somata (asterisks in Fig. 19D) are observable, each sending a neurite posteriorly to the pre-oral commissure (Fig. 19D). Three/four separate neurites run to the posterior side (filled arrowheads in Fig. 19D): halfway along their path they meet each other forming a single bundle which branches off in the proximity of the pre-oral commissure into several neurites (open arrowheads in Fig. 19D) which connect in part medially to the dorsal margin of the pre-oral commissure and in part

laterally to the proximal portion of the frontal tract. These four cell somata may represent four sensory retinular cells of the prospective lateral cups forming the nauplius eye complex. Additionally, two cells with elongated nuclei have newly formed lying directly adjacent and ventral to the four sensory cells (light blue circles in Fig. 19C). They may represent the anlage of the two pigment cells. No distinct connection of these cells with the brain is observed. A symmetrical arrangement of the cell nuclei surrounding the nauplius eye complex is maintained (Fig. 19C).

The two neurite bundles of the pre-oral commissure have increased in diameter (Fig. 19A, B). Already in the earliest phase of the stage, the anlage of the unpaired median inferior ventricular nerve is visible, medially connected to the posterior neurite bundle of the pre-oral commissure, (open arrowhead in Fig. 19B). This reveals the beginning of the formation of the stomatogastric nervous system (see below). The neurite bundle of antenna 1 has become thicker. Of the three branches the two more anterior start to fuse together in their proximal portion while the posterior most maintains a separate course (Fig. 19A). Posteriorly, a thin branch of the inter-segmental nerve 1 runs out laterally (arrows in Fig. 19A), and ends in a brightly stained structure diagonally located at the lateral surface of the ‘head’ shield (filled arrowheads in Fig. 19A). In the tritocerebral region both branches of antenna 2 nerve anlage have increased their diameter so that, at their proximal portion, they become closer together to constitute the nerve root (Fig. 19A). Posteriorly, the inter-segmental nerve 2 anlage has formed (open arrowheads in Fig. 19A). It runs from the lateral side of the connective of the nerve ring, slightly anterior to the post-oral commissure, towards the dorso-lateral side of the ‘head’ shield (Fig. 19A).

At the dorsal side of the nerve ring some neurons are stained in a bilateral symmetric arrangement (stars in Fig. 19C). They are associated with different neurite bundles: the one medio-dorsally to the anterior neurite bundle of the pre-oral commissure (upper) with the frontal tract and the nauplius eye nerves, the one dorsal to the connective in the deutocerebral region (medial) with antenna 1 nerve, and the one more posterior postero-lateral to the stomodeum (lower) with the inter-segmental nerve 2 (Fig. 19C). Also the post-oral commissure has become thicker and the sub-division into two neurite bundles becomes less obvious due to the interposition of additional neurites in between (Fig. 19A and E). In the same way, the mandibular commissure now results in a singular thick transversal neurite bundle running quite close to the post-oral commissure (Fig. 19A and E).

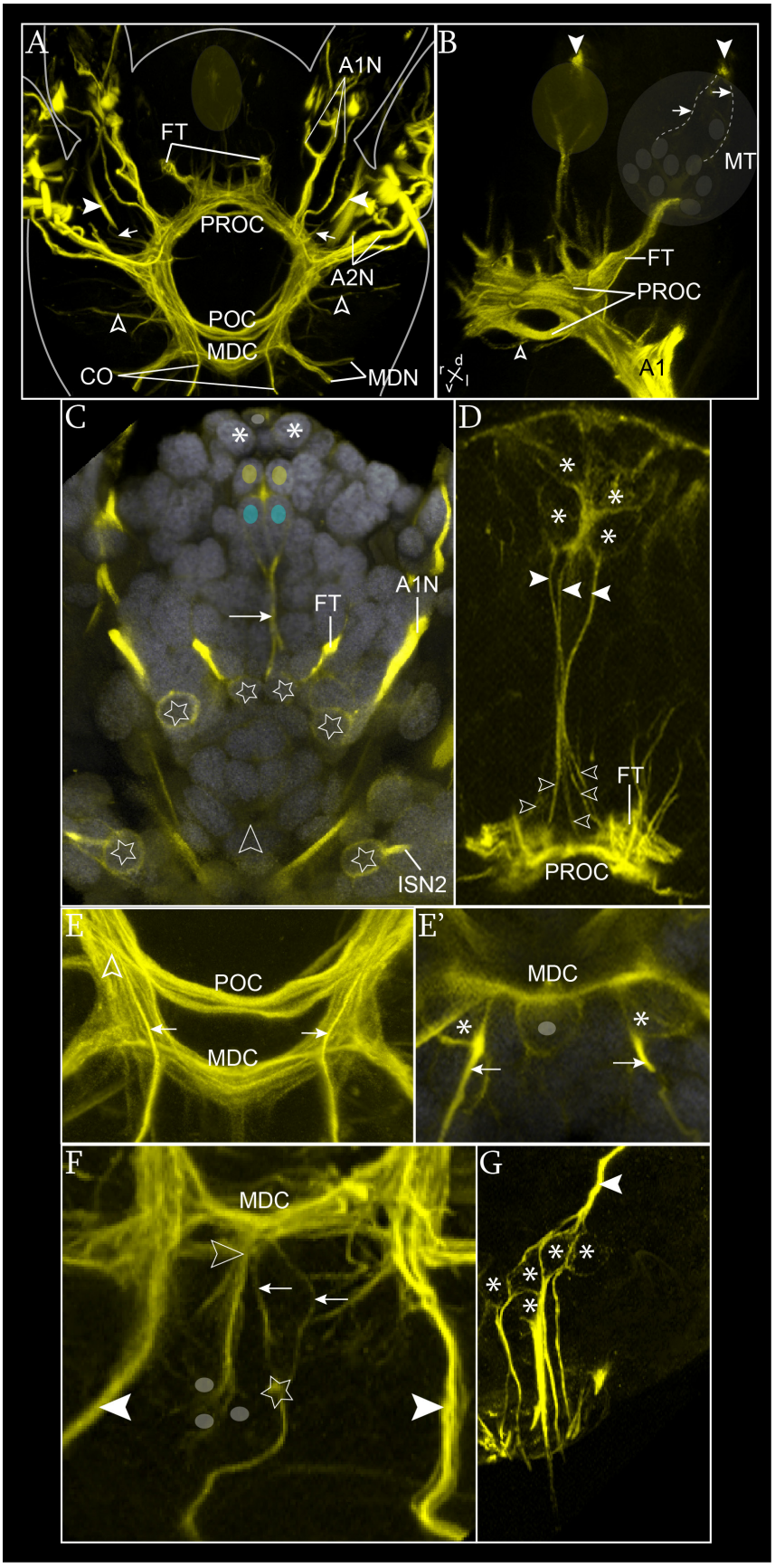

Fig. 19 - Axogenesis in *M. norvegica*, nauplius stage 2

Anti-ac-α-tubulin labelling shown in yellow. Sytox-green staining in grey. CLSM image stack. Imaris surpass mode: volume (blend in **B**, **C**), clipping plane in **B**, **D**, **E**, **F** and **G**, section mode in **C** and **E'**. **A -** View of the naupliar region (ventral view). The yellow area marks the position of the nauplius eye complex anlage. Arrows point at the inter-segmental nerve 1 anlage. Filled arrowheads point at a bright stained structure at the lateral surface of the 'head' shield. Open arrowheads point at the inter-segmental nerve 2 anlage. **B -** Detail of the protocerebral region (ventro-lateral view). The yellow area marks the position of the nauplius eye complex anlage. The grey area marks the position of the medulla terminalis. The transparent ovals included in the area indicate the location of some of the cell somata of the medulla terminalis. Filled arrowheads point at the frontal organs (note that they are located dorsally to the nauplius eye complex). Arrows point at single neurites connecting the frontal organs to the medulla terminalis. The open arrowhead points at the insertion of the inferior ventricular nerve anlage. **C -** Detail of the dorsal side of the naupliar region (ventral view). Small oval and asterisks mark some of the cell nuclei with a symmetrical arrangement. The four coloured ovals mark paired medial cell nuclei of the nauplius eye complex anlage. The yellow ones label two of the putative retinular cells, while the two light blue ones label the two putative pigment cell nuclei. Arrow points at the median neurite bundle which connects the cell cluster of the nauplius eye complex to the pre-oral commissure. Stars mark paired cell somata at the dorsal side of the nerve ring associated with the nauplius eye complex anlage and the frontal tract (upper), antenna 1 nerve (medial) and inter-segmental nerve 2 (lower). Open arrowhead marks the position of the stomodeum. **D -** Detail of the nauplius eye complex anlage (ventral view). Only part of the dorsal component of the pre-oral commissure and the proximal root of the frontal tract is visible in the section. Asterisks mark the four median cell somata forming the nauplius eye complex anlage. Filled arrowheads point at single neurite bundles running from the cell somata. Open arrowheads mark each of the posterior branches which connect the nauplius eye complex to the pre-oral commissure and to the frontal tract. **E -** Detail of the post-oral and mandibular commissures' ventral portion in the early phase of the stage (ventral view). Open arrowhead (on the left of the picture) points to the root of the inter-segmental nerve 2 anlage. Arrows point at the ventral component of the connective. **E' -** Detail of the of the mandibular commissure's dorsal portion (ventral view). Asterisks label single paired cell somata at the lateral side of the commissure connected to the dorsal portion of the longitudinal connective anlagen (arrows). Small oval labels the unpaired median cell soma adjacent to the commissure. **F -** Detail of the anlage of the mandibular commissure and of the median fiber tract in a late phase of the stage (ventral view). The open arrowhead points at the insertion of the ventral neural projections associated with a ventral cell cluster (small ovals). Arrows point at single neurites forming the anterior component of the median fiber tract anlage, which meet posteriorly (star) forming one single longitudinal neurite bundle. The filled arrowheads point at the connective anlagen. **G -** Detail of the telson (left half) in a late phase of the stage (ventral view). Asterisks label single stained cell somata connected, anteriorly, to the connective (filled arrowhead) and, posteriorly, to the terminal spines.

A1: antenna 1; A1N: antenna 1 nerve; A2: antenna 2; A2N: antenna 2 nerve; CO: connective; DC: deutocerebrum; FT: frontal tract; IVN: inferior ventricular nerve; MD: mandible; MDC: mandibular commissure; MDN: mandibular nerve; MT: medulla terminalis; MX1: maxilla 1; MX2: maxilla 2; PG: paragnaths; POC: post-oral commissure; PROC: pre-oral commissure; STG: stomatogastric ganglion; STN: stomatogastric nerve; TC: tritocerebrum; TH1: thoracopod 1.

The dorso-median big cell soma adjacent to the mandibular commissure is still observable in an earlier phase of the stage (small oval in Fig. 19E') while, in a later phase, when the anlage of the median fiber tract has formed, this is not visible any longer (Fig. 19F). The median fiber tract anlage is composed of two separate thin neurites running from the commissure to the posterior side (arrows in Fig. 19F) and meeting each other slightly posteriorly in one single median longitudinal neurite bundle (star in Fig. 19F). At the same median level several stained projections with a dorso-ventral orientation are spanned between the mandibular commissure (open arrowhead in Fig. 19F) and a ventral cell cluster (small ovals in Fig. 19F).

The post-naupliar connective has established anteriorly the connection with the naupliar neuromere (filled arrowheads in Fig. 19F). In the earliest phase of the stage, two distinguished neurites are observable along the naupliar connective proceeding longitudinally in posterior direction (arrows in Fig. 19E, E'). One has a ventral location and runs out from the more anterior connective of the nerve ring (arrow in Fig. 19E). The second is located more dorsally and is connected with a dorso-lateral cell soma adjacent to the dorso-posterior side of the mandibular commissure (arrows in Fig. 19E'). Later in development these components are fused together with the posterior neurites from the telson in one single longitudinal neurite bundle which spans continuously between the mandibular commissure and the telsonic cell cluster. The number of constituting cells of this last has increased proportionally to the increasing number of terminal spines to which each cell is posteriorly connected (asterisks in Fig. 19G).

In summary, the anlage of the connective of the ventral nerve cord results constituted by the projection of neurite bundles with three different origins: one posterior from the pioneers located in the telson, one antero-ventral from the brain neuromeres, and one antero-dorsal from the pioneers associated with the mandibular neuromere.

Stomatogastric nervous system

The first observable structure of the stomatogastric nervous system is the anlage of the median unpaired inferior ventricular nerve, which runs out ventrally from the medio-ventral side of the pre-oral commissure (Fig. 19B). Later in development, the inferior ventricular nerve bifurcates ventrally into two neurite bundles that run to the lateral sides in opposite directions (Fig. 20B and D) and connect the ventro-lateral sides of the post-oral commissure (stars in Fig. 20B, C). From a ventral view, together they form an arch, which represents the anlage of the labral commissure. Parallel to the inferior ventricular nerve but more posteriorly, the anlage of the stomatogastric nerve has grown (Fig. 20B and D). This runs on the antero-dorsal wall of the stomodeum spanned between the stomatogastric ganglion, dorsally (Fig. 20B), and the anterior margin of the stomodeum, ventrally (Fig. 20B, C). The root of the stomatogastric nerve anlage is composed of two distinct neurite bundles (Fig. 20B). Ventrally the stomatogastric nerve branches laterally and forms the anlage of the stomodeal commissure which surrounds the antero-dorsal margin of the stomodeum (Fig. 20C). The lateral end of the stomodeal commissure meets the one of the labral commissure at the lateral side of the post-oral commissure (stars in Fig. 20B, C).

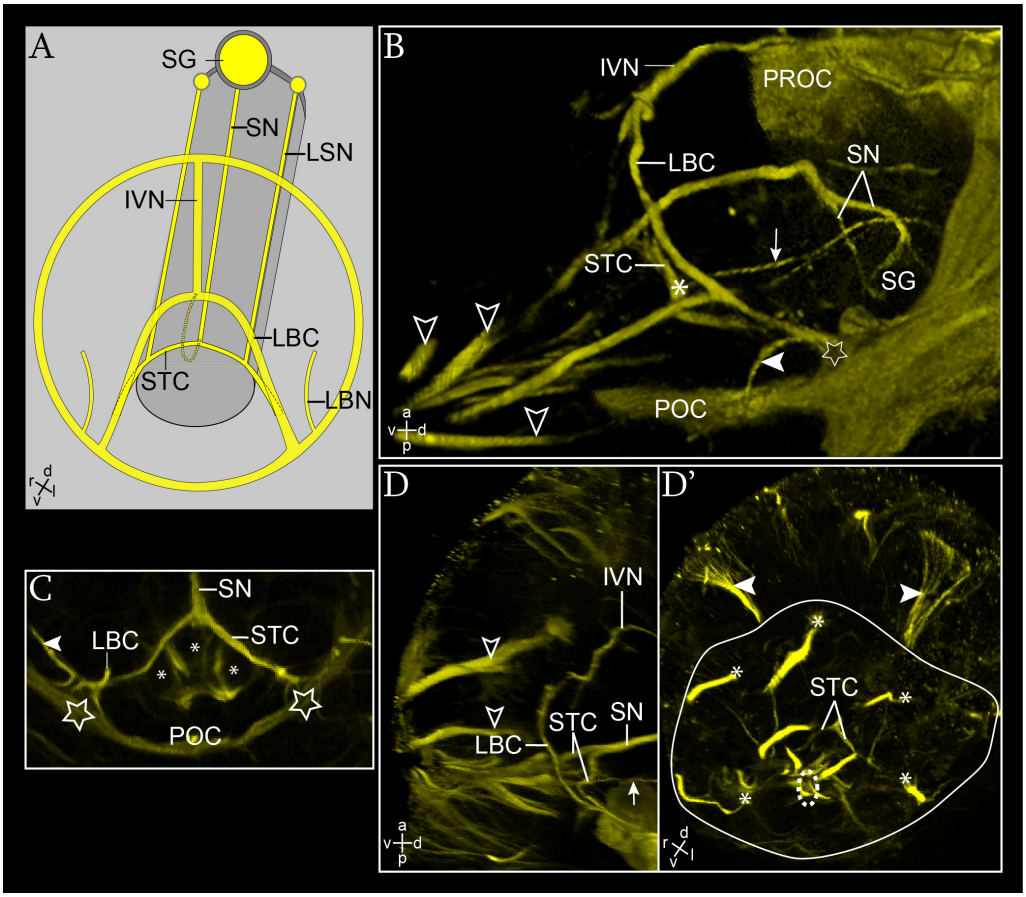

Fig. 20 - The anlage of the stomatogastric nervous system and the innervation of the labrum in *M. norvegica*, nauplius stage 2

A - Schematic illustration of the stomatogastric nervous system anlage (ventro-lateral view). Neural structures are labelled in yellow. The anlage of the digestive tube is represented by a grey cylinder. The circumesophageal nerve ring is schematized by the circular yellow ring in the foreground. The small yellow circles, lateral to the stomatogastric ganglion, represent the cell clusters of the lateral stomatogastric nerves.

B-D' - Anti-ac-α-tubulin labelling. CLSM image stack. Imaris surpass mode: volume (blend in **B** and **D**), clipping plane in **C-D'**. **B -** General overview (lateral view). The asterisk marks the intersection point between the lateral stomatogastric nerve (arrow) and the stomodeal commissure. The star marks the intersection point of the labral and stomodeal commissure with the post-oral commissure. The filled arrowhead points at the ventral neurite bundle running anteriorly to the labrum. Open arrowheads point at putative sensory structures around the stomodeum. **C -** Detail of the posterior portion (ventral view). Asterisks mark single cell nuclei of the stomodeum. The filled arrowhead points at the ventral neurite bundle running anteriorly to the labrum. Stars mark the points of intersection of the labral and stomodeal commissure with the post-oral commissure. **D**, **D' -** View of the anlage of the labrum and of part of the stomatogastric nervous system (lateral view in **D**; ventro-lateral view in **D'**). **D -** Open arrowheads point at the median putative sensory innervations of the labrum. The small arrow points to the lateral stomatogastric nerve anlage. **D' -** The dorsal side of the image stack has been cut out so that the circumesophageal nerve ring is not visible. The continuous line marks the border of the labrum anlage. Filled arrowheads point at the fun-like structure stained anterior to the labrum anlage. Asterisks mark the position of the cell cluster of the putative sensory structures of the labrum. A stippled circle marks the position of the ventral opening of the stomodeum.

IVN: inferior ventricular nerve; LBC: labral commissure; LSN: lateral stomatogastric nerve; POC: post-oral commissure; PROC: pre-oral commissure; SG: stomatogastric ganglion; SN: stomatogastric nerve; STC: stomodeal commissure.

Moreover, parallel to the stomatogastric nerve a lateral paired thin neurite bundle has formed running along the dorso-lateral wall of the stomodeum forming the lateral stomatogastric nerve (arrow in Fig. 20B). This spans between a small paired cell cluster lateral to the stomatogastric ganglion, dorsally, and the median half branch of the stomodeal commissure, ventrally (asterisk in Fig. 20B). At the same level as the insertion of the two commissures, at the lateral side of the post-oral commissure, one additional neurite bundle is observed running to the antero ventral side towards the labrum (filled arrowhead in Fig. 20B, C). In the ventral portion of the labrum, additional structures are stained (Fig. 20 D, D'). These are regularly distributed cell clusters in the labrum (asterisks in Fig. 20D') which are connected with stained projections with a dorso-ventral orientation ending at the external surface of the labrum (Fig. 20D, D'). These probably represent the anlage of sensory organs of the labrum. Similar structures are detected more posteriorly around the stomodeum (open arrowheads in Fig. 20A). Anterior to the labrum one paired lateral fun-shape structure is also stained by α-tubulin (filled arrowheads in Fig. 20D').

Serotonin-like expression pattern

One additional pair of SL-ir neurons appears dorsal to the one observed in the previous stage (stars in Fig. 21A, B). The SL-ir neuropilar layer intercalated within the dorsal portion of the pre-oral commissure has increased in volume and extends slightly to the antero-dorsal portion of the pre-oral commissure and to its postero-ventral side assuming a saddle-like shape (Fig. 21B, C).

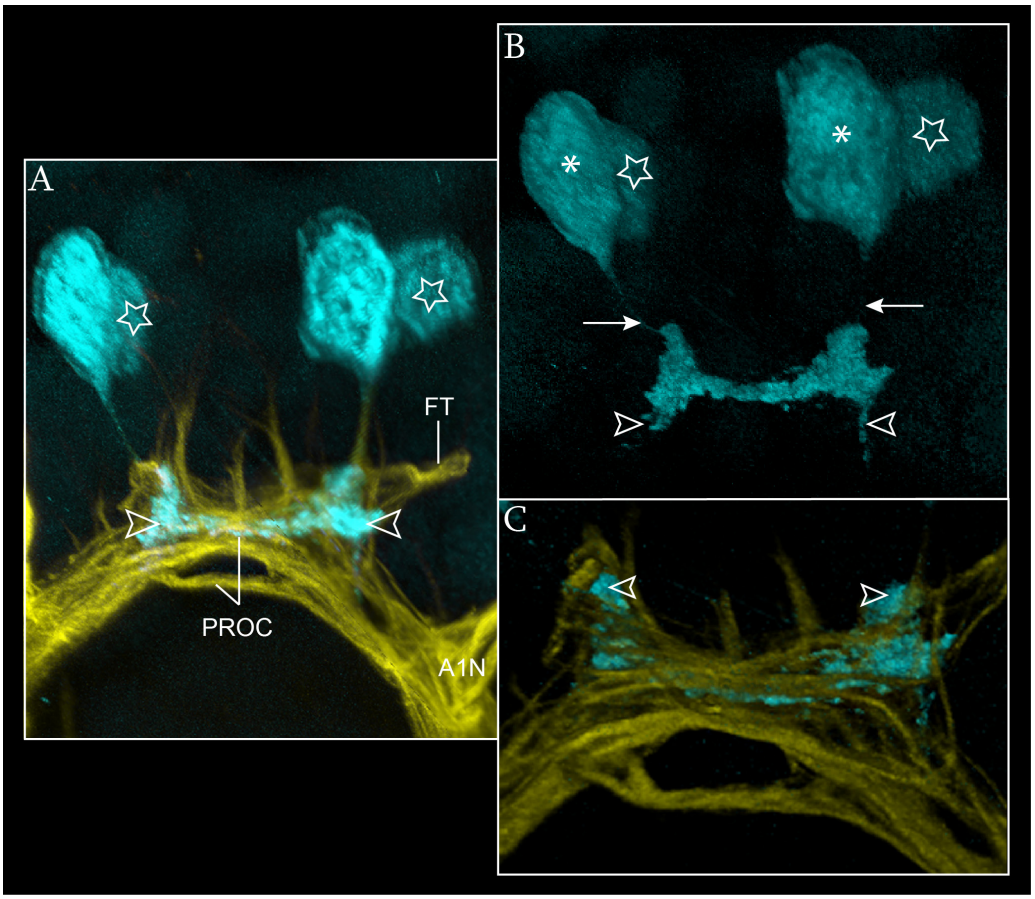

Fig. 21 - Distribution of SL-ir structures in *M. norvegica*, nauplius stage 2

Anti-ac-α-tubulin labelling. Anti-serotonin-like labelling in light blue. CLSM image stack. Imaris surpass mode: volume (blend in **B**, **C**), clipping plane. **A -** General overview (ventral view). The sample is slightly tilted to the right side. Stars mark the dorsal additional pair of SL-ir neurons. Open arrowheads point at the SL-ir neuropilar region. **B –** Detail of the SL-ir structures (ventral view). Asterisks mark the ventral SL-ir neurons. Stars mark the dorsal additional pair of SL-ir neurons. Arrows point at the thin SL-ir neurites connecting the ventral pair of SL-ir neurons to the SL-ir neuropilar layer. Open arrowheads point at the posterior extension of the SL-ir neuropilar layer. **C -** Detail of the pre-oral commissure (ventral view). Open arrowheads point at the antero-dorsal extension of the forming SL-ir neuropilar layer.

A1N: antenna 1 nerve; FT: frontal tract; PROC: pre-oral commissure.

3.1.2.5 Metanauplius stage

Axogenesis

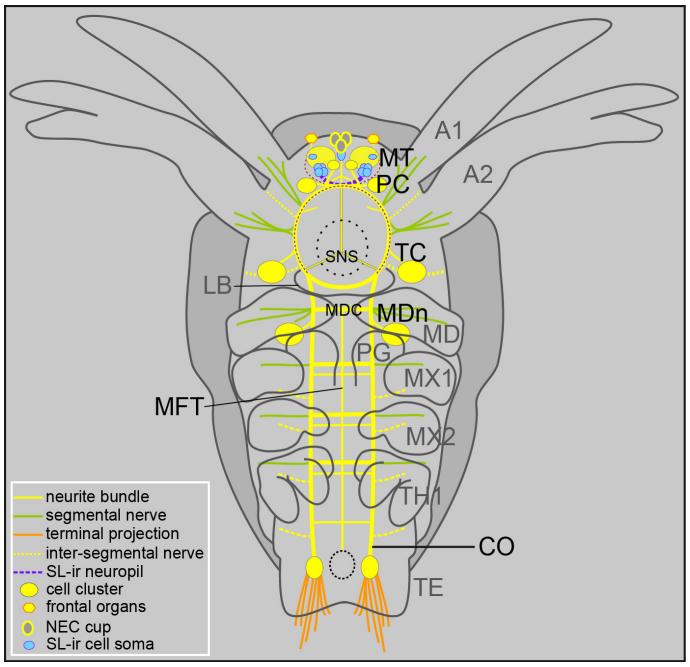

Fig. 22 - *M. norvegica*, metanauplius stage

Schematic illustration of the distribution of differentiated neural structures (ventral view). The carapace edge is represented by the dark grey frame around the body shape. Only the ventral portion of the SNS is represented. The region of the stomodeum is marked by black circular stippled line. The small stippled circle in the telson represents the proctodeum.

A1: antenna 1; A2: antenna 2; CO: connective; LB: labrum; MD: mandible; MDC: mandibular commissure; MDn: mandibular neuromere; MFT: median fiber tract; MT: medulla terminalis; MX1: maxilla 1; MX2: maxilla 2; PC: protocerebrum; PG: paragnaths; TC: tritocerebrum; TE: telson; TH1: thoracopod 1; SNS: stomatogastric nervous system.

The metanauplius stage is characterized by a gradual condensation of the neurite bundles in the naupliar region so that at the latest phase of the stage the brain appears as a solid homogeneous structure surrounding the stomodeum (Fig. 23A). The distinction of separate neurite bundles becomes less obvious and a certain decrease of the α-tubulin signal has been detected so that a detailed observation of the brain compartments becomes more difficult. Nevertheless, in the earliest phase of the stage, the brain anlage is still brightly stained and a certain distinction of separate neurite bundles is possible (Fig. 23B-D). In the protocerebral region the pre-oral commissure resembles one thick single unit (Fig. 23A -C). The medulla terminalis has noticeably increased in volume resulting in a massive bi-lobed dorsal mass composed of several cell somata which send their neurites to the frontal tract (Fig. 23C). The frontal organs have bulged out from the ‘head’ shield as cylindrical apical structures (filled

arrowheads in Fig. 23A, B). The frontal organ nerve has become a single short and thick neurite bundle, which appears as a basal peduncle (open arrowheads in Fig. 23C). The distance between the post-oral and the mandibular commissure increases during this stage and the connectives in the comprised region become thicker (Fig. 23A, B and D). Dorso-lateral cell clusters are noticeable in the deuto-, trito- and mandibular regions. They are connected to the naupliar connective at the level of the pre-oral, post-oral and mandibular commissure (stippled lines in Fig. 23D).

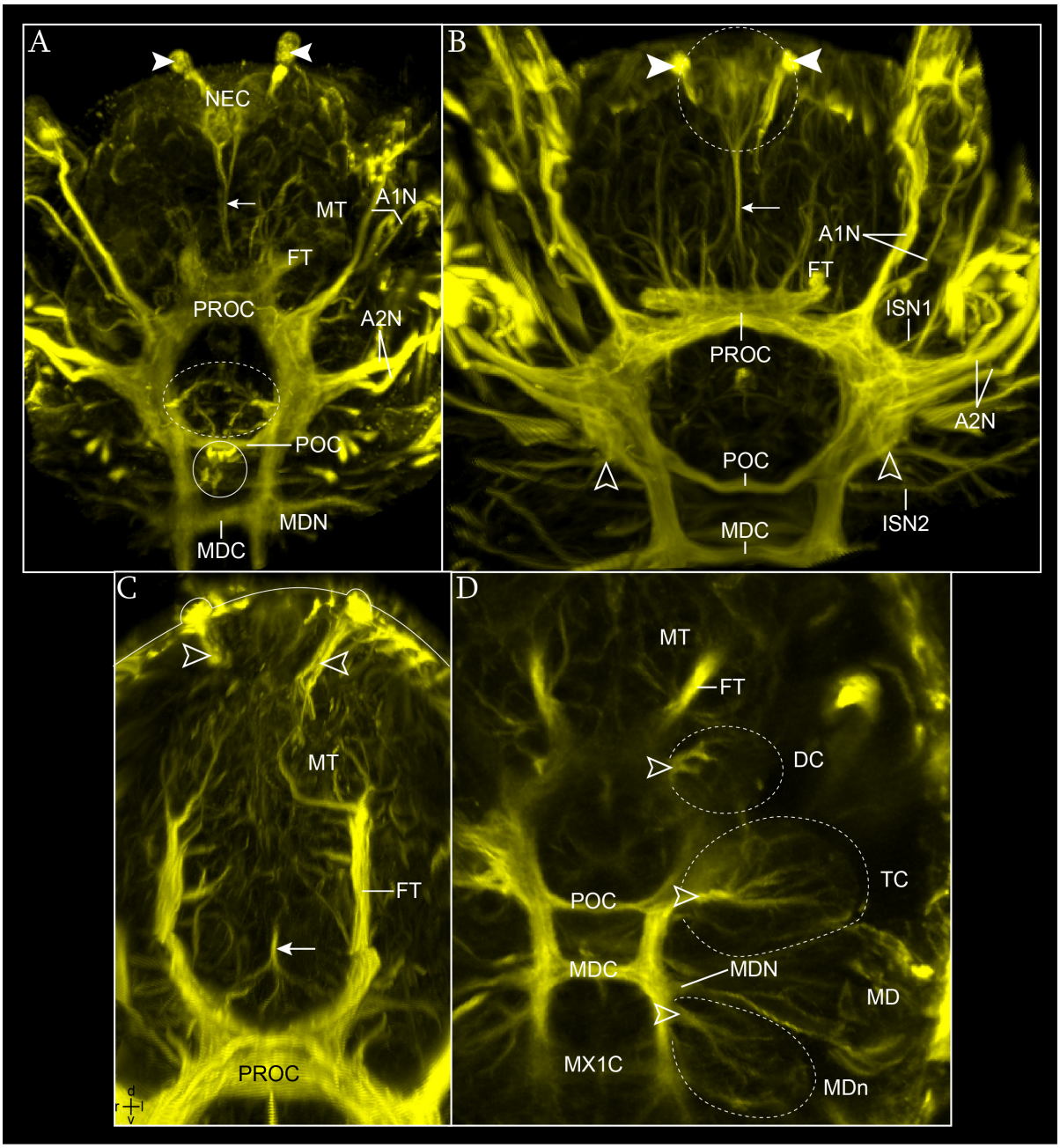

Fig. 23 – Axogenesis in the naupliar region of *M. norvegica*, metanauplius stage

Anti-ac-α-tubulin labelling in yellow. CLSM image stack. Imaris surpass mode: volume, clipping plane. **A -** General overview of the naupliar region in the latest phase of the stage (ventral view). Filled arrowheads point at the frontal organs. The small arrow points at the median neurite bundle of the nauplius eye complex. A stippled circle marks the region of the stomatogastric nervous system, while a circle marks the region of the stomodeum opening. **B -** General overview of the naupliar region in the early phase of the stage (ventral view). Filled arrowheads point at the frontal organs. A stippled circle marks the position of the nauplius eye complex anlage (note that it is located ventral to the frontal organs, compare with **C**). The small arrow points at the median neurite bundle of the nauplius eye complex. Open arrowheads mark the insertion point into the nerve ring of the dorsal cell cluster's neurites in the tritocerebral region. **C -** Detail of the protocerebral region (antero-ventral view). The antero-ventral portion of the image stack has been cut out from the picture (e.g. nauplius eye cups anlage). Open arrowheads mark the peduncle-like structure of the frontal organ nerve. The small arrow marks the posterior end of the median neurite bundle of the nauplius eye complex. **D -** Detail of the dorsal portion of the naupliar region (ventral view). The dorsal cell clusters are encircled by stippled lines. Open arrowheads point at the neurite bundles which run into the connective.

A1: antenna 1; A1N: antenna 1 nerve; A2: antenna 2; A2N: antenna 2 nerve; DC: deutocerebrum; FO: frontal organs; ISN2: inter-segmental nerve 2; FT: frontal tract; MD: mandible; MDC: mandibular commissure; MDN: mandibular nerve; MDn: mandibular neuromere; MT: medulla terminalis; MX1C: maxilla 1 commissure; NEC: nauplius eye complex; POC: post-oral commissure; PROC: pre-oral commissure; TC: tritocerebrum.

The nauplius eye complex differentiates during this stage (Fig. 24). Two main compartments are distinguishable: one unpaired medial at the ventral and one paired lateral in dorsal position (Fig. 24C-C"). These compartments are generally called cups of the nauplius eye. Each cup is composed of three cell somata (retinular cells) (asterisks in Fig. 24C-C") and is connected with the dorsal portion of the pre-oral commissure by one neurite bundle (open arrowheads in Fig. 24C-C"). The nauplius eye complex nerve resembles one median neurite bundle, which collects the three neurites from each cup at its anterior end, runs to the posterior (arrow in Fig. 24B and C"), and branches off to connect the protocerebrum in two different regions. These are: medially, the dorsal side of the pre-oral commissure and, laterally, the proximal portion of the frontal tract (open arrowheads in Fig. 24B). Moreover, two median elongated cells are imbedded in the nauplius eye complex and, possibly, correspond to the anlage of the pigmented cells (stippled line in Fig. 24C"). These are located dorsally to the median cup and, ventro-posteriorly, in between the lateral cups framed by the neurites coming out from the three cups (stippled line in Fig. 24C").

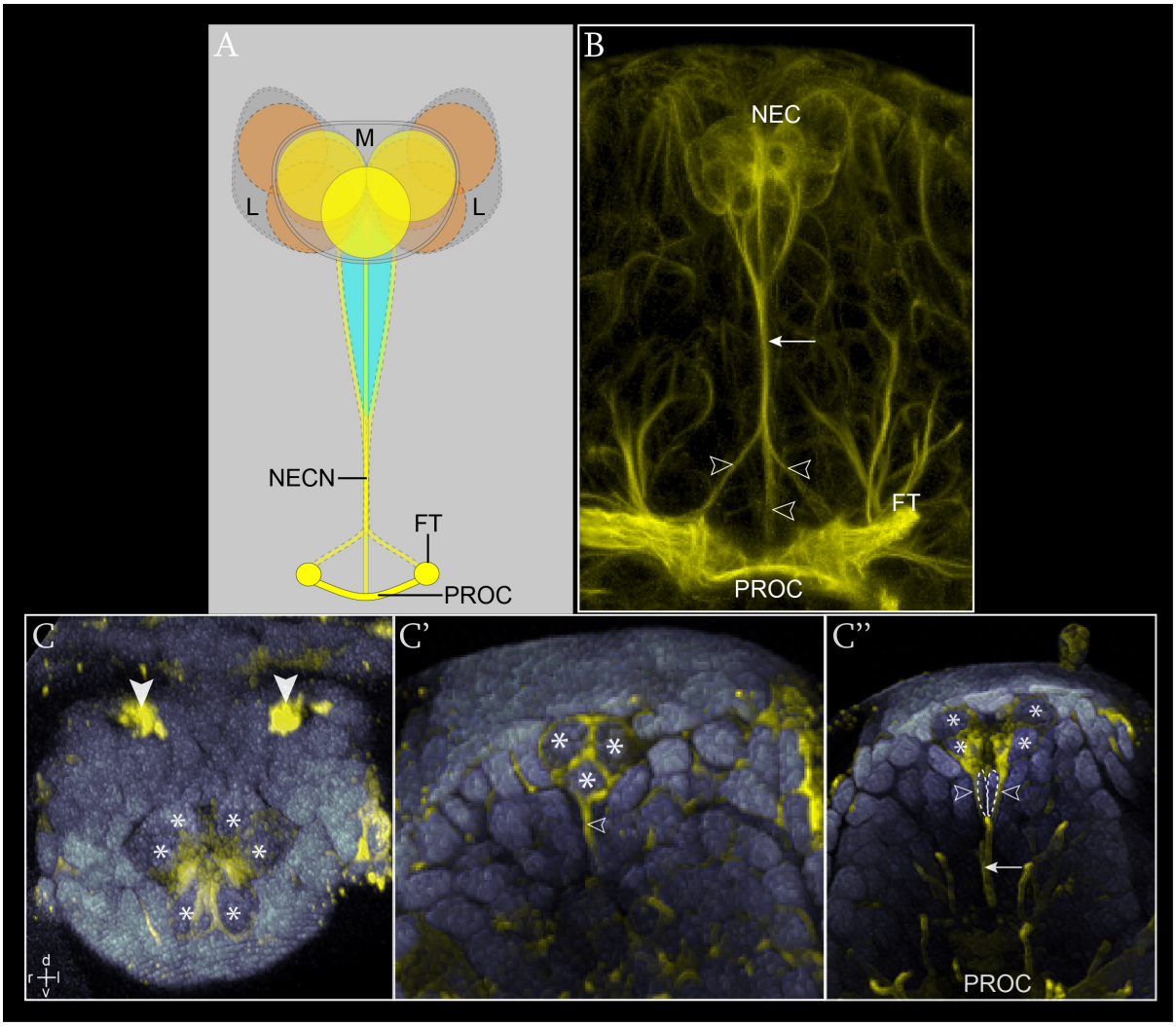

Fig. 24 – Development of the nauplius eye complex in *M. norvegica*, metanauplius stage

A - Schematic illustration of the nauplius eye complex anlage as it appears in the latest phase of the metanauplius (ventral view). Circles correspond to single cell somata (median cup in yellow; lateral cups in orange). Continuous lines encircle structures of the median cup (M). Broken lines encircle structures of the lateral cups (L). Light blue label the SL-ir pigmented cells anlage (see Fig. 27**A**, **B**). The frontal tract is represented in a frontal section.

B-**C" -** Anti-ac-α-tubulin labelling in yellow. Sytox-green staining in grey. CLSM image stack. Imaris surpass mode: volume (blend in **C**- **C"**), clipping plane. **B -** Detail of the dorsal portion of the pre-oral commissure and its connection with the nauplius eye complex (ventral view). Arrow points at the median neurite bundle of the nauplius eye complex. Open arrowheads point at its posterior branches. **C**-**C" -** Details of the nauplius eye complex. Asterisks label single cell somata forming the cups. **C –** Anterior view of the nauplius eye cups. Filled arrowheads point at the frontal organs. **C' –** View of the ventral cup (ventral view). Open arrowhead points at the median neurite bundle of the cup. **C" –** View of the lateral cups (ventral view). Open arrowheads point at single neurite bundle connected with each cup. Stippled lines encircle the two putative pigmented cells. Arrow points at the median neurite bundle which connects the nauplius eye complex to the protocerebrum.

FT: frontal tract; L: lateral cup; M: median cup; NEC: nauplius eye complex; NECN: nauplius eye complex nerve; PROC: pre-oral commissure.

In the post-naupliar region the architecture of the ventral nerve cord has been established (Fig. 25). In the early phase of the stage (Fig. 25A-C) the connective has become thicker and the anterior commissure of the first three post-naupliar segments (i.e. maxilla 1 and 2 and thoracopod 1) develop following an antero-posterior gradient, the more posterior being less developed than the more anterior ones (Fig. 25A). The segmental nerves of maxilla 1 and 2have formed: they run out laterally at the level of the commissure anlagen. Three inter-segmental nerves have also formed: one between maxilla 1 and 2 neuromeres (ISN 3), one between maxilla 2 neuromere and thoracomere 1 (ISN 4), and one posterior to thoracomere 1 (ISN 5) (arrows in Fig. 25A and C). They all run laterally towards the dorso-lateral side of the larva. No inter-segmental nerve occurs between the mandibular and the maxilla 1 neuromeres. At the lateral sides of each commissure, postero-medially, short neurites connect with pairs of median cell clusters which probably contain the pioneer neurons of additional connectival axons (e.g. filled arrowheads in Fig. 25B). The median fiber tract anlage extends from the mandibular commissure all along the nerve cord connecting each commissural anlage (Fig. 25A). It extends posterior to thoracomere 1, and ends onto the ventral surface of the proctodeum (stippled circle in Fig. 25C). In the middle of maxilla 1 and 2 commissure anlagen stained projections with a dorso-ventral course are observable (arrows in Fig. 25B). These are connected with a medio-ventral cell cluster in the external ectodermal layer (circles in Fig. 25B).

In the late phase of the stage, a commissure in the thoracomere 2 anlage has formed (Fig. 25D, E), and a posterior commissure has developed in all the first three post-naupliar neuromeres. These last also follow an antero-posterior gradient of development (Fig. 25D). The thoracomere 1 segmental nerve and thoracomere 2 inter-segmental nerve anlagen have grown out (arrows in Fig. 25D, E). The median fiber tract has extended further posterior to the thoracomere 2 anlage (filled arrowhead in Fig. 25E) running along the ventral wall of the proctodeum (stippled line in Fig. 25E). The telsonic cell cluster has grown further and flanks the proctodeum (asterisks in Fig. 25F).

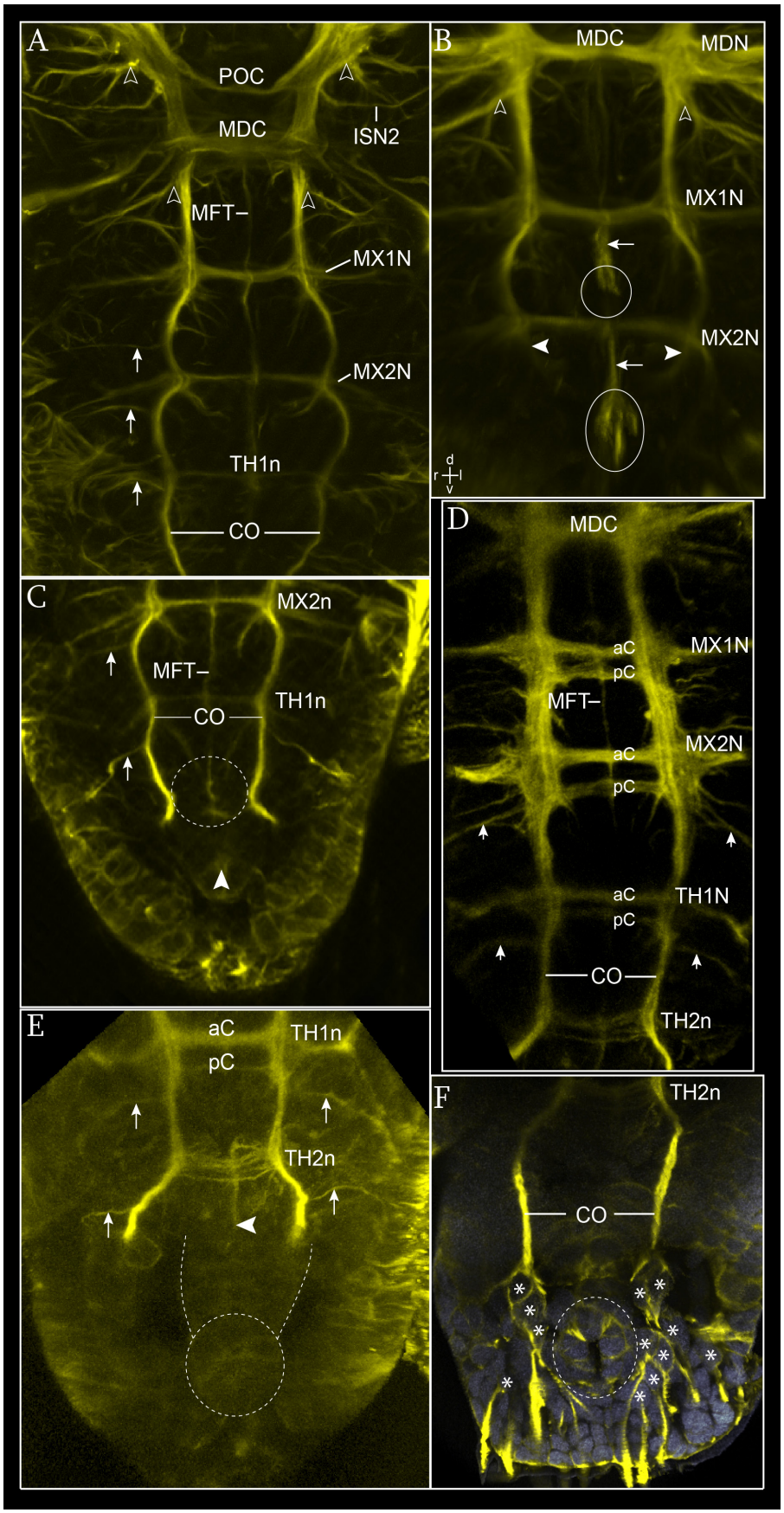

Fig. 25 – Axogenesis in the ventral nerve cord of *M. norvegica*, metanauplius stage

Anti-ac-α-tubulin labelling in yellow. Sytox-green staining in grey. CLSM image stack. Imaris surpass mode: volume (blend in **F**), clipping plane. **A-C -** General overview of the anlage of the ventral nerve cord in the early phase of the stage. **A –** View f the first three post-naupliar neuromeres anlagen (ventral view)Open arrowheads point at the dorso-lateral neurite bundles which run out from the dorsal cell cluster in the tritocerebrum and mandibular neuromeres and extend into the connective. Arrows point at the inter-segmental nerves. **B -** View of the anlage of the ventral nerve cord in the region comprised between the mandibular and the maxilla 2 neuromeres (antero-ventral view). Open arrowheads point at the dorsal neurite bundle running out from the dorsal cell cluster in the mandibular neuromere into the connective. Arrows point at the ventro-median projection spanned between the commissures and a ventral median cell cluster in the external ectodermal layer (circles). Filled arrowheads point at median neurite bundles sent by paired median cell clusters posterior to maxilla 2 commissure. **C -** View of the posterior end of the developing ventral nerve cord (ventral view). Arrows point at the inter-segmental nerves. A stippled circle marks the region of the posterior end of the median fiber tract. Filled arrowhead marks the position of the proctodeum. **D-F -** General overview of the developing ventral nerve cord in the late phase of the stage (ventral view). **D –** View of the first four post-naupliar neuromeres. Arrows point at the inter-segmental nerves. Note the antero-posterior developmental gradient. **E -** View of the posterior end of the ventral nerve cord (ventral view). Open arrowhead marks the posterior end of the median fiber tract. Stippled lines mark the borders of the proctodeum. **F -** Detail of the terminal portion of the ventral nerve cord and of the telson (ventral view). Asterisks mark single cell somata of the terminal cell cluster. A stippled circle marks the position of the proctodeum.

aC: anterior commissure; CO: connective; ISN2: inter-segmental nerve 2; MD: mandibular nerve; MDC: mandibular commissure: MFT: median fiber tract; MX1, 2: maxilla 1, 2; MX1, 2N: maxilla 1, 2 nerve; pC: posterior commissure; POC: post-oral commissure; TH1, 2N: thoracomere 1, 2 nerve; TH1, 2n: thoracomere 1, 2.

Stomatogastric nervous system

The general architecture of the stomatogastric nervous system has become more compact (Fig. 26). The labral and the stomodeal commissures have become thicker and are medially connected by a thin neurite bundle which continues ventrally the extension of the stomatogastric nerve and meets anteriorly the inferior ventricular nerve (arrow in Fig. 26B) with, possibly, the intercalation of neural somata (interneurons) (transparent ovals in Fig. 26B). Moreover, in some samples, a transversal thin neurite is observable spanned between the two branches of the labral commissure (open arrowhead in Fig. 26B). Several thick fibers with a symmetric distribution are stained around the stomodeum. Some are connected with cell clusters (transparent ovals in Fig. 26A) and probably correspond to the anlage of sensory structures of the forming mouth apparatus (open arrowheads in Fig. 26A), while others are intercalated among the neurite bundles and may represent some muscle anlagen (e.g. filled arrowheads in Fig. 26B).

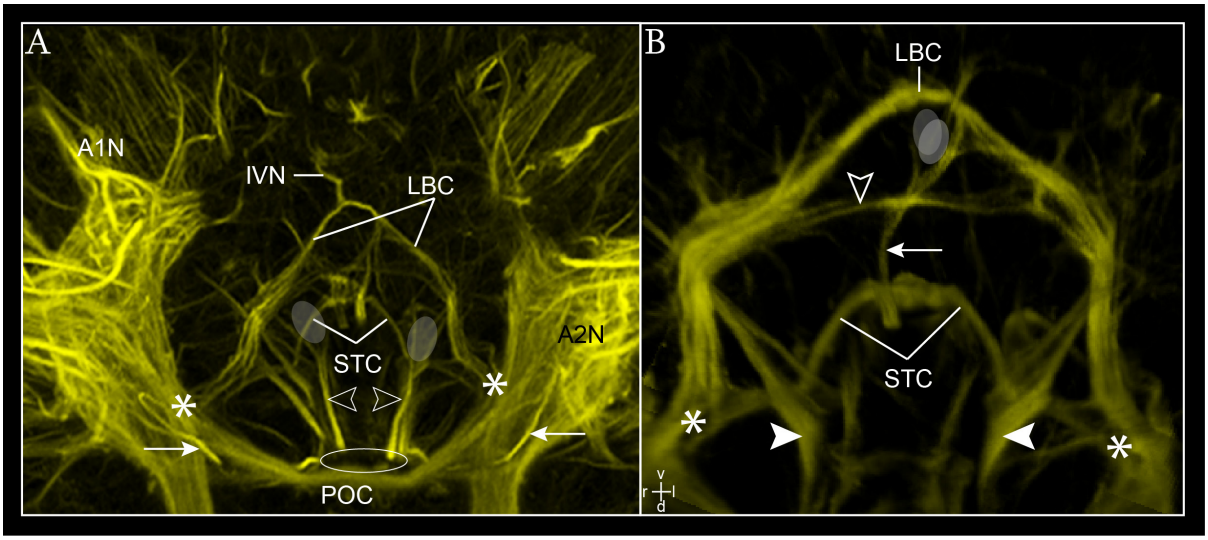

Fig. 26 – Development of the stomatogastric nervous system in *M. norvegica*, metanauplius stage

Anti-ac-α-tubulin labelling. CLSM image stack. Imaris surpass mode: volume, clipping plane. Asterisks label the region of connection of the two commissures with the connective. **A -** General overview (ventral view). The antero-dorsal portion of the image stack has been cut out from the picture (e.g. the pre-oral commissure). The white circle marks the position of the stomodeum opening. Open arrowheads point at putative sensory fibers around the stomodeum, while the transparent ovals mark the position of their associated cell clusters. Asterisks mark the point of intersection among the labral, the stomodeal, the post-oral commissures, and a lateral neurite bundle which runs ventrally into the labrum (arrow). **B -** Detail the ventral portion of the stomatogastric nervous system (postero-ventral view). Open arrowhead points at one additional transversal neurite bundle spanned between the lateral sides of the labral commissure. Arrow points to the prolongation of the stomatogastric nerve medially connecting the labral to the stomodeal commissure. Transparent ovals mark the putative cell somata intercalated between the stomatogastric and the inferior ventricular nerve at the level of the labra commissure. Filled arrowheads point at putative muscle anlagen around the stomodeum.

A1N: antenna 1 nerve; A2N: antenna 2 nerve; IVN: inferior ventricular nerve; LBC: labral commissure; POC: post-oral commissure; STC: stomodeal commissure.

Serotonin-like expression pattern

In the earliest phase of the stage SL-ir structures are still restricted to the naupliar region (Fig. 27A, B). In the protocerebral region two additional SL-ir cell somata occur at each side of the commissural neuropil (asterisks in Fig. 27) dorsal to the paired couple already observed in the previous stage (stars in Fig. 27A, B). The SL-ir distribution has extended dorsally along the frontal tract (open arrowhead in Fig. 27B) and postero-laterally along the nerve ring into the deutocerebral region (filled arrowhead in Fig. 27B). The postero-median region comprised among the three cups of the nauplius eye complex, which includes the two pigment cells, is transiently stained in some specimens (Fig. 27A, B). This probably represents an artefact rather than a specific SL immunoreactivity of the pigment cells.

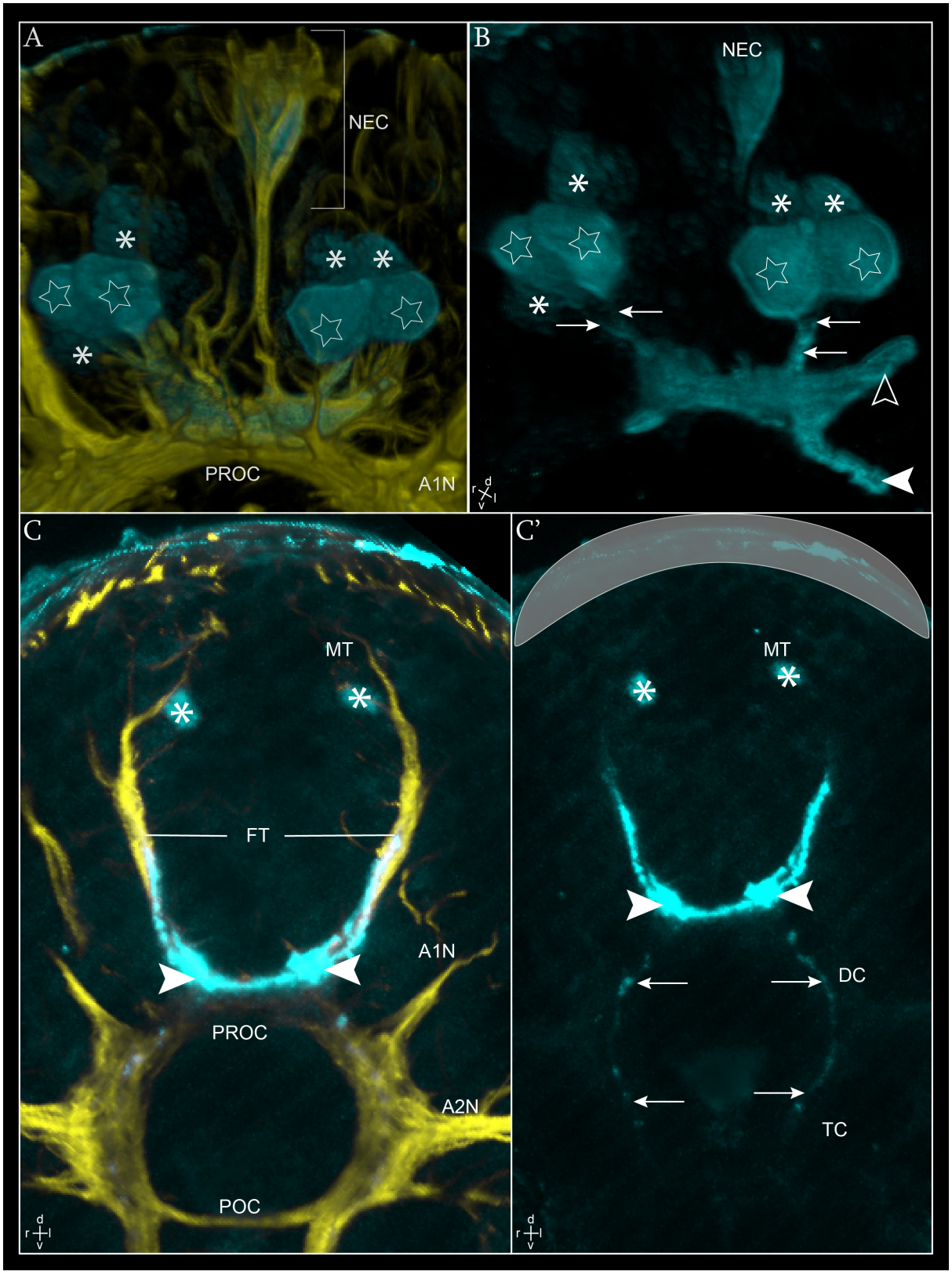

Fig. 27 – Distribution of Sl-ir structures in the naupliar region of *M. norvegica*, metanauplius stage

Anti-ac-α-tubulin labelling. Anti-serotonin-like labelling in light blue. CLSM image stack. Imaris surpass mode: volume (blend in **A**, **B**), clipping plane. **A**, **B –** View of the protocerebral region in the early phase of the stage (ventral view in **A**, ventro-lateral view in **B**). Stars mark SL-ir neurons in the same location as observe in the previous stage. Asterisks mark additional SL-ir neurons. Arrows point at single SL-ir

neurites connecting the ventral SL-ir neurons to the pre-oral commissure. Open arrowhead marks the dorsal extension into the SL-ir frontal tract. Filled arrowhead marks the posterior extension of SL signal along the connective into the deutocerebral region.

C, **C' -** Distribution of SL-ir structures in a slightly later phase of the stage (antero-ventral view). Asterisks mark the paired SL-ir neurons of the frontal organ center within the medulla terminalis. Filled arrowheads point at the antero-dorsal portion of the pre-oral commissure. In **C'** the transparent area at the top of the image covers the dorsal 'head' shield. Arrows mark the posterior extension of SL signal along the connective of the nerve ring.

A1N: antenna 1 nerve; A2N: antenna 2 nerve; DC: deutocerebrum; FT: frontal tract; MT: medulla terminalis; NEC: nauplius eye complex; POC: post-oral commissure; PROC: pre-oral commissure; TC: tritocerebrum.

Slightly later in development (Fig. 27C, C'), also the dorsal portion of the frontal tract expresses serotonin-like (Fig. 27 C) and one pair of SL-ir cell somata has occurred in the dorsal portion of the medulla terminalis. They mark a pair of neurons connected to the frontal organ marking the frontal organ center (asterisks in Fig. 27 C, C'). Moreover, a feeble SL-ir signal occurs along the connectives of the nerve ring reaching the level of the tritocerebral region (arrows in Fig. 27C').

At the latest phase of the stage, additional SL-ir cell somata are recognizable in the naupliar region and SL-ir structures have developed further posterior in the post-naupliar region (Fig. 28). In the protocerebral region, three paired SL-ir neurons are located ventro-lateral to the pre-oral commissure (asterisks in Fig. 28B) and two additional paired SL-ir neurons occurs more dorsally postero-lateral to the nauplius eye complex (asterisks in Fig. 28D). Further dorsally, SL-ir two paired lateral neurons are observable along the same plane, postero-dorsal to the frontal organs (arrowheads in Fig. 28C and E), posterior to the frontal tract (open arrowheads in Fig. 28C), and at the level of the deuto-, tritocerebrum and mandibular neuromere (Fig. 28C). This regular distribution of paired lateral SL-ir neurons occurs in the same plane in the first three post-naupliar neuromeres (Fig. 28E). The SL signal in the antero-dorsal portion of the pre-oral commissure has noticeably increased (Fig. 28D) possibly signing the development of the central complex anlage. In the naupliar region: SLI has extended further posterior to the postero-ventral component of the pre-oral commissure and along the connective until the mandibular neuromere (Fig. 28D). Also the post-oral and the mandibular commissures are slightly stained (Fig. 28D).

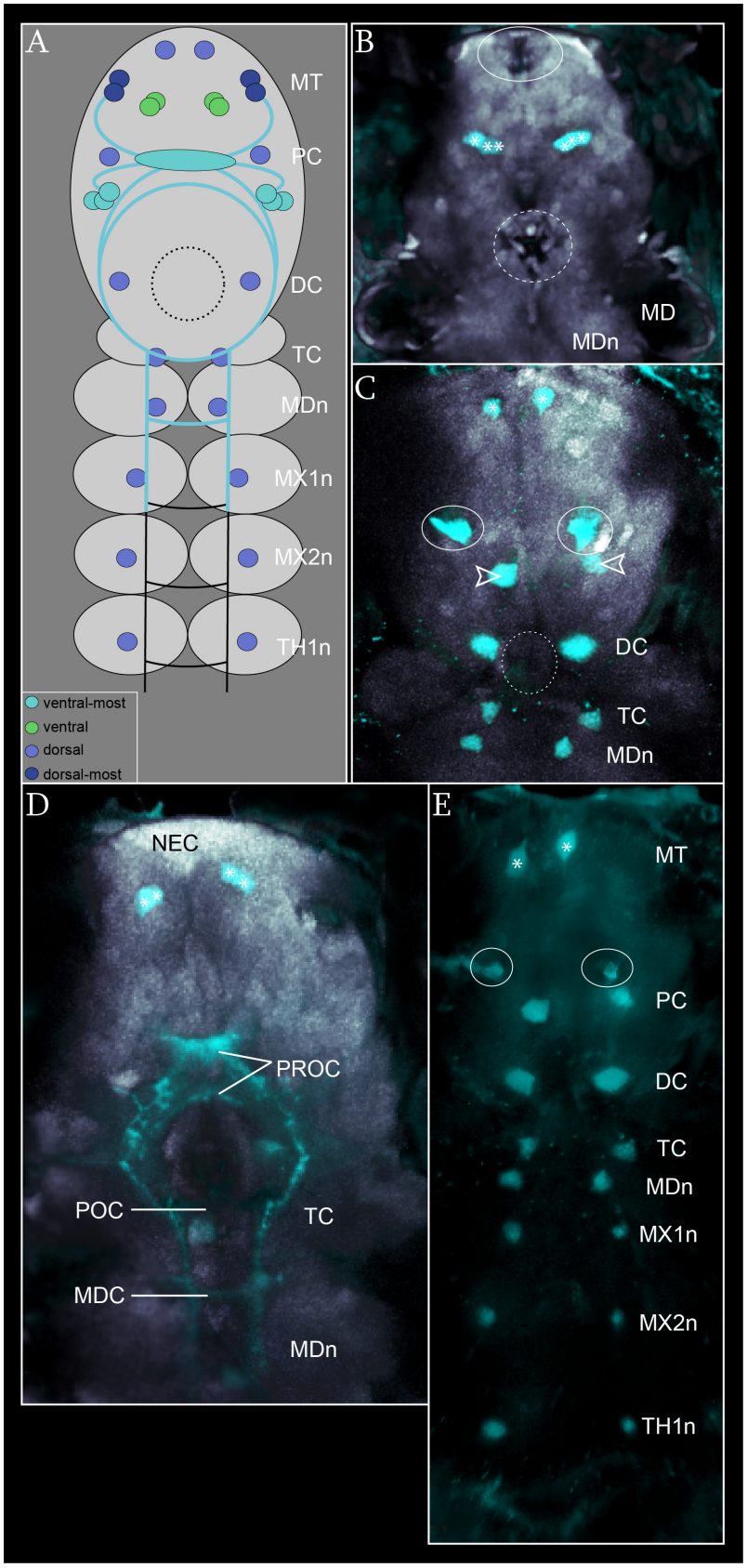

Fig. 28 – Distribution of SL-ir structures in *M. norvegica*, late metanauplius stage

A - Schematic illustration of the distribution of SL-ir neurons, neuropils and neurite bundles (ventral view). Coloured circles correspond to single SL-ir cell somata. Different colours are assigned to distinguish

their location along the z-axis (see figure legend). The median light blue oval marks the anlage of the central complex neuropil.

B-E - Anti-serotonin labelling in light blue. Sytox-green staining in grey. CLSM image stack. Imaris: surpass mode: oblique slicer. **B-D –** View of the naupliar region (ventral view).The three images have been performed with the same plane orientation at different depth along the z-axis of the sample: the most ventral plane in **B**, the most dorsal plane in **C** and the intermediate plane in **D**. **B –** The white circle marks the region of the nauplius eye complex. A stippled circle marks the region of the stomodeum. Asterisks point at single SL-ir neurons located antero-ventrally to the pre-oral commissure. **C –** White circles mark the position of the frontal tract. A stippled circle marks the position of the stomodeum. Asterisks point at single SL-ir neurons in the frontal organ center within the medulla terminalis. Open arrowheads point at single protocerebral SL-ir neurons posterior to the frontal tract (marked by circles). **D -** Asterisks point at single SL-ir neurons postero-lateral to the nauplius eye complex. The SLI has extended along the connective posterior to the mandibular neuromere. **E -** View of the dorsal-most side of the larva (ventral view). White circles mark the position of the frontal tract. Asterisks mark single SL-ir neurons of the frontal organ center within the medulla terminalis.

DC: deutocerebrum; MD: mandible; MDC: mandibular commissure; MDN: mandibular neuromere; MT: medulla terminalis; MX1n: maxilla 1 neuromere; MX2n: maxilla 2 neuromere; PC: protocerebrum; POC: post-oral commissure; PROC: pre-oral commissure; TH1n: thoracomere1; TC: tritocerebrum.

3.1.2.6 Calyptopis stage 1

Axogenesis

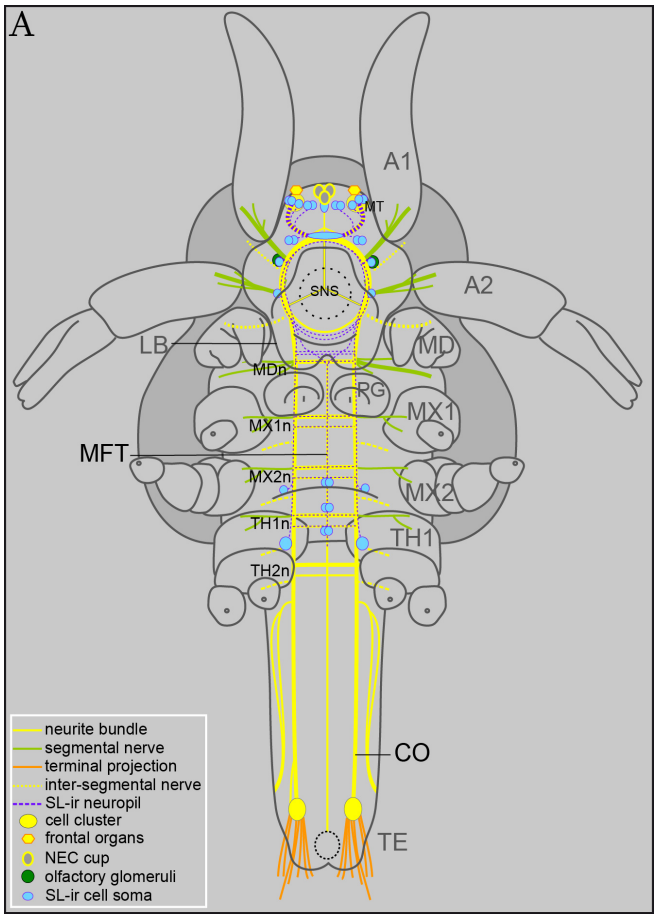

Fig. 29 - *M. norvegica*, calyptopis stage 1

Schematic illustration of the distribution of neural structures (ventral view). The carapace edge is represented by the dark grey frame around the body shape. Only the ventral portion of the SNS is represented. The region of the stomodeum is marked by black circular stippled line. The small stippled circle in the telson represents the proctodeum.

A1: antenna 1; A2: antenna 2; CO: connective; LB: labrum; MD: mandible; MDC: mandibular commissure; MDn: mandibular neuromere; MFT: median fiber tract; MT: medulla terminalis; MX1: maxilla 1; MX1n: maxilla 1 neuromere; MX2: maxilla 2; MX2n: maxilla 2 neuromere; PG: paragnaths; SNS: stomatogastric nervous system; TE: telson; TH1: thoracopod 1; TH1n: thoracopod 1 neuromere; TH2n: thoracopod 2 neuromere.

The condensation process of the neurite bundles proceeds further, and extends posteriorly into the post-naupliar neuromeres. A decrease of the α-tubulin signal is observed especially in some region of the brain. Nonetheless, a consistent thickening of all the main neurite bundles can be observed (Fig. 30). In the naupliar region the pre-oral commissure shows an intense signal which does not allow distinguishing individual structures but presumably corresponds to the increment of neural structures forming the anlage of the central complex (Fig. 30A). The posterior component of the pre-oral commissure is, on the contrary, only weakly stained (Fig. 30A). In the deutocerebral region the anlage of the olfactory glomeruli has formed ventro-posterior to the root of antenna 1, strictly adjacent to it and to the connective of the nerve ring (Fig. 30A). Only one thin neurite bundle of the post-oral commissure can be visualized (Fig. 30A). The mandibular commissure appears as a thick single transversal tract (Fig. 30A). The distance between the post-oral and the mandibular commissures has increased further. In between the two commissures, dorsally, one transversal structure is stained and is not connected with neural structures (stippled circle in Fig. 30A). This consists of a group of median cells and lateral projections (filled arrowheads in Fig. 30A) which probably correspond to glia cells and their processes, respectively. Both the segmental nerves of antenna 1 and 2 have increased diameter (Fig. 30A). The double composition of antenna 2 nerve root can be still distinguished (Fig. 30A). Three distinct lateral neurite bundles come out from the mandibular neuromere and extend into the limb (arrows in Fig. 30A). Eventually the mandibular neuromere is separate from the naupliar brain and is closer to the more posterior post-naupliar neuromere, i.e. the maxilla 1 neuromere (Fig. 30A).

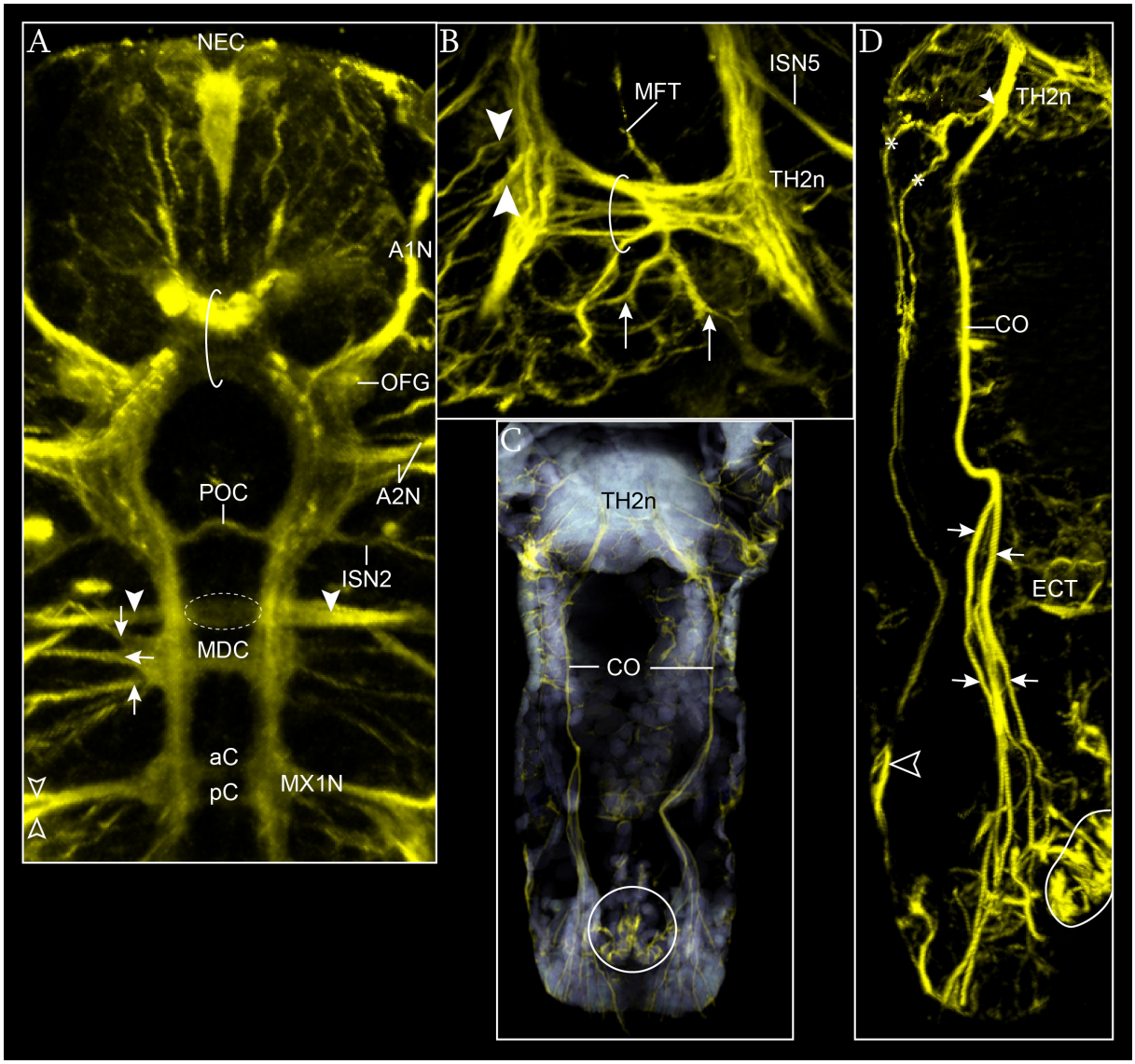

Fig. 30 - Axogenesis in *M. norvegica*, calyptopis stage1

Anti-ac-α-tubulin labelling in yellow. Sytox-green staining in grey. CLSM image stack. Imaris: surpass mode: volume, clipping plane. **A -** General overview of the naupliar region and of the maxilla 1 neuromere (ventral view). The extension of the pre-oral commissure is marked by open circle. A stippled circle marks the dorsal location of putative glia cells and filled arrowheads point at their lateral projections. Small arrows point at single lateral neurite bundles of the mandibular neuromere. **B**-**D -** Axogenesis in the post-naupliar region (ventral view). **B -** Detail of thoracomere 2 anlage. The open circle marks the commissure anlage. Filled arrowheads point at the two neurite bundles of segmental nerve anlage. Arrows point at the two terminal branches of the median fiber tract. **C -** General overview of the region posterior to the thoracomere 2. The white circle marks the position of the proctodeum. **D -** General overview of the half terminal portion of the connective. The profile section of the proctodeum is marked by a white line. Filled arrowhead points at the level in which one neurite bundle run off laterally from the connective. Asterisks mark the two of its posterior branches. The open arrowhead marks the end point in the telson of the two connectival branches. Arrows point at the terminal branches of the connectives.

aC: anterior commissure; A1N: antenna 1 nerve; A2N: antenna 2 nerve; CO: connectives; ECT: ectoteloblast ring; ISN2, 5: inter-segmental nerve 2, 5; MDC: mandibular commissure; MFT: median fiber tract; MX1N: maxilla 1 nerve; NEC: nauplius eye complex; OFG: olfactory glomeruli; pC: posterior commissure; POC: post-oral commissure; TH2: thoracomere2; TH2n: thoracomere 2 neuromere.

In the post-naupliar region, the maxilla 1 and 2 neuromeres and thoracomere 1 share a common architecture with the presence of two distinct commissural bundles and one single segmental nerve root. Each segmental nerve bifurcates into two branches which enter the limbs (e.g. open arrowheads in Fig. 30A). Posterior to the segmental nerve of thoracomere 1 the inter-segmental 5 nerve has formed (Fig. 30B). The diameter of the connective has increased, reinforcing the connection between the forming neuromeres. Additional neurites have formed at the level of the anlage of thoracomere 2 commissure and the primordium of the corresponding segmental nerve is composed of two slender neurite bundles (filled arrowheads in Fig. 30B). Posterior to the thoracomere 2 commissure, the median fiber tract ends bifurcating into two branches within the neuromere (arrows in Fig. 30B). At the same level, lateral to the connective one neurite bundle runs transversally out (filled arrowhead in Fig. 30D) and bifurcates into two long branches which turn to the posterior and run parallel to the connectives (asterisks in Fig. 30D). These end quite together at the dorso-lateral side of the telson (open arrowhead in Fig. 30C, D). Posterior to the thoracomere 2, the connective is thinner than in its anterior portion (Fig. 30D). Anterior to the level of the ectoteloblasts ring several branches of the connective (arrows in Fig. 20D) terminate posteriorly into the terminal spines lateral to the proctodeum (Fig. 30C, D).

Stomatogastric nervous system

The architecture of the stomatogastric nervous system could not be followed consistently at this stage.

Serotonin-like expression pattern

Additional SL-ir cell somata have formed in the protocerebral region and in particular in the dorsal-most portion of the medulla terminalis (small ovals in Fig. 31A). Some of these are connected to the dorsal-most portion of the frontal tract via a thin short SL-ir neurite. One SL-ir neuron of the frontal organ center (asterisk in Fig. 31A) is now distinctively connected by a SL-ir neurite to the SL-ir neuropil of the frontal tract (arrow in Fig. 31A). Also the pair of SL-ir neuron associated with the nauplius eye complex (stars in Fig. 31A) is connected via a slender SL-ir neurite to the proximal portion of the frontal tract (arrow in Fig. 31A). One pair of SL-ir neurons is located antero-ventrally to the pre-oral commissure (filled arrowheads in Fig. 31A). At the level of the antenna 1 nerve root the olfactory glomeruli anlage shows a diffused and weak SL signal (Fig. 31A) while one short SL-ir neurite surrounds its anterior margin (open arrowhead in Fig. 31A). Postero-ventrally to the root of antenna 2 nerve, one

additional SL-ir has formed (white circle in Fig. 31A). In general, the SL expression has noticeably increased and a meshwork of SL-ir neurites has formed all around the nerve ring and along the frontal tract (Fig. 31A, B). Especially the signal in the region of the anlage of the central complex is very intense and does not allow distinguishing individual structures (Fig. 31B). Two transversal thin SL-ir neurites have formed at the level of the post-oral commissure (open arrowheads in Fig. 31B'). They lie ventrally and slightly posterior to the neurite bundle stained by α-tubulin. Several distinct SL-ir neurites are also observable at the level of the mandibular commissure (Fig. 31B, B'). At this level, one lateral longitudinal SL-ir neurite running from anterior along the internal margin of the connectives (filled arrowheads in Fig. 31B') crosses the midline and meets the contra-lateral forming a median SL-ir neurite bundle corresponding to the median fiber tract (Fig. 31B, B'). This extends posteriorly reaching the region posterior to the thoracomere 1 commissure (filled arrowhead in Fig. 31B).

In the post-naupliar region one median pair of SL-ir cell somata have formed anterior and posterior to each commissure from maxilla 1 to thoracomere 1. Each pair is formed by one ventral and one dorsal soma (white and stippled circles, respectively in Fig. 31C). Moreover, dorso-lateral paired SL-ir somata are observable at the level of maxilla 2 neuromere and thoracomere 1 (asterisks in Fig. 31C). They are connected by single SL-ir neurites to the connective at the level of the posterior portion of the corresponding commissures (arrows in Fig. 31C). The dorso-lateral SL-ir neuron of thoracomere 1 is a large cell soma posterior to the neuromere (Fig. 31C) additionally connected with a dorso-lateral SL-ir longitudinal connective (filled arrowhead in Fig. 31C). This last is covered by several distinctive SL-ir neurites which reach the thoracomere 2. Each post-naupliar neuromere shows two to three transversal SL-ir neurites at the lever of the corresponding commissures (Fig. 31B, C). Noticeably, in some samples, one single transversal SL-ir neurite is observed spanning between the mandibular and the maxilla 1 neuromeres (small arrow in Fig. 31B).

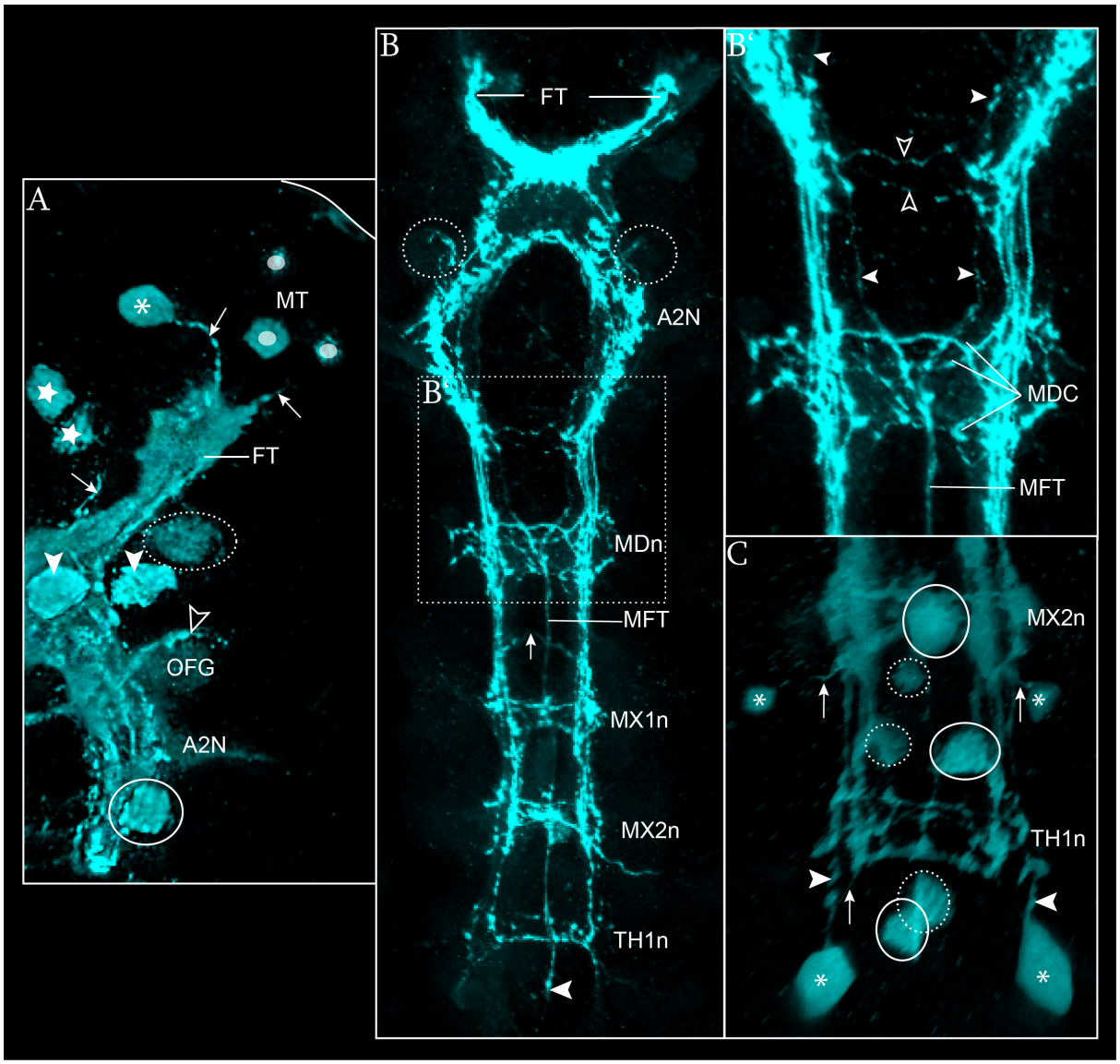

Fig. 31 - Distribution of SL-ir structures in *M. norvegica*, calyptopis stage 1

Anti-serotonin labeling. CLSM image stack. Imaris: surpass mode: volume (blend in **A**), clipping plane. **A -** View of the left half of the anterior brain (ventral view). The sample has been slightly tilted to the right side. Arrows point at single neurites connecting single neurons to the frontal tract. Small ovals mark the neurons in the dorsal portion of the medulla terminalis. The asterisk marks the neuron of the frontal organ center. Stars mark the pair of neurons associated with the nauplius eye complex. The stippled oval marks the neuron dorsal to the frontal tract. Filled arrowheads point at the ventral-most pair of neurons. Open arrowhead points at the short lateral neurite associated with the olfactory glomeruli (diffusely stained underneath). The white circle marks the ventral neuron posterior to the antenna 2 nerve root. **B, B' -** Distribution of SL-ir neuropils (ventral view). **B -** General overview. Stippled circles mark the position of the olfactory glomeruli anlagen. The filled arrowhead points at the posterior end of the median fiber tract. **B' -** Detail of the posterior portion of the naupliar region. Open arrowheads point at single neurites of the post-oral commissure. Filled arrowheads point at the anterior extension of the two anterior branches forming the median fiber tract. **C -** Detail of the maxilla2 neuromere and of thoracomere1 (ventral view). White circles mark the medio-ventral neurons. Stippled circles mark the medio-dorsal neurons. Asterisks mark dorso-lateral neurons. Arrows point at single neurites connecting the dorso-lateral cell somata to the connectives. Filled arrowheads mark the connectival dorso-lateral components.

A2N: antenna 2 nerve; FT: frontal tract; MDC: mandibular commissure; MDn: mandibular neuromere; MFT: median fiber tract; MT: medulla terminalis; MX1n: maxilla 1 neuromere; MX2n: maxilla 2 neuromere; OFG: olfactory glomeruli; TH1n: thoracomere1.

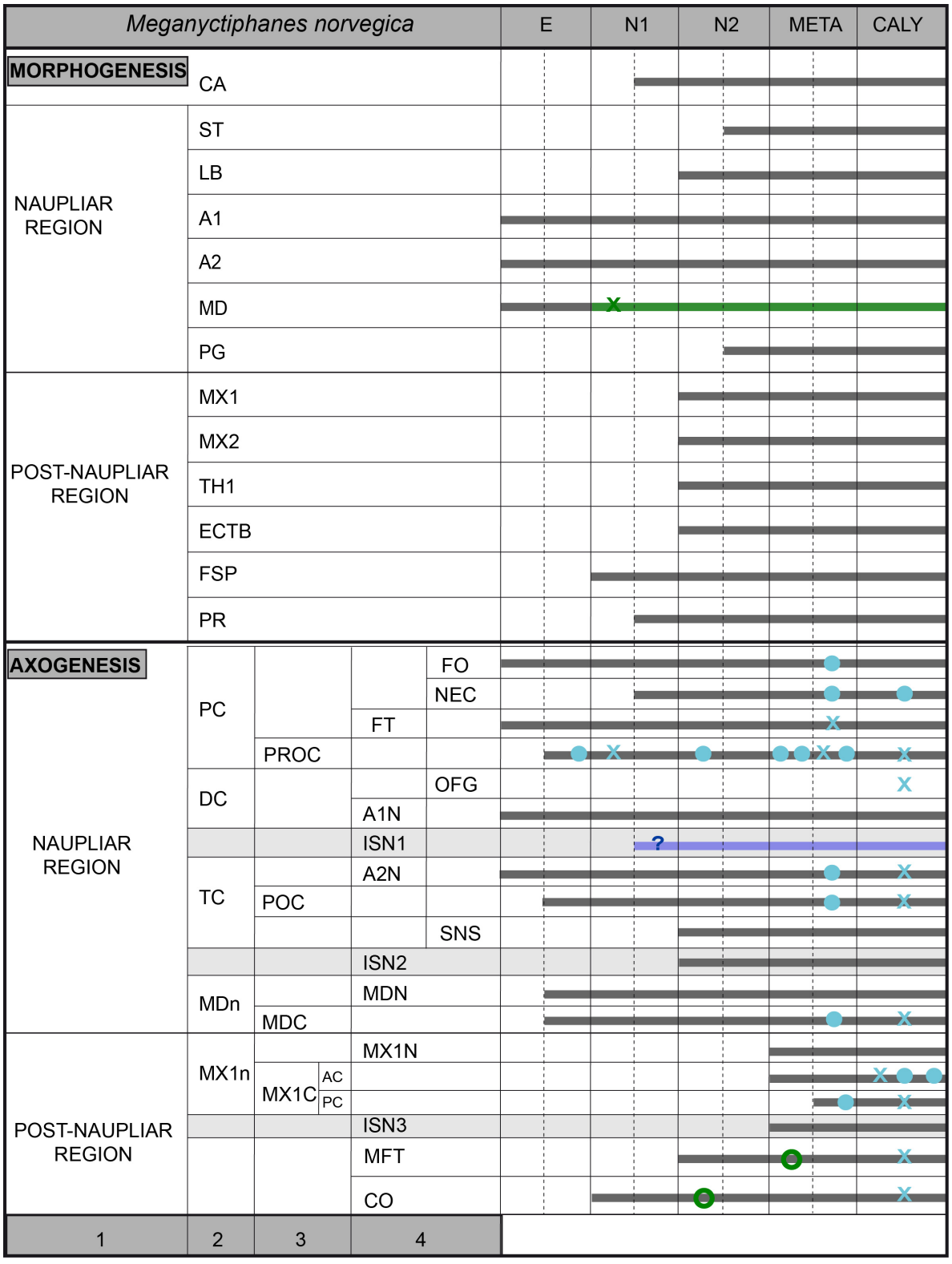

Table 3 - Summary of the main developmental events in *M. norvegica*

The anlagen of the main external morphological structures (**MORPHOGENESIS**) and of the relevant neural components (**AXOGENESIS**) are listed in the rows. They are ordered following the antero-posterior axis of the animal. The developmental stages are listed in the columns (**E**: embryonic stage; **N1**: nauplius stage 1; **N2**: nauplius stage 2; **META**: metanauplius stage; **CALY**: calyptopis 1 stage). Each stage is subdivided into two phases (one early and one late) separated by a vertical stippled line. The characters are organized in four columns (numbers at the bottom of the table) referring to: **1**=body regions; **2**=neuromeres;

3=commissures; **4**=neurite bundles. The **green X** marks the time in which the mandibles are transformed from functional limbs into components of the prospective mouth apparatus. The **green rings** mark the time in which the median fiber tract has reached the proctodeum (early phase of the metanauplius stage), and the time in which connectives have established their connection with the naupliar neuromeres (early phase of the nauplius 2 stage). The inter-segmental nerve 2 has not been identified but its presence is possible (**blue question mark**). The distribution of SL immunoreactivity in the neuraxis (**light–blue X**) and in the neural somata (**light blue circles**) is indicated. The inter-segmental nerves are underlined by light-grey to simplify the reading of the table.

Abbreviations are as indicated in the **List of abbreviations**.

3.2 *Penaeus monodon*

General remarks on the used staging system

The traditional staging system of *P. monodon* is based on intervals between moults after hatching and main changes of the external morphological characters (e.g. Motoh 1981). In this way six nauplius stages have been described before the first post-nauplius stage, i.e. the protozoea 1 stage. However, performing the present investigation has put on light how the changes of the nervous system during larval development do not strictly follow the staging system imposed by moults intervals. Instead, they follow relative broader time intervals, each including, roughly, two of the traditional nauplius stages. In this way, the description of development of the nervous system of the nauplii of *P. monodon* has been divided into three developmental stages called, in reference to the traditional staging nomenclature: nauplius 1-2, nauplius 3-4, nauplius 5-6. The last nauplius stage (stage 5-6) corresponds to the metanauplius stage (see Table 4 and Fig. 32). Changes occurring in a shorter time interval within the stage, if any, have been referred as happening within early or late phases of the corresponding stage. Eventually, one embryonic, two nauplius, one metanauplius and one protozoea stages are described in this chapter. Moreover, some observations on the nervous system development of protozoea stage 2 and 3 are included at the end of the section.

THIS STUDY	MOTOH (1981)
EMBRYONIC STAGE	Late embryonic stage
NAUPLIUS STAGE I	Nauplius 1 Nauplius 2
NAUPLIUS STAGE II	Nauplius 3 Nauplius 4
METANAUPLIUS STAGE	Nauplius 5 Nauplius 6

Table 4 - Correspondence of the staging system used in the present study and the traditional staging system referred to Motoh (1981)

3.2.1 Morphogenesis

Morphogenesis has not been followed in detail but some changes of the external morphology which run in parallel with neural differentiation have been highlighted (Fig. 32) and summarized in Table 5.

	E	N1-2	N3-4	N5-6 (MetaN)	Z1
Antenna 1		(uniramus)			
Antenna 2	(limb bud)	(biramus)			
Carapace					
Frontal organ				(Protruded)	
Terminal spines n.	1	3 (1ml +2 ls)	4 (1ml+2ls+1ls)	6 (1ml+2ls+3ls)	
Labrum			(protruded)	(extended)	
Mandible	(limb bud)	(biramus)			
Maxilla 1			(limb bud)	(biramus)	
Maxilla 2			(limb bud)	(biramus)	
Paragnath					
Proctodeum					
Thoracopod 1			(limb bud)	(biramus)	
Thoracopod 2			(limb bud)	(biramus)	
Thoracopod 3					

Table 5 – Formation and modification of the main external morphological characters during development of *P. monodon*

Characters are listed in the left column in alphabetical order. The number of terminal spines follows the nomenclature given by Motoh (1981): **ml**: median long; **ls**: lateral short. **E**: embryonic stage; **N**: nauplius stage; **MetaN**: metanauplius stage: **Z**: protozoea stage.

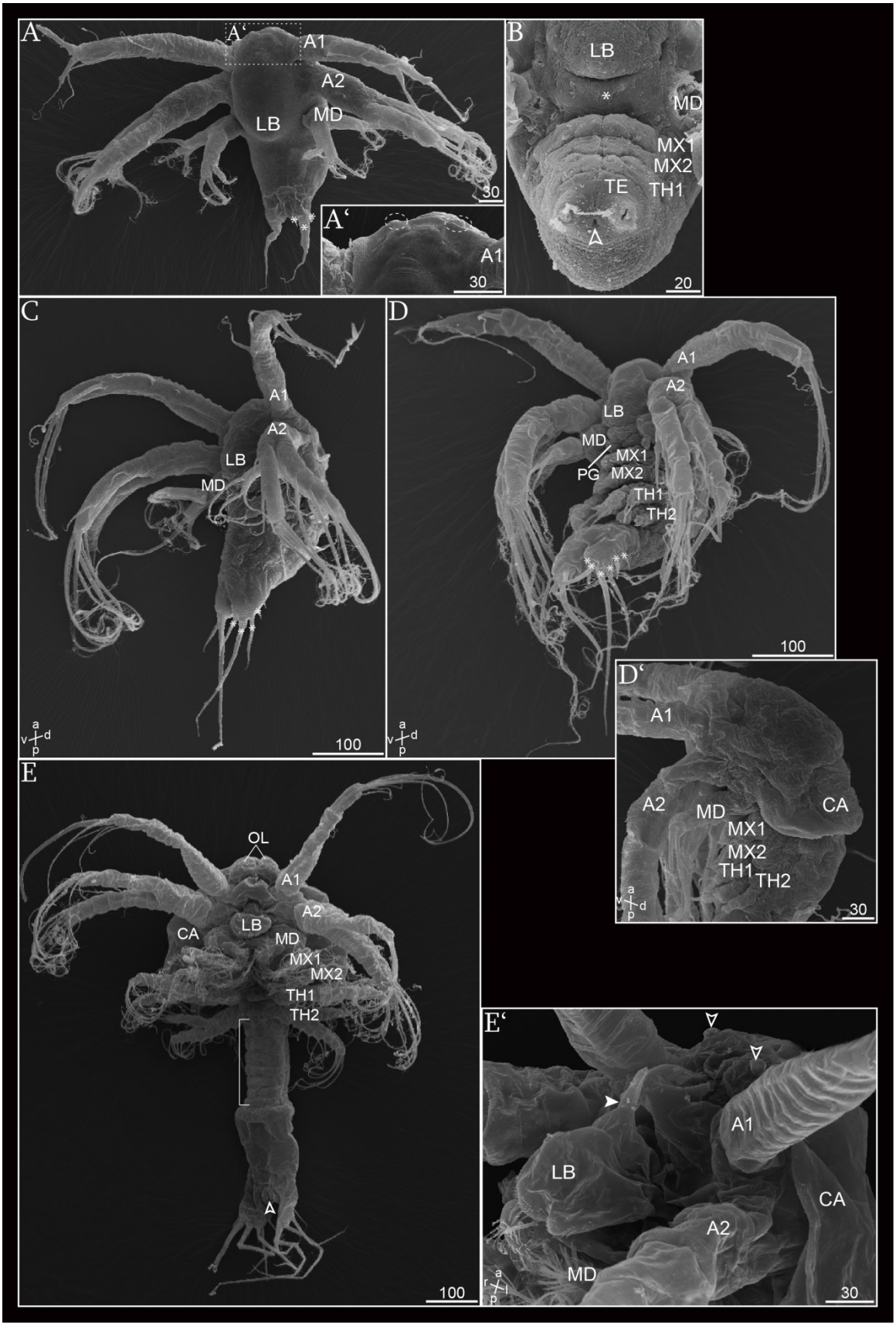

Fig. 32 - Morphogenesis in *P. monodon*

SEM micrographs. The cuticle has been manually dissected in **A-B** and partially in **D**. **A**, **A' -** Nauplius stage 1-2 [Nauplius 2 *sensu* Motoh (1981)] (ventral view). **A -** General overview. Asterisks mark single terminal spines. **A' -** Detail of the anterior pole of the nauplius. Stippled circles mark the position of the frontal organ anlagen. **B -** Nauplius stage 3-4 [Nauplius 3 *sensu* Motoh (1981)]. Detail of the post-naupliar region (ventral view). The asterisk marks the median sternal region of the prospective paragnaths. Open arrowhead points at the proctodeum. **C -** Nauplius stage 3-4 [Nauplius 4 *sensu* Motoh (1981)] (ventro-lateral view). Asterisks mark single terminal spines. **D**, **D' -** Nauplius stage 5-6 (Metanauplius) [Nauplius 6 *sensu* Motoh (1981)] (ventro-lateral view in **D**; dorso-lateral view in **D'**). **D -** Asterisks mark single terminal spines. **D' -** Detail of the carapace anlage. **E**, **E' -** Protozoea stage 1 (ventral view in **E**; antero-lateral view in **E'**). **E –** The square bracket marks the thoracic region posterior to thoracopod 2 segment. Open arrowhead points at the opening of the proctodeum. **E' -** Detail of the anterior pole. Open arrowheads point at the frontal organ anlagen medially popping out at the apical surface of the optic lobes. The filled arrowhead points at the median horn at the antero-dorsal margin of the labrum. **Scale bars** are as indicated in each image in micrometer (µm).

A1: antenna 1; A2: antenna 2; CA: carapace; LB: labrum; MD: mandible; MX1, 2: maxilla 1, 2; OL: olfactory lobe; PG: paragnath; TE: telson; TH1, 2: thoracopod 1, 2.

3.2.2 Nervous system development

3.2.2.1 Embryonic stage

Axogenesis

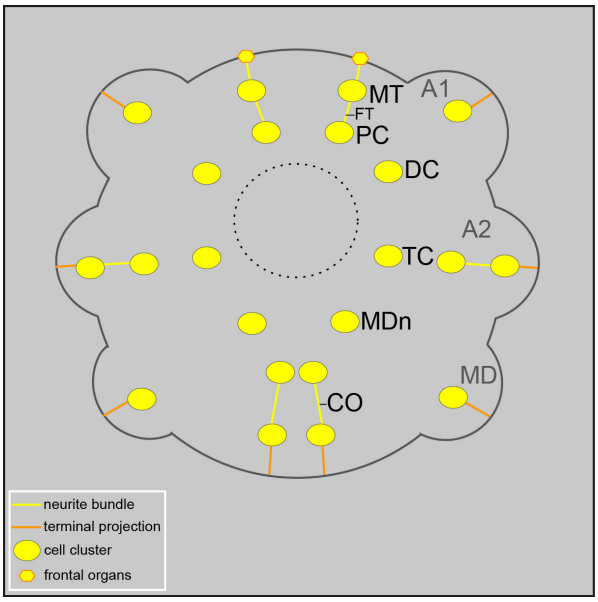

Fig. 33 - *P. monodon*, embryonic stage

Schematic illustration of the distribution of neural structures (ventral view). The region of the stomodeum is marked by a black stippled circle.

A1: antenna 1; A2: antenna 2; CO: connective; DC: deutocerebrum; FT: frontal tract; MD: mandible; MDn: mandibular neuromere; MT: medulla terminalis; PC: protocerebrum; TC: tritocerebrum.

In the naupliar region, the anlage of the brain is formed by paired cell clusters (asterisks in Fig. 34A) which surround the stomodeum (stippled circle in Fig. 34A). They represent the

anlagen of the naupliar brain neuromeres, i.e. from anterior to posterior, the protocerebrum; the deutocerebrum; the tritocerebrum; and the mandibular neuromere. Short longitudinal neural projections start to connect the clusters to each other forming the anlage of the connectives (e.g. open arrowhead in Fig. 34A). The anlage of the frontal organ is stained at the anterior pole of the embryo, dorsal to the region enclosed between the insertions of antenna 1 anlage (filled arrowheads in Fig. 34A). A feeble neural projection with a dorso-lateral course runs out the protocerebral cell cluster and connects the anlage of the medulla terminalis forming the anlage of the frontal tract (Fig. 34A). The anlage of the medulla terminalis is composed of a small number of bipolar neurons located antero-dorsally to the protocerebral cell cluster. This small cell cluster connected to the frontal organ corresponds to the frontal organ center of the prospective medulla terminalis (see Discussion) (Fig. 34A). The anlage of the segmental nerve of antenna 2 has formed (Fig. 34B, B'). This is composed of one neurite bundle which runs along the limb bud (open arrowhead in Fig. 34B'), but is not yet connected to the brain anlage (Fig. 34). Two clusters of stained cell somata are interposed along the antenna 2 nerve anlage, one proximal and one distal (asterisks in Fig. 34B') and probably contain the peripheral pioneers of the segmental nerve (see Discussion). The terminal spines at the tips of each of the three naupliar limb anlagen are also stained (e.g. antenna 2 and mandible: filled arrowheads in Fig. 34B', B").

In the post-naupliar region, two cell clusters are stained: one anterior, located posterior to the level of the mandible insertion, and one more posterior at the caudal pole of the embryo (asterisks in Fig. 34B"). This last is connected to the terminal spines, which are visibly stained at the posterior end of the embryo (arrows in Fig. 34B"), and represents the anlage of the telsonic cell cluster. A longitudinal neurite spans between the two cell clusters forming the anlage of the connective of the ventral nerve cord (open arrowheads in Fig. 34B").

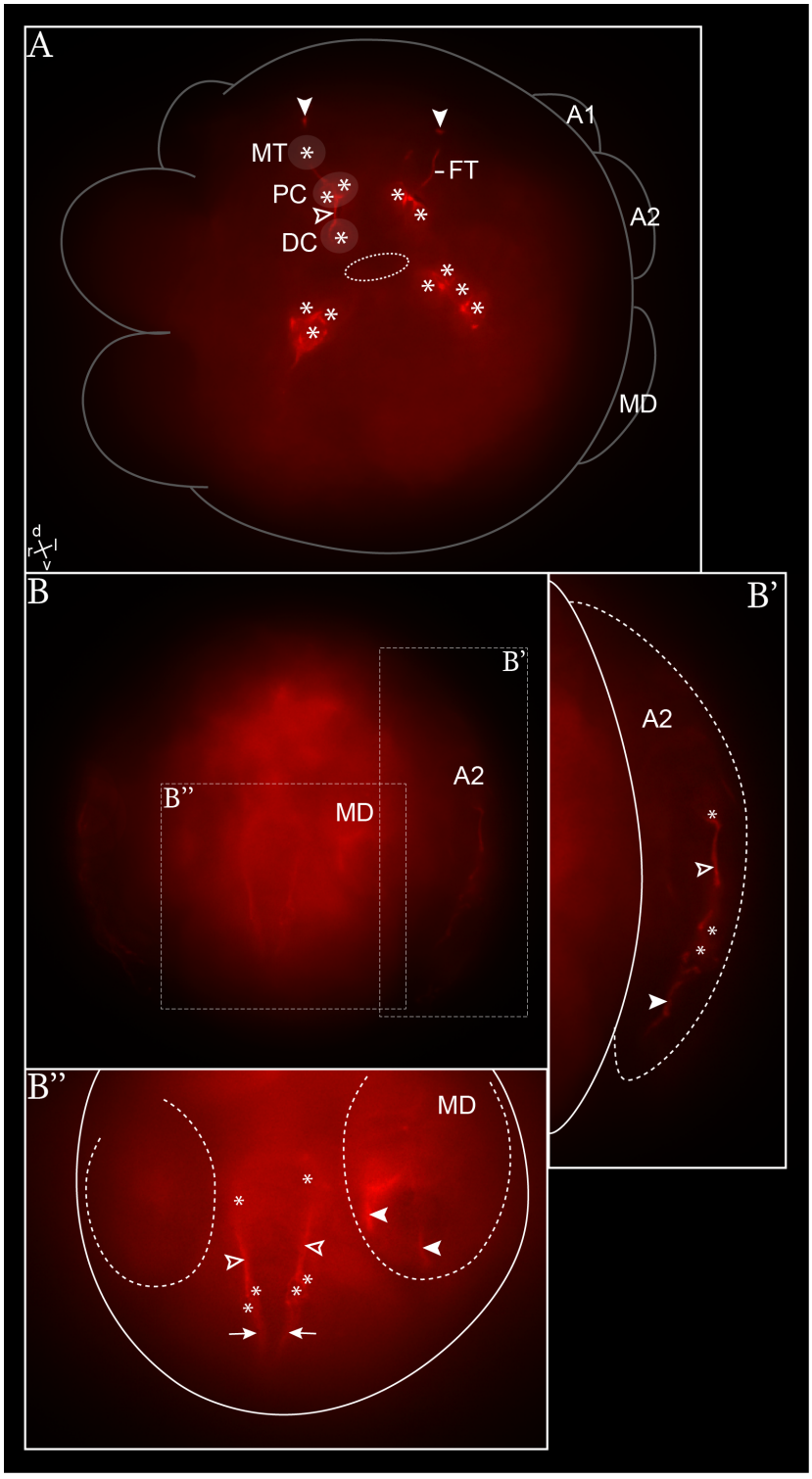

Fig. 34 - Axogenesis in *P. monodon*, embryonic stage

Anti-ac-α-tub labelling. Epifluorescence microscopic image. **A -** Overview of the naupliar brain anlage (postero-ventral view). The stippled oval marks the region of the stomodeum. Asterisks mark single cell somata within the cell clusters (transparent areas). Filled arrowheads point at the frontal organ anlagen. The open arrowhead points at a single neurite which spans between the protocerebrum and the deutocerebrum anlagen. **B**-**B" -** View of the postero-ventral side of the embryo (ventral view). Asterisks mark single cell somata. Filled arrowheads point at the terminal spines of antenna 2 anlage in **B'** and of the mandible in **B"**. **B -** General overview. **B' -** Detail of the left antenna 2 anlage neural structures. Open arrowhead points to the neurite which spans between the two cell clusters and forms the anlage of the

segmental nerve. **B" -** Detail of the post-naupliar region. Stippled lines mark the region of the mandible anlagen. Open arrowheads point at the anlage of the ventral connectives. Arrows point at the terminal spines in the telson.

A1: antenna 1; A2: antenna 2; DC: deutocerebrum; FT: frontal tract; MD: mandible; MT: medulla terminalis; PC: protocerebrum.

Serotonin-like expression pattern

No evidence of SL-ir structures emerged at this stage with the used methods.

3.2.2.2 Nauplius stage 1-2

Axogenesis

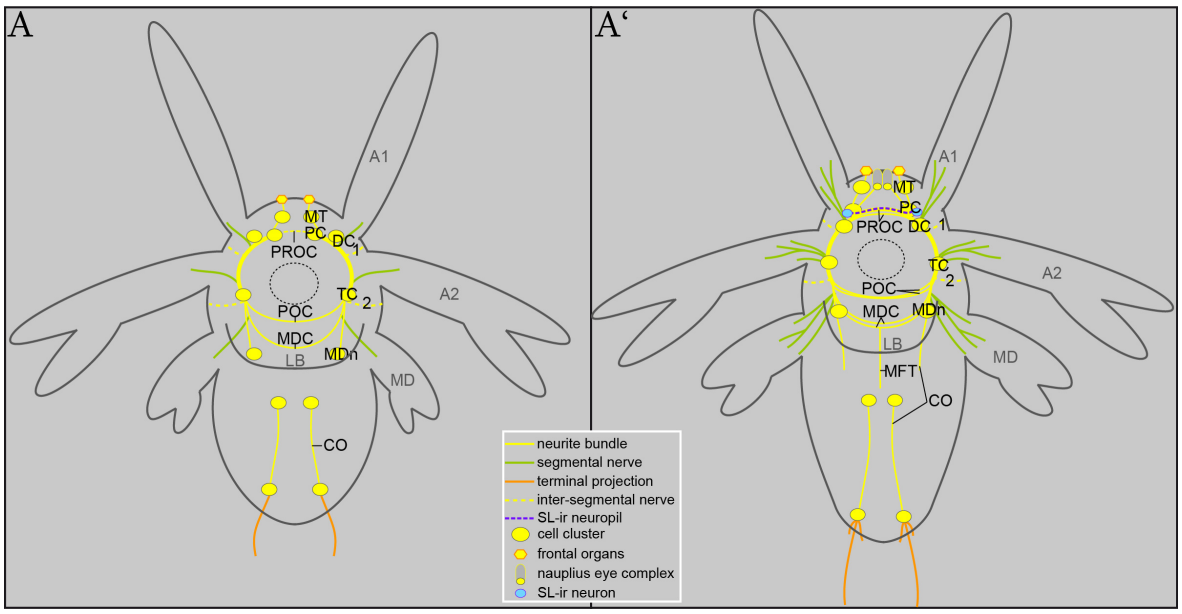

Fig. 35 - *P. monodon*, nauplius stage 1-2

Schematic illustration of the distribution of neural structures in the early (**A**) and in the late (**A'**) phase of the stage (ventral view). The region of the stomodeum is marked by a stippled circle.

A1: antenna 1; A2: antenna 2; CO: connective; DC: deutocerebrum; 1 and 2: inter-segmental nerve 1 and 2; LB: labrum; MDC: mandibular commissure; MD: mandible; MDn: mandibular neuromere; MFT: median fiber tract; MT: medulla terminalis; PC: protocerebrum; POC: post-oral commissure; PROC: pre-oral commissure; TC: tritocerebrum.

At the time of hatching, several neurite bundles have formed around the stomodeum, forming the anlage of the circumesophageal nerve ring (Fig. 36A, B). One thick longitudinal neurite bundle connects the protocerebrum to the mandibular neuromere passing through the deuto- and tritocerebrum, which constitutes the anlage of the nerve ring connective (Fig. 36A, B). Anteriorly, the nerve ring is closed by the anlage of the pre-oral commissure which is formed by a thin transversal neurite bundle between the two protocerebral hemi-neuromeres (Fig.

36C). An undefined number of cell somata are observable interposed within the commissure (asterisk in Fig. 36C). The anlage of the frontal tract has become thicker (Fig. 36D, E). The anlage of the frontal organ appears has a brightly stained disk-like structure (filled arrowheads in Fig.36D, E) connected to the medulla terminalis via short and feeble neurites which constitute the anlage of the frontal organ nerve (arrows in Fig. 36D). More ventrally, medially to the frontal tract anlage, a median cluster of cell somata results stained at the apical pole of the nauplius which probably represents the anlage of the nauplius eye complex (stippled oval in Fig. 36E). Very thin neurites are observed running from some of these cells to the dorso-lateral side of the pre-oral commissure proximal to the insertion site of the frontal tract anlage (arrows in Fig. 36E). The anlage of the deutocerebrum is located at the antero-lateral side of the stomodeum (Fig. 36A). At this level, lateral cell somata are observable sending neural projections to the connective (asterisk in Fig. 36A). The anlage of the segmental nerve of antenna 1 has formed as a single neurite bundle entering the antenna (Fig. 36A, B). The tritocerebrum anlage develops postero-laterally to the stomodeum. At this level the segmental nerve of antenna 2 anlage has joined the brain (Fig. 36B). Between the two segmental nerves of antenna 1 and 2, the anlage of inter-segmental nerve 1 has grown out running to the lateral side of the nauplius (filled arrowheads in Fig. 36B). The post-oral commissure encloses the posterior side of the nerve ring. This is made up of one transversal neurite bundle between the two tritocerebral hemi-neuromeres (Fig. 36A). Posterior to the tritocerebrum anlage, the mandibular hemi-neuromeres are transversally connected by the anlage of the mandibular commissure, which represents a single neurite bundle (Fig. 36A and F). Separate cell somata are observable postero-laterally sending their neurites to the lateral insertion of the mandibular commissure anlage (asterisks in Fig. 36F). From this region two neurite bundles run out laterally into the mandible, forming the segmental mandibular nerve anlage (Fig. 36B). Anteriorly, also the anlage of inter-segmental nerve 2 has formed (Fig. 36A and arrow in Fig. 36B). It runs off from the dorsal side of the nerve ring connective and is most likely pioneered by a dorsal stained cell soma which is located immediately posterior to the post-oral commissure (star in Fig. 36A). In the post-naupliar region, the anlage of the connective represents a thick neurite bundle spanning continuously between a cell cluster located posteriorly to the mandibular neuromere (stars in Fig. 36F) and the telsonic cell cluster (data not shown).

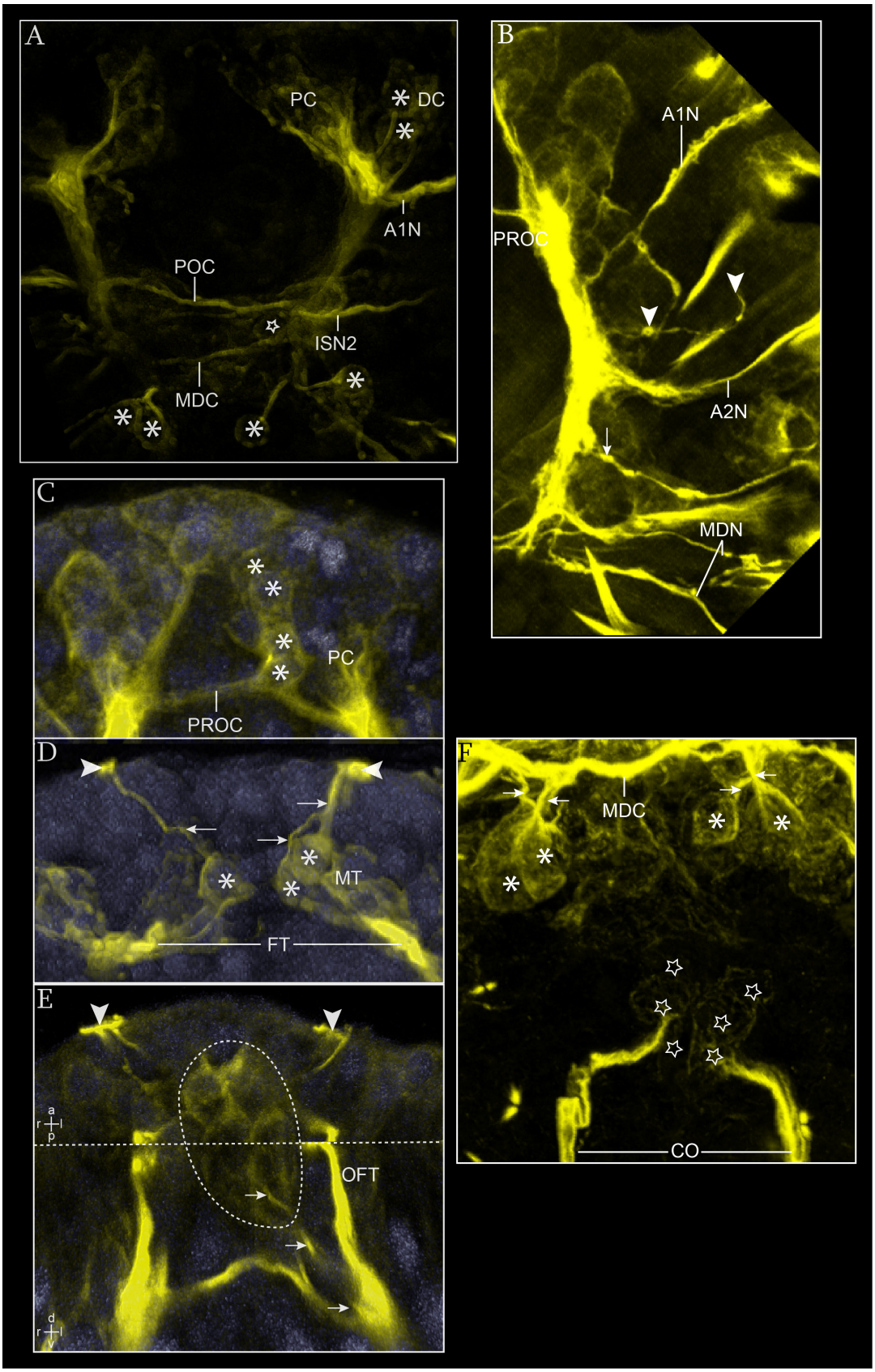

Fig. 36 - Axogenesis in *P. monodon*, early nauplius stage 1-2

Anti-ac-α-tubulin labelling, in yellow. Sytox-green staining, in grey. CLSM image stack. Imaris surpass mode: volume, clipping plane in **A**-**D**, oblique slicer in **E**. View of the naupliar region. **B -** View of the dorsal portion of the naupliar brain (ventral view). Asterisks mark single cell somata connected by separate neurites to the connective. Star marks the dorsal cell soma connected with the inter-segmental nerve 2, at the left side of the nauplius. **C -** View of the left half of the naupliar connective and its connection to the segmental and inter-segmental nerve anlagen (ventral view). Filled arrowheads mark the path of inter-segmental nerve 1. Arrow points at the proximal portion of inter-segmental nerve 2. **C -** Detail of the antero-ventral part of the protocerebrum. Asterisk marks one cell soma intercalated within the pre-oral commissure anlage. **D -** Detail of the antero-dorsal part of the protocerebrum (ventral view). Arrows point at single neurites connecting the frontal organs (filled arrowheads) to some of the cell forming the medulla terminalis (cell nuclei marked by asterisks). **E -** Detail of parts of the protocerebrum anlage (upper image: ventral view; lower image: anterior view). The image has been performed with the use of two intersected oblique slices; the stippled line signs the level of intersection. Filled arrowheads point at the frontal organ anlagen. Stippled oval marks the cell cluster forming the anlage of the nauplius eye complex. Arrows mark the path of a thin neurite from one of the cell somata of the nauplius eye complex cell cluster to the dorsal margin of the pre-oral commissure proximal to the insertion of the frontal tract anlage. **F -** View of the anterior portion of the post-naupliar region (ventral view). Part of the mandibular neuromere is included in the picture. Asterisks mark single cell somata connected to the lateral side of the mandibular commissure. Stars mark single cell somata connected to neurite bundle forming the post-naupliar connective.

A1: antenna 1; A1N: antenna 1 nerve; A2: antenna 2; A2N: antenna 2 nerve; CO: connective; DC: deutocerebrum; FO: frontal organ; FT: frontal tract; ISN1 and 2: inter-segmental nerve 1 and 2; LB: labrum; MFT: median fiber tract; MDC: mandibular commissure; MD: mandible; MDN: mandibular nerve; MDn: mandibular neuromere; MT: medulla terminalis; PC: protocerebrum; POC: post-oral commissure; PROC: pre-oral commissure; TC: tritocerebrum.

In a later phase of development, additional neurites have formed around the stomodeum, giving the nerve ring scaffold a solid shape (Fig. 37). In the protocerebral region, the pre-oral commissure has become thicker and is made up of two separate neurite bundles, one antero-dorsal and one postero-ventral (Fig. 37C). Antero-medially, several short neural projections run off from single cell somata (asterisks in Fig. 37C) connecting the pre-oral commissure at different sites (Fig. 37C). At the same level but more dorsally, the nauplius eye complex anlage is observable as a median cluster of cells (stippled contour below the stippled line in Fig. 37A) sending neural projections to the dorso-lateral margin of the pre-oral commissure, at the same level of the attachment of the frontal tract (arrows in Fig. 37A). Moreover, α-tubulin reveals the presence of anterior paired structures related to the nauplius eye complex anlage which bring the nauplius eye anlage in contact with the external surface (stippled contour above the stippled line in Fig. 37A). In the deutocerebral region two neurite bundles split off from the nerve root of antenna 1 (Fig. 37B). At the level of the proximal insertion of antenna 1 and mandible brightly stained structures connected by the branches of the segmental nerves are observable (stippled circles in Fig. 37B). They probably represent the anlage of tendons of the limbs. The anlage of antenna 2 nerve is composed of three main neurite bundles (Fig. 37B). The number of constituting neurites of the post-oral and

mandibular commissures has also increased. These neurites can be grouped into two main neurite bundles per commissure (Fig. 37C, C'). Moreover one thin neurite is visibly stained between the two commissural bundles (open arrowhead in Fig. 37C'). Anterior to the mandibular commissure anlage, a transversal row of four round cells is observable strictly adjacent to the anterior neurite bundle of the commissure (asterisks in Fig. 37C'). The mandibular nerve anlage is formed by two main neurite bundles and one thin posterior neurite (Fig. 37B). The neurite bundle in the middle bifurcates into two branches at the level of the limb insertion (arrows in Fig. 25B). Moreover, posterior to the mandibular commissure, the anterior anlage of the ventral nerve cord has formed (Fig. 37B, C). Several neurites are visible running out from the naupliar connectives towards the posterior (open circle in Fig. 37B, C). Medial to the mandibular commissure the unpaired median fiber tract has also formed (arrow in Fig. 37C).

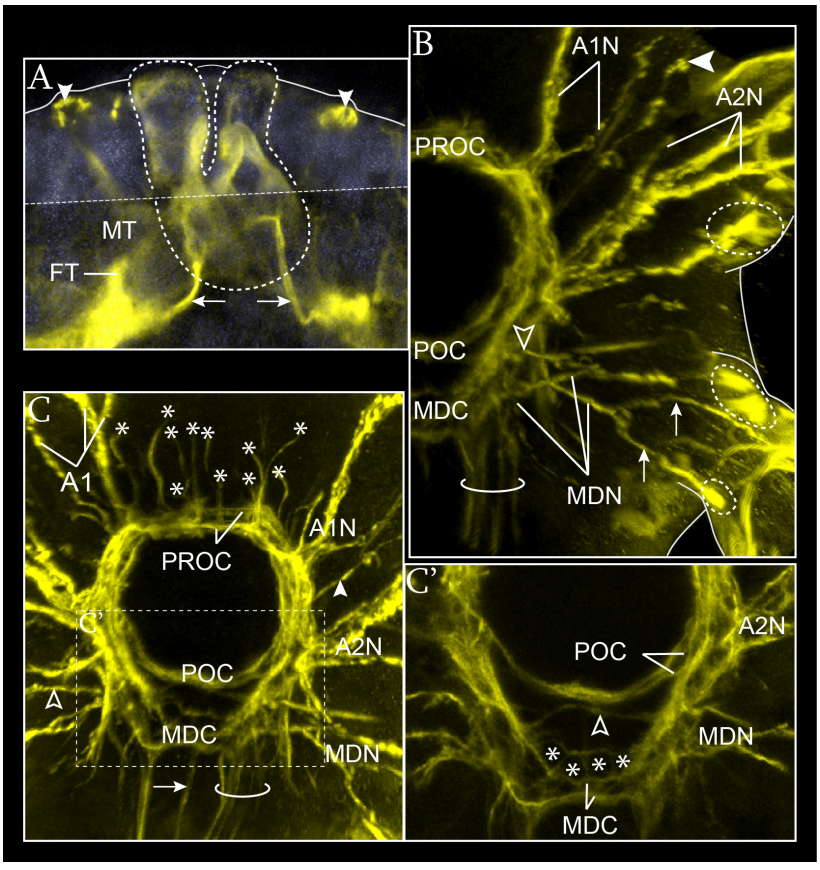

Fig. 37 - Axogenesis in *P. monodon*, late nauplius stage 1-2

Anti-ac-α-tubulin labelling, in yellow. Sytox-green staining, in grey. CLSM image stack. Imaris surpass mode: oblique slicer in **A**; volume, clipping plane in **B-C'**. View of the naupliar region. **A -** Detail of the dorsal portion of the protocerebrum (upper image: ventral view; lower image: anterior view). The image has been performed with the use of two intersected oblique slices; the stippled line signs the level of intersection. Filled arrowheads point at the frontal organ anlagen. Stippled contour marks the position of the nauplius eye complex anlage. Arrows point at the neurite bundles connecting the cell cluster forming the anlage of the nauplius eye complex to the dorso-lateral margin of the pre-oral commissure. **B -** View of

the left half of the naupliar region (ventral view). Filled arrowheads mark the distal end of inter-segmental nerve 1. Open arrowhead marks the insertion of inter-segmental nerve 2 to the connective. Arrows point at each of the branches of the median neurite bundle of the mandibular nerve. Open circle includes the group of neurites forming the anterior portion of the post-naupliar connective. Stippled circles mark the position of putative tendons at the insertion of antenna 2 and mandible. **C -** General overview of the naupliar region (ventral view). Asterisks mark single cell somata at the antero-ventral side of the protocerebrum. Filled arrowhead marks inter-segmental nerve 1. Open arrowhead marks inter-segmental nerve 2. Arrow points at the anlage of the median fiber tract. Open circle includes the group of neurites forming the anterior portion of the post-naupliar connective. **C' -** Detail of the post-oral and mandibular commissures anlage (ventral view). Asterisks mark single somata adjacent to the anterior margin of the mandibular commissure.

A1N: antenna 1 nerve; A2N: antenna 2 nerve; FT: frontal tract; MDC: mandibular commissure; MDN: mandibular nerve; MT: medulla terminalis; POC: post-oral commissure; PROC: pre-oral commissure.

Stomatogastric nervous system

The inferior ventricular nerve anlage occurs as a feeble unpaired neurite running ventrally from the median portion of the postero-ventral neurite bundle of the pre-oral commissure (data not shown).

Serotonin-like expression pattern

The first appearance of SL-ir structures occurs within the protocerebral region (Fig. 38). A lateral SL-ir soma located antero-ventrally to the pre-oral commissure (asterisk in Fig. 38) is connected to the pre-oral commissure via a thin SL-ir neurite (filled arrowhead in Fig. 38A'). A thin SL-ir neuropilar layer composed by two main SL-ir neurite bundles has differentiated within the antero-dorsal portion of the pre-oral commissure (arrows in Fig. 38A').

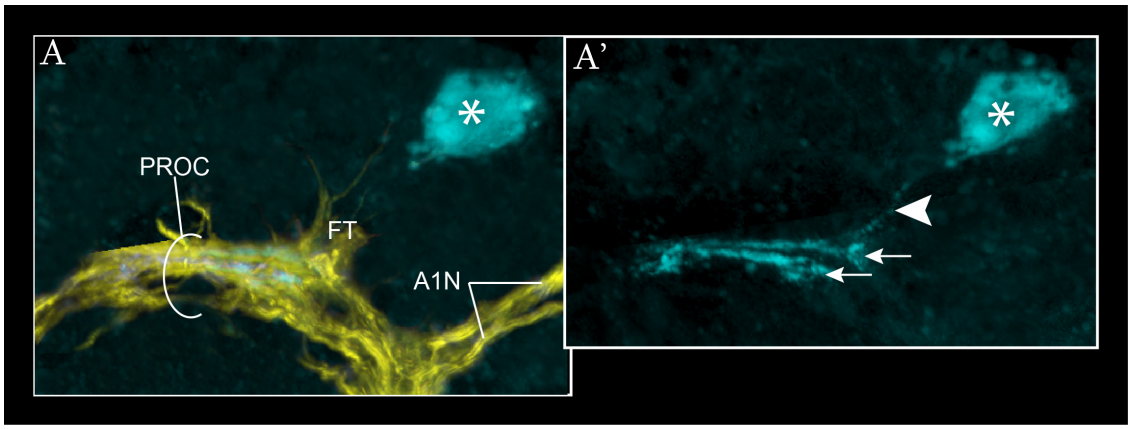

F8ig.38 - Distribution of SL-ir structures in the nauplius stage 1-2

Anti-ac-α-tubulin labelling in yellow. Anti-serotonin-like labelling in light blue. CLSM image stack. Imaris surpass mode: volume, clipping plane. View of the SL-ir structures in the left half of the protocerebral region (ventral view). Asterisks mark single SL-ir neuron. In **A'** filled arrowhead points at the SL-ir neurite which connects the SL-ir neuron to the commissural neuropil. Arrows point at each of the neurite bundles forming the pre-oral neuropil.

A1N: antenna 1 nerve; FT: frontal tract; PROC: pre-oral commissure.

3.2.2.3 Nauplius stage 3-4

Axogenesis

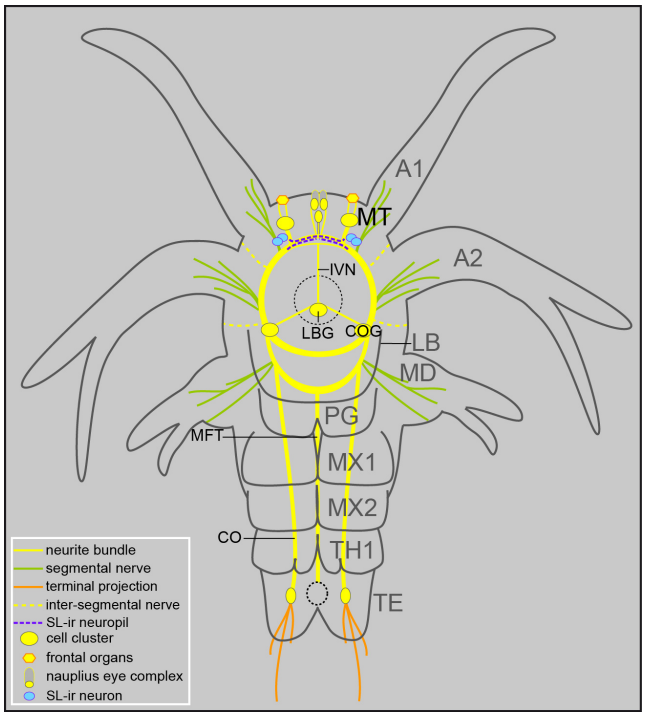

Fig. 39 - *P. monodon*, nauplius stage 3-4

Schematic illustration of the distribution of neural structures (ventral view). The region of the stomodeum is marked by black broken circular line. Only the ventral portion of the SNS is represented. The black broken circular line in the telson represents the proctodeum.

A1: antenna 1; A2: antenna 2; CO: connective; COG: commissural ganglion; DC: deutocerebrum; LB: labrum; LBG: labral ganglion; MD: mandible; MDn: mandibular neuromere; MFT: median fiber tract; MT: medulla terminalis; MX1: maxilla 1; MX2: maxilla 2; PC: protocerebrum; PG: paragnath; TC: tritocerebrum; TE: telson; TH1: thoracomere 1; TH2: thoracomere 2.

In the naupliar region additional neurites continue growing and gradually the neurite bundles of the nerve ring condense together giving the brain anlage a solid compact architecture around the stomodeum (Fig. 40A). The pre-oral commissure has noticeably increased its volume in both its components (stippled square bracket in Fig. 40A). The antero-dorsal neurite bundle of the pre-oral commissure is connected with the frontal tract and medially to the nauplius eye complex, while the postero-ventral one encloses the anterior margin of the nerve ring and connects medially to the stomatogastric nervous system anlage via the inferior ventricular nerve (Fig. 40A, B). The frontal organ starts to bulge out at the antero-dorsal pole of the nauplius. Several neurites are now observable connecting the frontal organ to the medulla terminalis (Fig. B'). More ventrally two additional components of the nauplius eye complex have formed: one paired, composed of two boomerang-like shaped cell somata (open

arrowheads in Fig. 40B') embedded medially to the lateral cups (data not shown) which represent the two pigment cells of the nauplius eye complex, and one unpaired, composed of three cell somata (asterisks in Fig. 40C) located medio-ventrally between the two pigment cells which represent the medio-ventral cup of the nauplius eye complex. Each of the two pigment cells is connected to the medio-dorsal site of the pre-oral commissure via one neurite bundle (arrows in Fig. 40B, B'). One neurite bundle runs out from the posterior-most cell of the medio-ventral cup towards the medio-dorsal margin of the pre-oral commissure (arrow in Fig. 40C). The roots of the segmental nerves of antenna 1 and 2 have become thicker (Fig. 40A, B). The course of inter-segmental nerves 1and 2 can be followed in their path to the dorso-lateral side of the nauplius (Fig. 40A, B and Fig. 41A, A'). In particular, the inter-segmental nerve 1 connects a brightly stained fan-like structure posterior to the medulla terminalis while the inter-segmental nerve 2 anlage connects the lateral-most of the dorsal longitudinal muscles (Fig. 41a, A'). The post-oral and the mandibular commissures have become thicker and their composition in two separate neurite bundles becomes less obvious due to the proximity of the forming neurites (Fig. 40A).

In the post-naupliar region the connective anlage are now formed by a continuous neurite bundle spanning between the postero-lateral margin of the mandibular commissure (stippled area marked in Fig. 41C) and the telsonic cell cluster. This last has taken a ventral location in the telson and the number of constituting cell somata has increased proportionally to the number of terminal spines (stippled ovals in Fig. 41B). The anlage of the median fiber tract extends as a single longitudinal neurite bundle spanning between the postero-medial margin of the mandibular commissure and the ventral wall of the proctodeum (Fig. 41C). In their terminal extension the connective and the median fiber tract flex to the ventral following the ventral flexure of the telson (data not shown).

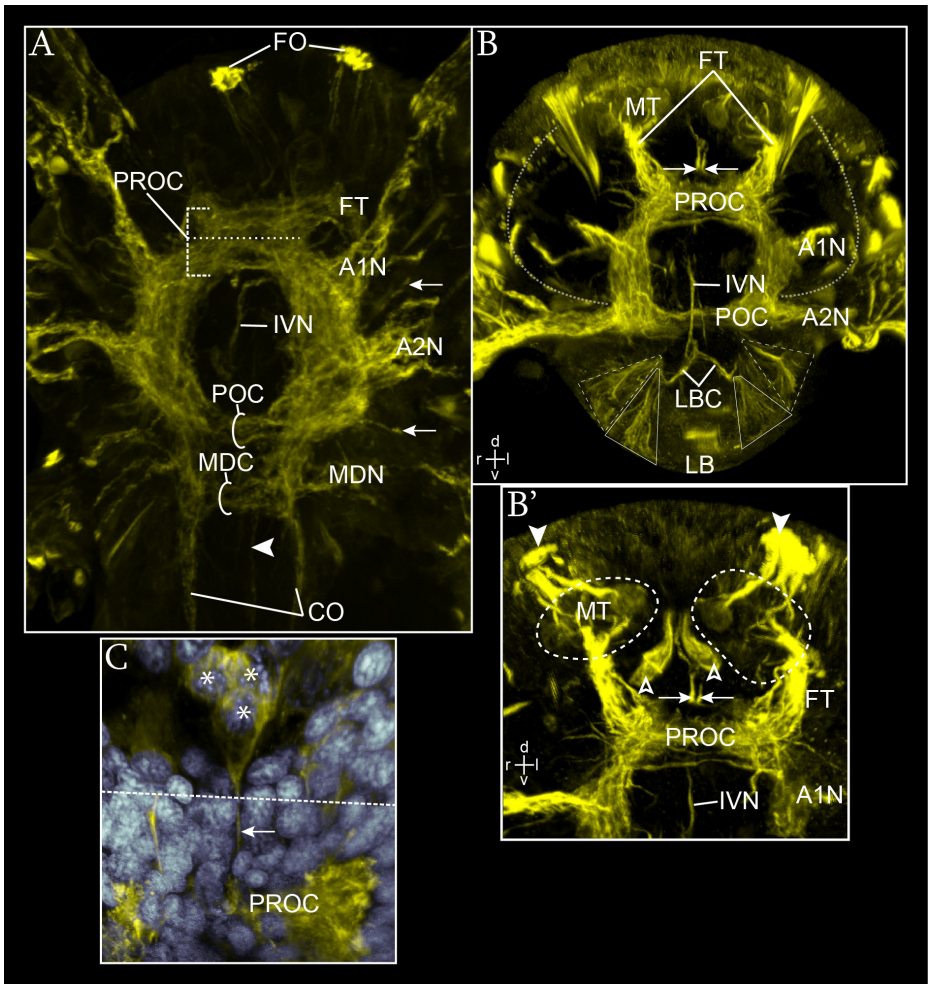

Fig. 40 - Axogenesis in the naupliar region of *P. monodon*, nauplius stage 3-4

Anti-ac-α-tubulin labelling, in yellow. SYTOX-green staining, in grey. CLSM image stack. Imaris surpass mode: volume, clipping plane, oblique slicer in **C**. **A -** General overview of the brain and of the anterior portion of the ventral nerve cord (ventral view). The sample is slightly tilted to the right side. The border between the two neurite bundles of the pre-oral commissure (stippled square brackets) is marked by stippled line. Arrows mark the inter-segmental nerve 1 and 2 at the left side of the nauplius. Filled arrowhead marks the median fiber tract. **B -** Detail of the circumesophageal nerve ring (antero-ventral view). The anterior-most pole has been cut out from the image. The image includes part of the stomatogastric nervous system and the labrum anlage. Two separate neurites (arrows) connect the pigment cells of the nauplius eye complex to the dorsal margin of the pre-oral commissure. Stippled transparent lines mark the course of the inter-segmental nerve (see detail in **Fig. 41 A, A'**). Triangles mark paired fan-like structures in the labrum anlage; stippled lines indicate a more posterior position. **B' -** Detail of the anterior pole (antero-ventral view). Filled arrowheads point at the frontal organs. The region of the medulla terminalis is encircled by stippled line. Open arrowheads mark the pigment cells of the nauplius eye complex. They lay more in an upper layer then the medulla terminalis. Arrows point at each of the neurite bundle connecting the pigment cells to the pre-oral commissure. **C -** Detail of the medio-ventral cup of the nauplius eye complex anlage (ventral view). The image has been performed with the use of two intersected oblique slices; the stippled line signs the level of intersection. Upper image: ventral view. Lower image: antero-ventral view. Asterisks mark single cell somata of the cup. Arrow points at the neurite bundle connecting the median cup to the dorsal margin of the pre-oral commissure (only partially visible in the section).

A1N: antenna 1 nerve; A2N: antenna 2 nerve; MT: medulla terminalis; FO: frontal organ; FT: frontal tract; IVN: inferior ventricular nerve; LB: labrum; MDC: mandibular commissure; MDN: mandibular nerve; POC: post-oral commissure; PROC: pre-oral commissure.

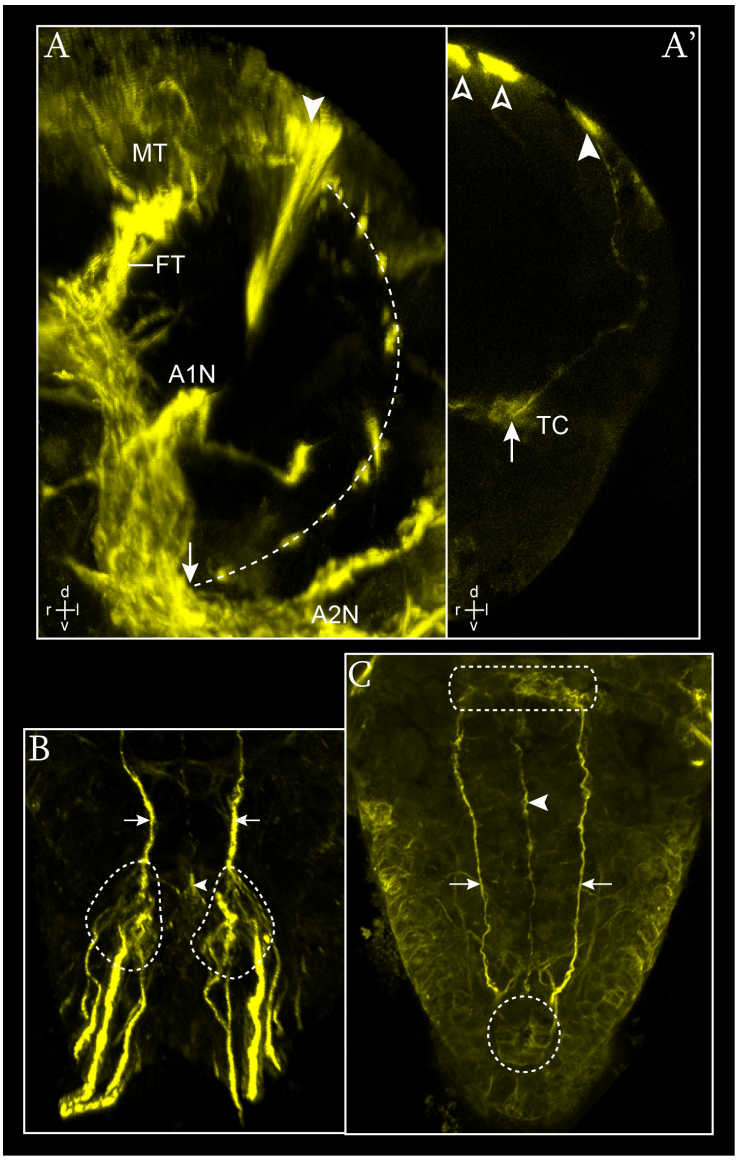

Fig. 41 - Axogenesis in *P. monodon*, nauplius stage 3-4

Anti-ac-α-tubulin labelling. CLSM image stack. Imaris surpass mode: oblique slicer in **A** and **A',** clipping plane in **B**, **C**. **A**, **A' -** Detail of the course of inter-segmental nerve 1 (in **A**) and 2 (in **A'**) in the right half of the nauplius (antero-ventral view). Arrow points at the insertion of the inter-segmental nerve at the level of the nerve ring. Filled arrowhead points to the position of the dorsal insertion of the inter-segmental nerve. In **A'** open arrowheads ark the position of two medio-dorsal longitudinal muscles. **B**, **C -** Axogenesis in the ventral nerve cord (ventral view). Arrows point at the longitudinal connective anlagen. **B -** Detail of the telson region. Filled arrowhead points at the posterior end of the median fiber tract. Stippled ovals mark the terminal cell clusters which connects posteriorly the terminal spines. **C -** General overview. The ventral-most portion of the telson has been cut out from the image. Filled arrowhead marks points at the median fiber tract. Stippled area marks the position of the mandibular commissure (here only its dorsal portion is visible). A stippled circle marks the position of the gut tube anlage.

A1: antenna 1; A1N: antenna 1 nerve; A2: antenna 2; A2N: antenna 2 nerve; MT: medulla terminalis; FO: frontal organ; FT: frontal tract; ISN1 and 2: inter-segmental nerves 1 and 2; POC: post-oral commissure; TC: tritocerebrum.

Stomatogastric nervous system

The stomatogastric nervous system anlage is visibly stained at this stage (Fig. 42). Two parallel neurite bundles run medially in dorso-ventral direction. On one hand, the inferior ventricular nerve connects the median portion of the postero-ventral margin of the pre-oral commissure to a medio-ventral cluster of cells at the antero-dorsal margin of the labrum (stippled oval in Fig. 42B-C'). This cell cluster is recognized as the anlage of the labral ganglion. At this level, two lateral branches run in opposite direction towards the ventro-lateral sides of the post-oral commissure and form the labral commissure (Fig. 42). The labral commissure meets laterally a group of cells clustered together ventrally to the tritocerebrum. This may represent the anlage of the commissural ganglion (circle in Fig. 42C, C'). On the other hand, the stomatogastric nerve runs along the dorsal surface of the stomodeum spanned between the anlage of the stomatogastric ganglion and the anterior margin of the stomodeum (Fig. 42B, C). Here, two lateral branches split off and run in opposite direction into the commissural ganglion forming the stomodeal commissure (in Fig. 42B, C). The stomatogastric nerve anlage extends further to the ventral side, turns to the anterior and connects the inferior ventricular nerve (arrow in Fig. 42B C). Stained projections with a ventro-dorsal orientation are observable surrounding the stomodeum (Fig. 42B). Whether they represent the anlage of sensory innervations or of muscles cannot be resolved with the used techniques.

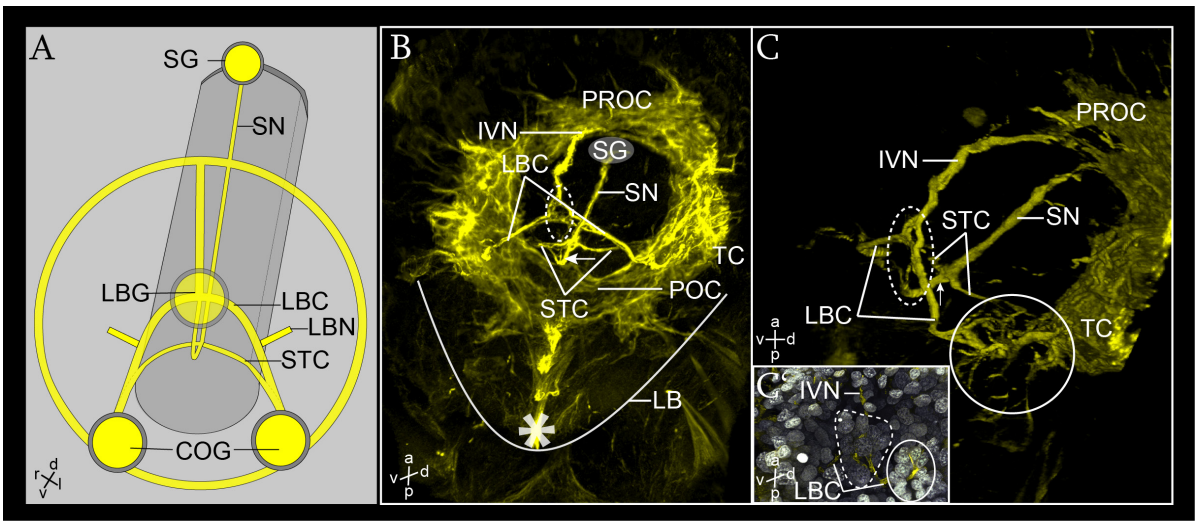

Fig. 42 - Axogenesis of the stomatogastric nervous system in *P. monodon*, nauplius stage 3-4

A - Schematic illustration of the stomatogastric nervous system anlage. Ventro-lateral view. Neural structures are labelled in yellow, non-neural structures in grey. The anlage of the digestive tube is represented by the grey cylinder. The circumesophageal nerve ring is schematized by the circular yellow ring in the foreground. Yellow circles with grey contour represent the ganglia. Stippled line marks the region of the labral ganglion. Circle marks the region of the commissural ganglion.

B-C' - Anti-ac-α-tubulin labelling, in yellow. SYTOX-green staining, in grey. CLSM image stack. **B –** General overview(ventro-lateral view). The stippled circle marks a small cluster of cells at the intersection among the inferior ventricular nerve, the stomatogastric nerve and the labral commissure, which may represent the anlage of the labral ganglion. The ventral margin of the labrum is underlined by a white line while the putative opening of the stomodeum is marked by an asterisk. **C, C' -** General overview (lateral view in **C**; ventro-lateral view in **C'**). The stippled circle marks the region of the anlage of the labral ganglion while the solid circle line marks the one of the commissural ganglion.

A1N: antenna 1 nerve; COG: commissural ganglion; IVN: inferior ventricular nerve; LB: labrum; LBC: labral commissure; LBG: labral ganglion; POC: post-oral commissure; PROC: pre-oral commissure; SG: stomatogastric ganglion; SN: stomatogastric nerve; STC: stomodeal commissure; TC: tritocerebrum.

Serotonin-like expression pattern

One additional SL-ir neuron has formed antero-ventrally to the pre-oral commissure dorsally to the one observed at the previous stage (asterisks in Fig. 43). Only one single neurite is still observable connecting the ventral neuron to the antero-dorsal margin of the pre-oral commissure (arrows in Fig. 43 A'). The SL-ir neuropil has expanded from the pre-oral-commissure dorso-laterally into the frontal tract (open arrowheads in Fig. 43) and postero-laterally along the nerve ring connectives towards the deutocerebral region (filled arrowheads in Fig. 43 A').

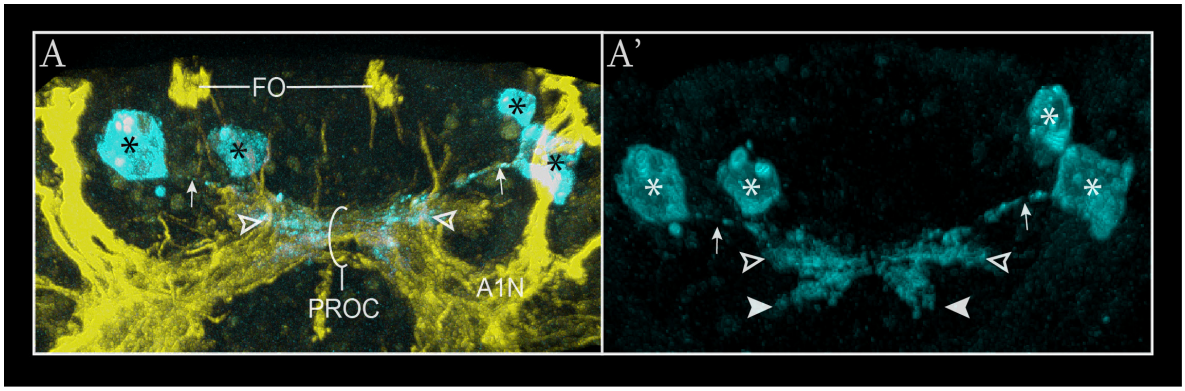

Fig. 43 - Distribution of SL-ir structures in the nauplius stage 3-4

Anti-ac-α-tubulin labelling in yellow. Anti-serotonin-like labelling in light blue. CLSM image stack. Imaris surpass mode: volume, clipping plane. View of SL-ir structures in the protocerebrum (ventral view). Asterisks mark single SL-ir cell somata. Arrows point at single SL-ir axons. Open arrowheads point at the dorso-lateral extension of the SL-ir neuropil into the frontal tract. Filled arrowheads in **A'** point at the posterior extension of the SL-ir neuropil along the nerve ring towards the deutocerebral region.

A1N: antenna 1 nerve; FO: frontal organ; PROC: pre-oral commissure.

3.2.2.4 Nauplius stage 5-6 (Metanauplius)

Axogenesis

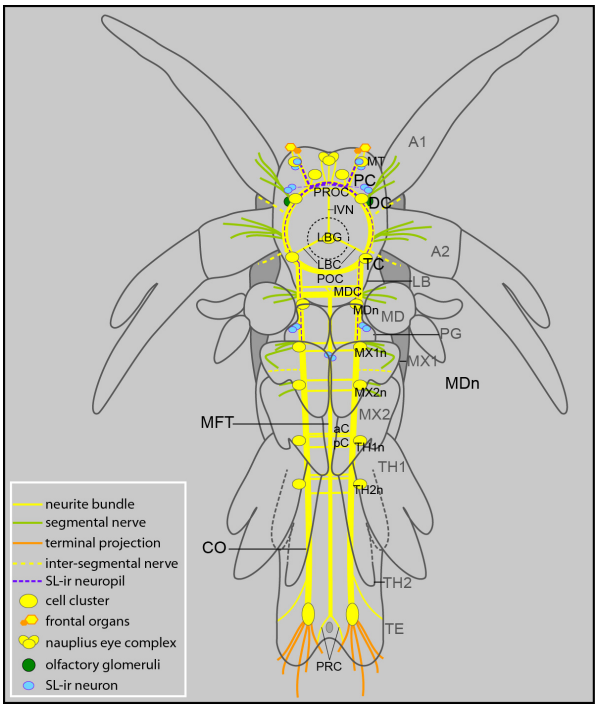

Fig. 44 - *P. monodon*, nauplius stage 5-6 (metanauplius)

Schematic illustration of the distribution of neural structures (ventral view). The region of the esophageal anlage is marked by black broken circular line. The proctodeum is represented by a small grey oval. Only the superior portion of the stomatogastric nervous system anlage is schematized.

A1: antenna 1; A2: antenna 2; aC: anterior commissure; CO: connective; COG: commissural ganglion; DC: deutocerebrum; LB: labrum; LBC: labral commissure; LBG: labral ganglion; MD: mandible; MDC: mandibular commissure; MDn: mandibular neuromere; MFT: median fiber tract; MT: medulla terminalis; MX1: maxilla 1; MX1n: maxilla 1 neuromere; MX2: maxilla 2; MX2n: maxilla 2 neuromere; PC: protocerebrum; pC: posterior commissure; PG: paragnath; POC: post-oral commissure; PRC: proctodeal commissure; PROC: pre-oral commissure; TC: tritocerebrum; TE: telson; TH1: thoracomere 1; TH1n: thoracomere 1 neuromere; TH2: thoracomere 2; TH2n: thoracomere 2 neuromere.

While the condensation process of the circumesophageal nerve ring proceeds further the brain anlage becomes more defined (Fig. 45A). In the protocerebral region, additional neurite bundles contribute to settle the structure of the anterior portion of the pre-oral commissure (Fig. 45A, B and F). Anteriorly in the protocerebrum, a voluminous lateral cell cluster sends several neurites to the ventro-lateral side of the commissure (Fig. 45A, B). This represents the anlage of cluster 6, *sensu* Sandeman et al. (1992). Posteriorly, the neural projections of the anlage of the olfactory lobe meet each other and contribute to the medial margin of the commissure (Fig. 45F, see below). Dorsally the medulla terminalis has grown further (Fig. 45C). At the latest time of the stage the dorsal end of the frontal tract has become thicker and

all around its diameter several short neural projections connect the surrounding cell layers radially (open arrowheads in Fig. 45C). The frontal organ protrudes further and its connection with the medulla terminalis become thicker (filled arrowheads in Fig. 45C). One additional median component can be distinguished (asterisk in Fig. 45C) which keeps a more basal position without protruding at the surface. Individual neurites connect this component directly to the frontal tract (arrows in Fig. 45C). Medially, the nauplius eye complex takes a more defined structure (Fig. 45B and D-E'). The three cups are now well-defined: one is medio-ventral, and two are lateral, dorsal to the previous one (Fig. 45D). Each cup is formed by three cells (asterisks in Fig. 45 D-E'). The cell somata of the lateral cup are disposed in a row obliquely oriented medio-laterally, dorsal to the antero-ventral cell cluster of the protocerebrum (asterisks in Fig. 45E'). In the deutocerebral region, anterior to the root of antenna 1 nerve a small cell cluster sends a short neural projection into the nerve ring (Fig. 45B). Posterior to the root of antenna 1, the anlage of the olfactory lobe has formed and is visibly stained as a round glomerular structure (open arrowheads in Fig. 45A and open circles in F). One neurite bundle runs out from the glomerulus in antero-median direction along the margin of the nerve ring, passes the posterior portion of the pre-oral commissure and meets the contralateral bundle at the posterior margin of the anterior component of the commissure itself (filled arrowheads in Fig. 45F). The post-oral commissure results in one single thick transversal neurite bundle (Fig. 45A) which receives the neural projection of a cell cluster located postero-ventrally to the root of the antenna 2 nerve (filled arrowheads in Fig. 45A). The mandibular commissure takes a more posterior position (Fig. 45A) and its neurite bundles start to fuse in one single thick transversal tract (Fig. 46). However, a dorsal component can be distinguished separate from a ventral one (Fig. 46B). The first is medially connected with the anterior part of the median fiber tract (upper image in Fig. 46B and Fig. 46C) which at this level is composed of two branches forming a Y intercalated within the neurites of the commissure (Fig. 46B, C). The ventral component receives laterally the neural projections of a voluminous cell cluster which has formed ventro-posteriorly to the root of the mandibular nerve (stippled circles in Fig. 46A, B). Another projection is observable connecting the commissure medially (open arrowhead in Fig. 46A) associated with a group of ventral (probably glia) cells. The segmental nerve of the mandible consists of three branches, one thicker anterior and two thinner posterior (arrows in Fig. 46A; see also Fig. 47B).

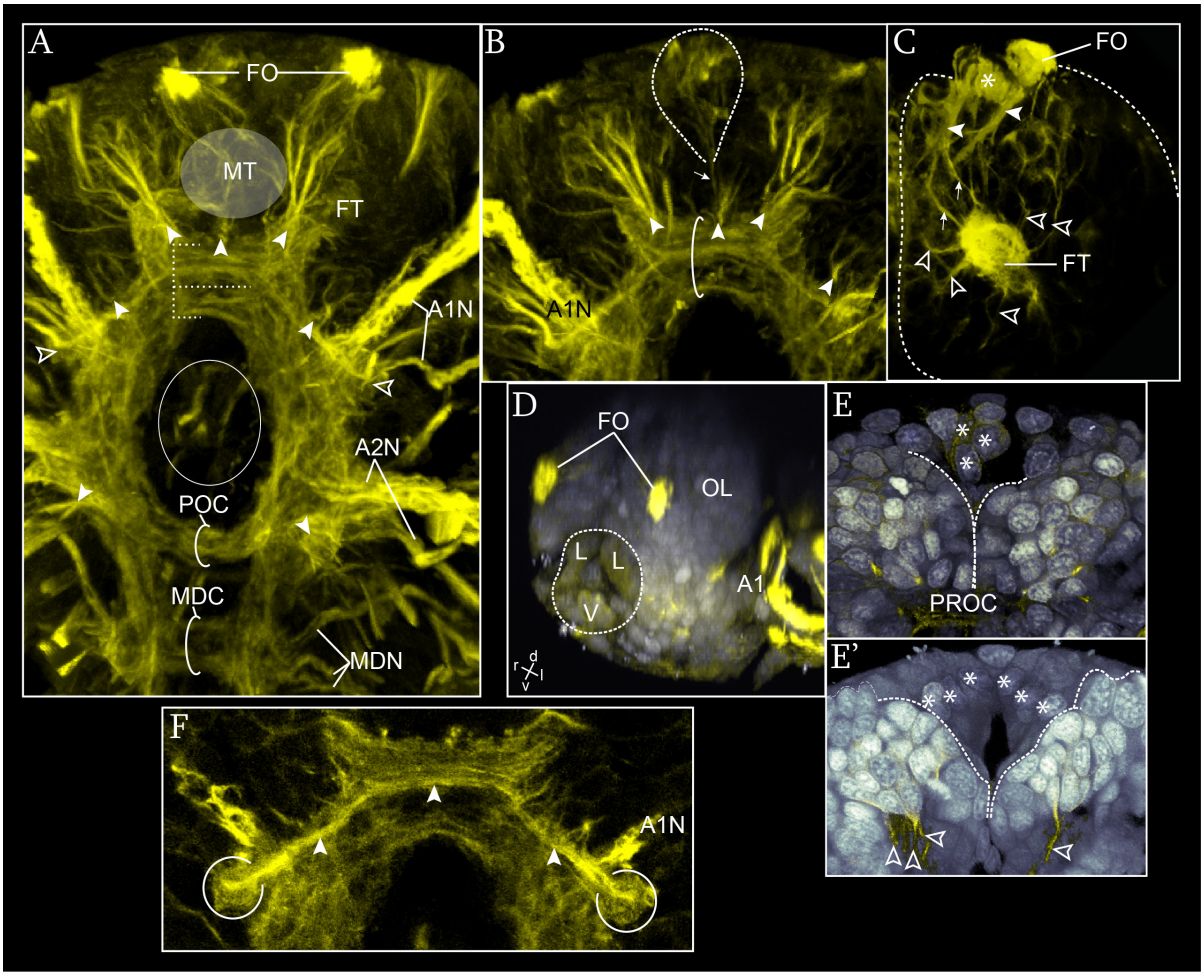

Fig. 45 - Axogenesis of the naupliar region in *P. monodon*, nauplius stage 5-6 (metanauplius)

Anti-ac-α-tubulin labelling, in yellow. Sytox-green staining, in grey. CLSM image stack. Imaris surpass mode: volume (blend in **C**, **E** and **E'**), clipping plane, section mode in **D**. **A**, **B -** View of the naupliar region (ventral view). Filled arrowheads point at the sites of insertion of neural projections from ventral cell clusters. **A -** General overview. The pre-oral commissure (stippled square bracket) is formed by two components separated by transversal stippled line. Open arrowheads mark the location of the anlage of the olfactory lobes. The position of the stomodeum and part of the stomatogastric nervous system is marked by a circle. **B -** Detail of the antero-ventral portion of the protocerebral region. T Stippled line marks the position of the ventral cup of the nauplius eye complex. Arrow points at the median neurite bundle connecting the ventral cup to the pre-oral commissure. **C -** Detail of left half of the medulla terminalis and its connection to the frontal organ (ventral view). The stippled line marks the extension of the medulla terminalis. The asterisk marks the medial component of the frontal organ. Filled arrowheads point at neurite bundle connecting the frontal organ to the medulla terminalis. Arrows mark single neurites connecting the frontal tract. Open arrowheads point at short neurites radially distributed around the frontal tract. **D -** View of the anterior pole of the metanauplius (dorso-lateral view). The nauplius eye complex anlage is encircled by stippled line. **E**, **E' -** View of part of the protocerebrum and of the nauplius eye complex (ventral view). The cuttings have been performed at different levels of the image stack maintaining the same position of the clipping plane. In **E** the cutting plane is more ventral than in **E'**. Asterisks mark single cell nuclei forming the cups of the nauplius eye complex. Stippled line marks the antero-medial border of the protocerebrum. **E -** Ventral cup. **E' -** Lateral cups. Open arrowheads point at some of the neurites projecting to the pre-oral commissure. **F -** Detail of the dorsal portion of the pre-oral commissure and of the deutocerebral region (ventral view). The anlage of the olfactory lobes is marked by open circles. Filled arrowheads point at the neural projections of the olfactory lobe to the pre-oral commissure.

A1: antenna 1; A1N: antenna 1 nerve; A2: antenna 2; A2N: antenna 2 nerve; FO: frontal organ; FT: frontal tract; L: lateral cup; MD: mandible; MDC: mandibular commissure; MDN: mandibular nerve; MT: medulla terminalis; OL: optic lobe; POC: post-oral commissure; PROC: pre-oral commissure; V: ventral cup.

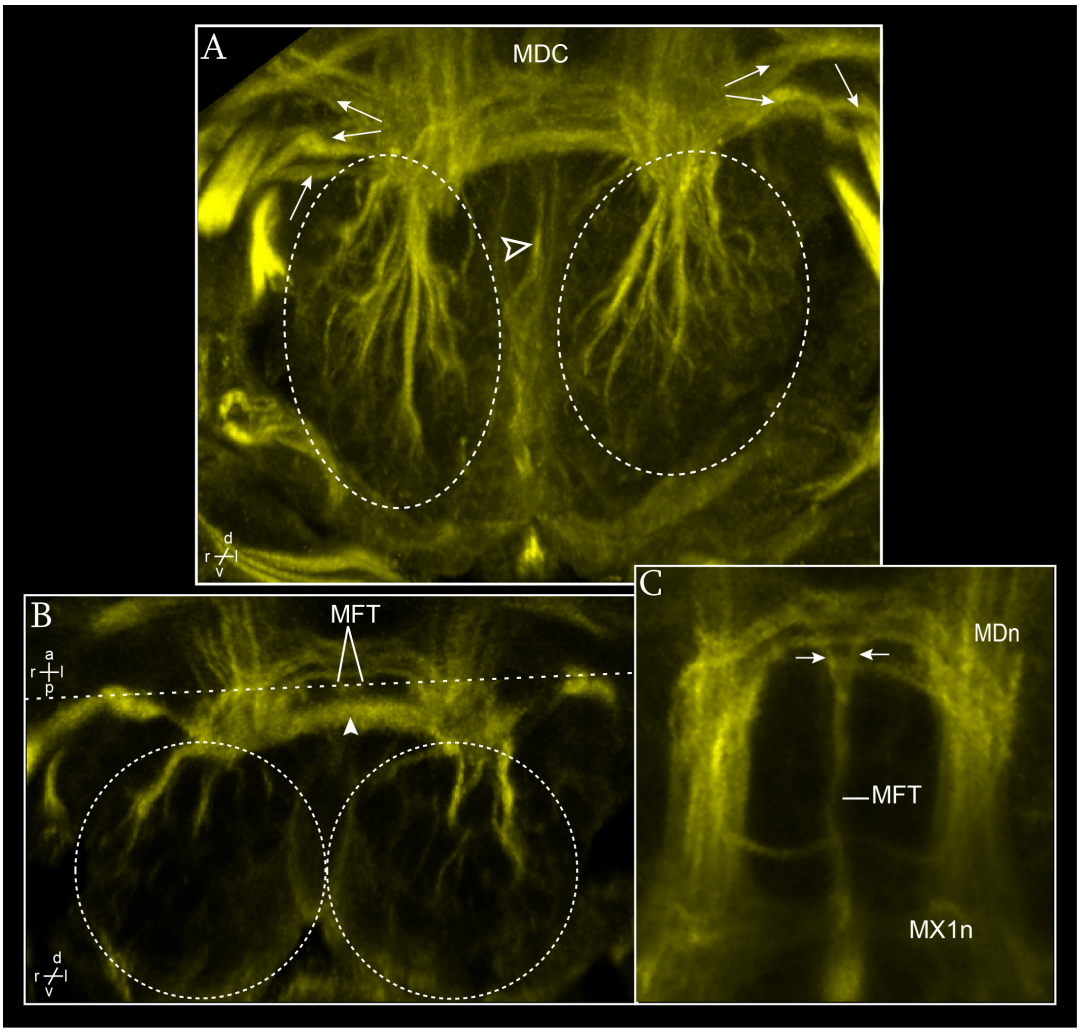

Fig. 46 – Axogenesis of the mandibular neuromere in *P. monodon*, nauplius stage 5-6 (metanauplius)

Anti-ac-α-tubulin labelling. CLSM image stack. Imaris surpass mode: volume, clipping plane in **A** and **C**, oblique slicer in **B**. **A -** View of the ventral-most side (antero-ventral view). Stippled circles mark the ventral cell clusters. Arrows point at each of the branches of the segmental nerve. Open arrowhead points at the medio-ventral projection spanned between the median side of the commissure and the ventral surface of the embryo. These probably represent projections of glia cells in the ventral ectoderm. **B -** Detail of the commissural architecture (upper image: ventral view; lower image: antero-ventral view). The image has been performed with the use of two intersected oblique slices; the stippled line signs the level of intersection. Stippled circles mark the anterior extension of the ventral cluster. Filled arrowhead points at the ventral portion of the commissure. **C -** Detail of the anterior path of the median fiber tract anlage at the dorsal side of the mandibular commissure (ventral view). Arrows point at the two anterior branches of the median fiber tract.

MDC: mandibular commissure; MDn: mandibular neuromere; MFT: median fiber tract; MX1n: maxilla 1 neuromere.

The post-naupliar neuromeres have started to differentiate following an antero-posterior developmental gradient (Fig.47A, B). At first, two transversal thin neurites form at the level of the first four post-naupliar neuromeres following an antero-posterior gradient of development. They represent the anlage of the anterior commissural bundles of maxilla 1 and 2 neuromeres and thoracomere 1 and 2 (Fig. 47A).

In a later phase of development a third commissure has formed posterior to the previous ones in each of the post-naupliar neuromeres (Fig. 47B). The two bundles of the anterior commissures of maxilla 1 and 2 have fused together while still distinctly separate in thoracomere 1 and 2 (Fig. 47B). The anlage of the segmental nerve has formed at the level of the anterior commissure of each post-naupliar neuromere as well as the corresponding inter-segmental nerves (Fig. 47B). The presence of inter-segmental nerve posterior to thoracomere 2 is uncertain. The segmental nerves of the thoracic segments share a common architecture. Here the maxilla 1 composition is taken as representative (Fig. 47C-C"). Two neurite bundles run out very close together at the level of the anterior commissure: one dorsal which bifurcates into two neurites running to the posterior of the limb (asterisks in Fig. 47C, C') and one ventral which runs through the ventral margin of the limb (arrows in Fig. 47C, C'). The ventral branch extends medially into the anterior commissure where meets the contralateral one (stippled oval in Fig. 47C"). Ventrally several lateral cell clusters have formed. Their neural projections are sent to the posterior margin of the anterior commissure (filled arrowhead in Fig. 47C') and to different levels of the segmental nerve root (open arrowheads in Fig. 47C'). The longitudinal connective has noticeably increased its diameter between the mandibular and the maxilla 2 neuromere anlagen while become thinner in its posterior path. In the telson, a lateral branch runs off from the connective and takes a dorso-lateral direction (open arrowheads in Fig. 47D). Several cell somata are observable surrounding the proctodeum and connecting the terminal projection of the connective on one side and the terminal spines on the other side (asterisks in Fig. 47D, D'). At the anterior margin of the proctodeum the terminal portion of the median fiber tract bifurcates and it lateral branches form the proctodeal commissure (arrows in Fig. 47D, D'). The two branches surround the wall of the proctodeum and enter in a cell cluster adjacent to it (asterisks in Fig. 47D').

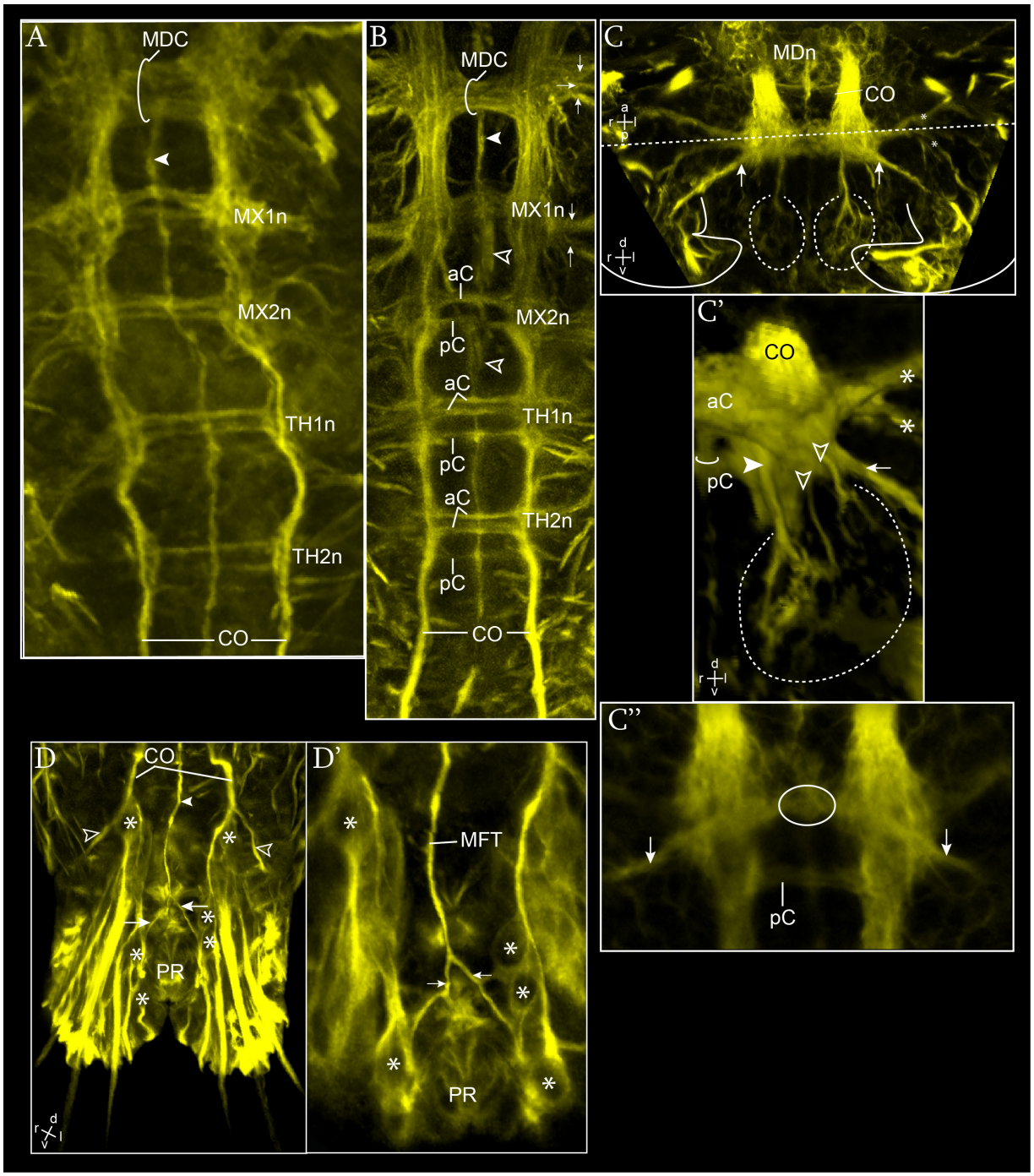

Fig. 47 – Axogenesis of the post-naupliar region in *P. monodon*, nauplius stage 5-6 (metanauplius)

Anti-ac-α-tubulin labelling. CLSM image stack. Imaris surpass mode: volume (blend in **C'**) clipping plane, oblique slicer in **C**. View of the ventral nerve cord in the early (**A**) and in the late phase of the stage (**B**). **A -** General overview of the anlage of the first four post-naupliar neuromeres in the early phase of the stage (ventral view). The anterior commissure, composed of two neurite bundles has formed in each neuromere anlage following an antero-posterior developmental gradient. Filled arrowhead marks the median fiber tract. **B -** General overview of the anlage of the first four post-naupliar neuromeres in the late phase of the stage (ventral view). Arrows point at singular neurite bundles forming the segmental nerve of the mandible and of the maxilla 1. Filled arrowhead points at the median fiber tract anlage. Its course posterior to the maxilla 1 and 2 commissures is partially hidden by ventral projections (open arrowheads) which probably represent glia cells projections. **C-C" -** Architecture of the maxilla 1 neuromere. Stippled lines encircle ventral cell clusters projecting into the anterior commissure. Arrows point at the postero-

ventral branch of the segmental nerve. Asterisks mark the two branches of the antero-dorsal branch of the segmental nerve. **C -** The image has been performed with the use of two intersected oblique slices; the stippled line signs the level of intersection (upper image: ventral view; lower image: anterior view). **C' -** Detail of the architecture of the left half of the maxilla 1 neuromere (antero-ventral view). Arrowheads point at the level of insertion of the neurites of the ventral cell cluster at different level of the neuromere. Thinner neurite bundles projecting from smaller ventro-lateral cell clusters insert at the level of the ventral component of the segmental nerve root (open arrowheads). The median fiber tract is encircled by open ring. **C" -** Detail of the ventral portion of the maxilla 1 commissure (ventral view). The circle marks the level of intersection of the ventral branches of the segmental nerve. **D**-**D' -** View of the telson region. Asterisks mark the single cell somata around the proctodeum. Arrows point to the two terminal branches of the median fiber tract. **D -** General overview (ventro-lateral view). The filled arrowhead points at the median fiber tract. Open arrowheads point at the lateral branch of the terminal portion of the connective. **D' -** Detail of the terminal portion of the median fiber tract (ventral view).

aC: anterior commissure; CO: connective; MD: mandible; MDn: mandibular neuromere; MDC: mandibular commissure; MFT: median fiber tract; MX1n: maxilla 1 neuromere; MX2n: maxilla 2 neuromere; pC: posterior commissure; PR: proctodeum; TH1n: thoracopod 1 neuromere; TH2n: thoracopod 2 neuromere.

Stomatogastric nervous system

The whole system has become more compact around the stomodeum (Fig. 48). The diameter of the labral commissure has noticeably increased (Fig. 48A'). Medially to each of its branches a neurite bundle has formed which projects to the ventral side towards the labrum forming the labral nerve (open arrowheads in Fig. 48 A'). The commissural ganglion is visible lateral to the labral commissure (stippled circle in Fig. 48).

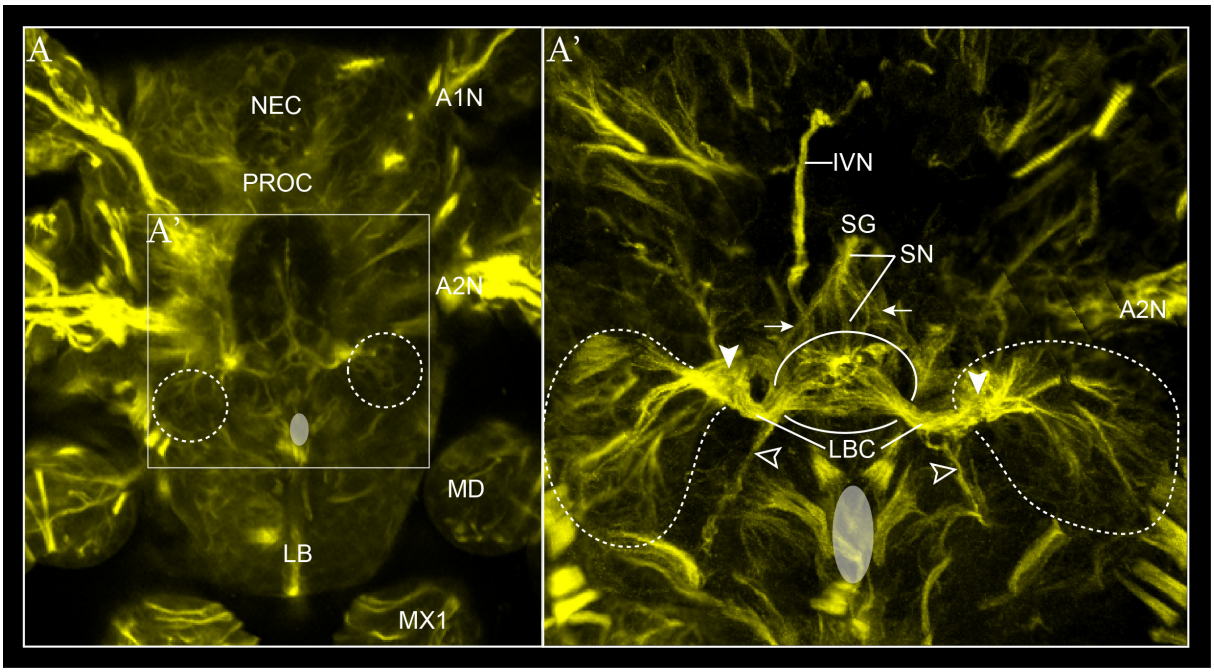

Fig. 48 – Axogenesis of the stomatogastric nervous system in *P. monodon*, nauplius stage 5-6 (metanauplius)

Anti-ac-α-tubulin labelling. CLSM image stack. Imaris surpass mode: volume, clipping plane. Stippled circles mark the ventral cell cluster projecting at the sides of the superior commissure. The position of the stomodeum opening is pointed by transparent oval. **A -** General overview of the ventral-most portion of the naupliar region (ventral view). The position of the forming stomatogastric nervous system is included

within the frame (magnified in **A'**). **A' -** Detail of the stomatogastric nervous system (ventral view). Arrows point at the neurite bundles forming the stomodeal commissure. Filled arrowheads point at the level of insertion of the ventral projection into the labral commissure. Open arrowheads point at the labral nerves. Open circle line marks the position of the labral ganglion.

A1N: antenna 1 nerve; A2N: antenna 2 nerve; IVN: inferior ventricular nerve; LB: labrum; LBC: labral commissure; MD: mandible; MX1: maxilla 1; NEC: nauplius eye complex; PROC: pre-oral commissure; SG: stomatogastric ganglion; SN: stomatogastric nerve.

Serotonin-like expression pattern

In the naupliar region the number of SL-ir neurons has increased and the SL-ir neuropilar region expanded (Fig. 49A-C). The paired SL-ir neurons ventral to the pre-oral commissure are still observable (filled arrowheads in Fig. 49A-C). They have taken a more lateral location and the SL-ir neurite which connects the commissure has elongated (arrows in Fig. 49A). More dorsally several SL-ir neurons have formed within the medulla terminalis at different levels (asterisks in Fig. 49C). One in particular is associated with the frontal organ and belongs to the frontal organ center (star in Fig. 49C). The SL staining has become more intense in the anterior portion of the pre-oral commissure and has expanded all along the frontal tract (Fig. 49A-C). Posteriorly it has expanded along the nerve ring connective intensely to the deutocerebrum (Fig. 49A) and more weakly to the posterior neuromeres reaching the maxilla 1 neuromere (Fig. 49D). One additional lateral pair of SL-ir neurons has formed posterior to the mandibular nerve (asterisks in Fig. 49D). Although no SL-ir neurites are visible connecting these neurons to any neuromere they are most probably associated with the anterior side of the maxilla 1 neuromere. Moreover one median pair of SL-ir neurons is observable right posterior to the maxilla 1 posterior commissure (stars in Fig. 49D), one more ventral and one more dorsal.

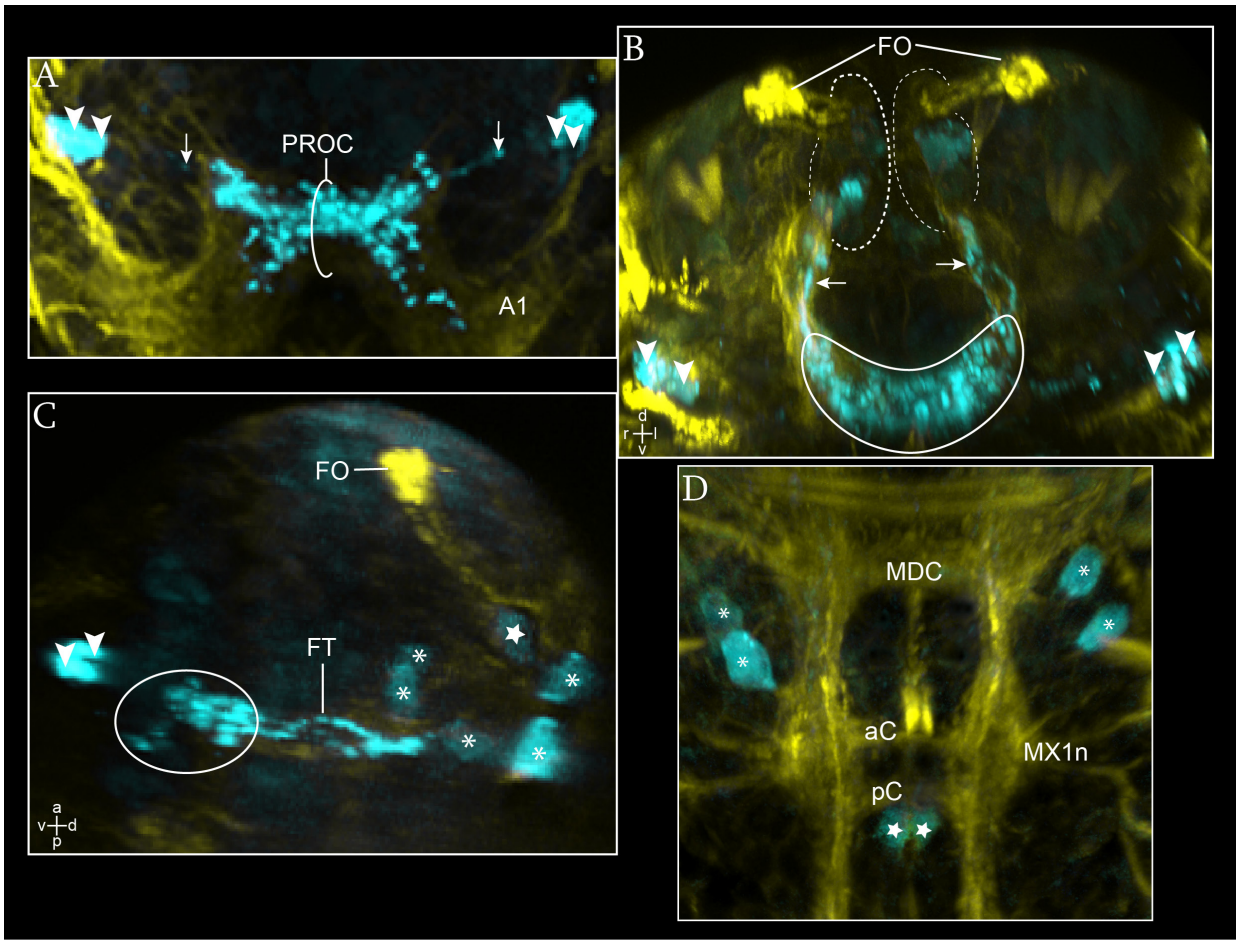

Fig. 49 – SL-ir structure distribution in *P. monodon*, nauplius stage 5-6 (metanauplius)

Anti-ac-α-tubulin labelling in yellow. Anti-serotonin-like labelling in light blue. CLSM image stack. Imaris surpass mode: volume, clipping plane in **A**, **B**; section mode in **C**. **A**-**C -** View of the SL-ir structures in the brain. **A -** View of the anterior region of the circumesophageal nerve ring (ventral view). Filled arrows point at single SL-ir neurons. They are connected to the SL-ir neuropilar region via one thin SL-ir neurite (arrow). **B -** Detail of the protocerebral region (antero-ventral view). The region of the medulla terminalis is encircled by stippled line. Arrows point at the extension of the neuropilar layer into the frontal tract. Filled arrowheads point at the ventro-lateral SL-ir cell somata. The SL-ir neuropilar region of the pre-oral commissure is encircled. **C -** View of the left half of the protocerebral region (lateral view). The filled arrowhead points to the pair of antero-ventral SL-ir neurons. Circle marks the position of the pre-oral commissure neuropil. Single SL-ir cell neurons in the medulla terminalis are marked by asterisks. Star marks the SL-ir neuron of the frontal organ center. **D -** View of the SL-ir structures in the ventral nerve cord (ventral view). Asterisks mark single SL-ir neurons associated with the maxilla 1 neuromere. Stars mark single median SL-ir neurons posterior to the posterior maxilla 1 commissure.

aC: anterior commissure; FO: frontal organ; FT: frontal tract; MDC: mandibular commissure; MX1n: maxilla 1 neuromere; pC: posterior commissure; PROC: pre-oral commissure.

3.2.2.5 Protozoea stage 1

Axogenesis

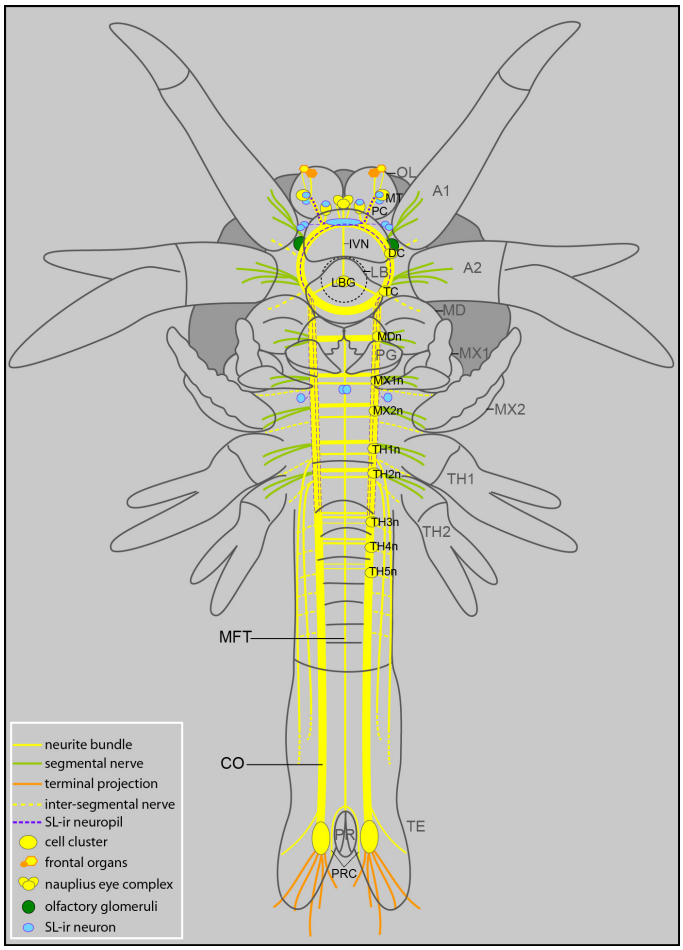

Fig. 50 – *P. monodon*, protozoea stage 1

Schematic illustration of the distribution of neural structures (ventral view). The region of the stomodeum is marked by black broken circular line. The proctodeum is represented by a small grey oval. Only the superior portion of the stomatogastric nervous system anlage is schematized.

A1: antenna 1; A2: antenna 2; aC: anterior commissure; CO: connective; COG: commissural ganglion; DC: deutocerebrum; LB: labrum; LBC: labral commissure; LBG: labral ganglion; MD: mandible; MDC: mandibular commissure; MDn: mandibular neuromere; MFT: median fiber tract; MT: medulla terminalis; MX1: maxilla 1; MX1n: maxilla 1 neuromere; MX2: maxilla 2; MX2n: maxilla 2 neuromere; PC: protocerebrum; pC: posterior commissure; PG: paragnath; POC: post-oral commissure; PR: proctodeum; PRC: proctodeal commissure; PROC: pre-oral commissure; TC: tritocerebrum; TE: telson; TH1: thoracomere 1; TH1n: thoracomere 1 neuromere; TH2: thoracomere 2; TH2n: thoracomere 2 neuromere.

In the protocerebral region the antero-dorsal portion of the pre-oral commissure has become an intricate thick meshwork of neurites which probably represents the architecture of the central complex anlage (Fig. 51). This cannot be stated at this stage because of the lack of data that could provide a view on individual neuropils (e.g. SLI; see next paragraph). The ventro-lateral cluster of protocerebrum, i.e. cluster 6, *sensu* Sandeman et al. (1992) has

increased its volume, becoming a bi-lobed median structure antero-ventrally to the pre-oral commissure (Stippled circles in Fig. 51B). Medially the nauplius eye complex is located. The median neurites which connect the complex to the protocerebrum have become closer and form one single median unpaired neurite bundle (asterisk in Fig. 51B). The frontal tract has noticeably increased its diameter and at its dorsal extension the anlage of the optic lobe is observable (Fig. 51). Included in the optic lobe, the frontal organs are still observable, composed of two different structures (Fig. 51). The lateral one (filled arrowhead in Fig. 51) is now smaller. It pops out from the optic lobe rim and maintains a weak connection with the medulla terminalis. The median one has become bigger (stars in Fig. 51) and is embedded within the optic lobe, connected to the medulla terminalis and to the frontal tract. In the deutocerebral region the olfactory glomeruli have become more voluminous and a thick neurite bundle is observable spanned between the glomerulus and the pre-oral commissure (arrows in Fig. 51).

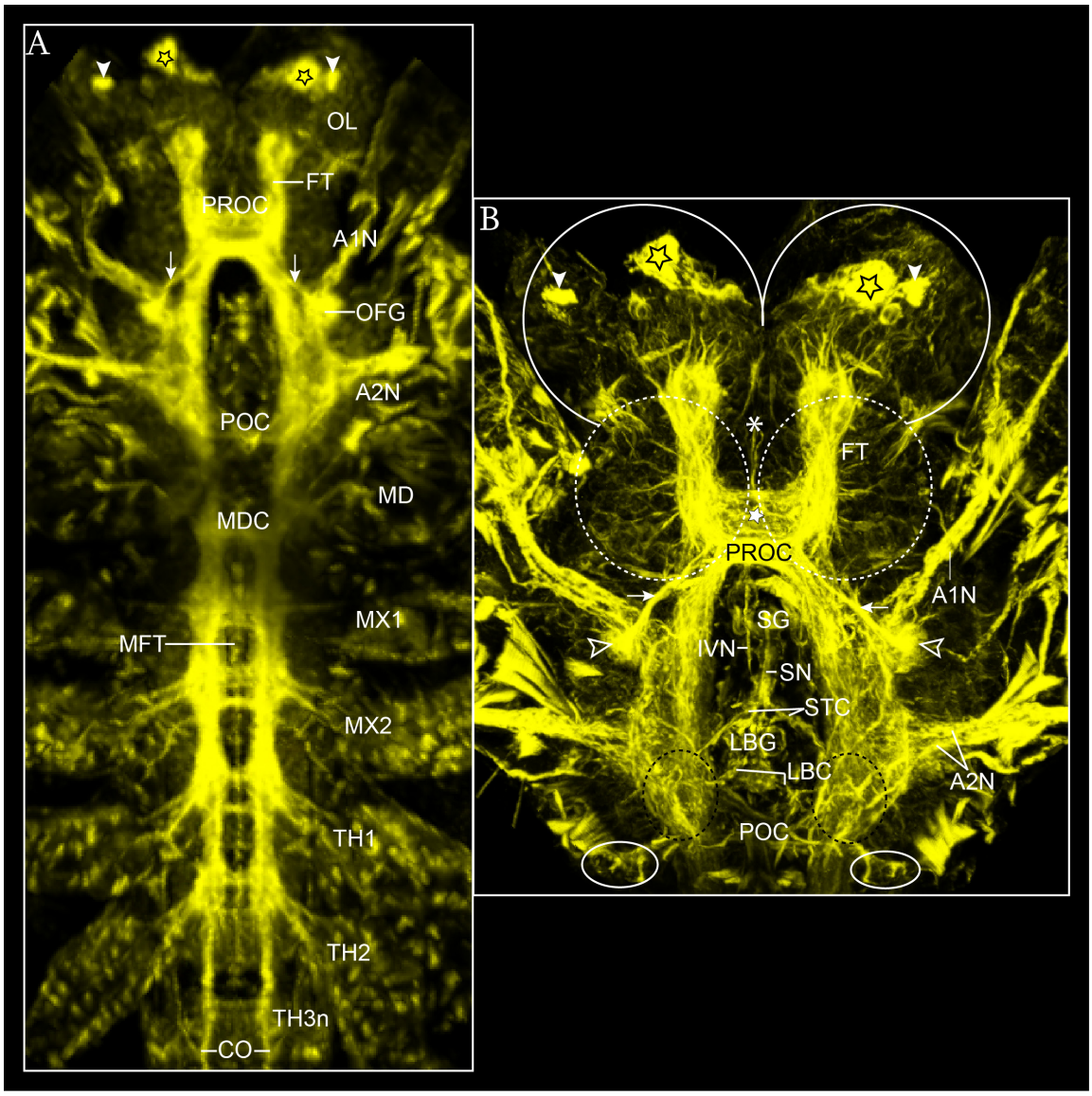

Fig. 51 – Axogenesis in *P. monodon*, protozoea stage 1

Anti-ac-α-tubulin labelling. CLSM image stack. Imaris surpass mode: volume, clipping plane. **A -** General overview of the naupliar region and of part of the ventral nerve cord (ventral view). The thoracic neuromeres posterior to thoracomere 3 are excluded from the picture. Filled arrowheads point at the external portion of the frontal organs while black stars mark their internal component. Arrows point at the neurite bundles which connect the olfactory glomeruli to the pre-oral commissure. **B -** General overview of the architecture of the brain and its connection with the peripheral nervous system (ventral view). The stomatogastric nervous system is included in the picture. Filled arrowheads point at the external portion of the frontal organs while black stars mark their internal component. White star marks the neuropilar layer forming the anlage of the central complex. Arrows point at the neurite bundles which connect the olfactory glomeruli (open arrowheads) to the pre-oral commissure. Lines surround the border of the optic lobe. Stippled circles mark the position of the antero-ventral cell cluster forming of the protocerebrum. Ovals at the bottom of the image mark the position of the ventro-lateral cell clusters connected with the putative commissural ganglion (the black stippled circles). Asterisk marks the anterior end of the nauplius eye nerve.

A1N: antenna 1 nerve; A2N: antenna 2 nerve; CO: connectives; FT: frontal tract; LBG: labral ganglion; IVN: inferior ventricular nerve; MD: mandible; MDC: mandibular commissure; MX1: maxilla 1; MX2: maxilla 2; TH1: thoracopod 1; TH2: thoracopod 2; TH3n: thoracomere 3; OL: optic lobe; POC: post-oral commissure; PROC: pre-oral commissure; SG: stomatogastric ganglion; SN: stomatogastric nerve; STC: stomodeal commissure.

In the post-naupliar region, the first four post-naupliar neuromeres (i.e. maxilla 1, 2 and thoracomere 1, 2) are all composed of a double commissure, one anterior and one posterior (Fig. 51A and Fig. 52A, A'). The nerve roots of the segmental nerves have become thicker. Posterior to the segmental nerve of thoracomere 1 one neurite bundle runs laterally and extends posteriorly (open arrowheads in Fig. 52A'). In the same way one neurite bundle runs out posteriorly to the segmental nerve of thoracomere 2 and extends to the posterior medially to the previous bundle (filled arrowheads in Fig. 52A'). The posterior end of these two longitudinal neurite bundles could not be followed. The anlage of the last six thoracic neuromeres has formed and the anlage of the anterior commissures of thoracomere 3, 4 and 5 is observable (arrows in Fig. 52A'). Feeble neurites run out from the connective at the level of each neuromere (asterisks in Fig. 52A'). These neurites run to the lateral side and turn to the dorsal following the shape of the caudal papilla. Here they connect to a single cell soma located at the lateral side of the gut tube (open arrowheads and small ovals in Fig. 52A"). Because of their location, timing of appearance and connection to the gut, these neurites most likely represent the anlagen of the inter-segmental nerve in the posterior portion of the thorax. A very thin longitudinal neurite runs adjacent to the dorso-lateral wall of the gut tube (arrows in Fig. 52A"). This is associated with a cell cluster located posterior to the level of thoracomere 2 (stippled ovals in Fig. 52A"). The number of neurites forming the connectives have noticeably increased at the level of the first four post-naupliar segments while more posteriorly they result thinner (Fig. 52A, A'). At their posterior end they split into a median and a lateral neurite bundles (Fig. 52A"'). The lateral bundle branches further innervating the terminal spines (Fig. 52A"'). From the anterior margin of the proctodeum the two terminal branches of the median fiber tract extend further posteriorly and end in the internal margin of the telson close to the median branch of the connective (filled arrowheads in Fig. 52A"').

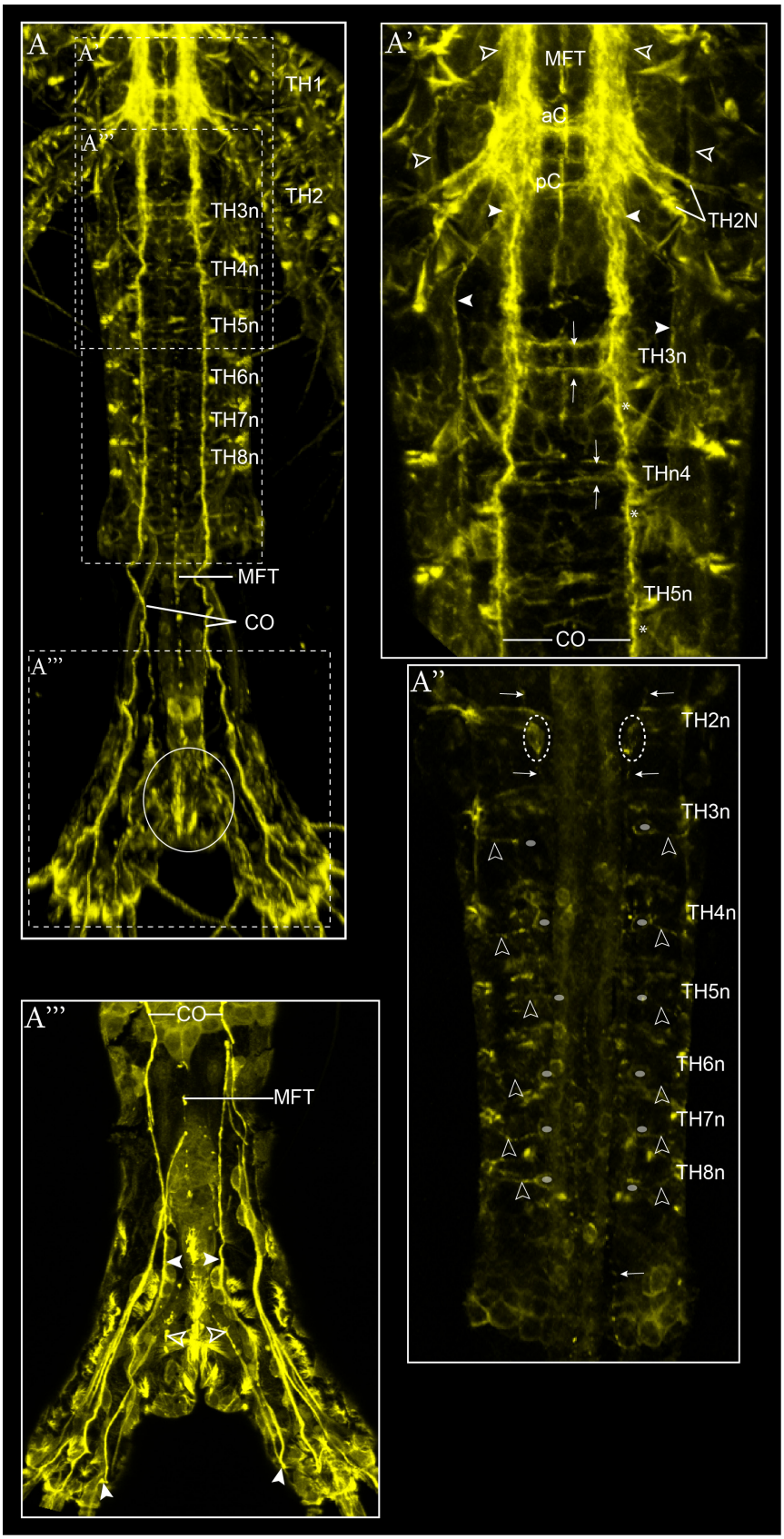

Fig. 52 – Axogenesis in *P. monodon*, protozoea stage 1

Anti-ac-α-tubulin labelling. CLSM image stack. Imaris surpass mode: volume, clipping plane. . Axogenesis in the posterior thoracic segments and in the telson (ventral view). **A -** General overview. Circle marks the position of the proctodeum. Stippled line squares refers to the corresponding areas shown in details in **A'**, **A"** and **A"'**. **A' -** Detail of axogenesis at the level of thoracomere 2-5 anlagen. Open arrowheads point at the extension of the lateral most longitudinal neurite bundle. Filled arrowhead point at the extension of the longitudinal neurite bundle running in between this last and the connective. Arrows point at the commissural anlagen in thoracomere 3-5. Asterisks mark the level of connection of the inter-segmental nerves. **A" -** Axogenesis in the dorsal side of the thoracic segment anlagen. Arrows point at the extensions of the dorsal neurites running adjacent to the dorso-lateral wall of the gut tube. Stippled oval marks the cell clusters associated with them. Small oval mark single cell somata connected with the inter-segmental nerves (open arrowheads). **A"' -** Axogenesis in the terminal portion of the tail. Filled arrowheads point at the extension of the median branches of the terminal portion of the connectives. Open arrowheads point at the two terminal branches of the median fiber tract.

aC: anterior commissure; CO: connectives; MFT: median fiber tract; pC: posterior commissure; TH1, 2:thoracopod1, 2; TH2N: thoracopod2 nerve; THn3-8: thoracomere3-8.

Stomatogastric nervous system

The architecture of the stomatogastric nervous system becomes more solid and compact being enriched by neurites in all its components (Fig. 51B). Ventrally in the labrum paired fan-like structures, which project some neurites dorsally to the labral commissure, are visibly stained (encircled in Fig. 51B).

Serotonin-like expression pattern

Unfortunately no SL labelling was successfully performed for this stage.

3.2.2.6 The distribution of SL-ir structures in the protozoea stage 2

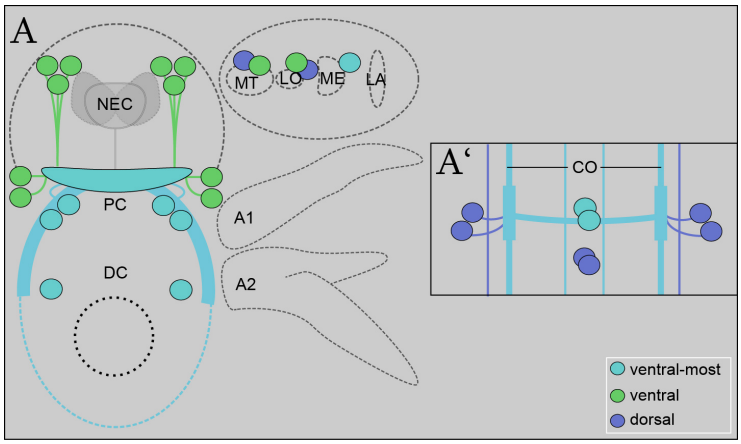

Fig. 53 – Distribution of SL-ir structures in *P. monodon*, protozoea stage 2

Schematic illustration of the distribution SL-ir structures in the naupliar region (**A**) and in each of the post-naupliar neuromeres (**A'**) (ventral view). Colored circles represent single SL-ir cell somata (minimum number observed). Color-codes refer to different positions of the neural structures along the ventro-dorsal axis, as indicated in the legend.

A1N: antenna 1 nerve; DC: deutocerebrum; LA: lamina; LO: lobula; ME: medulla; MT: medulla terminalis; MX1n: maxilla 1 neuromere; MX2n: maxilla 2 neuromere; NEC: nauplius eye complex; OFG: olfactory glomeruli; PC: protocerebrum; TH1-3n: thoracomere 1-3.

In the protocerebral region it is possible to observe three distinct paired SL-ir cell clusters connected with a broad unpaired median SL-ir neuropil which probably represents the anlage of the central body (star in Fig. 54A, B). The anterior-most SL-ir cell cluster is located adjacent to the nauplius eye complex, right at its lateral side, keeping a dorsal position relative to the other two cell clusters (stippled circle in Fig. 54A). It is possible to distinguish at least three SL-ir cell somata at this level which are weakly stained (asterisks in Fig. 54B). These are embedded in a sizeable mass of cell somata which constitute the antero-dorsal portion of the head i.e. cluster 6, *sensu* Sandeman et al. (1992). The other two SL-ir cell clusters are located more posterior at the level of the protocerebrum, one lateral and one ventral, the latter one being the most ventral of the three mentioned clusters (Fig. 54A, B). Due to their distinct location relative to the growing protocerebral neuropil, I suggest they correspond to cluster 8 and cluster 7, respectively, *sensu* Sandeman et al. (1992). The signal of SL along the brain neuropils has a diffuse distribution more condensed at the level of the protocerebrum, which gradually fades to the posterior so that at the level of the tritocerebrum there is no clear detectable signal. Although weak, SLI is detectable at the level of the deutocerebrum along the median connective where the olfactory glomeruli (which does not show any SLI) is located and extends a bit more posterior reaching the insertion of the antenna 2 nerve (Fig. 54A, B). At the same level but more ventral, one or two SL-ir cell somata are located at each median side (Fig. 54A, B). It is quite uncertain to which brain neuromere these paired cell cluster belongs to since there are no evident neural connections. These cells lie in front of the stomatogastric nervous system, just behind the labrum.

The compound eye has developed and it is possible to recognize the eye neuropil anlagen: the lamina and the medulla anlagen have formed in addition to the medulla terminalis. The lobula anlage is located between the medulla terminalis and the medulla (Fig. 54C). Several SL-ir cell somata are visibly stained within the proximal portion of the compound eye which can be subdivided in three separate clusters. One, the most numerous, is associated with the medulla terminalis, i.e. cluster 4, *sensu* Sandeman et al. (1992), one with the lobula, i.e. cluster 3, *sensu* Sandeman et al. (1992) and the third, consisting of few cell somata only weakly stained, is connected with the medulla, i.e. cluster 2, *sensu* Sandeman et al. (1992) (Fig. 54C). To note the presence of a medio-ventral structure stained by α-tubulin and connected to the medulla terminalis (open star in Fig. 54C). There is no trace of frontal organ within the rhyme of the stalked eye.

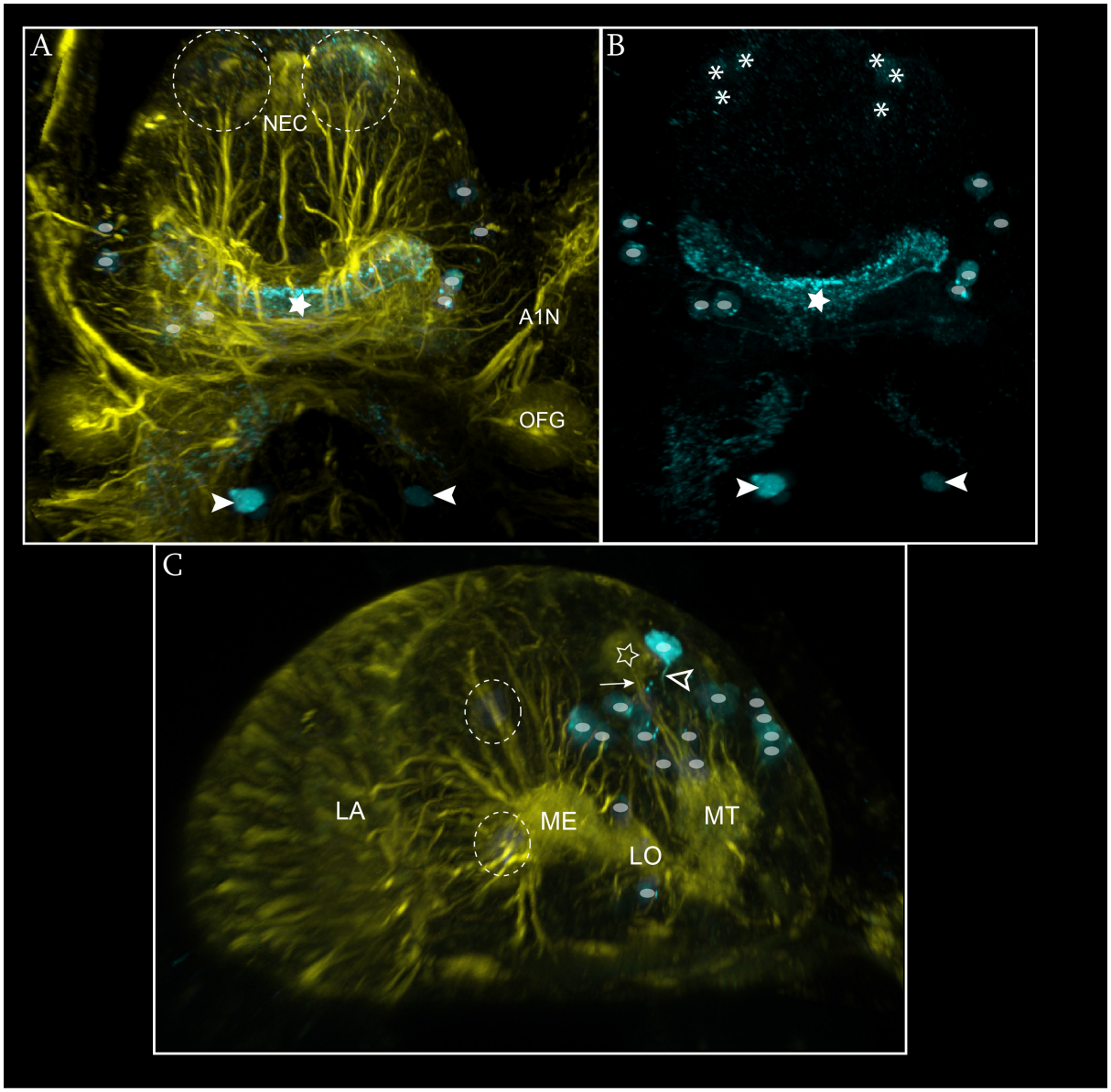

Fig. 54 – Distribution of SL-ir structures in the naupliar region in *P. monodon*, protozoea stage 2

Anti-ac-α-tubulin labelling in yellow. Anti-serotonin-like labelling in light blue. CLSM image stack. Imaris surpass mode: volume, clipping plane. **A**, **B -** General overview of the protocerebral region (ventral view). Part of the deutocerebrum is included in the picture i.e. the root of antenna 1 and the olfactory glomeruli anlage. Small oval mark single SL-ir cell somata of the ventral and lateral clusters. Filled arrowheads mark single ventral SL-ir neurons dorsal to the anterior margin of the labrum (not shown). Stippled ovals in **A** mark the position of the SL-ir cell cluster in the apical region. Asterisks in **B** mark single SL-ir cell somata in the apical cluster. **C -** Detail of the compound eye (ventral view). Small oval mark single SL-ir cell somata. Stippled ovals mark two weakly stained SL-ir cell somata at the ventral, distal most portion of the eye. Open arrowhead marks one SL-ir neurites running off from one SL-ir neuron. The star marks the position of the putative SP-X organ and the arrow its connection with the medulla terminalis. Numbers name cell clusters putatively referred to the classification followed by Sandeman et al. (1992).

A1N: antenna 1 nerve; DC: deutocerebrum; LA: lamina; LO: lobula; ME: medulla; MT: medulla terminalis; MX1, 2n: maxilla 1, 2 neuromere; NEC: nauplius eye complex; OFG: olfactory glomeruli; PC: protocerebrum; TH1-3n: thoracomere 1-3.

In the post-naupliar region the presence of SL-ir structures has grown consistently along the ventral nerve cord. A part from a diffused but quite strong signal at the level of each

neuromere it is possible to distinguish distinct SL-ir neurite bundles running longitudinally and some very thin ones crossing transversally at the level of each commissure (Fig. 55).

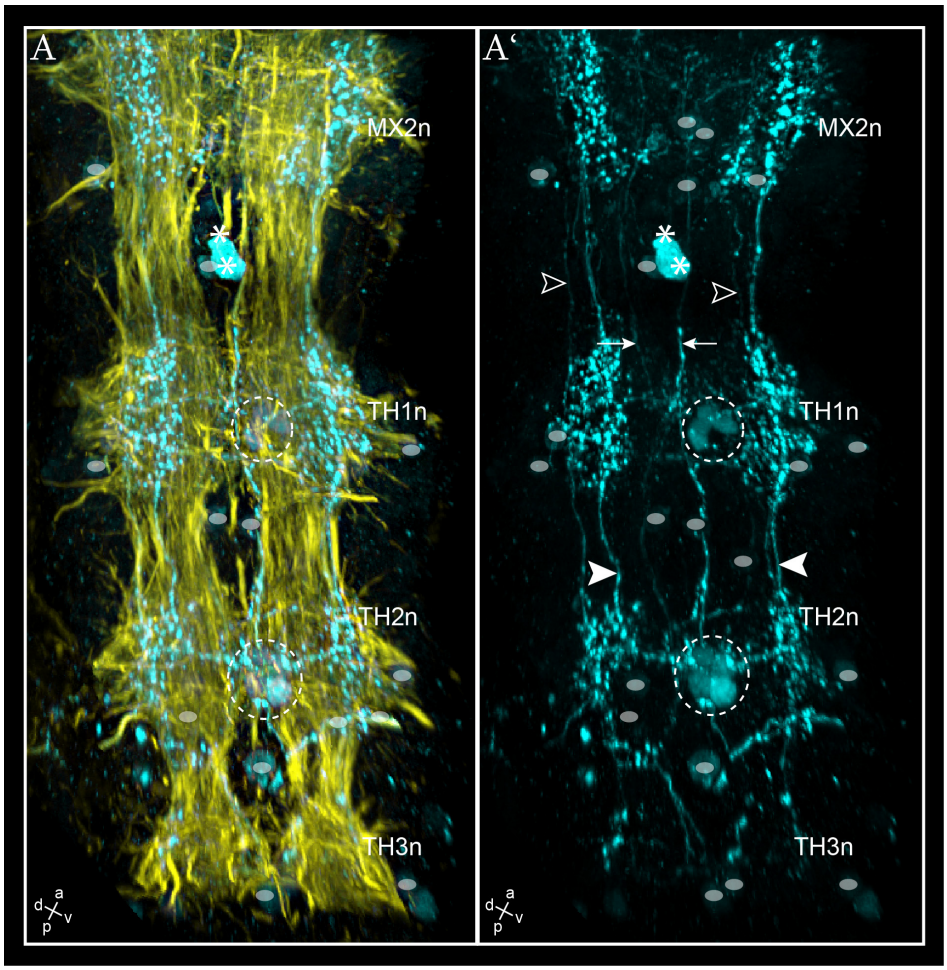

Fig. 55 – Distribution of SL-ir structures in the VNC of *P. monodon*, protozoea stage 2

Anti-ac-α-tubulin labelling in yellow. Anti-serotonin-like labelling in light blue. CLSM image stack. Imaris surpass mode: volume, clipping plane. View of the anterior portion of the ventral nerve cord (ventro-lateral view). Asterisks mark single brightly stained SL-ir neurons. The small ovals mark single weakly stained SL-ir neurons. Arrows point at single neurites running medially along the connective. Filled arrowheads point at single neurites running ventro-laterally along the connective while open arrowheads to single dorso-lateral neurites.

MX2n: maxilla 2 neuromere; TH2-3n: thoracomere 2-3.

Three distinct longitudinal SL-ir neurite bundles are distinguishable: one median, running lateral to the median fiber tract (arrows in Fig. 55A’), and two lateral, one thicker ventral (arrowheads in Fig. 55 A’) and one thinner dorsal (open arrowheads in Fig. 55 A’), both embedded into the thick connective. The SL-ir cell somata have a regular distribution at the level of each neuromere and a pattern which develops following an antero-posterior gradient is recognized. Two unpaired paired SL-ir cell cluster are located medially at the ventral and at the dorsal side of each neuromere (asterisks and stippled circles in Fig. 55). The number of

SL-ir cell somata in each cluster is generally four, but sometimes only of two or three. One pair of SL-ir cell somata is observed at the dorso-lateral side of each neuromere (small ovals in Fig. 55) and is connected to the neuropil by a pair of thin SL-ir neurites.

3.2.2.7 Short note on the development of the protocerebrum and the nauplius eye complex in the protozoea stage 3

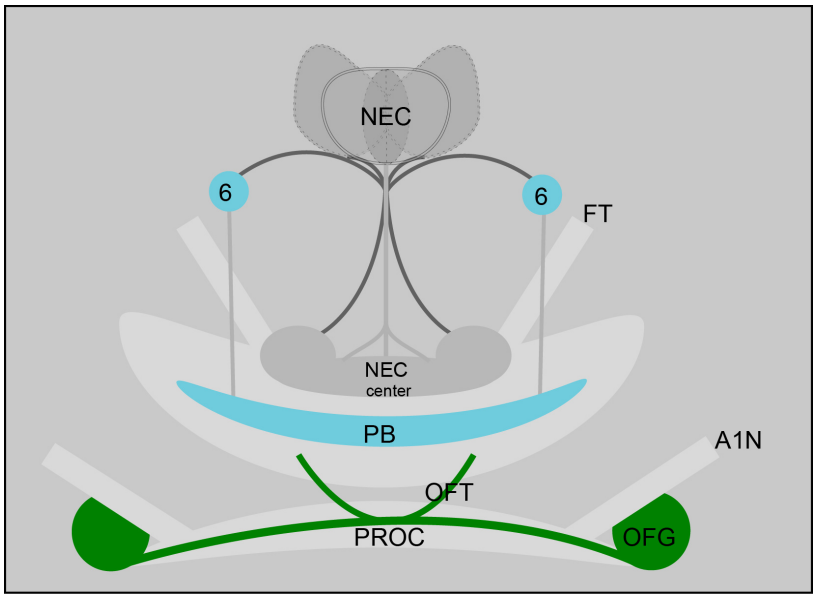

Fig. 56 – Architecture of the protocerebrum and of the nauplius eye complex in *P. monodon*, protozoea stage 3

Schematic illustration of the architecture of the protocerebrum and its connection with the nauplius eye complex and the olfactory glomeruli (in green) (ventral view). SL-ir structures are labelled in light blue. They correspond to the putative cell cluster 6, *sensu* Sandeman et al. (1992), and protocerebral bridge.
A1N: antenna 1 nerve; FT: frontal tract; NEC: nauplius eye complex; OFG: olfactory glomeruli; OFT: olfactory tract; PB: protocerebral bridge; PROC: pre-oral commissure.

The protocerebrum has condensed into a massive antero-dorsal unit in which it is no longer possible to identify separate neurite bundles (Fig. 57A). Ventrally the protocerebrum is organized in horizontal layers in which three portions are distinguishable: two anterior compact neuropils and one posterior layer which represents the pre-oral commissure. The most anterior neural layers are geometrically organized into a compact midline unpaired SL-ir neuropil which probably represents the anlage of the protocerebral bridge (Fig. 57 A, B). The anterior surface is connected laterally to the bunch of neurite bundles associated with the antero-ventral cell cluster, i.e. cluster 6, *sensu* Sandeman et al. (1992), and, medially and medio-dorsally, to the nauplius eye complex (Fig. 57B, C). This last has increased in size and additional neurites bundles have formed. One neurite bundle branches off posteriorly from the

median nauplius eye nerve (open arrowheads in Fig. 57B and C') and connects to the dorsal portion of the protocerebrum where the anlage of a three parted nauplius eye centre is now recognizable (open stars in Fig. 57B and C'). The second neurite bundle branches off from the median nauplius eye nerve more anteriorly, just behind the insertion of the cups (arrows in Fig. 57C'), and goes laterally connecting to the cell somata of cluster 6, *sensu* Sandeman et al. (1992) (Fig. 57A and C). Posteriorly, the neural layers are connected to the pre-oral commissure via a thick tract corresponding to the olfactory tract (open arrowhead in Fig. 57A). From the dorsal portion of this compact mass the thick frontal tract runs out (filled stars in Fig. 57 C) and constitutes the stalk of the prominent compound eye (not shown).

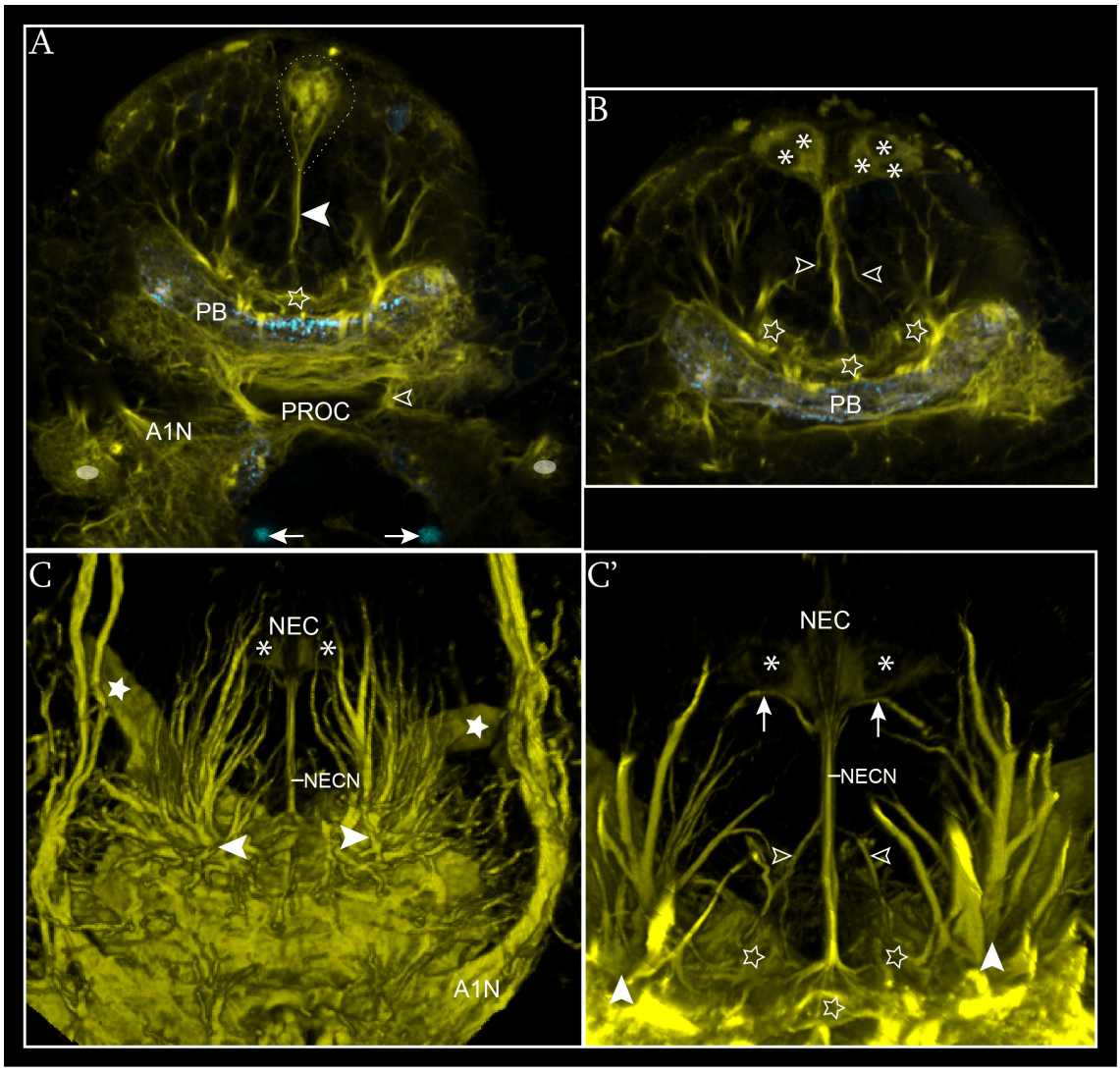

Fig. 57 – Architecture of the protocerebrum in *P. monodon*, protozoea stage 3

Anti-ac-α-tubulin labelling in yellow. Anti-serotonin-like labelling in light blue. CLSM image stack. Imaris surpass mode: volume (blend in **C**, **C'**); clipping plane in **B** and **C'**. **A -** General overview of the protocerebral region (ventral view). Part of the deutocerebrum is included in the picture i.e. the root of

antenna 1 and the olfactory glomeruli (small ovals). The ventral cup of the nauplius eye complex is encircled by a stippled line and the nauplius eye complex nerve is marked by the filled arrowhead. The open star marks the medial portion of the nauplius eye complex neuropil (the nauplius eye complex center). The putative protocerebral bridge is a massive anterior SL-ir neuropil. The open arrowhead points at the olfactory tract. A diffuse SL-ir neuropil occurs medially in the deutocerebral region (asterisks) and one pair of SL-ir neurons is located ventrally slightly posteriorly to it (arrows) and it probably belongs to the SNS. **B –** Detail of the protocerebral bridge and of the dorsal portion of the nauplius eye complex (ventral view). Asterisks mark each of the neurons of the lateral cups. Open arrowheads point at the lateral posterior branches of the nauplius eye complex nerve. The stars mark the three regions of the nauplius eye complex center. **C**-**C' –** Detail of the anterior-most portion of the protocerebrum and of the nauplius eye complex' dorsal components (ventral view). Filled stars in **C** mark the frontal tract. Filled arrowheads point to the site of connection of the bunch of neurite bundles of the antero-ventral cell cluster, i.e. cluster 6, *sensu* Sandeman et al. (1992) with the protocerebrum. Asterisks mark the lateral cups of the nauplius eye complex. Arrows point at the anterior branches of the nauplius eye complex nerve. Open arrowheads mark the posterior ones. The open stars in **C'** mark each of the three portions of the nauplius eye complex center.

A1N: antenna 1 nerve; NEC: nauplius eye complex; NECN: nauplius eye complex nerve; PB: protocerebral bridge; PROC: pre-oral commissure.

Table 6 (next page)

The anlagen of the main external morphological structures (**MORPHOGENESIS**) and of the relevant neural components (**AXOGENESIS**) are listed in the rows. They are ordered following the antero-posterior axis of the animal. The developmental stages are listed in the columns (**E**: embryonic stage; **N1-6**: nauplius stages 1- 6; **ZOEA**: protozoea stage 1). The characters are organized in four columns (numbers at the bottom of the table) referring to: **1**=body regions; **2**=neuromeres; **3**=commissures; **4**=neurite bundles. The **green X** marks the time in which the mandibles are transformed from functional limbs into components of the prospective mouth apparatus. The **green rings** mark the time in which the median fiber tract has reached the proctodeum and the time in which the connectives have established their connection with the naupliar neuromeres (both at the nauplius stage 3-4). The distribution of SL immunoreactivity in the neuraxis (**light–blue X**) and in the neural somata (**light blue circles**) is indicated. The inter-segmental nerves are underlined by light-grey to simplify the reading of the table.

Abbreviations are as indicated in the **List of abbreviations**.

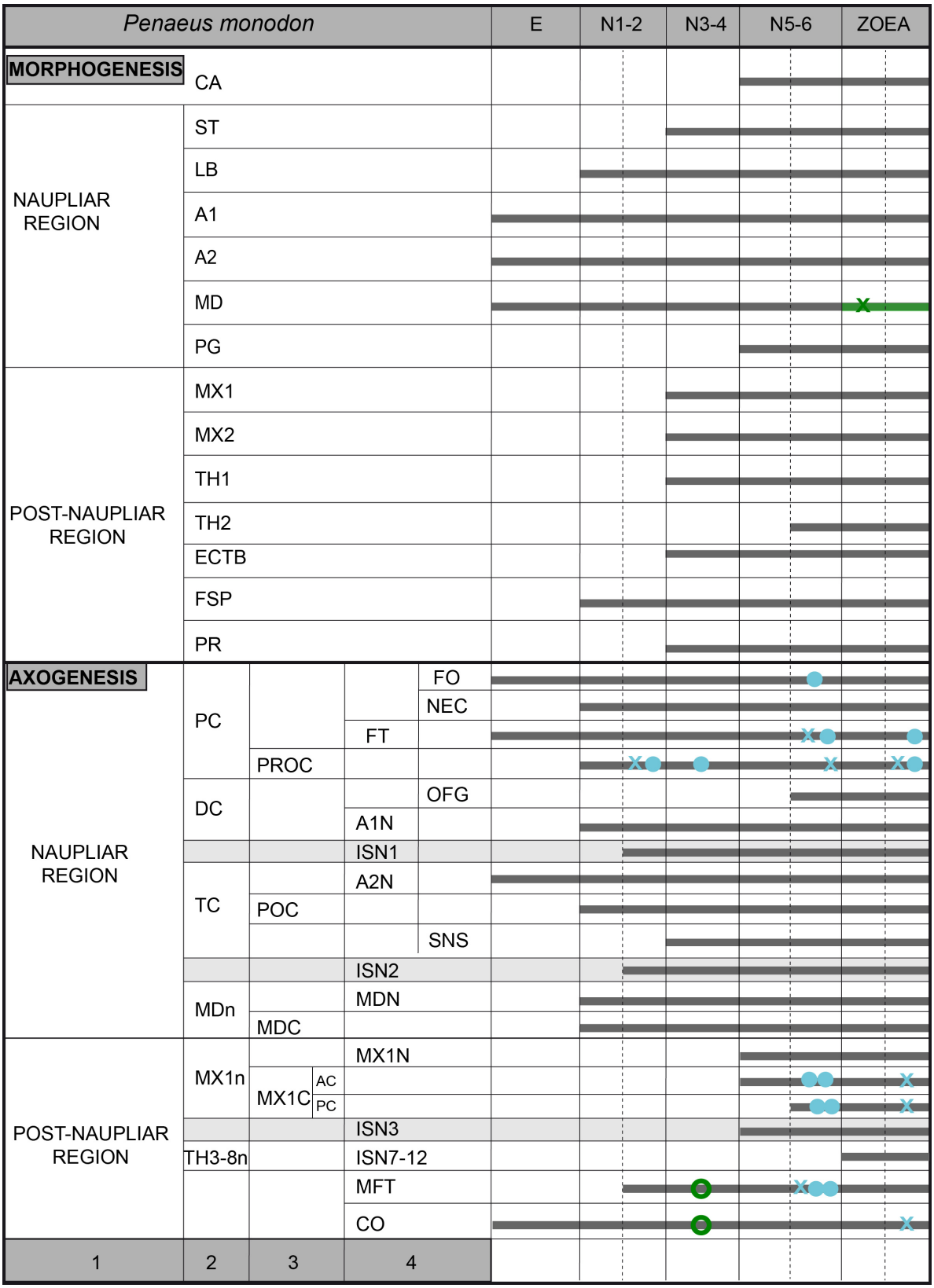

Table 7 - Summary of the main developmental events in *P. monodon*

3.3 Procambarus fallax (Hagen, 1870) f. virginalis

General remarks on the used staging

In this study, the staging of the embryonic morphogenesis of *P. fallax* refers to the system presented by Alwes and Scholtz (2005). Embryonic stage 3 represents the stage in which the first differentiating neural structures have been consistently observed. Nervous system differentiation has been followed up to embryonic stage 7. Some notes are added on the serotonin-like expression pattern at stage 8.

3.3.1 Morphogenesis

Since the external morphological changes according to the staging system herein adopted have been described in detail in the study of Alwes and Scholtz (2005), the present study offers only a brief resume of those. The external morphological characters used to discriminate between the stages are summarized in Table 7 and shown in Fig. 58.

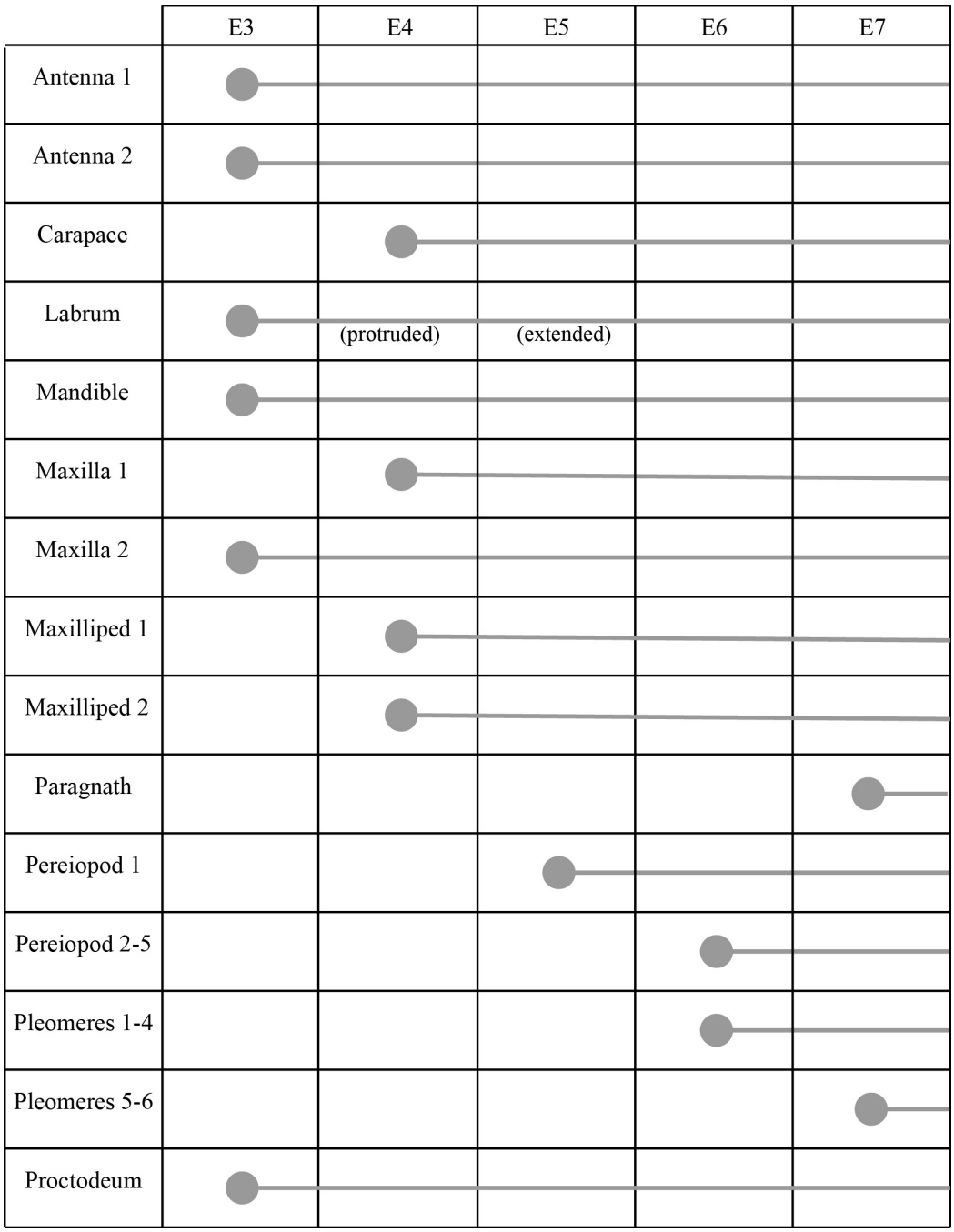

Table 8 – Formation and modification of the main external morphological characters during development of *P. fallax*

Characters are listed in the left column in alphabetical order. **E**: embryonic stage.

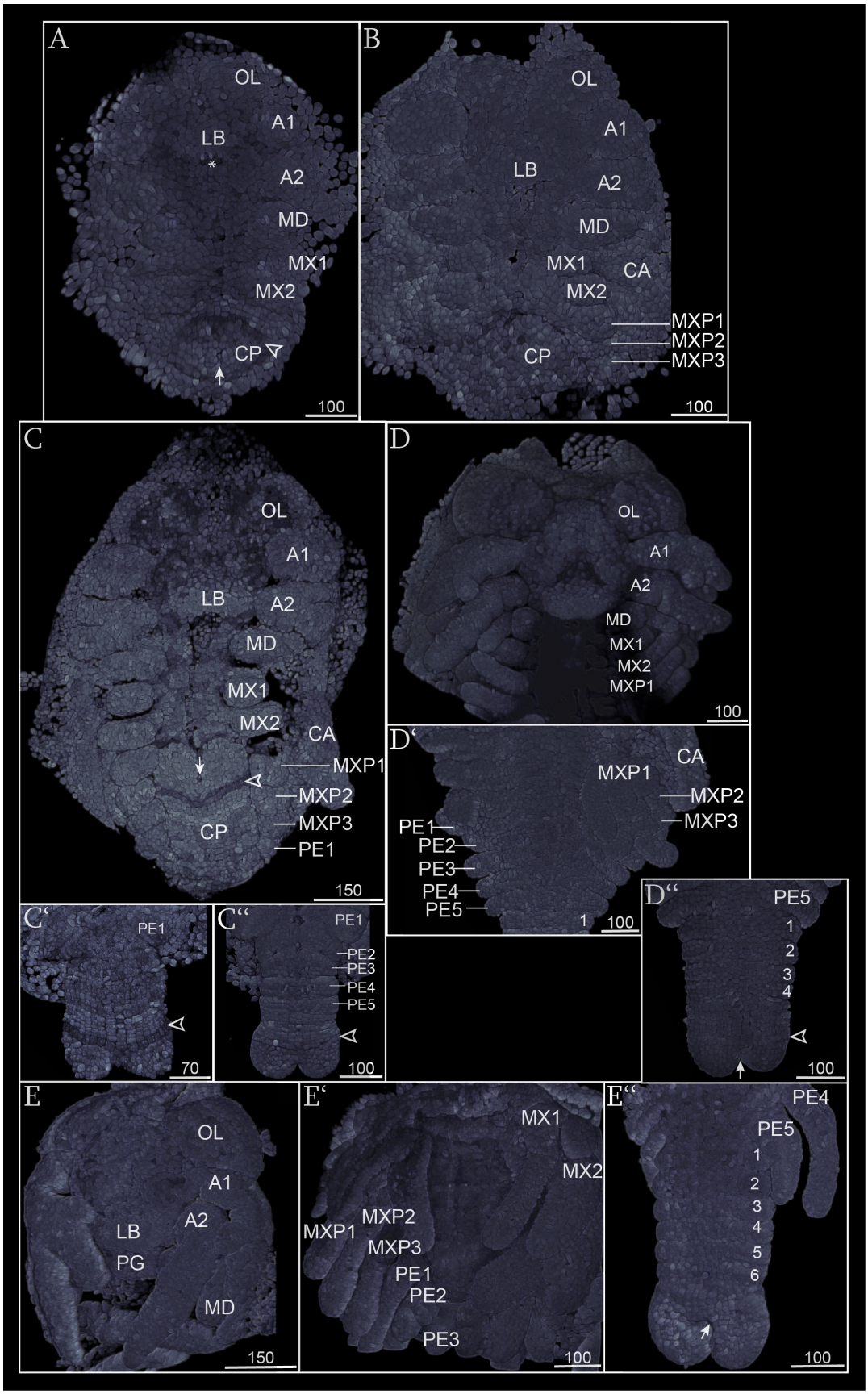

Fig. 58 – Morphogenesis in *P. fallax*, embryonic stages 3-7

Hoechst staining. CLSM image stack. Surpass mode: volume (blend). Arrows point at the anlage of the proctodeum. Open arrowheads point at the level of the ectoteloblast ring. Asterisk in **A** mark the position of the stomodeum. Ventral view. **A -** Embryonic stage 3. **B -** Embryonic stage 4. **C-C" -** Embryonic stage 5. **C' -** Detail of the caudal papilla in an early phase of the stage. **C" -** Detail of the caudal papilla in a late phase of the stage. **D-D" -** Embryonic stage 6. **D -** View of the naupliar region and of the first three thoracic segments. **D' -** View of the thoracic segments. **D" -** View of the caudal papilla and the anlage of the first four pleonal segments. **E-E" -** Embryonic stage 7. **E -** View of the naupliar region. **E' -** View of part of the thorax. **E" -** View of the caudal papilla and the anlage of the pleonal segments. **Scale bars** are as indicated in each image in micrometer (µm).

A1: antenna 1; A2: antenna 2; CA: carapace; CP: caudal papilla; ECTB: ectoteloblasts; LB: labrum; MD: mandible; MX1, 2: maxilla 1, 2; MXP1-3: maxilliped 1-3; OL: optic lobe; PE 1-5: pereiopod 1-5; PG: paragnaths; PL1-6: pleopod 1-6; PR: proctodeum; ST: stomodeum; TE: telson.

3.3.2 Nervous system development

3.3.2.1 Embryonic stage 3

Axogenesis

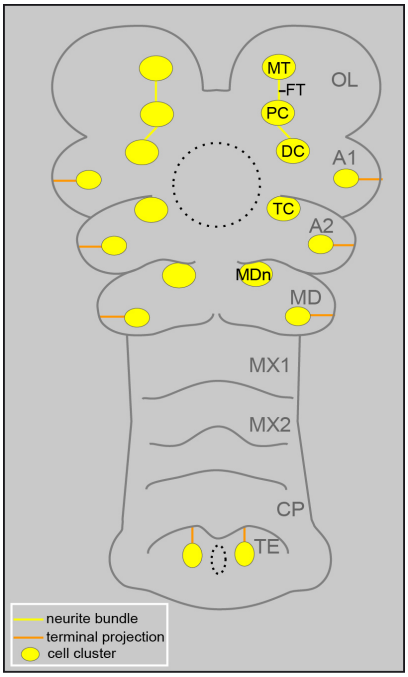

Fig. 59 – Axogenesis of *P. fallax*, embryonic stage 3

Schematic illustration of the distribution of neural structures (ventral view). The region of the stomodeum is marked by a black stippled circle, the proctodeum by the stippled oval in the telson.

A1: antenna 1; A2: antenna 2; CP: caudal papilla; DC: deutocerebrum; FT: frontal tract; LB: labrum; MD: mandible; MDn: mandibular neuromere; MT: medulla terminalis; PC: protocerebrum; MX1, 2: maxilla 1, 2; OL: optic lobe; PR: proctodeum; TC: tritocerebrum; TE: telson.

In the naupliar region, five cell clusters can be distinguished, symmetrically distributed at the sides of the stomodeum and clearly separate from each other (open arrowheads in Fig. 60A,

A'). They represent the anlagen of the brain neuromeres, the proto-, deuto- and tritocerebrum, and of the mandibular neuromere. Anterior to the stomodeum two separate cell clusters are recognizable, one proximal to the stomodeum which represents the anlage of the protocerebrum, and one distal, more anterior, which represents the anlage of the medulla terminalis (Fig. 60A). The anlage of the deutocerebrum lies at the level of the antenna 1 bud and antero-laterally adjacent to the stomodeum (Fig. 60A, A'). The anlage of the tritocerebrum is located at the level of the antenna 2 bud, postero-lateral to the stomodeum (Fig. 60A, A'), while the mandibular neuromere anlage takes a posterior position antero-medial to the mandible bud (Fig. 60A, A').

Slightly later in development, the first axons start to differentiate in each brain neuromere anlage, connecting one another (Fig. 60B, B'). In the periphery, short axonal projections are stained at different levels at the tips of the naupliar limb buds (arrows in Fig. 60B'). The projections extend from cell somata grouped in small clusters in the distal portion of the buds (e.g. asterisks in the A1 bud in Fig. 60B'). They most likely represent the pioneer innervations of sensory structures that lie underneath the ectodermal surface of the limb anlagen.

In the post-naupliar region, a cell cluster is distinguishable in the telson, antero-lateral to the proctodeum, and represents the anlage of the telsonic cell cluster (asterisks in Fig. 60C, C'). These cells lie in a more basal position than the ventral ectodermal layer and slightly posterior to the forming ectoteloblasts and of the corresponding proliferating mesoderm layer (Fig. 60C and D). They send short projections posteriorly towards the ventral side of the telson anlage (filled arrowheads in Fig. 60B and C, C'). Their terminal ends are visible at the external surface antero-lateral to the opening of the proctodeum (encircled in Fig. 60D).

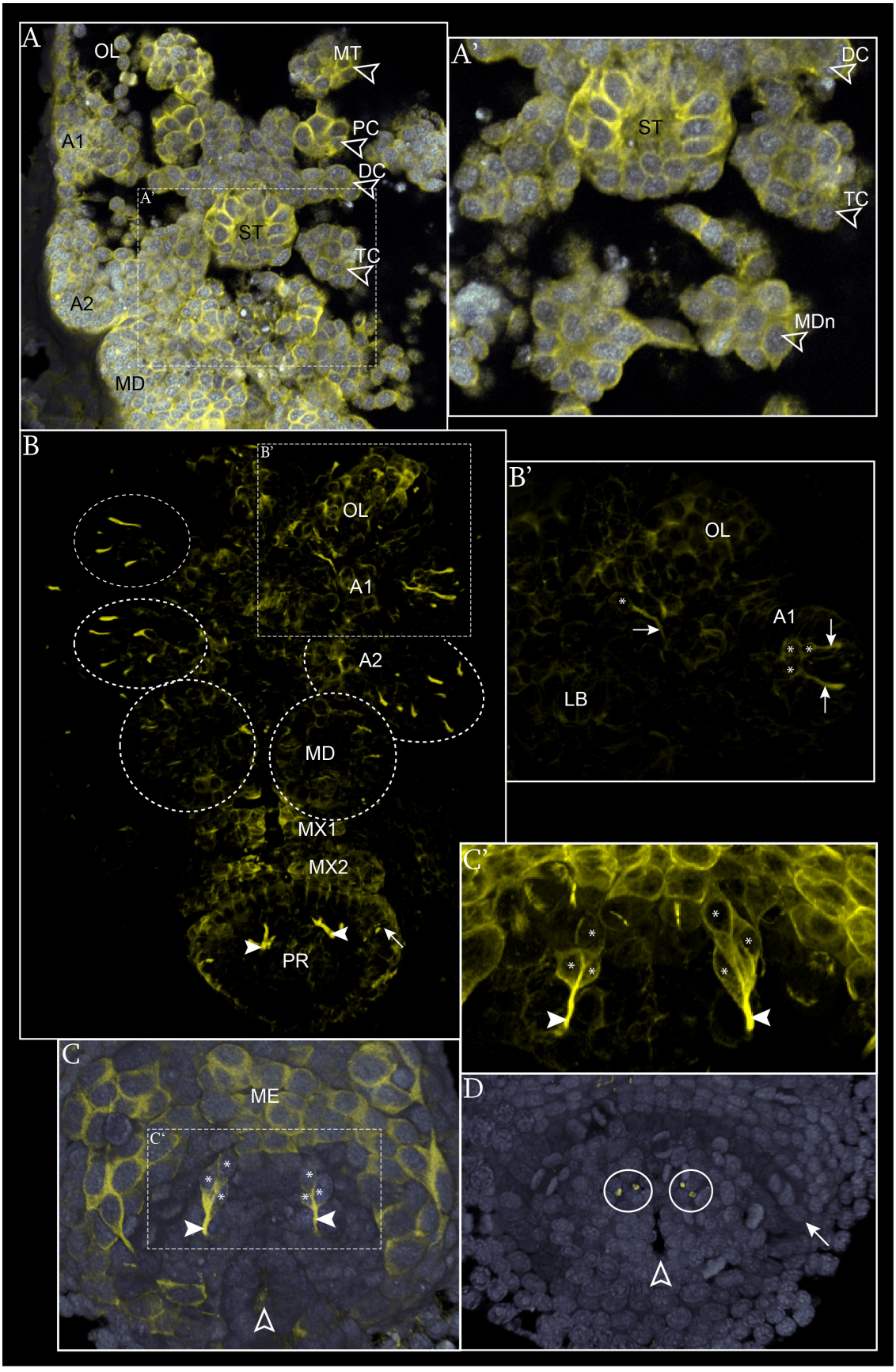

Fig. 60 – Axogenesis of *P. fallax*, embryonic stage 3

Anti-ac-α-tubulin labelling in yellow; Hoechst staining in grey. CLSM image stack. **A**, **A' -** View of the naupliar region in the early stage 3 (ventral view). Imaris surpass mode: volume, clipping plane (blend). Open arrowheads point at the cell clusters representing the anlagen of the naupliar neuromeres. In **A'** the selected plane is slightly more dorsal than in **A**. **B**, **B' -** Onset of axogenesis in a late stage 3 (ventral view). Imaris surpass mode: volume. **C**. General overview of the entire embryo. Stippled circles mark the naupliar limb anlagen. The arrow points at one side of the forming ectoteloblast ring. Filled arrowheads point at the terminal axonal projections. **B'** Detail of the left anterior-most part of the brain anlage. Asterisks mark single cell somata in the protocerebrum anlage and in the periphery within the antenna 1 limb bud. Pioneering neurite projections are labelled by arrows. **C**-**D -** Onset of axogenesis in the telson anlage (dorsal view in **C**, **C'**; ventral view in **D**). Imaris surpass mode: volume, clipping plane (blend in **C**, **D**). Asterisks label single cell somata within the terminal neuron cluster. Filled arrowheads point at their neural projections. Ovals in **D** mark the area of the neurites' external ends (two per side). The level of the growing ectoteloblasts ring is indicated by the arrow. Anterior to the terminal neuron clusters in the telson anlage mesodermal proliferating cells (ME) are visible.

A1: antenna 1; A2: antenna 2; CP: caudal papilla; DC: deutocerebrum; LB: labrum; MD: mandible; MDn: mandibular neuromere; ME: mesoderm; MT: medulla terminalis; MX1, 2: maxilla 1, 2; OL: optic lobe; PC: protocerebrum; PR: proctodeum; ST: stomodeum; TC: tritocerebrum.

Stomatogastric nervous system (SNS)

No evidence of differentiating neural structures of the stomatogastric nervous system has been observed at this stage.

3.3.2.2 Embryonic stage 4

Axogenesis

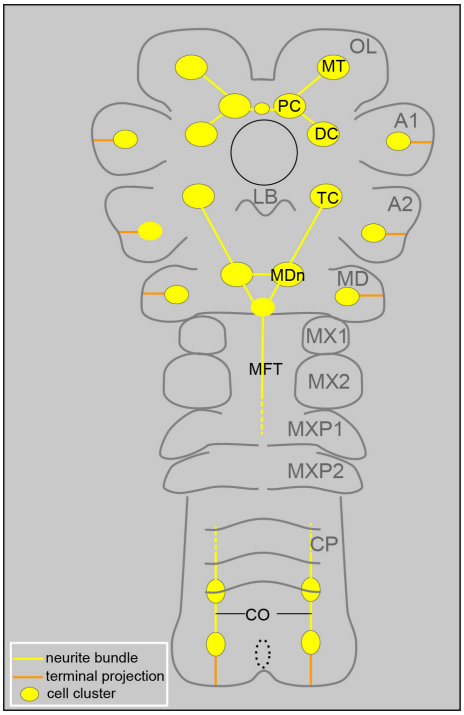

Fig. 61 – Axogenesis of *P. fallax*, embryonic stage 4

Schematic illustration of the distribution of neural structures (ventral view). The stomodeum is marked by the black circle. The stippled oval indicates the position of the proctodeum.

A1: antenna 1; A2: antenna 2; CP: caudal papilla; DC: deutocerebrum; FT: frontal tract; LB: labrum; MD: mandible; MDn: mandibular neuromere; MT: medulla terminalis; MX1, 2: maxilla 1, 2; OL: optic lobe; PC: protocerebrum; PR: proctodeum; TC: tritocerebrum.

In the naupliar region the first axonal projections are observable in the protocerebral and in the mandibular regions (Fig. 62). In the protocerebrum an antero-median cell cluster is visibly stained (open arrowheads in Fig. 62B') together with some cell somata intercalated in the forming pre-oral commissure (asterisks in Fig. 62A'). Short neurites span antero-laterally between the protocerebrum and the medulla terminalis forming the anlage of the frontal tract (Fig. 62A', B). Several neurites span between the protocerebrum and the deutocerebrum and, more posteriorly, between the tritocerebrum and the mandibular neuromere (Fig. 62A-A") constituting the anlage of the connective of the circumesophageal nerve ring. The anlage of the mandibular commissure has formed between the two mandibular hemi-neuromeres (Fig. 62A and A"). Posterior to the forming mandibular commissure about six distinct cell somata form a transversal row (asterisks in Fig. 62A"). The two more lateral ones are probably the commissural pioneer neurons while the four medial pioneer the connection with the more anterior neuromeres (i.e. the tritocerebrum anlage). Dorsally, in median position a seventh cell soma is observable (small oval in Fig. 62A"), representing, likely, the pioneer neuron of the median fiber tract (filled arrowhead in Fig. 62A").

In a later phase of the stage the anlage of the frontal tract has become thicker and has elongated (Fig. 62B). The anlage of the circumesophageal connective has also become thicker and has extended far posterior to the deutocerebrum but has as yet not joined the tritocerebrum anlage (open arrowheads in Fig. 62B). The pre-oral commissure anlage still retains a primordial shape and no compact neurite bundles are observable between the two protocerebral hemi-neuromeres (filled arrowhead in Fig. 62B). Posterior to the mandibular commissure a median cell cluster has formed, the mandibular median cell cluster, which includes the pioneer neurons of the median fiber tract (small oval in Fig. 62B') and the neurons connected anteriorly with the brain (asterisks in Fig. 62B').

At this stage, in the periphery, the terminal neural projections in the distal portion of the naupliar limb buds elongate and increase in number proportionally to the number of associated cell somata (asterisks in Fig. 62A and B).

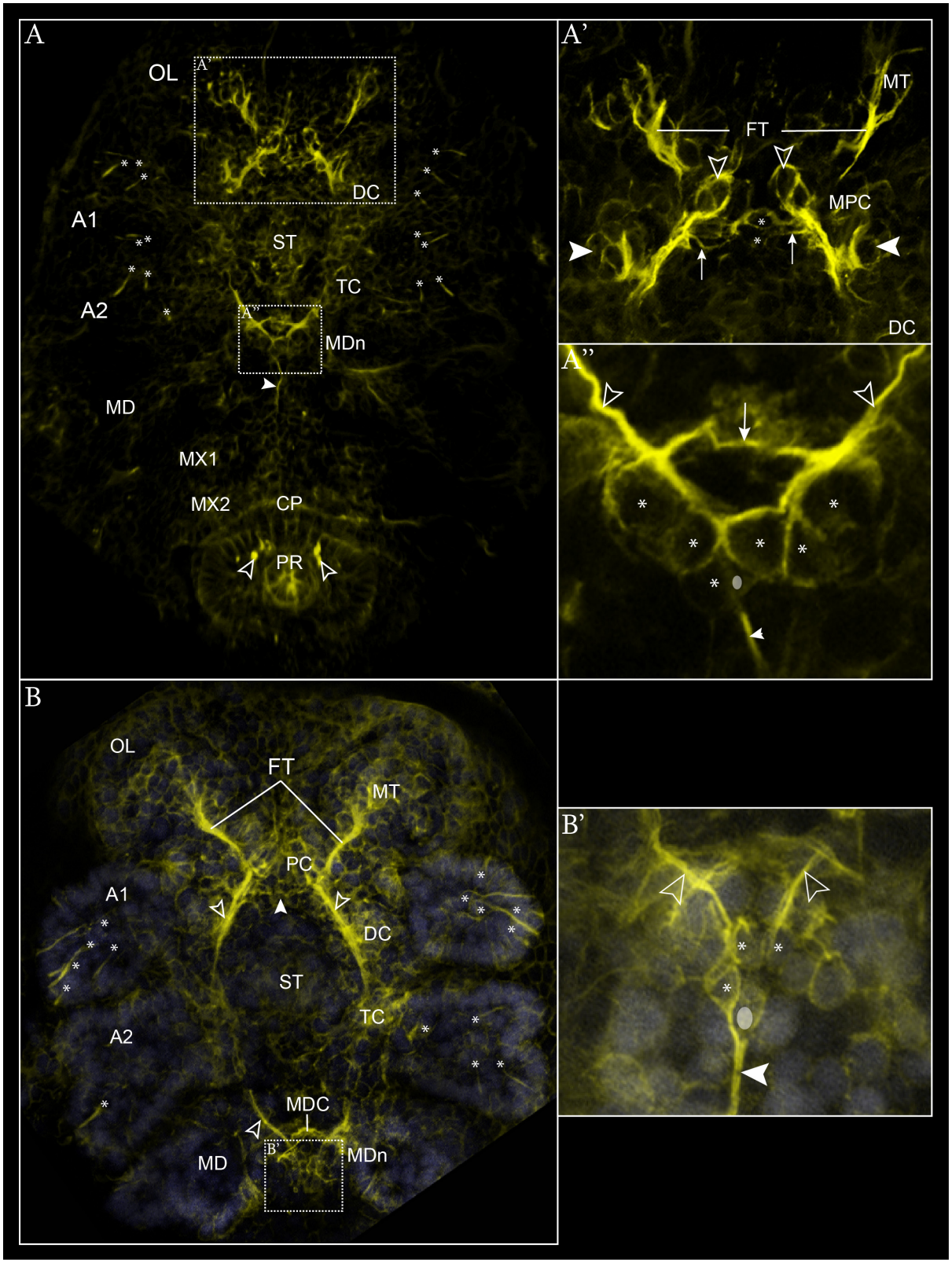

Fig. 62 – Axogenesis in the naupliar region of *P. fallax*, embryonic stage 4

Anti-ac-α-tubulin labelling in yellow; Hoechst staining in grey. CLSM image stack. **A-A" -** Overview of axogenesis in an early phase of the stage (ventral view). Anti-ac-α-tubulin labelling. Imaris surpass mode: volume, clipping plane. **A -** Asterisks mark single cell somata connected with terminal sensory structures at the tip of the limb buds (i.e. A1 and A2). Filled arrowhead points at the anlage of the median fiber tract anlage. Open arrowheads point at the terminal sensory structures in the tip of the caudal papilla anlage. **A'**

- Detail of the protocerebral region. Asterisks mark two cell somata interposed between the protocerebrum hemi-neuromeres. Arrows point at single neurites running from these cell somata and constituting the anlage of the pre-oral commissure. Open arrowheads point at the antero-median clusters of the protocerebrum while filled arrowheads to the lateral one. **A" -** Detail of the mandibular region. Open arrowheads point at the connective between the tritocerebrum and the mandibular neuromere. Asterisks label single cell somata posterior to the anlage of the mandibular commissure (arrow). Grey oval marks a medio-dorsal cell soma connected with the anlage of the median fiber tract which probably represents its anterior pioneer neuron. **B**, **B' -** Overview of the naupliar region of an embryo in a later phase of the stage (ventral view). Imaris surpass mode: volume, clipping plane. **B -** Asterisks mark single cell somata connected with terminal sensory structures at the tip of the limb buds (i.e. A1 and A2). Open arrowhead points at the connective. Filled arrowhead points at the region of the forming pre-oral commissure. **B' -** Detail of the basal region posterior to the anlage of the mandibular commissure anlage. Open arrowheads point at the posterior extension of the connective anlage. Asterisks mark single cell somata forming a median cluster which includes the cell soma pioneering the median fiber tract.

A1: antenna 1; A2: antenna 2; CP: caudal papilla; DC: deutocerebrum; FT: frontal tract; LB: labrum; MD: mandible; MDn: mandibular neuromere; MT: medulla terminalis; MX1, 2: maxilla 1, 2; OL: optic lobe; PC: protocerebrum; PR: proctodeum; ST: stomodeum; TC: tritocerebrum.

In the post-naupliar region, the terminal sensory structures at the tip of the telson have increased in number (open arrowheads in Fig. 63A) proportionally to the number of cell somata connected to them (asterisks in Fig. 63A). The latter are grouped into a cell cluster, and have started to send neurite bundles anteriorly (arrows in Fig. 63), pioneering the posterior portion of the connective of the future ventral nerve cord. Following the shape of the forming caudal papilla, they describe a curve ventral to the proctodeum (arrows in Fig. 63A), turn dorsally and proceed straight anteriorly (arrows in Fig. 63A") but do not connect to the naupliar brain anlage as yet. Single cell somata (interneurons) are observable intercalated along their path, with a bilaterally symmetric distribution in the two neurite bundles (e.g. small oval in Fig. 63A and A").

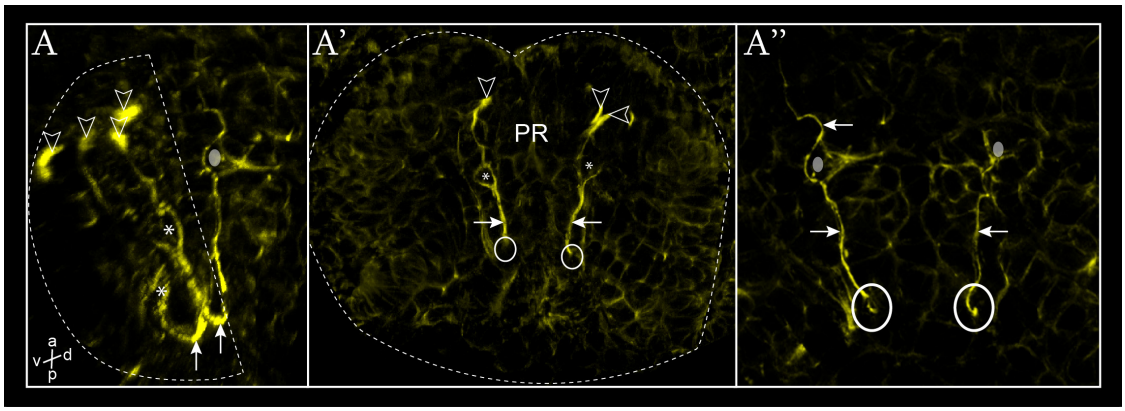

Fig. 63 – Axogenesis in the telson of *P. fallax*, embryonic stage 4

Anti-ac-α-tubulin labelling. CLSM image stack. Imaris surpass mode: volume, clipping plane. **A -** General overview of one half of the posterior pole of the embryo (ventro-lateral view). Stippled line marks the ventral portion of the caudal papilla anlage. Filled arrowheads point at the tip of the terminal sensory structures. Asterisks mark single ventral cell somata connected to the sensory structures and to the longitudinal connective anlage. Arrows point at the turning point of the connective to the antero-dorsal

side following the curvature of the caudal papilla. Small oval marks one cell soma interposed along the connective. **A' -** Detail of the ventral portion of the caudal papilla (ventral view). Filled arrowheads point at the terminal sensory structures. Asterisks mark single cell somata with a bilaterally symmetric distribution at the ventral-most side of the caudal papilla. Arrows point at the connective anlage. The point of their turning to the dorsal side is marked by small circles. **A" -** Detail of the ventral surface of the post-naupliar region covered by the caudal papilla (ventral view). Arrows point at the connective anlagen. Small oval mark single bilaterally symmetric cell somata interposed at each side in between the connective bundles. Small circles mark the turning point of the connective anlagen.

PR: proctodeum.

Stomatogastric nervous system

No evidence of differentiating neural structures of the stomatogastric nervous system has been observed at this stage.

3.3.2.3 Embryonic stage 5

Axogenesis

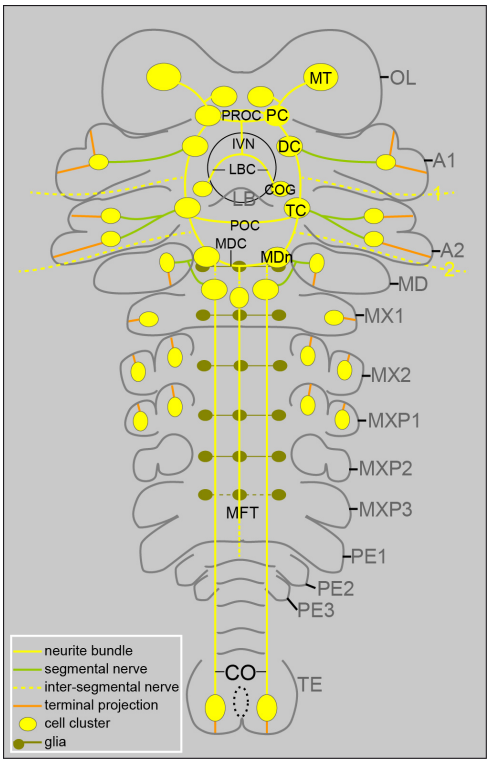

Fig. 64 – Axogenesis of *P. fallax*, embryonic stage 5

Schematic illustration of the distribution of neural structures (ventral view). The region of the stomodeum is marked by black circular line. The proctodeum is represented by a small oval (broken-line) in the telson. The antero-ventral portion of the stomatogastric nervous system is included in the scheme.

A1: antenna 1; A1N: antenna 1 nerve; A2: antenna 2; A2N: antenna 2 nerve; CO: connective; DC: deutocerebrum; FT: frontal tract; IVN: inferior ventricular nerve; LB: labrum; LBC: labral commissure; MD: mandible; MDC: mandibular commissure; MDN: mandibular nerve; MDn: mandibular neuromere; MFT: median fiber tract; MT: medulla terminalis; MX1-2: maxilla 1-2; MXP1-2: maxilliped 1-2; MXP3: maxilliped 3 anlage; oral commissure; TC: tritocerebrum.

During embryonic stage 5, the circumesophageal nerve ring becomes complete (Fig. 65A). Medially, anterior to the pre-oral commissure the protocerebrum consists of a sizeable cell cluster sending neural projections slightly anterior to the level of insertion of the pre-oral commissure anlage (open arrowheads in Fig. 65B). The frontal tract anlage has become thicker and the pre-oral commissure anlage has become more distinct (Fig. 65A, B). The latter is composed of two main neurite bundles: one antero-dorsal and one postero-ventral (Fig. 65A, B). In an earlier phase of the stage, the postero-ventral bundle is thicker than the antero-dorsal one (Fig. 65B) and is connected to the forming stomatogastric nervous system via the inferior ventricular nerve anlage (Fig. 65A, B, see also in the next sub-section). Posterior to the stomodeum, the post-oral commissure anlage has also formed at the same level as the insertion of antenna 2 (Fig. 65A). Posteriorly, the mandibular commissure anlage represents a single thick neurite bundle that spans between the two hemi-neuromeres (Fig. 65A and C). The connective now appears as a well-defined longitudinal neurite bundle spanning between the protocerebrum and the mandibular neuromere (Fig. 65A). All three naupliar segmental nerves have formed, extending between the lateral margin of the nerve ring connective and the terminal cell cluster of their corresponding naupliar limb (Fig. 65A). The antenna 2 nerve anlage is composed of two separate neurite bundles, while the other two anlagen consist of only one neurite bundle each (Fig. 65A). Interestingly, the roots of the segmental nerve anlagen are characterized by a branching pattern at their connection to the nerve ring (open arrowheads in Fig. 65A). In particular, in the mandibular nerve root anlage a distinct posterior branch can be distinguished (open arrowheads in Fig. 65C). This is connected with medial cell somata located posterior to the commissure anlage (whether this is a single soma or more grouped in a cluster cannot be further resolved). At this level, a layer of numerous cell somata has formed interposed between the mandibular neuromere and the more posterior region (stippled square bracket in Fig. 65C). Here the anterior end of the median fiber tract is observable still not connected to the anterior-most neurite bundles (Fig. 65A and C). At the same level the anterior end of the post-naupliar connective has formed (arrows in Fig. 65C). The connective of the forming ventral nerve cord eventually runs as a continuous longitudinal neurite bundle connecting the brain to the telsonic cell cluster.

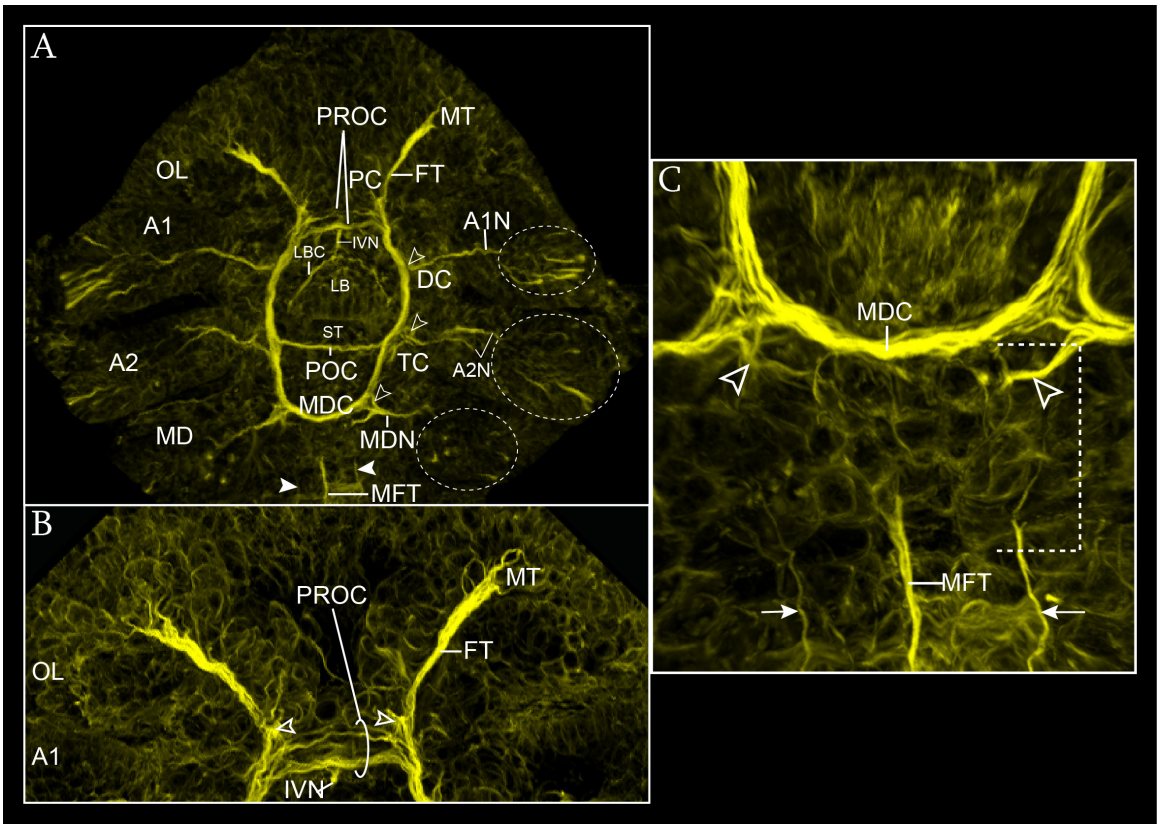

Fig. 65 – Axogenesis in the naupliar region of *P. fallax*, embryonic stage 5

Anti-ac-α-tubulin labelling in yellow; Hoechst staining in grey. CLSM image stack. View of the naupliar region in an early phase of the stage. Anti-ac-α-tubulin labelling. Imaris surpass mode: volume clipping plane. **A -** General overview (ventral view). Open arrowheads point the roots of the segmental nerve anlagen. Stippled circles mark the terminal portion of the naupliar limbs and include the terminal cell clusters and their projections to the terminal sensory structures. Filled arrowheads point at the anterior ends of the connective anlagen. **B -** Detail of the protocerebral region (ventral view). White arrowheads point at the level of insertion of neurites of the antero-median portion of the protocerebrum. The open circle includes the two neurite bundles forming the pre-oral commissure anlage. **C -** Detail of the mandibular neuromere (ventral view). Open arrowheads point at the posterior branch of the mandibular nerve root connected with the posterior cell somata layer (stippled square bracket). Arrows point at the anterior-most extension of the connectives.

A1: antenna 1; A1N: antenna 1 nerve; A2: antenna 2; A2N: antenna 2 nerve; CO: connective; DC: deutocerebrum; FT: frontal tract; IVN: inferior ventricular nerve; LB: labrum; LBC: labral commissure; MD: mandible; MDC: mandibular commissure; MDN: mandibular nerve; MDn: mandibular neuromere; MFT: median fiber tract; MT: medulla terminalis; MX1-2: maxilla 1-2; MXP1-2: maxilliped 1-2; MXP3: maxilliped 3 anlage; OL: optic lobe; PC: protocerebrum; PE1-3: pereiopod anlagen 1-3; POC: post-oral commissure; PROC: pre-oral commissure; ST: stomodeum; TC: tritocerebrum.

In a later phase of the stage, the general architecture of the brain anlage has become more solid: the commissures and connectives as well as the roots of the naupliar segmental nerves have become thicker (Fig. 66A). Moreover, two inter-segmental nerves have formed (Fig. 66A): one between the antenna 1 and 2 nerves, the second between the antenna 2 and the mandibular nerve. They appear simultaneously and run dorso-laterally towards the wall of the carapace anlage (more clear in the following stage). The mandibular commissure and the

ventral nerve cord anlage start to connect each other: medial and lateral longitudinal projections run posteriorly from the mandibular commissure to adjoin the longitudinal commissure and the median fiber tract anlagen (open arrowheads in Fig. 66A, A'). Two distinct neurite bundles form the anterior-most end of the median fiber tract anlage (arrows in Fig. 66A), extending from two cell somata embedded in the mandibular median cell cluster (asterisks in Fig. 66A) and meeting each other posterior to the maxilla 1 neuromere anlage (see below).

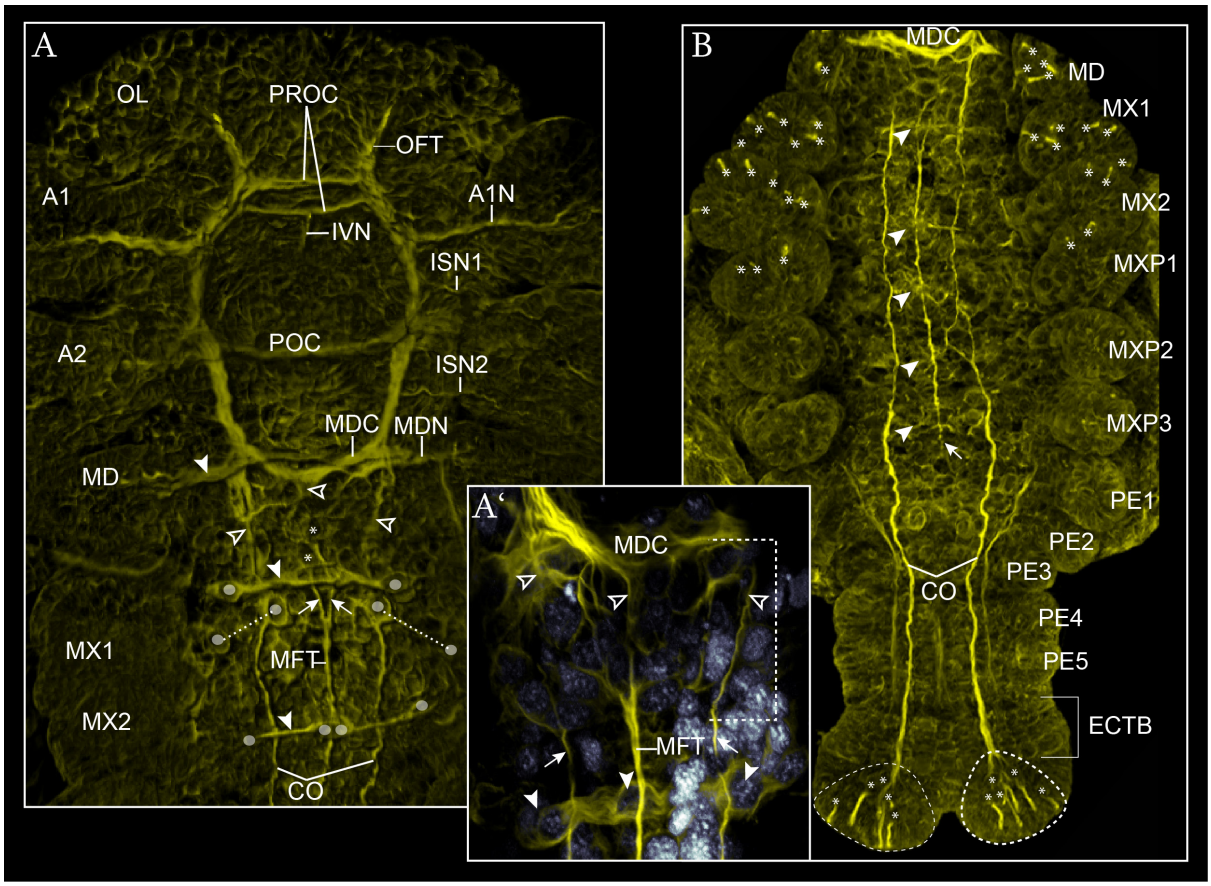

Fig. 66 – Axogenesis of *P. fallax*, later phase of embryonic stage 5

Anti-ac-α-tubulin labelling in yellow; Hoechst staining in grey. CLSM image stack. Imaris surpass mode: volume, clipping plane, blend mode in **A**. **A -** General overview of the naupliar region, and of the first two post-naupliar segments (i.e. MX1, 2) (dorsal view). Open arrowheads point at the posterior neural projections from the mandibular commissure to adjoin the anlagen of the connectives and of the median fiber tract. The two asterisks mark the two cell somata connected with the two anterior neurites of the median fiber tract (arrows). Filled arrowheads and small ovals label the projections and the cell somata of the glial cells, respectively. **A' -** Detail of the region posterior to the mandibular commissure (ventral view). Stippled squared bracket mark the extension of the cellular layer posterior to the mandibular commissure. Open arrowheads as in **A**. Arrows point at the anterior ends of the connectives. Filled arrowheads point at the cell somata of glial cells at the level of the maxilla1 neuromere. **B -** Overview of axogenesis in the post-naupliar region (ventral view). Filled arrowheads point at the neuromeres where the signal of the staining is more intense. Asterisks mark the position of cell somata connected with terminal sensory structures in the limb anlagen and in the caudal region. The stippled outlines include the posterior end of the connective, the terminal cell cluster and the projections connected with the terminal sensory structures.

A1: antenna 1; A1N: antenna 1 nerve; A2: antenna 2; A2N: antenna 2 nerve; CO: connective; ECT: ectoteloblasts; FT: frontal tract; ISN1, 2: inter-segmental nerve 1, 2; IVN: inferior ventricular nerve; LB: labrum; MD: mandible; MDC: mandibular commissure; MDN: mandibular nerve; MFT: median fiber tract; MX1-2: maxilla 1-2; MXP1-2: maxilliped 1-2; MXP3: maxilliped 3 anlage; OL: optic lobe; PE1-3: pereiopod 1-3; POC: post-oral commissure; PROC: pre-oral commissure; TC: tritocerebrum.

In the post-naupliar region, the connective extends continuously to the telsonic cell cluster (stippled line in Fig. 66B). The number of cells of the telsonic cell cluster has increased in number proportionally to the number of cell somata to which they are connected to (asterisks in Fig. 66B). The median fiber tract extends until the level of the posterior margin of the anlage of the maxilliped 3 neuromere (arrow in Fig. 66B). Axogenesis has begun in the post-naupliar neuromeres in an antero-posterior developmental gradient from maxilla 1 to maxilliped 3 neuromeres (filled arrowheads in Fig. 66B). This in accordance with the presence at the dorsal side of each segment of regularly distributed large cells connected transversally via elongated processes recognized also at the level of the mandibular commissure (filled arrowheads and small ovals in Fig. 66A). They most likely represent glial cells, probably involved in the structural support of development of the ventral nerve cord axonal scaffold. At the distal ends of maxilla 1 and 2 and of maxilliped1 limb anlage terminal sensory structures have formed with the same arrangement as observed in the limb buds of the naupliar segments in the previous stages (asterisks in Fig. 66B).

Stomatogastric nervous system

The anlage of the stomatogastric nervous system consists of two parallel neurite bundles spanning medially in dorso-ventral direction anterior to the stomodeum (Fig. 67). They are the anlage, anteriorly, of the inferior ventricular nerve which is connected to the pre-oral commissure (Fig. 67A), and, posteriorly, of the stomatogastric nerve, which is connected dorsally to the to the stomatogastric ganglion on the dorsal wall of stomodeum (Fig. 67C). These bundles run ventrally and meet at the antero-ventral surface of the anlage of the labrum (stippled circle in Fig. 67A, B). At the same level, two neurite bundles run off laterally in opposite direction, forming an arch which represents the anlage of the labral commissure (Fig. 67A, and filled arrowheads in Fig. 67B, C). The lateral ends of the labral commissure connect some cell somata lateral to the stomodeum (asterisks in Fig. 67B, C). Although the formation of a true ganglion cannot be detected at this level, these cells are interpreted here as the anlage of the commissural ganglion (see Discussion). Additional neurites with a ventro-dorsal orientation are stained within the labrum connected to small cluster of cells distally in the

labrum (open arrowhead in Fig. 67C) which may represent the anlage of some sensory structures.

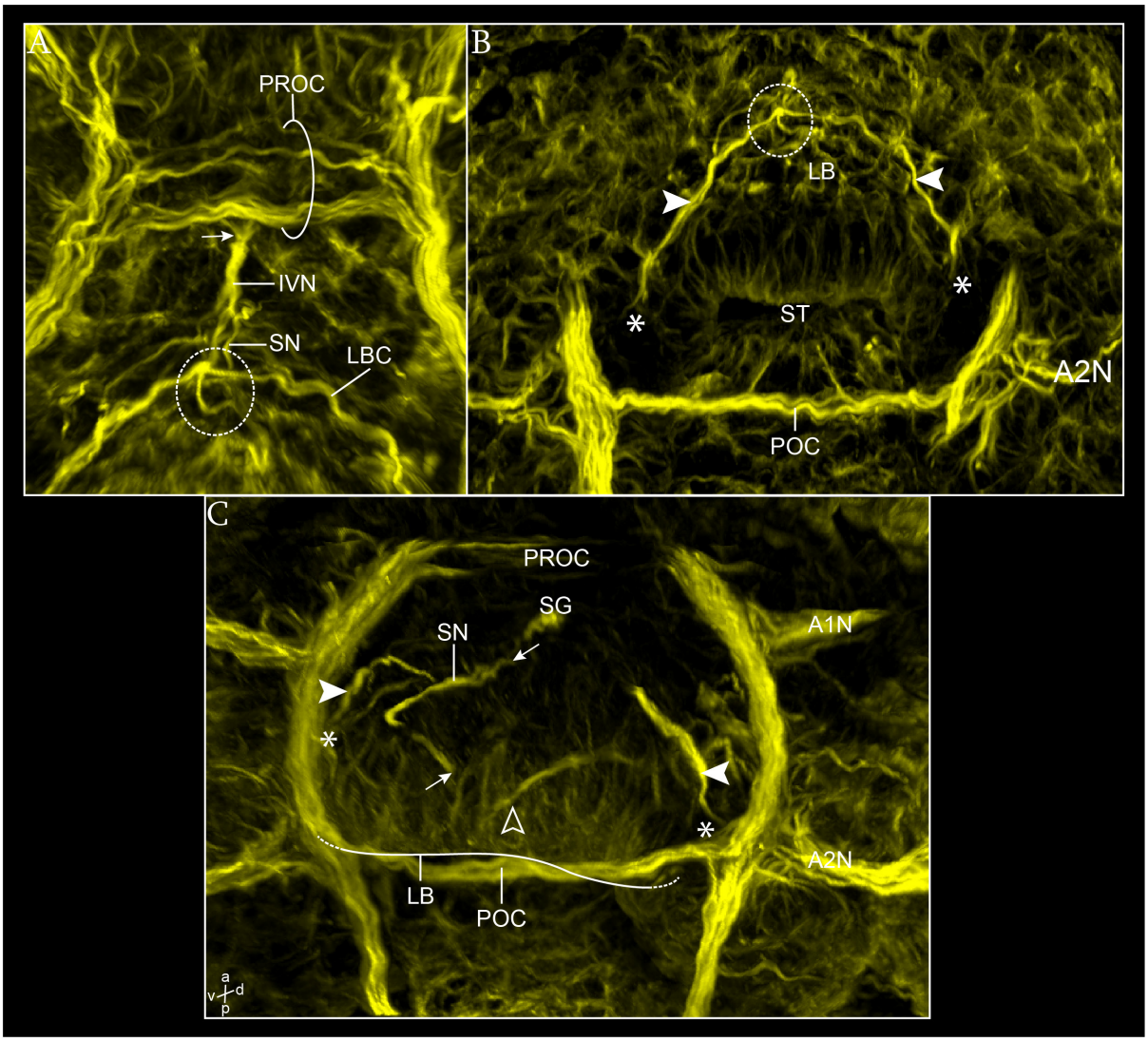

Fig. 67 – Axogenesis of the stomatogastric nervous system of *P. fallax*, embryonic stage 5

Anti-ac-α-tubulin labelling. CLSM image stack. Ventral view in **A**, **B**. in **C**. **A -** Detail of the antero-ventral portion of the STNS anlage (ventral view). The stippled circle marks the point of intersection of the inferior ventricular nerve, the stomatogastric nerve and the labral commissure. Note the inferior ventricular nerve contacts the postero-ventral component of the pre-oral commissure (open circle). **B -** Detail of the postero-ventral portion of the SNS anlage (ventral view). Open arrowhead points at the ventral end of the stomatogastric nerve anlage. Filled arrowheads point at the branches of the labral commissure. Asterisks mark the region of the forming commissural ganglia. **C -** Detail of the dorsal portion of the SNS anlage (ventro-lateral view). Arrows point at the ends of the extension of the stomatogastric nerve anlage. Filled arrowheads point at the posterior ends of the labral commissure (note that the anterior portion has been cut out from the picture). Open arrowhead point at the left neurite running in parallel to the stomatogastric nerve anlage (the right one is not visible in the picture). The posterior margin of the labrum (which lies ventrally to the post-oral commissure) is marked by stippled line.

A1N: antenna 1 nerve; A2N: antenna 2 nerve; IVN: inferior ventricular nerve anlage; LB: labrum; LBC: labral commissure; POC: post-oral commissure; PROC: pre-oral commissure; SG: stomatogastric ganglion; SN: stomatogastric nerve; ST: stomodeum.

3.3.2.4 Embryonic stage 6

Axogenesis

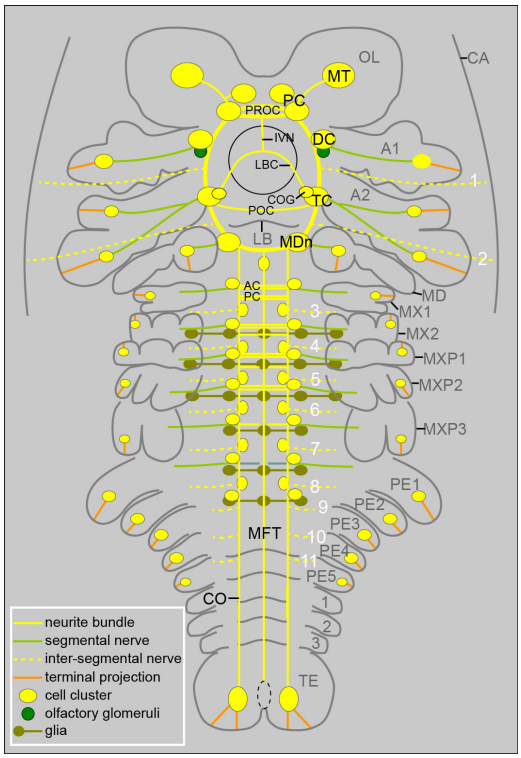

Fig. 68 – Axogenesis of *P. fallax*, embryonic stage 6

Schematic illustration of the distribution of neural structures (ventral view). The region of the stomodeum is marked by black circular line. The inter-segmental nerves are numbered in white. The proctodeum is represented by a small oval (broken-line) in the telson. The superior portion of the stomatogastric nervous system is included in the scheme.

A1: antenna 1; A2: antenna 2; CO: connective; CA: carapace; DC: deutocerebrum; FT: frontal tract; IVN: inferior ventricular nerve; LB: labrum; LBC: labral commissure; MD: mandible; MDN: mandibular nerve; MFT: median fiber tract; MT: medulla terminalis; MX1-2: maxilla 1-2; MXP1-3: maxilliped 1-3; OL: optic lobe; PC: protocerebrum; PE1-5: pereiopod 1-5; POC: post-oral commissure; PROC: pre-oral commissure; STG: stomatogastric ganglion; STN: stomatogastric nerve; TC: tritocerebrum; TE: telson.

In the naupliar region, the developing nervous system shows a further thickening of the neurite bundles and a swelling of the naupliar neuromeres, which can still be distinguished as separate compartments (Fig. 69A-C). In the protocerebral region, the two components of the pre-oral commissure have become thicker and – in a late phase of this stage – they start to be more close to each other as a consequence of the increasing number of constituting neurites (Fig. 69C, D). The neuropil of the medulla terminalis has enlarged (filled arrowheads in Fig. 69C). In the region of the deutocerebrum, the anlage of the olfactory glomeruli has formed (encircled by stippled line in Fig. 69D). It is represented by a small cluster of cell somata located posteriorly to the root of the antenna 1 nerve sending its neurites anteriorly into the

nerve ring. These form together a neurite bundle which runs along the external margin of the connective (filled arrowheads in Fig. 69D) reaching the pre-oral commissure. In the distal portion of each naupliar limb, new terminal sensory structures grow (Fig. 69A and C). From the distal end of nerve root of antenna 2 two additional thin neurites branch off (arrows in Fig. 69C). The segmental and inter-segmental nerve anlagen continue to elongate during the stage (Fig. 69A and C). The two inter-segmental nerves extend to the wall of the forming carapace (Fig. 69E). The root of the mandibular nerve has become thicker while its distal end has branched into two neurite bundles (Fig. 69C).

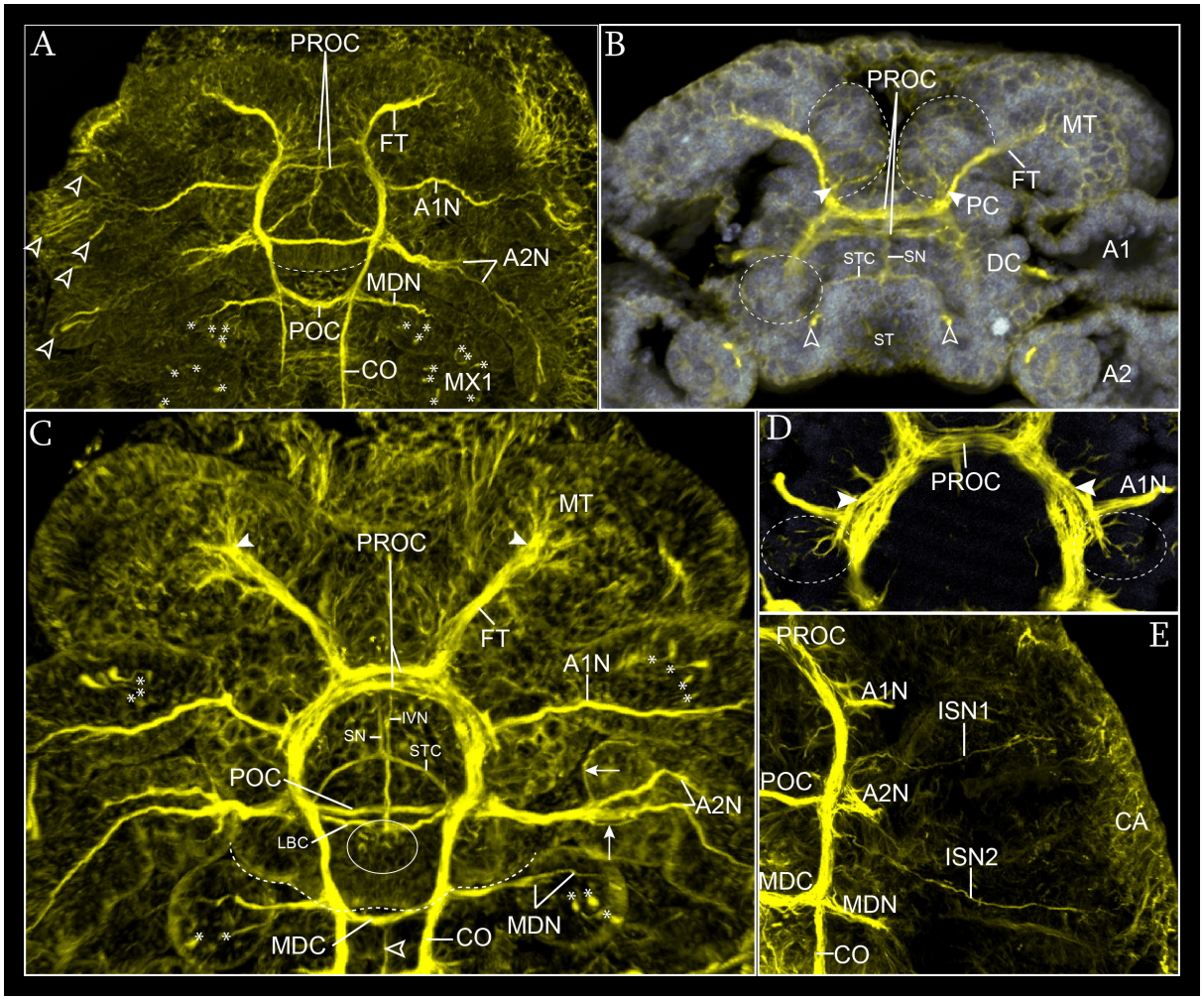

Fig. 69 – Axogenesis in the naupliar region of *P. fallax*, embryonic stage 6

Anti-ac-α-tubulin labelling in yellow; Hoechst staining in grey. CLSM image stack. Imaris surpass mode: volume, clipping plane in **A**; oblique slicer in **B** and **D**. **A -** General overview the naupliar region and of the maxilla 1 segment at the early phase of the stage (ventral view). The stippled line marks the posterior border of the labrum. Open arrowheads on the left side of the picture point at the antennal terminal sensory structures. Asterisks mark the neurons of the terminal sensory structures in the mandible and in maxilla 1. **B -** Detail of the antero-ventral portion of the brain anlage (ventral view). Stippled line encircles the antero-median cell cluster of the protocerebrum and filled arrowheads the point to the insertion of its neurites in the frontal tract. A stippled circle marks the position of the deutocerebrum at the right side of the embryo. The section includes also part of the stomatogastric nervous system i.e. the stomodeal

commissure and the stomatogastric nerve. Open arrowheads point at the lateral ends of the stomodeal commissure laterally to the stomodeum. **C-E -** Axogenesis in the later phase of the stage (ventral view). **C -** General overview. The stippled line marks the posterior border of the labrum. Filled arrowheads point at the ventral branches in the distal portion of the frontal tract. Arrows point at two additional neurites of the antenna 2 nerve. Asterisks mark the terminal sensory structures of the limbs. The median cell cluster encircled by the white line represents the anlage of the labral ganglion. Open arrowhead points at the median fiber tract anlage. **D –** Detail of the anlage of the olfactory glomeruli. Stippled circles mark the cell cluster. Filled arrowheads mark the neurite bundle at the external margin of the nerve ring. **E -** Detail of the left lateral side of the naupliar region. The distal extension of the segmental nerves has been cut out from the picture to allow the vision of the course of the anlage of the inter-segmental nerves projecting to the carapace.

A1: antenna 1; A1N: antenna 1 nerve; A2: antenna 2; A2N: antenna 2 nerve; CO: connective; CA: carapace; DC: deutocerebrum; FT: frontal tract; IVN: inferior ventricular nerve; LB: labrum; LBC: labral commissure; MD: mandible; MDN: mandibular nerve; MT: medulla terminalis; OL: optic lobe; PC: protocerebrum; POC: post-oral commissure; PROC: pre-oral commissure; SN: stomatogastric nerve; ST: stomodeum; STC: stomodeal commissure; TC: tritocerebrum.

The median fiber tract and the connectives have joined the mandibular commissure (Fig. 69C and Fig. 70A, A'). In an earlier phase of the stage, two separate neurites form the median fiber tract anlage in its anterior-most end (Fig. 70A, A'). One ventral is connected directly to the mandibular commissure (filled arrowhead in Fig. 70A'), while the one dorsal runs off from a median cell soma embedded in the post-commissural cell layer (asterisk in Fig. 70A, A'). Additional neurites can be distinguished also in the anterior-most portion of the connective, which has gained in diameter (Fig. 70A').

The post-naupliar neuromeres differentiate following a spatial and temporal stereotyped pattern in an antero-posterior gradient. In the earliest phase of the stage, axogenesis is detectable only at the level of the maxillar segments (Fig. 70A). A thin neurite spans between the two hemi-neuromeres at the level of maxilla 1, representing the first anlage of the segmental commissure (filled arrowhead in Fig. 70A). At the level of maxilla 2, no transversal neurites are observable as yet. Only a thin lateral neurite (open arrowhead in Fig. 70A) originates from a lateral cell cluster external to the connective (solid circle in Fig. 70A). No segmental nerves have been formed yet, but the inter-segmental nerve anlage is present (arrows in Fig. 70A). The latter runs off from the connectives towards the lateral side of the embryo. A cell cluster in a slightly dorsal location lies immediately posterior to the anlage of the maxilla 1 commissure medially to the connective (stippled circles in Fig. 70A) and may be connected to the inter-segmental nerve. At the dorsal side of each neuromere (including the mandibular and, far posterior, also the first two maxilliped neuromeres) cell somata resembling the morphology of glial cells with their processes form transversal bridges

between the contralateral insertion sites of each corresponding limb anlage (small ovals in Fig. 70A and Fig. 70B).

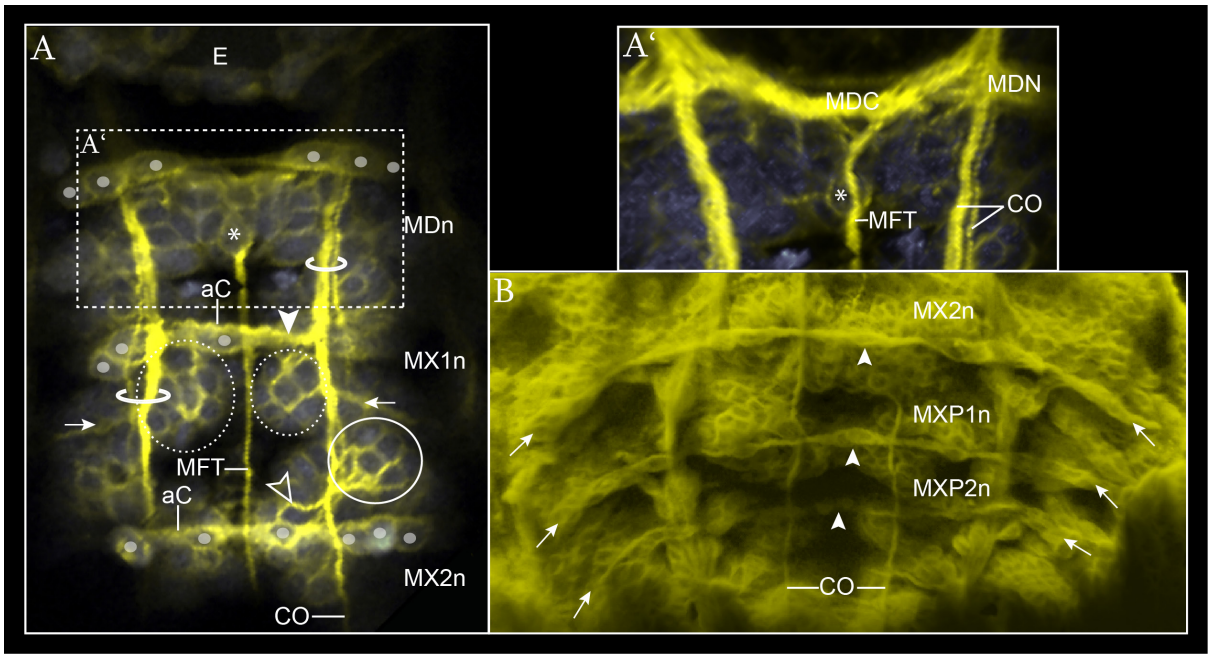

Fig. 70 – Axogenesis in the anterior portion of the ventral nerve cord of *P. fallax*, embryonic stage 6 (early phase)

Anti-ac-α-tubulin labelling in yellow; Hoechst staining in grey. CLSM image stack. Imaris surpass mode: oblique slicer in **A**, volume, clipping plane in **A'**; volume (shadow projection) in **B**. **A -** General overview of the posterior portion of the mandibular and of the two maxillar neuromeres (ventral view). The asterisk marks the medio-dorsal cell soma at the antero-dorsal end of the median fiber tract. The open circles include the neurites forming the connectives. Filled arrowhead points at the anterior commissure anlage of the maxilla 1 neuromere. Stippled circles mark the paired median cell clusters, which probably pioneer the inter-segmental nerve 3 (arrows). Open arrowhead points at single neurite forming the anterior commissure of the maxilla 2 neuromere, running off from a lateral cell cluster (solid circle). Small ovals mark the nuclei of putative glial cells. **A' -** Detail of the antero-ventral component of the median fiber tract (ventral view). The asterisk marks the medio-dorsal cell soma at the antero-dorsal end of the median fiber tract (compare with **A**). The ventral neurite bundle is connected with the mandibular commissure. **B -** Distribution of the putative glial cells at the level of maxilla 2 and of the first two maxilliped neuromeres (dorsal view). Filled arrowheads point at the median cells, while arrows mark the lateral end of each transversal bridge.

aC: anterior commissure; CO: connective; MDC: mandibular commissure; MDN: mandibular nerve; MDn: mandibular neuromere; MFT: median fiber tract; MX1-2: maxilla 1-2; MX1-2N : maxilla 1-2 nerve; MX1-2n: maxilla 1-2 neuromeres; MXP1-3n: maxilliped 1-3 neuromeres; ST: stomodeum.

In a later phase of development, the differentiation of the ventral nerve cord has proceeded posteriorly, including by then all the maxilliped and the pereiopod neuromeres (Fig. 71). Two commissural neurite bundles have formed at the level of the maxillar neuromeres, one anterior and one posterior (Fig. 71A, B). They are composed of two main neurite bundles each, which gradually become thicker and fuse together (square brackets in Fig. 71B). The establishment of the posterior commissure of maxilla 2 is delayed in comparison to maxilla 1 (compare in

Fig. 71A, B) while in the maxilliped neuromeres, only the anterior commissure has formed (Fig. 71A). At the level of maxilliped 1, scattered transversal neurites projecting medially from the lateral side of the connectives can be distinguished, constituting the rudiment of the posterior commissure anlage (Fig. 71A, B). At the level of maxilliped 3 and of the first two pereiopods, only one thin neurite forms the anterior commissure anlage (Fig. 71A and D) while no clear commissure anlagen are observable in the following neuromeres. Moreover, in between the pereiopod 1 and 2 neuromeres, the distal end of the median fiber tract is observable (asterisk in Fig. 71C). Lateral cell clusters external to the connectives characterize each neuromere at the level of the anlage of the anterior commissure from maxilla 1 to pereiopod 2 (stippled ovals in Fig. 71B, C). The segmental nerves have formed at the level of the maxillae and of the maxillipeds (Fig. 71A, B). They run off from the connectives in close proximity to the neurites of the lateral cluster and extend to the forming longitudinal trunk muscle (this last marked by the arrow in Fig. 71A). From there, only the maxillary nerves proceed already into the limb anlagen (Fig. 71A). The inter-segmental nerves 3 (between maxilla 1 and 2) to 11 (between pereiopod 4 and 5) have formed (numbered in Fig. 71). Each inter-segmental nerve spans between the connective and the wall of the longitudinal forming muscles. Posterior to the level of the prospective anterior commissure anlage, paired medial cell clusters are visibly stained (stippled circles in Fig. 71C) which may be connected to the corresponding inter-segmental nerves. Terminal sensory structures have formed all along the maxillae and maxilliped 1 and 2 (asterisks in Fig. 71A).

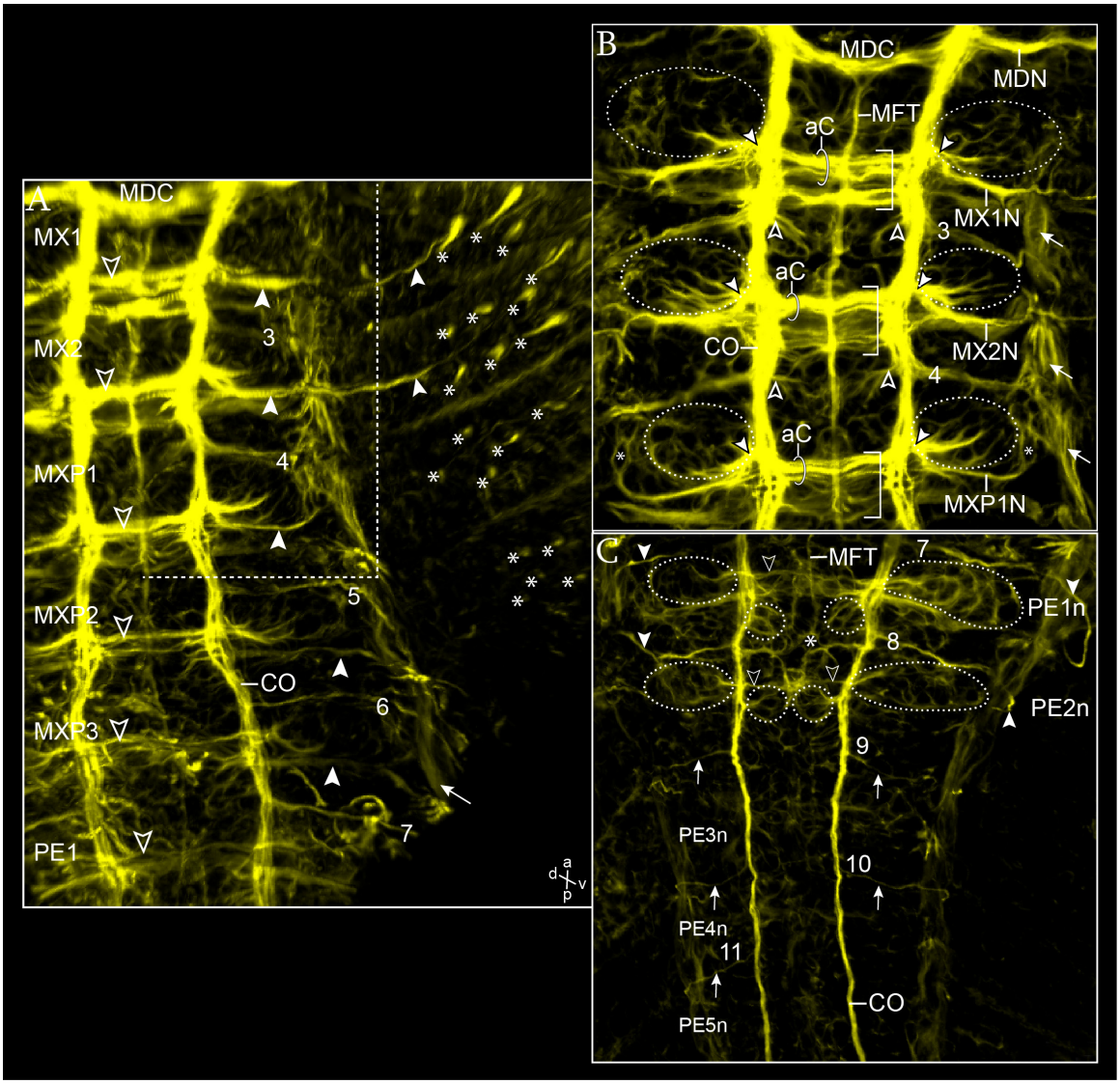

Fig. 71 – Axogenesis in the ventral nerve cord of *P. fallax*, embryonic stage 6 (late phase)

Anti-ac-α-tubulin labelling in yellow; Hoechst staining in grey. CLSM image stack. Imaris surpass mode: volume, clipping plane. **A -** Overview of the first six thoracic neuromeres (i.e. maxilla 1, 2; maxillipeds 1-3, pereiopod 1) (ventro-lateral view). The segmental axogenesis follows a stereotyped spatial and temporal pattern along the antero-posterior axis. Open arrowheads point at the anlage of the anterior commissures. Filled arrowheads point at the segmental nerve anlagen. Note their extension into the limbs in the maxilla 1 and 2 segments. Asterisks mark the terminal sensory structures in each limb anlage. The arrow at the right bottom of the image points at the anlage of the longitudinal muscles. Stippled line marks the portion of the image shown in **B**. **B -** Detail of the first three thoracic neuromeres (i.e. maxilla1, 2 and maxilliped 1) ventral view. Square brackets include the anterior and the posterior commissure in each neuromere. Open arrowheads point to the insertion of the neurites of the median clusters into the axonal scaffold of the connectives. Stippled ovals mark the lateral cell clusters, while filled arrowheads indicate the point of insertion of their neural projections into the connectives. Asterisks at the level of maxilliped 1 mark the cell somata at the distal end of the segmental nerve anlage close to the wall of the longitudinal muscles (arrows). **C -** Overview of the pereiopod neuromeres ventral view. Open arrowheads point at the anlagen of the anterior commissures. Stippled ovals mark the lateral cell clusters, while stippled circles outline the paired median ones. Filled arrowheads point at the lateral extension of inter-segmental nerves 7 and 8. Arrows point at inter-segmental nerves 9-11 (11 visible only at the right side of the embryo. Asterisk mark the posterior end of the median fiber tract.

aC: anterior commissure; CO: connective; MDC: mandibular commissure; MDN: mandibular nerve; MFT: median fiber tract; MX1-2: maxilla 1-2; MX1-2N : maxilla 1-2 nerve; MXP1-3: maxilliped 1-3; MXP1N: maxilliped 1 nerve; PE1-5n: pereiopod 1-5 neuromeres; 3-11: inter-segmental nerves 3-11.

Stomatogastric nervous system

The components of the stomatogastric nervous system have become more distinct due to the thickening of the constituting neurite bundles (Fig. 72). The inferior ventricular nerve and the stomatogastric nerve have elongated while the labral commissure has shifted ventrally following the ventral protrusion of the labrum (Fig. 72B and E). Moreover, an additional transversal neurite bundles has formed, spanning between the commissural ganglion and the stomatogastric nerve, where it meets its contralateral counterpart forming the stomodeal commissure (Fig. 72B, C and E). The stomodeal commissure runs transversally directly on the antero-dorsal wall of the stomodeum (Fig. 72C). The lateral stomatogastric nerve runs out from a cluster of cells situated in the dorsal wall of the digestive tube at the same level as the stomatogastric ganglion (circles in Fig. 72D) and meets ventrally the stomodeal commissure (open arrowheads in Fig. 72C). The position of the stomatogastric ganglion and of the lateral cell clusters changes during the development of the embryo following posteriorly the elongation of the digestive tube (compare Fig. 72C, D).

In a later phase of development the lateral ends of the labral and stomodeal commissures have fused together with the ventral margin of the nerve ring connective at the same level of the insertion of the post-oral commissure and of the segmental nerve of antenna 2 (filled arrowheads in Fig. 72B and E). The ventral cell cluster corresponding to the commissural ganglion has increased in volume, embedded into the labral tissue (stippled circles in Fig. 72B and E).

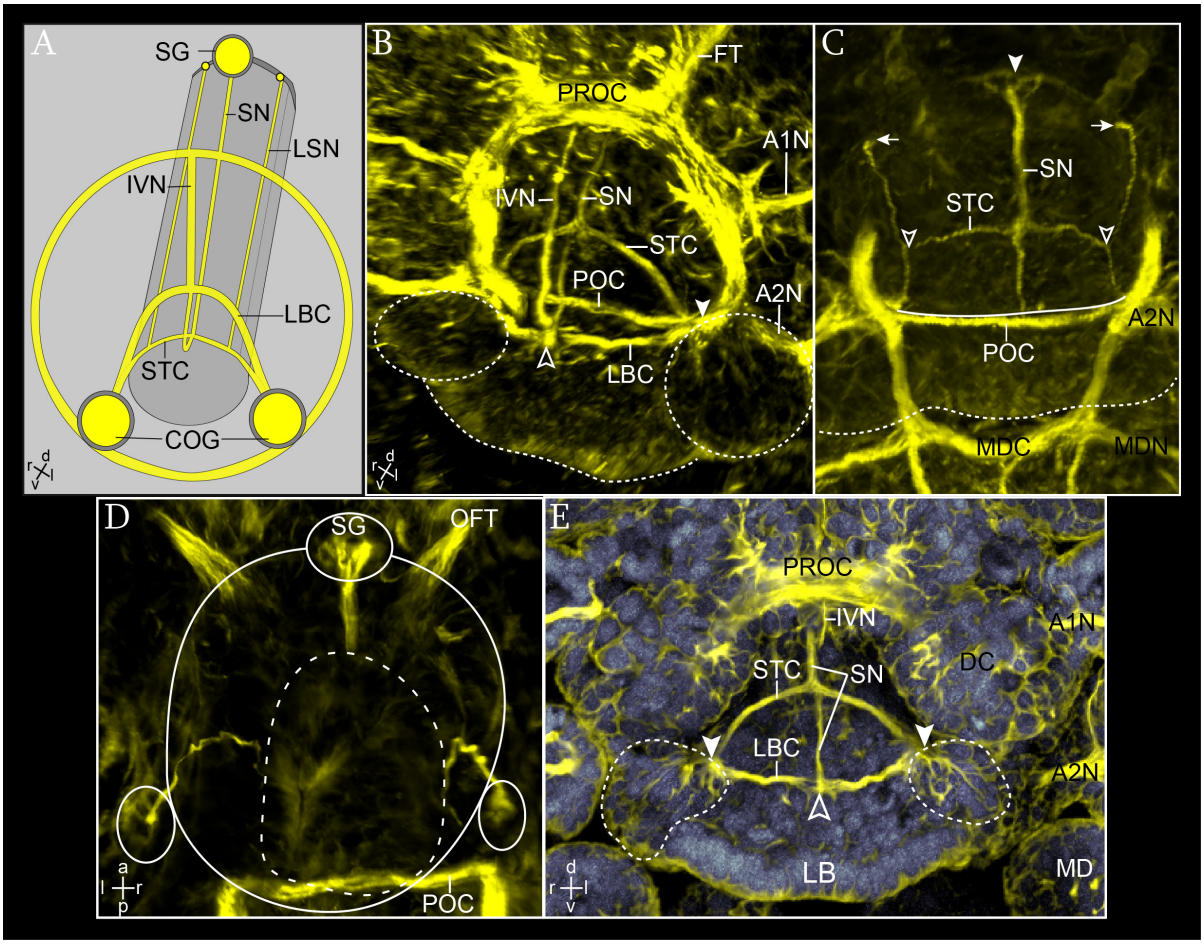

Fig. 72 – Axogenesis of the stomatogastric nervous system of *P. fallax*, embryonic stage 6

A – Schematic illustration of the stomatogastric nervous system anlage (ventro-lateral view). Neural structures are labelled in yellow. The anlage of the digestive tube is represented by the grey cylinder. The circumesophageal nerve ring is schematized by the circular yellow ring in the foreground. Yellow circles with grey rim represent the anlage of the ganglia. The small lateral circle at the side of the stomatogastric ganglion represents the stomatogastric lateral cell cluster.

B-**E -** Anti-ac-α-tubulin labelling in yellow; Hoechst staining in grey. CLSM image stack. Imaris surpass mode: volume, clipping plane; orto-slicer in **D**, **E**. **B -** General overview of the SNS. Filled arrowhead points at the point of connection of the larval and stomodeal commissures to the nerve ring (antero-lateral view). Stippled circles mark the cell clusters corresponding to the commissural ganglia. Stippled line marks the postero-ventral margin of the labrum. Open arrowhead points at the point of intersection of the inferior ventricular nerve and stomatogastric nerve with the labral commissure. **C -** Detail of the dorsal wall of the digestive tube anlage (ventral view). The filled arrowhead points at the stomatogastric ganglion. Arrows point to the dorsal insertion of the lateral nerves, running in parallel to the stomatogastric nerve. Open arrowheads mark at the point pf intersection of the lateral stomatogastric nerves with the stomodeal commissure. The transversal line close to the post-oral commissure labels the postero-ventral margin of the stomodeum. The stippled line close to the mandibular commissure marks the postero-ventral margin of the labrum. Note that the posterior margin of the stomodeum is located more ventrally than the post-oral commissure and the labral margin lies in the ventral-most plane (not visible in the perspective of the image). **D -** Detail of the dorsal-most portion of the SNS (dorsal view). Stippled line marks the ventral margin of the stomodeum, while the continuous line marks its dorsal sectioned margin. Circles mark the dorsal cell clusters of the lateral stomatogastric nerves. **E -** Detail of the anterior portion of the SNS within the brain (antero-ventral view). Only the proximal portion of the inferior ventricular nerve is included in the section. Filled arrowheads point at the connection of the labral and stomodeal commissures with the commissural ganglion marked by stippled outlines. Open arrowhead points at intersection of the inferior ventricular nerve and of the stomatogastric nerve with the labral commissure (compare with **B**).

A1N: antenna 1 nerve; A2N: antenna 2 nerve; COG: commissural ganglion; DC: deutocerebrum; FT: frontal tract; IVN: inferior ventricular nerve; LB: labrum; LBC: labral commissure; LSN: lateral stomatogastric nerve; MD: mandible; MDC: mandibular commissure; MDN: mandibular nerve; POC: post-oral commissure; PROC: pre-oral commissure; SG: stomatogastric ganglion; SN: stomatogastric nerve; STC: stomodeal commissure.

3.3.2.5 Embryonic stage 7

Axogenesis

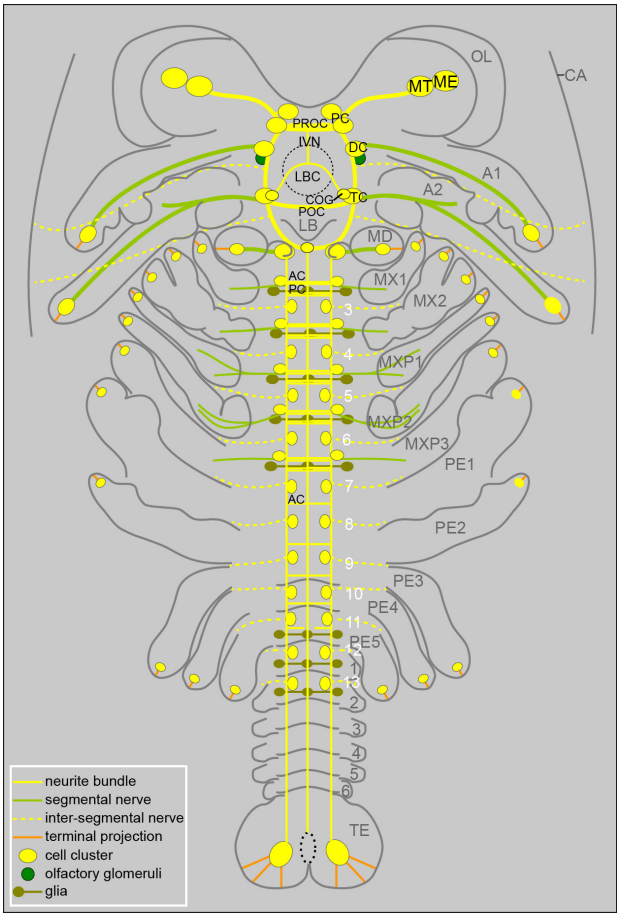

Fig. 73 – Axogenesis of *P. fallax*, embryonic stage 7

Schematic illustration of the distribution of neural structures (ventral view). The superior portion of the stomatogastric nervous system (i.e. the inferior ventricular nerve, the labral commissure and the commissural ganglion) is included in the scheme. The region of the stomodeum is marked by black circular line. The inter-segmental nerves are numbered in white (1-13). The anlage of each pleopod is marked by grey number (1-6). The proctodeum is represented by a small oval stippled-line in the telson.

aC: anterior commissure; A1: antenna 1; A2: antenna 2; CA: carapace; CO: connective; COG: commissural ganglion; DC: deutocerebrum; FT: frontal tract; IVN: inferior ventricular nerve; LB: labrum; LBC: labral commissure; MD: mandible; MFT: median fiber tract; ME: medulla; MT: medulla terminalis; MX1-2: maxilla 1-2; MXP1-3: maxilliped 1-3; OL: optic lobe; PC: protocerebrum; pC: posterior commissure; PE1-5: pereiopod 1-5; POC: post-oral commissure; PROC: pre-oral commissure; TC: tritocerebrum; TE: telson.

In addition to the increasing diameter of the neurite bundles of each tract in the naupliar region, a certain condensation process of the neuropilar structures occurs during this stage and a general decrease of the α-tubulin signal is noticeable (Fig. 74A). In the protocerebral region, the pre-oral commissure has noticeably thickened. Both of its components have approached each other and their distinction has become more difficult (Fig. 74A). The antero-median cell cluster of the protocerebrum has enlarged (green field in Fig. 74B) and touches its contra-lateral medially, forming an even externally protruding bi-lobed mass of somata at the antero-median side of the brain. A consistent cell cluster is also noticeable at the lateral side of the protocerebrum, nested between the frontal tract and the antenna 1 (grey field Fig. 74B). Within the optic lobe, additionally the medulla terminalis, the hemi-ellipsoid body and the medulla anlagen have formed (Fig. 74C). The hemi-ellipsoid body lies in antero-ventral position with respect to the medulla terminalis and protrudes medio-ventrally in the optic lobe. At the medio-dorsal side of the mandibular commissure, a cell cluster of around four cells is connected to the anterior end of the median fiber tract (Fig. 75A, A').

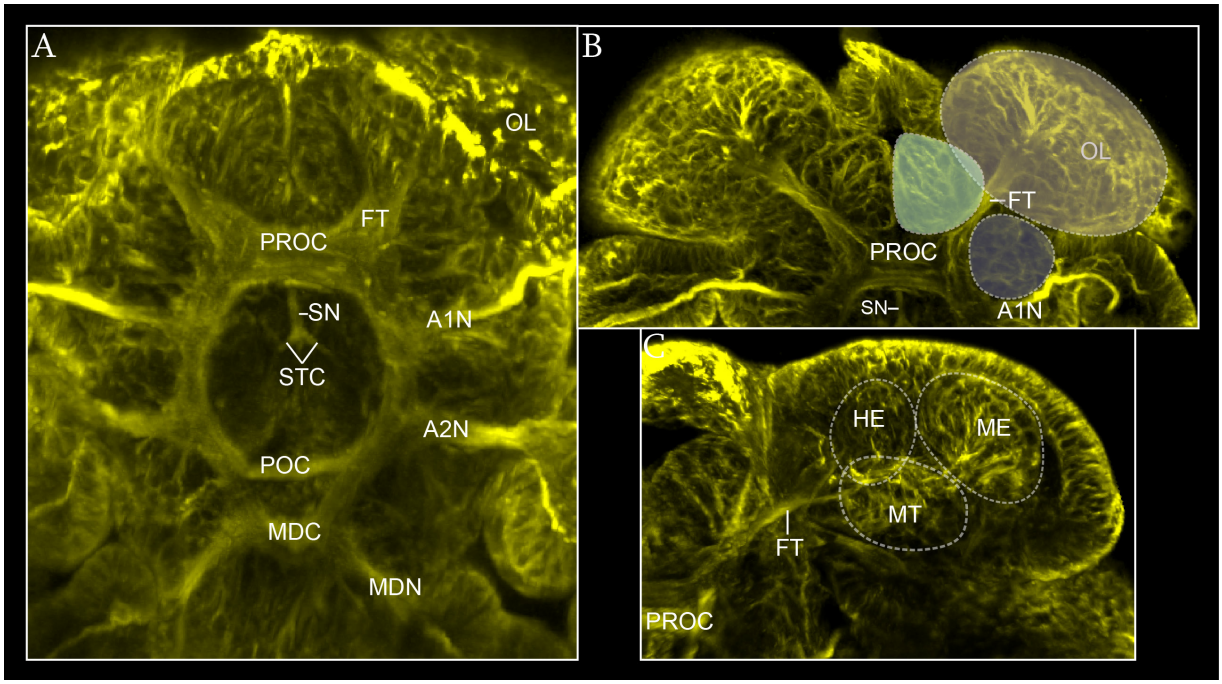

Fig. 74 – Axogenesis in the naupliar region of *P. fallax*, embryonic stage 7

Anti-ac-α-tubulin labelling. CLSM image stack. Imaris volume mode, clipping plane. **A -** General overview (ventral view). Note that the image includes part of the stomatogastric nervous system (i.e. SN; STC). **B -** Overview of the protocerebral region (ventral view). Three cell clusters are marked by transparent coloured area delimited by stippled line. They correspond to the postero-lateral and the antero-median cell clusters and to the optic lobe. **C -** Detail of the optic lobe anlage (ventral view). The three cell clusters in the optic lobe are marked by circular broken line. Note that the cell cluster of the hemi-ellipsoid body lies in a more ventral position than the others and is partially cut out in the section.

A1N: antenna 1 nerve; A2N: antenna 2 nerve; FT: frontal tract; HE: hemi-ellipsoid body; ME: medulla; MDC: mandibular commissure; MDN: mandibular nerve; MT: medulla terminalis; OL: optic lobe; POC:

post-oral commissure; PROC: pre-oral commissure; SN: stomatogastric nerve; STC: stomodeal commissure.

The differentiation of the ventral nerve cord has progressed further, following an antero-posterior gradient (Fig. 75A-D). The anterior and the posterior maxillary commissures have fused in one single neurite bundle each (e.g. MX1 in Fig. 75A), while at the level of the three maxilliped neuromeres the anterior and posterior commissures are composed of two distinct neurite bundles (e.g. MXP1 in Fig. 75B). The posterior commissure of maxilliped 3 neuromere shows a somehow delayed differentiation. In the pereiopod neuromeres only the anterior commissures have formed, showing an antero-posterior decrease of differentiation so that at the level of pereiopod 5 only a thin neurite constitutes the anlage of the anterior commissure (filled arrowhead in Fig. 75D). The segmental nerves of the maxillipeds have now a defined shape and each run off as a single neurite bundle, which branches at the level of the longitudinal muscle anlage into two neurites that enter the limb anlage (Fig. 75C). The inter-segmental nerves have formed in between all the five pereiopod neuromeres. The inter-segmental nerve 11, between pereiopod 4 and 5, is the most posterior, (Fig. 75D). Additionally, two thin neurites are observable running off the connectives between the pereiopod 5 and pleon 1 neuromeres and between the latter and the pleon 2 neuromere (i.e. ISN12, 13 anlagen in Fig. 75D). The somata of putative glia cells and their longitudinal projections are still visible at the dorsal side each neuromere, posterior to the anterior commissure (small grey ovals Fig. 75A, B and D) and their occurrence has extended as far posterior as the pleon 2 segment (small grey ovals in Fig. 75D). In the telson region, the terminal cluster has noticeably enlarged (stippled line in Fig. 75E) proportionally to the increasing number of terminal sensory structures visibly stained at the surface (filled arrowheads in Fig. 75E).

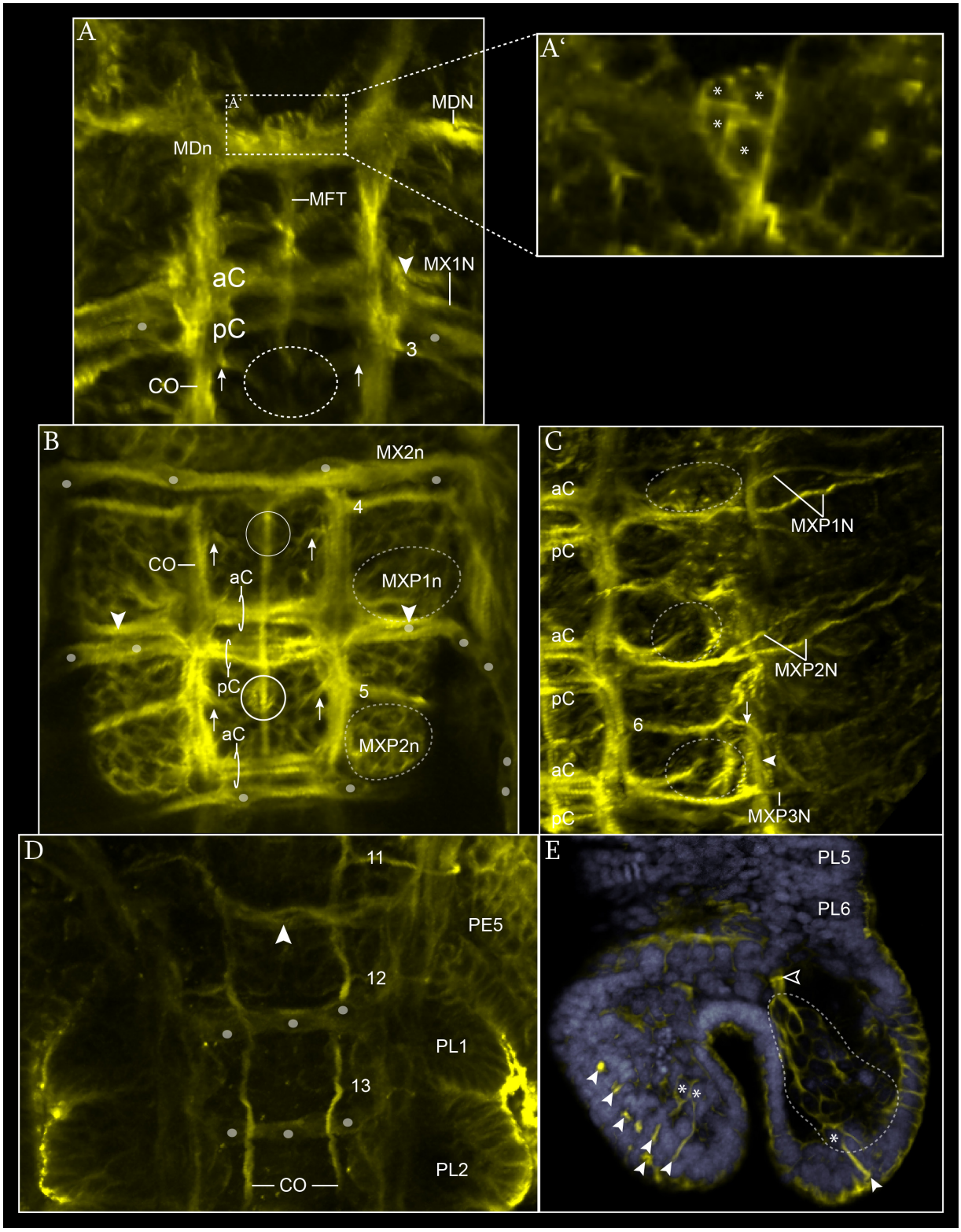

Fig. 75 – Axogenesis in the post-naupliar region of *P. fallax*, embryonic stage 7

Anti-ac-α-tubulin labelling in yellow; Hoechst staining in grey. CLSM image stack. Imaris volume mode, clipping plane; oblique slicer in **B**. **A -** View of the mandibular and the maxilla 1 neuromeres (ventral view). The filled arrowhead on the right points at the group of neurites running into the connectives from the lateral cluster of the maxillar neuromere (stippled circles in **B**). Small grey ovals mark single glial cell somata, putatively of glia cell. Arrows point at the insertion of the neurites of the medio-ventral cluster into the connectives. The stippled circle includes the region where the two medio-ventral cell clusters

meet the median fiber tract. **A' –** Detail of the median cell cluster at the level of the mandibular neuromere (ventral view). Each cell soma is marked by an asterisk. **B -** View of the maxilliped 1 neuromere (ventral view). The section includes also the postero-dorsal portion of the maxilla 2 neuromere and the antero-dorsal part of maxilliped 2 neuromere. Circles mark the medio-ventral cell clusters of the median fiber tract. Arrows point at the level of insertion of the neurites of the medio-ventral cell clusters into the connectives. The stippled circles mark the antero-lateral cell clusters at the left of the maxilliped neuromeres. Small ovals mark single glial cell somata. **C -** View of the left half of the ventral nerve cord and of the maxilliped segmental nerves (ventral view). Stippled circles mark the antero-lateral cell clusters. The arrow points at inter-segmental nerve 6, extending ventral to the longitudinal musculature anlage (filled arrowhead). **D –** View of the anlagen of the last pereiopod and the first two pleon neuromeres (ventral view). The filled arrowhead points at the anlage of the anterior commissure in the pereiopod 5 neuromere. Small ovals mark single glial cell somata. **E -** Axogenesis in the telson (ventral view). Filled arrowheads point at the terminal sensory structures. The stippled line encircles the terminal cell cluster that is anteriorly connected to the connective (open arrowhead). Asterisks mark single cell somata directly connected to the terminal sensory structures.

aC: anterior commissure; CO: connective; MDC: mandibular commissure; MDN: mandibular nerve; MFT: median fiber tract; MX1-2: maxilla 1-2; MX1N: maxilla 1 nerve; MXP1-3: maxilliped 1-3; MXP1-3N: maxilliped 1-3 nerve; pC: posterior commissure; PE1-5: pereiopod 1-5; PL1-6: pleonal segment 1-6.

Stomatogastric nervous system

In general, the stomatogastric nervous system has become more compact (Fig. 76). The lateral cell cluster corresponding to the commissural ganglion has further enlarged (stippled circles in Fig. 76A, B) and is covered by the labral tissue (Fig. 76B). The stomatogastric nerve extends further dorso-posteriorly along the dorsal wall of the forming digestive tube (data not shown).

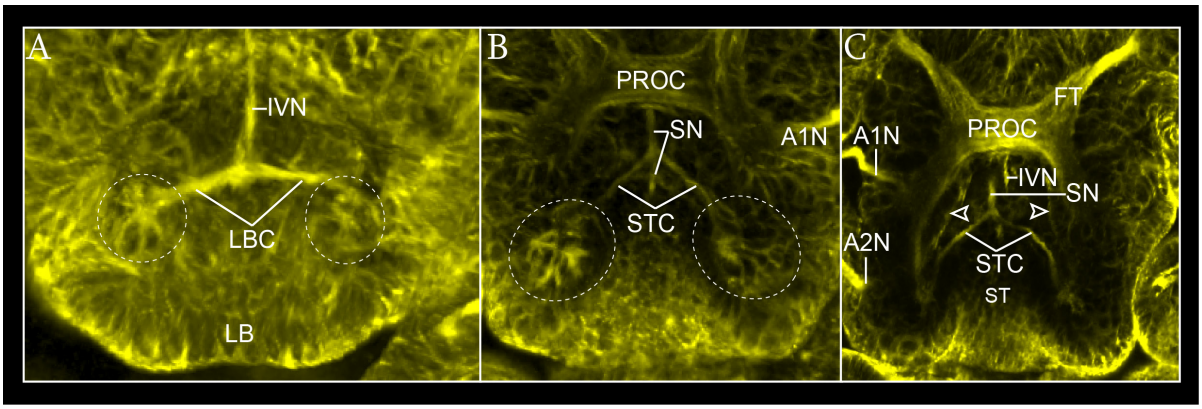

Fig. 76 – Axogenesis in the stomatogastric nervous system of *P. fallax*, embryonic stage 7

Anti-ac-α-tubulin labelling. CLSM image stack. Imaris volume mode, clipping plane. In **B**, **C** the antero-ventral portion of the image stack has been cut out. **A –** View of the superior portion of the stomatogastric nervous system and of the labrum (antero-ventral view). The anterior portion of the labrum has been cut off the image. The position of the commissural ganglion is marked by stippled circle at each side. **B –** View of the inferior portion of the stomatogastric nervous system (antero-ventral view). The clipping plane is oblique to the x-axis of the image. The position of the commissural ganglion is marked by stippled circle at each side. **C –** View of the stomatogastric nervous system in relation to the position of the stomodeum (antero-ventral view). The clipping plane is perpendicular to the x-axis of the image. Open arrowheads point at the lateral stomatogastric nerves.

A1N: antenna 1 nerve; A2N: antenna 2 nerve; FT: frontal tract; IVN: inferior ventricular nerve; LB: labrum; LBC: labral commissure; PROC: pre-oral commissure; SN: stomatogastric nerve; ST: stomodeum; STC: stomodeal commissure.

3.3.2.6 Note on the distribution of SL-ir structures in stage 8

The first evidence of SL positive expression has been consistently observed in the later phase of stage 8 (Fig. 77A, B). Stained SL-ir neuropilar regions include: the frontal tract and the median region of the optic lobe (Fig. 77A, B); the connectives between the protocerebrum and the tritocerebrum (Fig. 77A and C). SL-ir longitudinal neurites extend more posteriorly into the mandibular and maxilla 1 neuromeres (data not shown). Paired SL-ir neurons are observable: at the ventral side of the median region of the optic lobe (Fig. 77A); in the ventro-lateral cell cluster of the protocerebrum (Fig. 77B); medio-ventrally in the deutocerebral region; laterally within the tritocerebrum, the mandibular and the maxilla 1 neuromeres (Fig. 77C). Moreover, along the antenna 2, SL-ir bipolar neurons connected to thin SL-ir terminal branches of the segmental nerve terminal (Fig. 77D). Terminal axons are also stained, although more blandly, at the distal tip of the appendage (open arrowhead in Fig. 77D).

Fig. 77 (next page)

Anti-serotonin labelling. CLSM image stack in **A**-**C**. Imaris surpass mode; oblique slicer in **A**, volume, clipping plane in **B**, **C**. Epifluorescence microscopic image (Helicon-Focus) in **D**. Stippled circles mark single SL-ir neurons. **A -** Overview of the naupliar region and of the maxilla 1 neuromere (ventral view). **B -** Detail of the SL-ir structures in the protocerebral region (ventral view). Stippled lines surround the median region of the optic lobe at the terminal side of the frontal tract. Circles mark the lateral region of the protocerebrum. **C -** Detail of SL-ir structures in the deuto- and tritocerebrum, in the mandibular and maxilla 1 neuromeres (ventral view). The median SL-ir neurons at the level of the deutocerebrum are marked by stippled circles. They are located medially within the nerve ring. **D -** Detail of antenna 2. Arrows point at single SL-ir neurites connected to the SL-ir (bipolar) neurons (stippled circles). Open arrowheads point at terminal sensory neurites, only feebly stained.

DC: deutocerebrum; MDn: mandibular neuromere; MX1n: maxilla 1 neuromere; OL: optic lobe; PC: protocerebrum; TC: tritocerebrum.

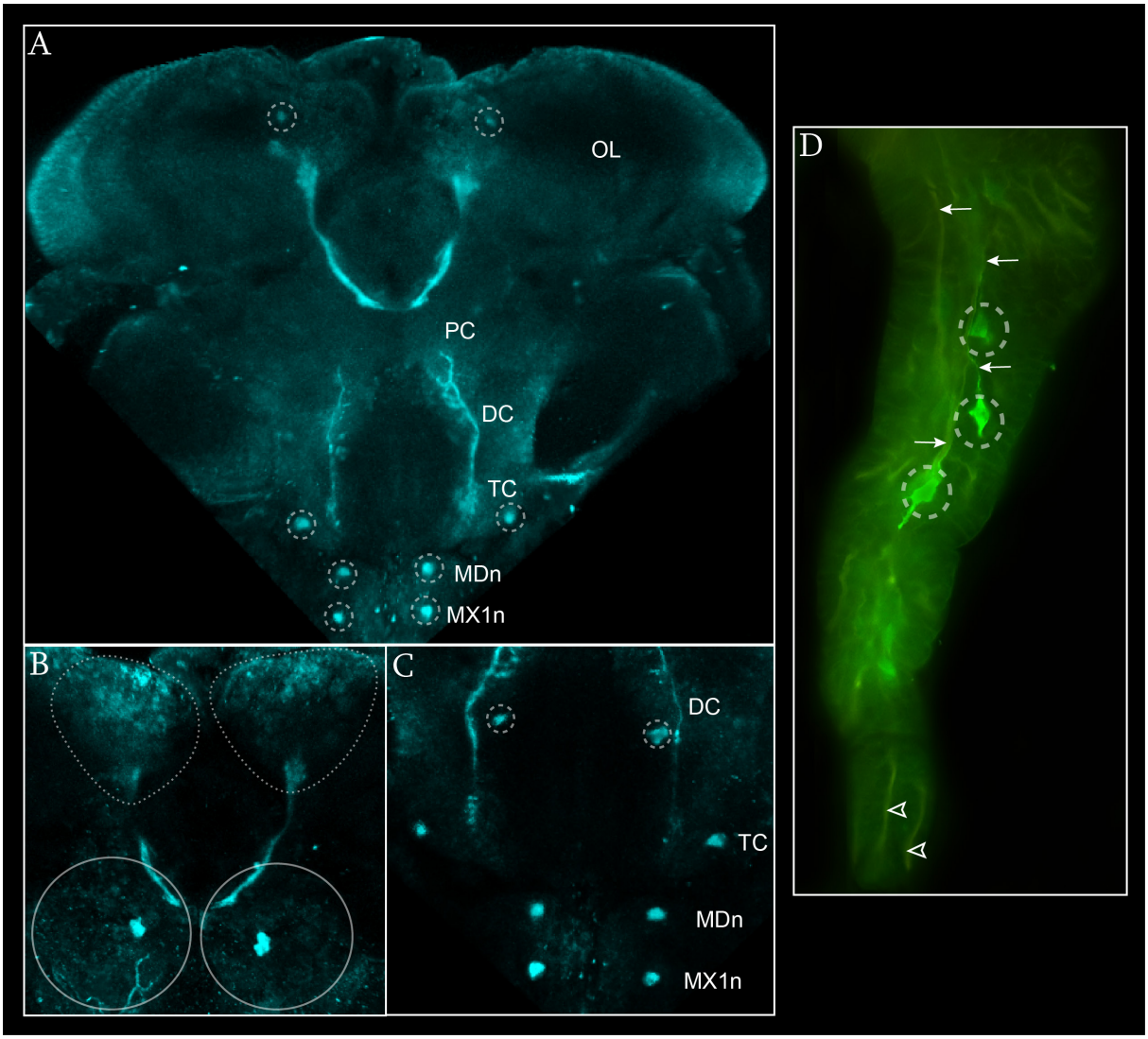

Fig. 77 – Expression of SL immunoreactivity in the development of *P. fallax*, embryonic stage 8

Table 8 (next page)

The anlagen of the main external morphological structures (**MORPHOGENESIS**) and of the relevant neural components (**AXOGENESIS**). They are ordered following the antero-posterior axis of the animal. The developmental stages are listed in the columns (**ST3**-**7**). The neural characters are organized in four columns (numbers at the bottom of the table) referring to: **1**=body regions; **2**=neuromeres; **3**=commissures; **4**=neurite bundles. The **green ring** marks the time in which the connectives have established their connection with the naupliar neuromeres (embryonic stage 5). The inter-segmental nerves are underlined by light-grey to simplify the reading of the table.

Abbreviations are as indicated in the **List of abbreviations**.

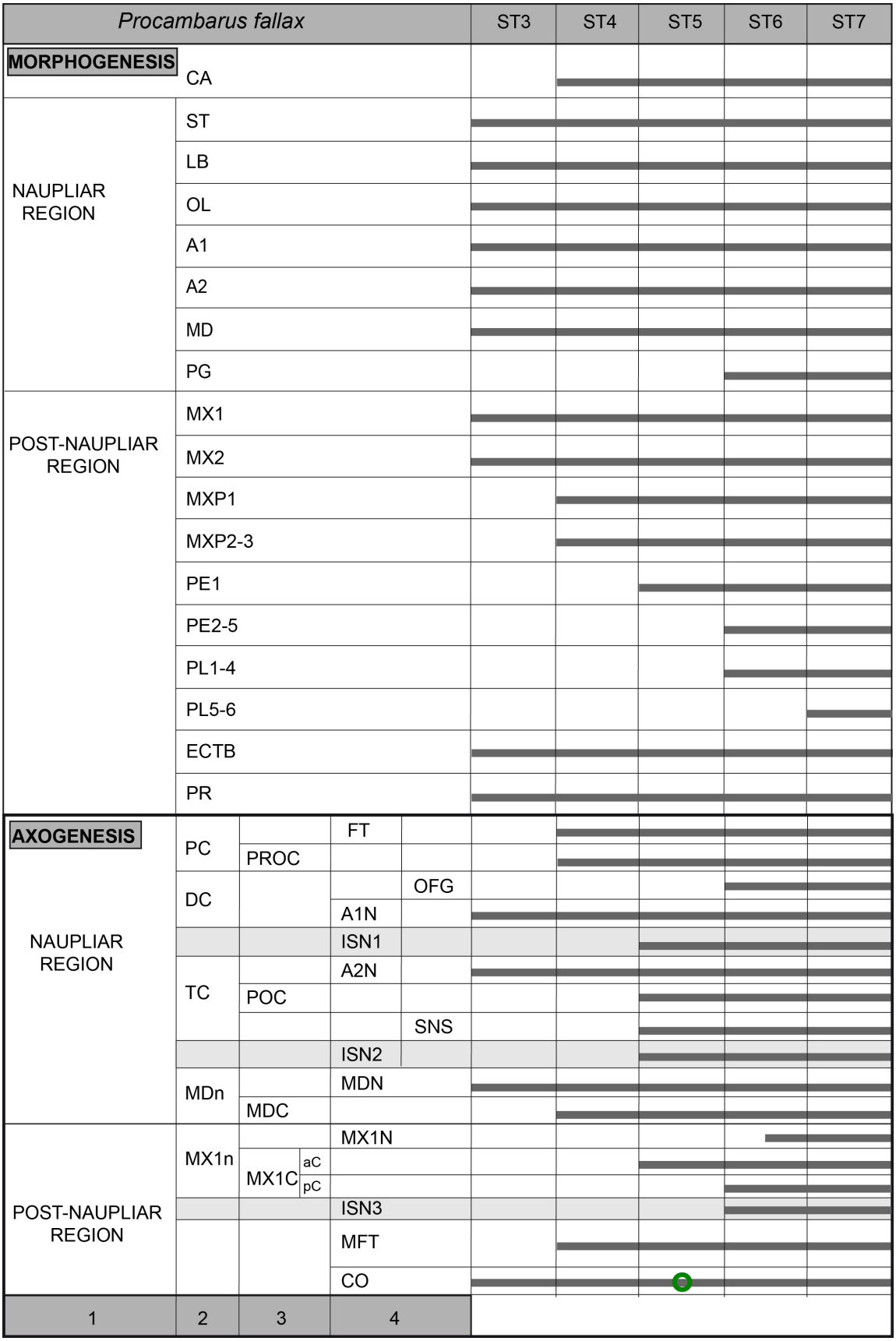

Table 9 – (next page) **- Summary of the main developmental events in *P. fallax***

4. Discussion

4.1 The development of the Central Nervous System (CNS)

4.1.1 The development of the central nervous system in Crustacea: an overview

The developmental unit of the CNS is represented by the neuromere which is defined as a cluster of cells consisting of all the developing nervous tissue that is part of one of the several anterior-posterior repetitive units of the nervous system (Richter et al. 2010). Each neuromere is a paired lateral unit composed of two hemi-neuromeres.

The brain is composed of the protocerebrum, associated with the compound eyes, the deutocerebrum, associated with the antenna 1, the tritocerebrum, associated with the antenna 2. The VNC is composed of the mandibular neuromere and of the following posterior neuromeres i.e. of the maxillar, thoracic and pleon neuromeres, each associated with a pair of limb buds.

In malacostracan crustaceans the development of the CNS proceeds in two phases, reflecting the developmental gap (*sensu* Scholtz 2000) observed in the development of the external morphological units. The brain and the mandibular neuromere develop in the first phase and form the naupliar region, also named the naupliar brain (e.g. Vilpoux et al. 2006), while the following posterior neuromeres, develop in the second phase and form the post-naupliar region (e.g. Vilpoux et al. 2006; Fischer and Scholtz 2010).

The axonal scaffold of the CNS is composed of longitudinal neurite bundles, the connectives, by transversal commissures crossing the midline spanned between the hemi-neuromeres, and by the lateral segmental and inter-segmental neurite bundles connecting the CNS to the periphery. The brain axonal scaffold is a nerve ring which surrounds the stomodeum with an anterior pre-oral commissure and a posterior post-oral commissure, while the VNC is a ladder-like axonal scaffold constituted by one anterior and one posterior commissure (or sub-commissure) at the level of each neuromere. The development of the VNC which proceeds according to a stereotypic developmental pattern along the antero-posterior axis of the animal has been studied in detail, but we have only incomplete data on the early development of the brain.

The present study shows in detail the very early development of the axonal scaffold of the brain and of the ventral nerve cord and reveals a general developmental pattern common to

the three investigated species (Fig. 78 and 79). In agreement with previous studies, the developmental pattern observed in the present study includes two major phases: the formation of the naupliar brain and, at certain time interval, the metameric formation of the post-naupliar region. Moreover, the present study describes for the first time a developmental pattern of the naupliar brain, and also brings to light additional observations on the developmental pattern of the VNC, leading to new insights on the interpretation of the CNS development.

4.1.2 The development of the central nervous system in the naupliar region

The developmental pattern

The first neural structures visibly stained in the naupliar region in all three investigated species are small cell clusters which appear simultaneously around the stomodeum and constitute the anlage of the four central neuromeres: the proto, deuto, tritocerebrum and the mandibular neuromere (Fig. 78). At the same time, smaller cell clusters are visibly stained at the periphery of each of the naupliar segments: the anlage of the medulla terminalis (see next chapter for discussion) and the peripheral sensory cell clusters in the distal portion of the limb buds of the antenna 1 and 2, and of the mandible. Those cell clusters, both the central neuromeres and of the peripheral sensory cell clusters, include the pioneer neurons of the axonal projection of the naupliar axonal scaffold. The first visible developing axons are the radial branches of peripheral neurites spanning between the central neuromeres and the peripheral sensory cell clusters, which form the anlage of the segmental nerves, and some of the longitudinal projection forming the first connectives. The connectives between the protocerebrum and the deutocerebrum are the first to develop, while the ones between the deutocerebrum and the tritocerebrum are the last (Fig. 78B). Subsequently, transversal neurites develop and form the anlage of the naupliar commissures: the post-oral commissure is the last to develop among the three (Fig. 78B). Eventually, once the connection between the neural elements has been established, additional neurites are added to reinforce that primary axonal scaffold (grey line in Fig.78C). The neurite at the level of each commissure distributes into two separate neurite bundles (Fig. 78C) (see below for discussion).

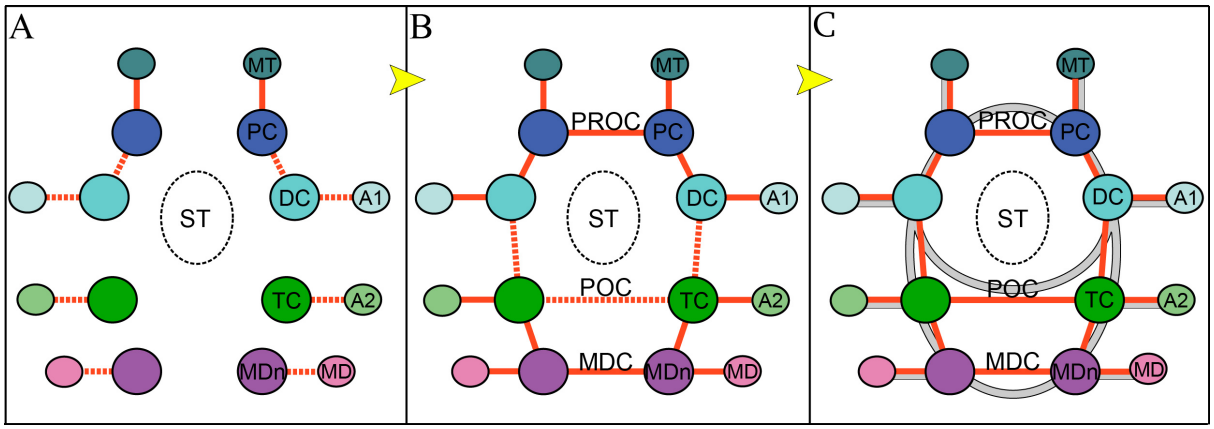

Fig. 78 – Schematic representation of the developmental pattern of the naupliar brain

A, **B** and **C** show three consecutive developmental stages and the yellow arrows indicate the time direction (ventral view). The stomodeum is represented by a circular broken line. The big coloured circles represent the anlage of each of the hemi-neuromeres of the naupliar brain. The small coloured ovals mark the peripheral ganglia within the limb bud anlagen associated with the corresponding neuromere. The colour code is consistent with the visualization of the different segmental units. The red broken lines indicate the anlage of the neurite bundles when their connections are not yet established. The continuous red lines represent the anlage of the neurite bundles with their connections set. The grey lines indicate additional neurites which contribute to form the neural network of the naupliar brain. **A -** The connectives spanned between the proto- and the deutocerebrum are the first neural projections to develop together with the anlage of the frontal tract (between the protocerebrum and the medulla terminalis) and of the segmental nerves. **B –** The development of the pre-oral and of the mandibular commissures precedes the development of the post-oral commissure. The connectives between the deutocerebrum and the tritocerebrum are the last to form. **C -** Once the axonal scaffold of the naupliar brain is established (*primary axonal scaffold*), additional neurites are added, including axons from each of the central neuromeres and afferences from the peripheral sensory centres to the nerve ring. At the commissure level, the neurites distribute at first into two separate neurite bundles which will fuse together in the following developmental stages.

A1 antenna 1; A2 antenna 2; DC deutocerebrum; MD mandible; MDC mandibular commissure; MDn mandibular neuromere; MT medulla terminalis; PC protocerebrum; POC post-oral commissure; PROC pre-oral commissure; ST stomodeum; TC tritocerebrum.

This spatio-temporal developmental pattern excludes an antero-posterior gradient of development of the naupliar brain. There is however a certain priority in the formation of the anterior-most neural structures, i.e. the connection of the protocerebrum with the medulla terminalis and the formation of the pre-oral commissure. The same arrangement could be deduced in the development of the nervous system of the stomatopod *G. falcatus* (Fischer and Scholtz 2010) and in the amphipod *O. cavimana* (Ungerer et al. 2011) suggesting the occurrence of such pattern in the ground pattern of the Malacostraca. Unfortunately, however, detailed studies on these early developmental stages of the naupliar brain are still scarce and a broader comparison for evolutionary considerations cannot be applied.

The development of the naupliar commissures and head segmentation

As shown in the present study, each naupliar commissure, i.e. the pre-oral, the post-oral and the mandibular one, is composed of several neurites, which include: axons spanned between the contralateral hemi-neuromeres, prolongation of the segmental neurite bundles (afferents), and prolongation of the connectival axons from each of the other naupliar neuromere. In a first phase of development, these neurites group into two main bundles. Later, with the exception of the pre-oral commissure, the two neurite bundles of each commissure unite to form one single tract. The composition and number of the commissures of the brain and of the mandibular neuromere have been a source of debate in the past, and several arguments have been taken as evidence for different scenarios on the segmental composition of the head of crustaceans and arthropods in general. Some are reviewed in the present study in the light of the observed developmental pattern.

The position of the stomodeum

There is an ongoing debate about the exact position of the mouth opening in euarthropods (e.g. Bitsch & Bitsch 2010). Observing that deutocerebral fibers run both anterior and posterior to the esophagus in representatives of chelicerates, crustaceans and insects (Boyan et al. 2003; Mittmann and Scholtz 2003; Harzsch 2004; Brenneis et al. 2008; Fischer and Scholtz 2010) it has been proposed that in the ground pattern of euarthropods the esophagus runs through the deutocerebrum (e.g. Scholtz and Edgecombe 2006). In accordance with this view recent studies on the development of the nervous system in malacostracans have confirmed the presence of deutocerebral neurites in the anlage of both pre- and post-oral commissures, suggesting that the stomodeum passes through the deutocerebrum (e.g. Vilpoux et al. 2006; Fischer and Scholtz 2010; Ungerer et al. 2011). The present study shows instead that each commissure receives neurites from all the segments of the naupliar brain once the neural pathway has been established by a "primary" connection. The pre- and post-oral commissures are constituted by neurites coming from the proto-, deuto-, tritocerebrum and the mandibular neuromere. This excludes the assignment of the stomodeum so far given exclusively to the deutocerebrum, considering the fact that protocerebral neurites extend posteriorly to join the post-oral commissure. The developmental pattern observed in the present study reminds of a developmental process already observed in the developing brain of insects in which a "*self-organizational process generates a set of initial axonal pathways that link all of the proliferative clusters in the embryonic brain, and provides an axonal*

framework for follower neurons in a given cluster to extend processes to any other cluster in the brain" (Reichert and Boyan 1997).

Thus, the traditional interpretation does not correspond to the actual nature of a commissure which connects and coordinates neural signals from the two halves of the body, beyond any segmental border. In summary, a commissure is "*a neurite bundle transversally oriented*" (Richter et al. 2010), a bridge connecting contralateral areas of the nervous system (central and peripheral) independently from the segment in which it is located. It would be of great interest to perform further studies to reveal the precise composition of each of the commissures of the naupliar brain, by identifying individual pioneer neurons and their axons, and to verify the exact developmental sequence in the addition of constituting neurites in different species, in order to check for the occurrence of a conserved pattern in the development of brain commissures in crustaceans and, eventually, in arthropods.

The mandibular commissure

Another interesting ongoing debate is about the number of "*sub-commissures*" constituting the mandibular commissure in the ground pattern of Crustacea. A double composition is considered the plesiomorphic condition for the Crustacea (Harzsch 2004a). The presence of two distinct neurite bundles, so called "*sub-commissures*", forming the mandibular commissure is considered to be the "*full set*" of the commissure itself (Harzsch 2004a). This is the layout described for some representatives of major crustacean taxa (Cephalocarida: Elofsson and Hessler 1990; Branchiopoda: Waloszek and Müller 2003; Kirsch & Richter 2007; Fritsch & Richter 2010; Remipedia: Fanenbruck et al. 2004). In contrast to the Malacostraca, a single neurite bundle forming the mandibular commissure has been observed (Harzsch et al. 1997; Vilpoux et al. 2006; Fischer and Scholtz 2010; Ungerer et al. 2011). The single nature of the mandibular commissure in malacostracans has been interpreted as the consequence of the loss of an anterior component, which, during evolution, has moved anteriorly to join the post-oral commissure (Harzsch et al. 1997).

The present study does not support this hypothesis but shows that the single nature of the mandibular commissure is the result of the fusion of multiple neurites which were distributed into two main neurite bundles in earlier stages of development. This reflects an early developmental pattern common to the naupliar commissures, and the mandibular commissure is no exception to it. This is clearly visible in the early nauplius larva of *M. norvegica* and *P. monodon*, while the double distribution is less obvious in the embryo of *P. fallax*. In this

species, the presence of neurites from the more anterior neuromeres can be easily recognized within the single neurite bundle. In my view, this could be explained by the unfortunate lack of data in the present study for intermediate stages at the time of formation of the debated commissure. There is a clear gap in the development of the nervous system between stage 4 and 5 in the present study in which we miss the details of the intermediate morphology of the mandibular commissure between its very first feeble single axon anlage appearing at stage 4, and the presence of a defined neurite-bundle as shown at stage 5. Moreover, in *M. norvegica* two distinct SL-ir neurites are clearly running within the post-oral commissure, and at least three in the mandibular commissure at the later stages of development observed in the present study. This shows and reinforces the presence and persistency of multiple neurites within a commissure, and confirms there is no migration of any "*sub-commissure*" from one neuromere to another. Interestingly, recent studies on the nervous system of the mystacocarid *D. remanei* have shown the presence of one single mandibular commissure (Brenneis et al. 2010). Here, the more anterior tritocerebral fibers are found to be involved in the formation of the mandibular commissure in the same way as shown for the investigated species in the present studies. In contrast to previous speculation about this matter (e.g. Elofsson and Hessler 2005) the authors propose that the posterior tritocerebral commissure is shifted backwards and fused to the mandibular one (Brenneis et al. 2010). However, they also advocate the need for developmental studies in order to address the issue on the plesiomorphic condition of the mandibular neuromere in crustaceans.

In summary, the present study shows that the axons which cross the midline at different levels of the naupliar brain do not invariably remain confined within the segment of origin of the neuroblasts. This reinforces the idea that the formation of a commissure goes beyond the segmental borders of the neuromeres (e.g. Bitsch and Bitsch 2010) and suggests that, in order to be able to define the ancestral condition of a commissure, one has to take into consideration the origin and the distribution of individual axons and define the exact composition of this neurite bundle during development e.g. identification of the pioneer neurons by single cell tracings. The definition of a commissure and of a sub-commissure also has to be revisited.

4.1.3 The development of the central nervous system in the post-naupliar region

Most of the studies on the development of the VNC in crustaceans have been directed towards understanding the metameric pattern of formation of the central neuromeres. Aspects of

neurogenesis and axogenesis in the developing neuromeres have been widely investigated (e.g. Harzsch and Dawirs 1994; Harzsch et al. 1998; Harzsch 2001; Sullivan and Macmillan 2001; Gerberding and Scholtz 1999, 2001; Harzsch 2002a; Harzsch 2003b; Whitington 2004; Ungerer and Scholtz 2008), including observations on the distribution of neurotransmitters and localization of individually identified neurons (e.g. Beltz and Kravitz 1987; Harzsch and Dawirs 1995; Vilpoux et al. 2008; Rieger and Harzsch 2008). The present study shows that metameric VNC construction represents only part of its development, while the pioneer neurites of its axonal scaffold are indeed established by the ascending axons of the connectives from the telson to the naupliar brain and by the descending axon of the median fiber tract from the mandibular segment towards the proctodeum.

The developmental pattern

In all three species investigated here, the development of the VNC begins together with neurogenesis in the naupliar region. The anlage of the VNC consists two longitudinal neurite bundles: the anlage of the paired lateral connective and of the unpaired median fiber tract (Fig. 79A). The paired connective is pioneered by a single lateral paired bipolar neuron in the telson, which is flanking the proctodeum. This neuron shows the typical morphology of a sensory neuron, bearing one short terminal-free sensory neural projection exposed at the distal surface of the telson, (i.e. the receptor or sensillum), and one long ascendant neurite projecting anteriorly towards the naupliar region (i.e. the afferent axon). With the proceeding of development, the terminal sensillum elongates and forms the terminal spine in the two nauplii of *M. norvegica* and *P. monodon*, while it remains embedded within the distal margin of the telson in *P. fallax*. In parallel, but slightly later, the afferent axon extends anteriorly and reaches the mandibular neuromeres, forming the anlage of the VNC connective. With progress in development, numerous other sensory neurons grow flanking the first pioneer, each forming one new terminal sensillum and each contributing to the thickening of the connective. In this respect, the telsonic cell cluster which grows lateral to the proctodeum represent the anlage of a paired sensory ganglion. The unpaired median fiber tract is pioneered by one single small neuron, within a small cell cluster, located in the mandibular region dorso-posteriorly to the forming mandibular commissure. The pioneer axons of the median fiber tract appear very early in the development of the two decapods, contemporary to the formation of the axonal scaffold of the naupliar brain. Instead, in the euphausiid *M. norvegica* the anlage of the median fiber tract begins in an advanced naupliar stage (i.e. nauplius 2), time at which the axonal scaffold of the naupliar brain is well established. The

median fiber tract extends posteriorly and reaches the proctodeum in the two nauplii of *M. norvegica* and *P. monodon* while in the embryo of *P. fallax* this is not clear (see Discussion below). Once the connective reaches the mandibular neuromere, descendant neural projections from the brain are visibly contributing to both the connective and the median fiber tract, forming continuous longitudinal neurite bundles spanning between the naupliar and the post-naupliar region, and reinforcing the "primary" longitudinal scaffold of the VNC and its connection to the brain.

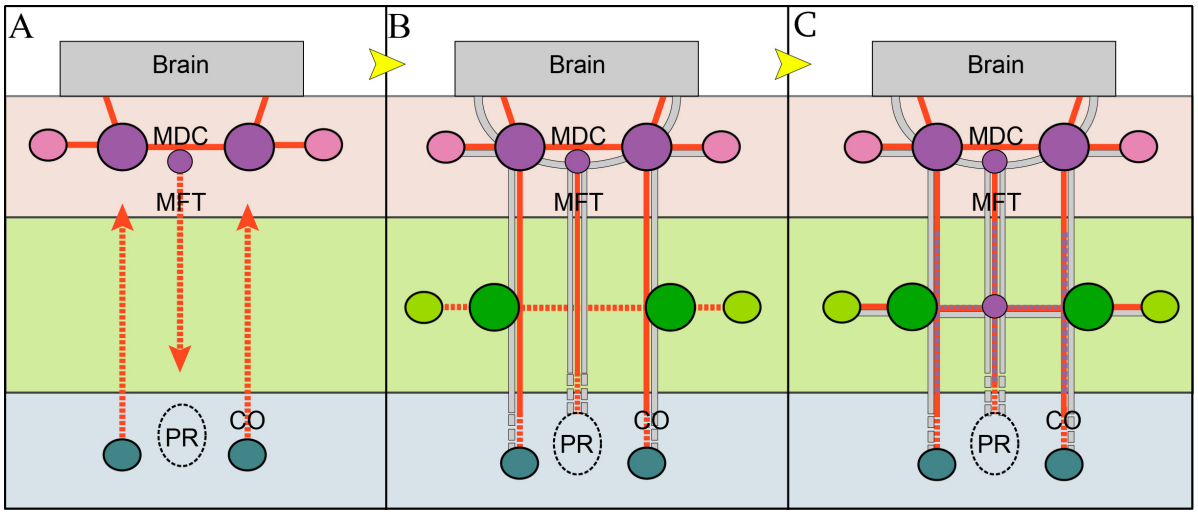

Fig. 79 – Schematic representation of the developmental pattern of the VNC

A, **B** and **C** show three consecutive stages, the yellow arrow point at time direction (ventral view). The brain is represented by the grey rectangle. The proctodeum is represented by the broken line circle in the telson. The different coloured areas mark the region of the mandibular segment, in purple, of the post-naupliar segments, in green, and of the telson, in blue. The one post-naupliar neuromere herein schematized is representative of all the post-naupliar segments. The big circles represent the hemi-neuromeres of the mandibular segment, in purple, and of the post-naupliar segments, in green. The small ovals represent the peripheral cell clusters which pioneer the segmental nerves of the mandible, in purple, of the post-naupliar segmental nerves, in green and of the longitudinal connectives, in blue. The small circles represent the cell cluster connected to the median fiber tract. The purple broken line marks the neural contribution of the median cell clusters metamerically arranged along the median fiber tract. The red lines indicate the pioneer axons of the nervous system. The grey lines mark the neurites which are connected to the brain. **A -** The longitudinal connective anlage develops running anteriorly from the posterior pioneer neuros clustered in the telson. The median fiber tract anlage is represented by a neurite which runs posteriorly from a small cell cluster located medially in the mandibular commissure. **B -** The connectives and the median fiber tract connect the mandibular neuromere, and they both receive posterior projections from the brain. The anlage of the post-naupliar commissure (the anterior component first) and segmental nerves start to form. Notice that the metameric development of the post-naupliar neuromeres follows a gradual developmental pattern from anterior to posterior. **C -** The median fiber tract is enriched by neurites from a metameric median cell cluster which also contribute to the commissure and the connective.

CO: connective; MDC mandibular commissure; MFT median fiber tract; PR proctodeum.

It is only after these events that axogenesis starts in the post-naupliar neuromeres with the gradual addition of neural units along the antero-posterior axis. This will eventually form the

typical ladder-like structure of the VNC. The sequence of development of the axonal components of the neuromeres follows the same pattern in the three investigated species. This is implemented by the formation, first, of the inter-segmental nerve, then, of the anterior commissure and the segmental nerve, and finally, of the posterior commissure. The formation of the anterior commissure and of the segmental nerve proceeds in parallel. While the anlage of the commissure is pioneered by central neurons within the neuromere, the anlage of the segmental nerve starts to grow at the periphery. At the distal tip of the limb buds small clusters of sensory cells project their afferences towards the forming VNC. In the same way as we have observed in the naupliar region, once the peripheral neurites interlock with the central ones, the efferent axons run off the central neuromeres and reach the periphery. Additionally, median neurites run out from median cells clustered in repetitive units along the midline and contribute to the growth and consolidation of the "primary" axonal scaffold of the VNC.

The non-segmental anlage of the ventral nerve cord

The anlage of the connectives

In their studies on the development of the ventral nerve cord performed by individually labelling early differentiating neurons, Whitington et al. (1993) observed that in decapods the pioneer axons of the connectives are descending neurites originating from neurons located anteriorly in the brain. These axons enter the segmental ganglia when the neurons in those ganglia begin axogenesis.

In the three species investigated in the present study, the pioneer axons of the connectives correspond instead to ascending neurites originating from neurons located posteriorly in the telson while the descending neurites from the brain, which probably correspond to the pioneer axons observed by Whitington and coauthors (1993), contribute to the anlage of the connectives only in a second phase of development but are not the pioneers.

The presence of posterior neurons pioneering the connectives has been previously observed in the marbled crayfish (Jirikowski et al. 2010) and in the stomatopod *G. falcatus* and it has been proposed to be part of the ground pattern of malacostracans (Fischer and Scholtz 2010). Additionally, the present study shows that these neurons are sensory neurons, which become part of a telsonic sensory ganglion flanking the proctodeum. Interestingly, among the crustaceans other than Malacostraca, the presence of posterior neurons pioneering the connectives occurs also in branchiopods (Blanchard 1986; Fritsch and Richter 2010; Frase

and Richter 2016) and some axons of these neurons have been observed to innervate posterior sensory elements and setae (Fritsch and Richter 2010; Frase and Richter 2016). Moreover, posterior neurons clustered together with setal neurons, potentially pioneering the connectives have been recently observed also in the development of the nervous system of cephalocarids (Stegner and Richter 2015). In this respect, we could advance the hypothesis that the connective of the VNC in crustaceans are pioneered by terminal sensory neurons of the telson which, initially, also act as guidance for the neural structures which follows throughout axogenesis.

The anlage of the median fiber tract

The median fiber tract in malacostracans is pioneered by a median unpaired neuron at the level of the mandibular neuromere (Whitington et al. 1993; Vilpoux et al. 2006; Fischer and Scholtz 2010). This neuron sends one median unpaired neurite towards the posterior and one paired lateral projection anterior to the brain (Whitington et al. 1993). This arrangement of the axons results in a Y-like shape which characterizes the anlage of the median fiber tract. The same arrangement has been observed during the development of the median fiber tract of the stomatopod *G. falcatus* (Fisher and Scholtz 2010) and has been proposed as representing the ancestral condition of the anlage of the median fiber tract in the stem species of the Eumalacostraca (Fischer and Scholtz 2010).

In the present study the same arrangement of the neurite bundle forming an Y-like shape at the level of the mandibular neuromere is found in all the three investigated species. However it is attained only later in development. In facts, the pioneer of the median fiber tract is represented by a small number of median cells clustered dorso-posteriorly to the forming mandibular commissure, thus called the mandibular median cell cluster. The first axons of the mandibular median cell cluster run posteriorly, while the Y-like shape as described in previous studies is achieved only in a later phase of development when bilateral axons descend from the brain, meet at the midline in the mandibular segment and adjoin the median fiber tract. This indicates that the Y-like shape is indeed a peculiar morphology of the median fiber tract anlage as proposed by previous studies but it is attained later in development, and as a consequence of the formation of descending axons from the brain. Possibly, lateral branches of the mandibular median cell cluster to the brain form in a later phase of development and do not represent the anlage of this tract.

Identification of the median fiber tract

The median fiber tract, sometimes called median neurite bundle or simply the median nerve, occurs in many malacostracan crustaceans (e.g. Amphipoda: Gerberding and Scholtz 2001; Decapoda: Whitington et al. 1993; Harzsch et al. 1997, 1998; Vilpoux et al. 2006; Isopoda: Whitington et al. 1993; Leptostraca: Pabst 2004; Stomatopoda: Chaudonneret 1957; Fischer and Scholtz 2010) and also in some non-malacostracans (Cirripedia: Semmler et al. 2008; Schulz van Endert 2009; Copepoda: Klann 2008; Mystacocarida: Brenneis and Richter 2010; Cephalocarida: Stegner et al. 2014; Stegner and Richter 2015), but not in branchiopods (Harzsch and Glötzner 2002; Kirsch and Richter 2007; Fritsch and Richter 2012).

Developmental studies have revealed that the median fiber tract extends to the proctodeum at a relatively early stage of development in most malacostracans investigated so far (Whitington et al. 1993; Fischer and Scholtz 2010). In *G. falcatus* the median fiber tract reaches the proctodeum at the time of hatching. However, its further development and correspondence with adult structures has not been defined yet. In the present study, the connection of the median fiber tract and the proctodeum in the development of *P. monodon* is manifest from the first nauplius stage. During the metanauplius stage the antero-ventral margin of the proctodeum is surrounded by the proctodeal commissure. The proctodeal commissure is pioneered by small cells lateral to the proctodeum included within the telsonic sensory cell cluster, and by the lateral branches of the median fiber tract itself. In this way, the arrangement of the neurites of the median fiber tract and of the proctodeal commissure is reminiscent of the *nervus intestinalis* and of its branches which innervate the anus in adult decapods (e.g. Sandeman 1982; Audehm et al. 1993) and may correspond to its anlage.

The segmental development of the ventral nerve cord

In the three species investigated in the present study, the addition of metameric units to the axonal scaffold is the last developmental event in the construction of the anlage of the VNC. This proceeds from anterior to posterior following a spatio-temporal developmental pattern which corresponds to the one described in other crustaceans (e.g. Whitington et al. 1993; Scholtz 1995b; Harzsch et al. 1997; Harzsch and Glötzner 2002; Fritsch and Richter 2010), including the formation of the inter-segmental nerve, followed by the segmental nerve and the anterior commissure, and eventually by the posterior commissure. As in previous studies the pioneers of those neurite bundles include paired neurons of the hemi-neuromeres and median unpaired neurons, probably originating from a median neuroblast clone (Gerberding and

Scholtz 2001). The neuromere neurons pioneer the inter-segmental nerves, contribute to the formation of the commissures, add neurites to the connectives and send efferents (motoneurons) to the periphery, contributing to the anlage of the segmental nerve. The median neurons contribute to the median fiber tract, to the formation of the commissure and to the connective. Moreover, in the present study a third unit of pioneer neurons is advocated. This corresponds to the neurons at the periphery of the limb buds, identified as peripheral sensory cell clusters which send their afferences to the central ganglia and pioneer the segmental nerves. Their axons also contribute to the formation of the commissures and of the connectives. In their study on the development of the nervous system in the amphipod *O. cavimana*, Ungerer et al. (2011) described the presence of sensory structures in the terminal portion of each appendage and named these "*cone-like sensory structures*". In the same way as described in the present study, these sensory structures send axons to the central neuromeres in parallel to the construction of the VNC axonal scaffold. Interestingly, examples of sensory pioneer neurons projecting into the CNS have been observed in the development of insects both in the brain and in the thoracic appendages (Ghysen1980; Keshishian1980; Ho and Goodman1982; Boyan and Ehrhardt 2015) and it has been pointed out that the placement of peripheral cells may constitute the initial guidance mechanism underlying long-distance pathfinding (Bentley and Keshishian1982; Ho and Goodman 1982; Edwards 1977), which might be the case in the species described here.

The relative development time of neural and external morphological units

When observing the relative development of the limb buds and the central neuromeres, there is a divergent sequential pattern among the species considered here. The sequential pattern is divergent in the egg-nauplius and in the free-living nauplius. While in the embryos of *P. fallax* the formation of the limb bud precedes the formation of the neuromeres invariantly from anterior to posterior until the completion of the thoracic ganglia, in the nauplii of *P. monodon* and of *M. norvegica* the development of the thoracic limb buds is interrupted at the metanauplius stage, while the development of the thoracic neuromeres proceeds posteriorly. The condition in the embryonic development of *P. fallax* is very similar to the developmental sequence in the stomatopod *G. falcatus* observed by Fischer and Scholtz (2006). Interestingly, the development of the naupliar limb buds also precedes the formation of the neural units in the amphipod *O. cavimana*, but here the time interval between the two events is much more pronounced. In the amphipod, in fact, even neurogenesis of the naupliar regions starts at the

time in which not only the thoracic buds have formed but also some of the pleonal ones. It has been already observed that, in contrast to decapods in peracarids the pioneer neurons of the VNC are located in the segmental ganglia before the axons from the brain reach the ventral ganglia (Whitington et al. 1993; Ungerer et al. 2011). So far, instead, the formation of neural structures in the post-naupliar segments prior to the corresponding appendage, as observed in the two nauplii in the present study, has only been observed in the development of cephalocarids (Stegner and Richter 2015). *H. macracantha* hatches at the metanauplius stage, which only exhibits the anlagen of the two maxillae but an additional six post-naupliar neuromeres (Stegner and Richter 2015).

The development of the post-naupliar commissures

As in all malacostracans, in all three species investigated in the present study each post-naupliar neuromeres is composed of two commissures, one anterior and one posterior. The anterior commissure develops before the posterior commissure in all three investigated species as in all malacostracans investigated so far. However, the number of constituting neurite bundles of each of the two commissures is variable. In *P. monodon*, 2 anterior neurite bundles form the anterior commissure and 1 posterior neurite bundle forms the posterior commissure; in *P. fallax*, 2 anterior and 2 posterior neurite bundles forms each of the two commissures; while in *M. norvegica*, 1 single neurite bundle form each of the two commissures. As a consequence of a condensation process, the number of neurite bundles becomes homogenous in the three species with the proceeding of development, with a final number of two commissures per each neuromere. The distribution of neurite bundles in the development of the stomatopod *G. falcatus* corresponds to the one observed in *P. monodon* in the present study with 2 anterior and 1 posterior neurite bundles while in the amphipod *O. cavimana*, 1 anterior and 2 posterior. In crustaceans the plesiomorphic condition of a commissure is represented by the composition of two neurite bundles.

In summary, the development of the VNC includes the formation of a primary axonal scaffold and the addition of the segmental neural units. The primary axonal scaffold is pioneered by the neurites which connect the telson to the brain. The segmental units are formed by the neurites of the peripheral sensory centers connecting the central neuromeres. The peripheral and the central nervous systems build in concert a network of efferences and afferences interlocking the primary axonal scaffold. In summary, the developmental pattern observed in the present study offers an example of an old and simple observation that the axonal pathways

are pioneered early in development when the "*distances are short and the terrain relatively simple*" (Harrison 1910) and leads to a new view on the development of the nervous system, shifting the attention from the central nervous system and underlying the fundamental role of the peripheral nervous system.

4.2 The development of the medulla terminalis: the anlage of a peripheral ganglion associated with an apical sensory organ

4.2.1 Subdivision of the protocerebrum in malacostracan crustaceans

In malacostracan crustaceans, the protocerebrum is traditionally subdivided in three parts. These are from posterior to anterior: the "*median protocerebrum*", the "*lateral protocerebrum*" and the ganglia of the compound eye medulla and lamina (e.g. Sandeman et al. 1992). The "*median protocerebrum*" includes the protocerebral bridge and the central body (for a review see Harzsch et al. 2012). The "*lateral protocerebrum*" is composed of two neuropils called the medulla terminalis and the hemi-ellipsoid body (e.g. Hanström 1947; Sandeman et al. 1992; Sullivan and Beltz 2001a; Harzsch et al. 2012). This last, as secondary olfactory processing area, has been extensively studied (e.g. Hanström 1925; Strausfeld and Hildebrand 1999; Blaustein et al. 1988; Sullivan and Beltz 2001a, b; Sullivan and Beltz 2004; Harzsch and Hansson 2008; Krieger et al. 2010; Wolff et al. 2012; Kenning and Harzsch 2013). Several studies have also addressed their interest into the identification of the visual neuropils, seeking for homologies throughout the pancrustacean groups (e.g. Elofsson and Dahl 1970; Nilsson and Osorio 1997; Harzsch and Waloszek 2001; Harzsch 2002b; Wildt and Harzsch 2002; Strausfeld 2005; Kress et al. 2016). Instead, while the medulla terminalis has not been taken in the same consideration in the past, it has attracted the attention of some authors in more recent years as a constant component of the crustacean brain (e.g. Strausfeld 2012; Kenning et al. 2013; Stegner et al. 2015).

The medulla terminalis is a complex neuropil

The medulla terminalis has been recently defined as a complex multi-layered aggregation of several structured and unstructured neuropils rather than one coherent neuropil (Strausfeld 2012), serving as a multi-modal integration center (Harzsch et al. 2012). During development of the compound eye in decapod crustaceans, the medulla terminalis gives rise to the lobula and together they form the most proximal visual neuropils (e.g. Harzsch 2006). The medulla

terminalis also integrates second order olfactory inputs in addition to the hemi-ellipsoid body (e.g. Maynard and Yager 1968; Ache 1982; Blaustein et al. 1988; Sullivan and Beltz 2004; Stegner et al. 2015), and includes the neuro-endocrine secretory organ X-organ, also known as organ of Bellonci or the cavity receptor organ, which is part of the neuro-endocrine secretory system known as the medulla terminalis ganglionic X-organ, sensory-pore-X (SPX)-sinus gland secretory organ (e.g. Hanström 1939; Carlisle 1953; Knowles and Carlisle 1956; Dahl 1957; Carlisle and Knowles 1959; Kauri 1966; Chaigneau 1969, 1971a, b; Gabe 1966; Elofsson and Lake 1971; Lake and Ong 1972; Chaigneau and Chataigner 1977; Cooke and Sullivan 1982). Developmental studies on Malacostraca have observed that the X-organ is generated by neuroblastic activity in the medulla terminalis (Hanström 1925, 1934; Pyle 1943; Carstam 1942; Carlisle 1953; Dahl 1957; Hubschman 1963; Fingerman 1987; Spiridonov and Casanova 2010).

The present study offers, for the first time, a detailed description of the development of the medulla terminalis in representatives of malacostracans and introduces a new interpretation on the development and evolution of this enigmatic neuropil.

4.2.2 The development of the medulla terminalis in Malacostraca

The development of the "lateral protocerebrum" and the current state of the character in the evolution of Malacostraca

Studies on the development of the compound eye have led to the commonly accepted assumption that in Crustacea, the "*median*" and the "*lateral protocerebrum*" are part of the brain as suggested by the given nomenclature (Elofsson 1966, 1969; Elofsson and Dahl 1970; Elofsson and Klemm 1972; Sandeman 1982; Harzsch et al.1997, 1999; Nilsson and Osorio 1998; Harzsch 2002b; Fischer and Scholtz 2010) as well as the lamina and the medulla which, however, develop as separate ontogenetic unit in a later stage of development (Harzsch and Dawirs 1996a; Harzsch and Waloszek 2001; Harzsch 2002b; Wildt and Harzsch 2002; Strausfeld 2005; Sintoni et al. 2007). In this respect, despite some debate (e.g. Strausfeld 2005; Kress et al. 2016), the simple sessile eye of branchiopods, and therefore the "*median*" and the "*lateral protocerebrum*" close together, is generally considered as representative of the plesiomorphic condition for crustaceans (e.g. Wildt and Harzsch 2001). The architecture of the visual neuropils in most malacostracans, which displays the "*lateral protocerebrum*" detached from the "*median*" protocerebrum, displaced into the eye stalk, represents instead an apomorphic condition of this taxon, and is the consequence of the "*lateral protocerebrum"*

secondarily moved into the eye-stalk (e.g. Hanström 1924, 1928; Strausfeld and Nässel 1981; Harzsch 2002). As a consequence, the close position of the "*lateral protocerebrum*" to the brain of some malacostracans, as, for instance, in representatives of peracarids and some decapods, is explained as the relocation of the "*lateral protocerebrum*" to its original (primary) position, i.e. into the cephalic capsule together with the brain (Hanström 1928; Sandeman et al. 1993; Stegner et al. 2015).

In malacostracans, the medulla terminalis is formed by typically dividing neuroblasts (Harzsch and Dawirs 1996a) and is the first neuropil of the "*lateral protocerebrum*" to develop (Vilpoux et al. 2006). However, only a few studies have documented the early stages of brain development and the derivation of the medulla terminalis from the lateral portion of the brain. All other authors refer to these, without in fact contributing any additional evidence. The existence of a "*lateral protocerebrum*" splitting off the brain during the ontogeny and the evolution of malacostracan crustaceans has become, nonetheless, common belief.

The ontogeny of the medulla terminalis: new insights from modern techniques

In the past, studies on the development of the protozoea stages of representatives of dendrobranchiates described the optic lobe in the first protozoea stage, which includes the medulla terminalis, as a sessile anlage. The optic lobe and the medulla terminalis will migrate into the eye-stalk during the subsequent protozoea stages (e.g. Hanström 1924a; Sandeman et al. 1993). Later, Elofsson (1969), in his study on the development of the penaeid shrimp *P. duorarum*, has described in detail the development of the protocerebrum in the nauplius stages of this animal by means of histological sections. Here, the author shows the anlage of the medulla terminalis at the first nauplius stage, corresponding to a specific group of 10 cells with small nuclei forming behind the eye anlage in the ectoderm. He specifies that those cells "*belong to the nervous system despite being detached from it*". He follows up his interpretation of the data with the statement that these cells might come from the brain, due to histological similarities of the cells interposed between the ten cells and the "*horns*", these latter constituting a neuropil coming out from the lateral portion of the protocerebrum: "*In my view,*" we read, "*these two cell groups behind the eye anlage in the ectoderm are cells coming from the anterior swelling of the nerve ring* [...] *They are bound to form the medulla terminalis and the medulla interna in the future eye-stalk*". At the fourth nauplius stage, the medulla terminalis anlage is further described as being clearly separate from the brain and forming "*two balls*" of cells "*sitting on the dorso-lateral surface of the brain anlage*".

The present study

In the present study, in the penaeid shrimp *P. monodon*, as in all the species investigated here, the anlage of the medulla terminalis is visibly stained by α-tubulin already at the embryonic stage synchronously with the four naupliar neuromeres. The medulla terminalis anlage is represented by a small number of cells clustered dorsally at the apical pole of the embryo and clearly separate from the protocerebrum, which forms in turn, a defined cell cluster more posteriorly. Comparing their position, the timing of their formation and further development, these cells are proposed as corresponding to the group of 10 cells observed in *P. duorarum* in the ectoderm of the optic lobe (Elofsson 1969). Further in development, the cell cluster increases its volume in *P. monodon*, constituting a bilateral dorso-lateral round neuropil, which corresponds for its morphology to the "*two balls*" at the dorsal side of the brain described in *P. duorarum* (Elofsson 1969). As a consequence, the two "*horns coming out of the protocerebrum*" in *P. duorarum* (Elofsson 1969) correspond to the anlage of the frontal tract of *P. monodon*, which forms between the protocerebrum and the medulla terminalis (Fig. 80).

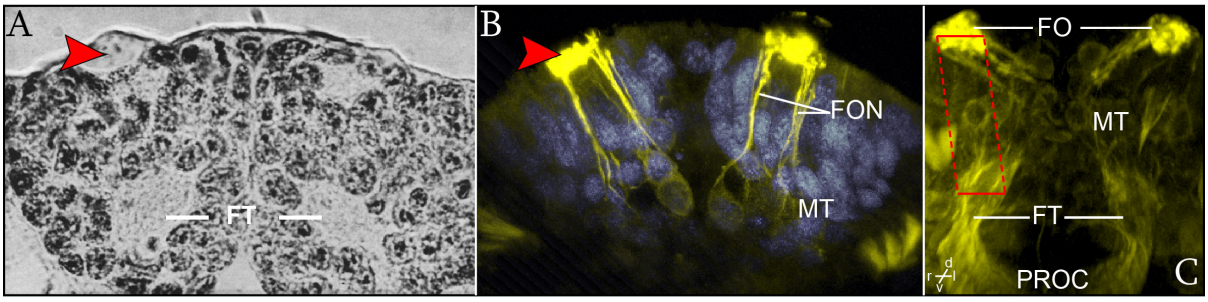

Fig. 80 – Correspondence of the SPX organ of *P. duorarum* to the frontal organ of *P. monodon* at corresponding developmental stage

A - *P. duorarum*, nauplius stage, modified from in Elofsson (1969) (Fig. 8 p. 332). Histological section of the dorsal portion of the anterior pole of the nauplius, (ventral view). The section includes the SPX organ which is marked by the red arrowhead and the frontal tract, more posteriorly. **B -** *P. monodon*, nauplius 3-4 stage (ventral view). Anti-ac-α-tubulin labelling in yellow; Sytox-green staining in grey. CLSM image stack. Imaris volume mode, oblique slicer. The section includes the frontal organs and the dorsal-most portion of the medulla terminalis. The frontal organs nerves connect the medulla terminalis to the frontal organs. **C -** *P. monodon*, nauplius 5-6 stage (antero-ventral view). Anti-ac-α-tubulin labelling. CLSM image stack. Imaris volume mode, clipping plane. The 3D view includes the anterior-most part of the nauplius including the course of the frontal tract from the protocerebrum to the medulla terminalis and the frontal organs. The frontal organs are positioned more ventrally than the medulla terminalis, so that the course of the frontal organ nerves is oblique dorso-ventrally and slightly laterally oriented. Eventually, a possible horizontal section performed at the level of the frontal organ (red quadrant at the left side of the image) would include the section of the frontal organ and of the optic fiber tract, but exclude the medulla terminalis and its neural connection to the frontal organ, as in the histological section in **A**.

FON: frontal organ nerve; FT: frontal tract; MT: medulla terminalis; PROC: pre-oral commissure.

In the light of the present data, the assumption that the medulla terminalis derives from a migration of cells from the brain to the region of the optic lobe as proposed by Elofsson (1969) is discouraged. In the same way, looking at the protozoea stage of *P. monodon*, it is clear that, despite the optic lobe still being incorporated within the head margins, and thus sessile as observed in the previous studies (see above), the medulla terminalis is clearly set apart from the brain and connected to it through an already prominent neurite bundle, which corresponds to the frontal tract. It has to be noticed that the particular architecture of this region during the development of the nauplius could be challenging to be disclosed by the use of traditional histological sectioning. The 3D render images provided by the present study clearly show the spatial relationship between the frontal tract and the developing ganglia constituting the optic lobe (Fig. 80). The frontal tract in fact extends dorsally, slightly oblique towards the anterior, and bends antero-ventrally while connecting the medulla terminalis which sits anteriorly on it. Moreover, given the delicate nature of the samples and the short distances among the neural components, particular care is required to avoid artefacts during the preparation of the objects which can be easily squeezed between the glasses and as a consequence the ventro-dorsal volume of the sample would be reduced.

The development of the medulla terminalis in the ground pattern of malacostracans

As stated above, in all three species investigated in the present study the medulla terminalis develops as a separate antero-lateral cell cluster at the very early stages of neurogenesis. While there is full correspondence between the neural architecture described here in the embryonic and larval development of *P. monodon* and *M. norvegica*, the medulla terminalis and in general, the entire optic lobe in the embryos of *P. fallax* develops in a clearly detached way from the brain as well, but antero-laterally and not dorsally. As a consequence the course of the anlage of the frontal tract in crayfish takes a straight antero-lateral direction. This morphology corresponds to the one described in the early embryo of the stomatopod *G. falcatus* (Fischer and Scholtz 2010): here the first axons forming the anlage of the frontal tract span between the protocerebrum and an antero-lateral cell cluster called the "*lateral lobe*" which, as the first ganglia of the optic lobe to develop, corresponds to the medulla terminalis as described in the present study.

The anlage of the medulla terminalis detached from the brain, although described with the use of a different nomenclature, can be observed in amphipods. For instance, in the early stages of

development of *O. cavimana* a "*medial lobe*" and an "*optic lobe*" form synchronously with the protocerebrum, antero-laterally to it (Ungerer et al. 2011). Moreover, the "*medial lobe*" is initially connected to the protocerebrum through a short neurite, an aspect not however mentioned by the authors but observable in their Fig. 4, p. 35 (Ungerer et al. 2011). This neurite disappears later as a consequence of the swelling of the "*medial lobe*" itself which becomes adjacent to the protocerebrum. I suggest that the "*medial lobe*" observed in the development of *O. cavimana* (Ungerer et al. 2011) corresponds to the medulla terminalis observed in the species investigated herein. As a consequence, the "*optic lobe*", *sensu* Ungerer et al. (2011), would represent the anlage of the medulla+lamina. Interestingly, the observations on the architecture of the brain anlage in the amphipod *Gammarus pulex pulex* accurately drawn by Weygoldt (1958) also reveal the presence of an anterior ganglion (called the "*ganglion opticum*") ontogenetically separated from the brain ganglia Weygoldt (1958). Here, a prominent neurite bundle (simply called "*connective*"), spanned between the "*ganglion opticum*" and the brain, is visibly embedded within the cell masses of these two ganglia which lie adjacent to each other (Weygoldt 1958).

Adult peracarids have a sessile eye with the medulla terminalis incorporated into the brain, a low number of ommatidia compared to other malacostracans, and, for some authors, they lack a lobula (e.g. Elofsson and Dahl 1970; Stegner et al. 2015). In the light of the present considerations, the developmental sequence of the optic lobe in amphipods mirrors the anagenetic reduction of the compound eye from primitive-stalked, to derived-sessile. This implies that the acquisition of a sessile eye in peracarids is the consequence of a derived ontogenetic mechanism. The same architecture, whit the "*lateral protocerebrum*" attached to the brain, which occurs in some decapods, e.g. in Anomala and Brachyura (Hanström 1924a, 1928; Helm 1928; Sandeman et al. 1992, 1993; Sandeman and Scholtz 1995) is presumably a derived condition driven by the same developmental sequence as observed in amphipods (see also Fig. 81 in the next section).

In the light of these observations, I propose that the medulla terminalis anlage in the ground pattern of malacostracans develops as a stand-alone ontogenetic unit, and as the first of the ganglia of a peripheral neuropil (formerly recognized as the "*lateral protocerebrum*") in the region of the optic lobe. In this respect, the medulla terminalis anlage represents a neuropil independent from the brain and connected to it via a specific neural bundle, the frontal tract which connects the brain to the prospective eye-stalk. The close proximity of the medulla terminalis anlage to the brain in some species is attained as the consequence of a derived

developmental process. This assumption is reinforced by the fact that the medulla terminalis anlage develops in association with apical sensory organs, the frontal organs in the nauplii of *P. monodon* and *M. norvegica* as discussed in the following section.

4.2.3 The development of the frontal organ in Malacostraca

The development of the frontal organ in the malacostracan nauplii

The anlage of the medulla terminalis in the embryos of *P. monodon* and *M. norvegica* is constituted by bipolar neurons, forming the frontal organ center, which connect postero-ventrally to the protocerebrum (via the frontal tract) and antero-ventrally to a pair of neural structures, identified as the frontal organ. The frontal organ gradually protrudes at the animal's apical pole medially to the first antennae and eventually pops out the optic lobe, in the advanced larval stages. At the metanauplius stage the medulla terminalis has increased in volume but one inter-neuron within the frontal organ center is specifically SL-ir in a corresponding position in both species. There is, nonetheless, a slightly difference in the external morphology of the two species which become more prominent in the advanced stages of development: the frontal organ in *P. monodon* is less protruding and has a button-like shape, while in *M. norvegica* it looks like a small cylinder. Moreover, in *P. monodon* the frontal organ undergoes a modification during the protozoea stages and is not recognizable in the eye-stalk once this protrudes. Nonetheless, the frontal organs of *M. norvegica* and *P. monodon* are assumed to be homologous.

The occurrence of the frontal organ in dendrobranchiates and euphausiids: a review of former studies

In the past, the presence of paired apical organs with the same location and morphology as the one described for the investigated species in the present study during development of the nauplius larvae in both euphausiids and dendrobranchiates has been documented. Apical sensory organs are reported as externally visible morphological features of these nauplii in the drawings of old textbooks (e.g. Korschelt and Heider 1891) and in several more recent studies. For instance, apical sensory organs called "*frontal sense organ*" have already been described in *P. monodon* (Motoh 1981). They appear during the nauplius and metanauplius stages, but are not mentioned in further larval development. Apical sensory organs have also been described in *P. duorarum* at the metanauplius stage (Dobkin 1961). Among euphausiaceans, apical sensory organs named "*sensory papillae*" are located at the median

side of the optic lobe in the nauplius larvae of *E. superba* (Fraser 1936), while small papillae are detected in *E. eximia* on the anterior margin of the body and beneath the carapace at the metanauplius stage (Knight 1980). Similar to the frontal organs described in the present study, the apical organs reported in those former works: 1) share a common antero-ventral position at the apical pole of the nauplius in between the attachment sites of the two antennae 1; 2) are the sole visible apical protruding structures at this site at comparable stages of development; 3) are associated with the optic lobe; 4) are not detected any longer once the eye stalk protrudes. As such, these are considered here homologous organs and referred to as the frontal organs.

The frontal organ is associated with the endocrine SPX-organ in the development of dendrobranchiates and euphausiaceans

The development of the apical sensory organ of *P. duorarum* studied by Dobkin (1961) has been reinvestigated in detail by Elofsson (1969) by means of histological sections. Elofsson (1969), however, refers to this structure as the "*sensory pore X-organ*" (SPX-organ) replacing the term "*apical sensory organs*" used by Dobkin (1961). This was done in order to distinguish those structures from different kinds of apical sensory organs which are linked instead to the nauplius eye (see e.g. Elofsson 1963, 1965). When comparing the development of the SPX-organ in *P. duorarum* to the development of the frontal organ in *P. monodon* at comparable stages, the correspondence of the two structures becomes clear (Fig. 80). They correspond in their external morphology and in their position. There is, however, a lack of information in the sections of Elofsson (1969) where the neural connection between the SPX-organ and the medulla terminalis is not well documented. In fact, the frontal section perpendicular to the organ meets the neurite bundles forming the frontal tract posteriorly but leaves the medulla terminalis and the neurites which connect the SPX-organ (i.e. the frontal organ) dorsally to it and therefore not visible (Fig. 80). Moreover, the SPX-organ in *P. duorarum* is reduced during development and is not detected at the surface of the compound eye once the eye becomes stalked, as is the frontal organ in *P. monodon*. From Elofsson's study (1969) we learn that such transformation is linked to the reduction of the SPX-organ into the neuroendocrine X-organ. In the same way, the transformation of a larval sensory papilla which gives rise to the X-organ has also been documented in representatives of euphausiaceans by Hanström (1947) in his detailed examination of the brain and of the visual neuropils. This leads to the conclusion that the frontal organs in dendrobranchiates and

euphausiaceans are homologous structures, which occur in the nauplius larva as sensory organs and at later stages become part of the endocrine organ SPX-organ associated with the medulla terminalis within the compound eye. The development of the frontal organs is associated with the development of the medulla terminalis which, from a small cluster of bipolar cells (the frontal organ center) becomes gradually a more complex neuropil and includes the endocrine organ.

The occurrence of frontal organs is widespread among Malacostraca

In the present study, no structure associated with the developing medulla terminalis which could correspond to the frontal organ has been detected during the embryonic development of *P. fallax.* Are the frontal organs specific organs of the malacostracan nauplius larva?

The presence of various apical sensory organs is known in Malacostraca (reviewed in Elofsson 1963, 1965) and screening through the old literature clearly shows that frontal organs homologous to the frontal organs described in the present study are not a peculiarity of the nauplius larva but occur during the embryonic development of other representatives of this group. For instance, among decapods, a developing "*sensory papilla*" associated with the X-organ occurs in various caridean species (Dahl 1957; Carlisle 1959; Hubschman 1963), and an eye papilla connected with the medulla terminalis and associated with a secretory organ has been described in the embryos of various reptants (Hanström 1939; Pyle 1943; Rotllant et al. 1994). Among peracarids, an embryonic eye papilla has been described in representatives of mysids (Dahl and Macklenburg 1969), and the same organ has been described as the "*organ of Bellonci*" or, again, the "*SPX-organ*" (Kauri and Dahl 1975).

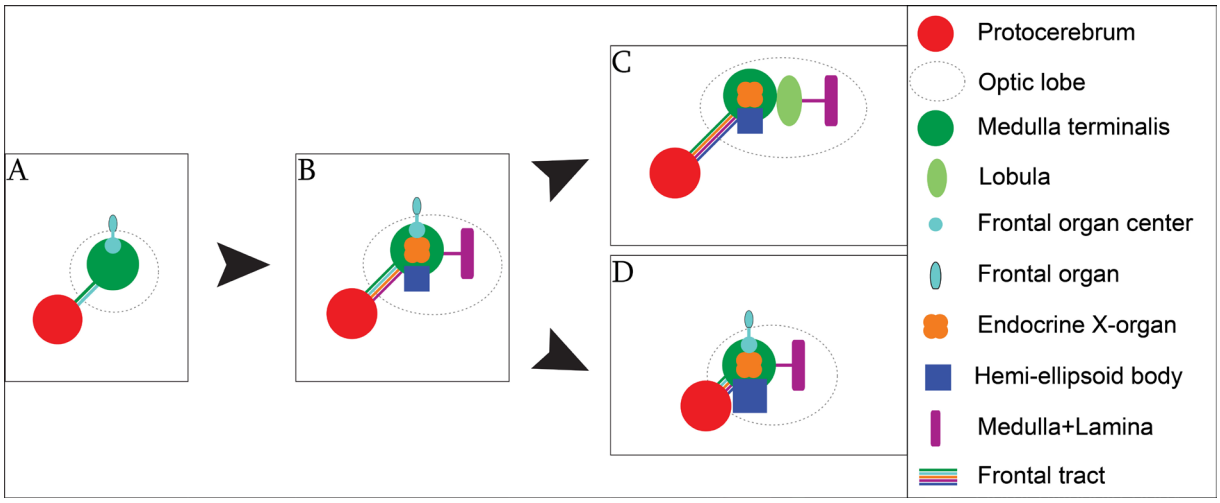

Fig. 81 – Schematic representation of the development of the medulla terminalis and the optic lobe in Malacostraca

The medulla terminalis develops in the early neurogenic stages. **A** – Embryonic stage. The early medulla terminalis is represented/includes a small number of cells connected to the frontal organ, indicated as the *frontal organ center*. It is connected to the brain (protocerebrum) via a neurite bundle which is composed of the afferences from the frontal organ and the efferences from the brain (the latter are not represented in the scheme). This represents the anlage of the frontal tract. **B** – Late developmental stage (e.g. protozoea1 in *P. monodon*; calyptopis 1 in *M. norvegica*). The medulla terminalis in the later developmental stages is composed of the endocrine organ X-organ which develops in association with the frontal organ. The medulla and the lamina anlagen develop and connect the medulla terminalis. The medulla terminalis, the medulla and lamina are included within the optic lobe (circle black line). This is connected to the brain via the frontal tract which is enriched with the afferences of the X-organ and of the medulla+lamina. **C** – Adult condition in species with a compound stalked eye. The frontal organ is reduced. The lobula forms as a derivative of the medulla terminalis. The hemi-ellipsoid body develops. The optic lobe (stippled circle) corresponds to the eye-stalk and is connected to the brain through the frontal tract which is enriched with the afferences and efferences of the hemi-ellipsoid body. **D** – Adult condition in species with reduced sessile eye. The medulla terminalis includes a small frontal organ ("*eye papilla*", see text) and the endocrine X-organ, and is close to the brain (protocerebrum). The lobula is not developed. The hemi-ellipsoid body has developed. The optic lobe (stippled circle) includes all these structures and the medulla+lamina. The frontal tract is enriched with the afferences and efferences of the hemi-ellipsoid body, Its length is reduced due to the short distance between the brain (protocerebrum) and the medulla terminalis.

The persistence of the frontal organ in adult malacostracans is linked to eye reduction

An apical organ named simply the "*eye papilla*" or the "*sensory pore organ*" or, alternatively, the "*eye papilla-sensory pore complex*" associated with a neurosecretory SPX organ has been described in various adult decapods (Hanström 1934; Dahl 1957, 1965; Chaigneau and Besse 1994). The same organ has been referred to as the "*organ of Bellonci*" in other studies (Lake and Ong 1970, 1972; Chaigneau 1971b, 1973; Smith 1974; Rotllant et al. 1994, 1995). An eye papilla occurs also in adult mysids (Dahl and Macklenburg 1969) while homologous secretory organs referred to as "*organs of Bellonci*" are reported in adult representatives of amphipods

(Elofsson and Hallberg 1980; Steele 1984; Steele and Oshel 1989) and isopods (Chaigneau and Chataigner 1977; Chaigneau et al. 1991). The "*organ of Bellonci*" of adult syncarids has been also described as homologous of these organs (Kauri and Lake 1972). Interestingly, a serotonin-like substance marks the "*organ of Bellonci*" in the eye-stalks of the prawn *P. serratus* in embryos, larvae, and adults (Bellon-Humbert and Van Herp 1988). Moreover, adult specimens of deep-sea euphausiaceans (Thysanopoda) bear tubercles protruding from their simple, highly reduced compound eyes (Brinton 1987; Herring 2002). Particularly well-developed "*organs of Bellonci*" are characteristic of some shrimps living in caves with a consequent reduction of compound eyes (Chaigneau and Jubertihie-Jupeau 1975). Likewise, an eye papilla is present in those fresh water isopods that live in caves in which the compound eyes are completely missing (Martin 1976; Chaigneau and Chataigner 1977).

In summary, despite some slight variation in external morphology, the frontal organs are widespread among malacostracans and, as indicated by the present study, these organs share the following characteristics during development: 1) they are apical sensory organs associated with the medulla terminalis, which form at the very early stages of neurogenesis; 2) they are connected to specific bipolar neurons (the frontal organ center) of the medulla terminalis which become SL-ir later in development; 3) they are associated with the neuro-endocrine X-organ (also called "*sensory pore X-organ*" or "*organ of Bellonci*") within the medulla terminalis; 4) in most species with a prominent stalked compound eye they become reduced or disappear while they are maintained in species with reduced compound eyes, where they still protrude out of the eye capsule.

4.2.4 Development and evolution of the frontal organ in Crustacea: an apical sensory organ associated with the medulla terminalis

The frontal organs in Crustacea: homology of apical sensory organs associated with the medulla terminalis

The presence of apical sensory organs is known to characterize the forehead of the representatives of most crustacean taxa (e.g. Elofsson 1963, 1965, 1966). In particular apical sensory organs referred to as "*frontal filaments*" are considered to be part of the ground pattern of the Crustacea (e.g. Scholtz and Edgecombe 2006). These organs have been observed during development in the nauplii of representatives of cirripeds (Kauri 1962, 1966; Walker 1974; Semmler et al. 2008) and of remipeds (Koenemann et al. 2007), and more

recently they have also been recognized as homologous in the nauplii of representatives of branchiopods (Fritsch and Richter 2010; Fritsch et al. 2013b; Frase and Richter 2016). The frontal filaments characterize adult remipeds (Fanenbruck et al. 2004; Fanenbruck and Harzsch 2005). Those organs are considered homologous structures based on the fact that they correspond in position and are connected directly with the medulla terminalis (e.g. Fritsch and Richter 2010).

The development of the "frontal filaments" of cirripeds and the frontal organs of malacostracans: a comparison

The "*frontal filaments*" are particularly prominent structures which characterize the embryonic and larval stages of cirripeds. Those apical sensory organs have attracted the attention of many scientists in the past and have been the subject of evolutionary considerations (e.g. Bate 1851; Darwin 1854; Kauri 1962; Walker 1974, 1992; Scholtz and Edgecombe 2006; Semmler et al. 2008; Richter et al. 2013). Differently from the modest outer appearance of the frontal organs of malacostracans, the "*frontal filaments*" of cirripeds protrude as a long and thick articulated thread at the apical pole of the nauplius. However, in the same way as the frontal organs of malacostracans, the "*frontal filaments*" of cirripeds are present from the embryonic stages (Kauri 1966; Semmler et al. 2008; Schulz van Endert 2009; Ponomarenko 2014) and develop as part of a complex of structures associated with the medulla terminalis, named in former studies the "*frontal filaments-medulla terminalis complex*" (Kauri 1962; Kauri 1966).

Moreover, recent developmental studies performed with the use of α-tubulin stainings, show the neural architecture of these animals' frontal filament in detail (Schulz van Endert 2009; Ponomarenko 2014) and leave very few doubts about the correspondence of those structures between cirripeds and malacostracans. "*frontal filaments*" in cirripeds form at the early stages of axogenesis connected to the medulla terminalis, which is a consistent cell cluster ("*fronto-lateral lobe*" in Schulz van Endert (2009); "*anterior ganglion*" in Ponomarenko (2014) located antero-dorsally in the brain with a spatial arrangement which corresponds to the one observed in the species investigated in the present study. The medulla terminalis of cirripeds is connected with the protocerebrum via a neurite bundle ("*fronto-lateral tract*" in Schulz van Endert (2009); "*frontal filament tract*" in Ponomarenko (2014)) with a dorso-lateral course, which is identical to the path of the anlage of the frontal tract observed in the present study. Later in development, the "*frontal filaments*" protrudes at the anterior margin of the

compound eye in the post-naupliar larva, the cypris larva (Kauri 1962; Walley and Rees 1969; Walker 1974: Gallus et al. 2009). At this stage, the frontal filament starts to be reduced and is gradually incorporated into a pocket within the eye, called the "*eye chamber*" (e.g. Kauri1962). This corresponds to the time of formation of the endocrine organ "*frontal filament base*", homologous of the SPX-organ of malacostracans (Kauri 1962; 1966). This is reminiscent of the transformation of the medulla terminalis and of the frontal organ within the optic lobe, and the subsequent formation of the endocrine X-organ observed in the present study in *P. monodon* at the post-naupliar stage, the protozoea stage 1.

Curiously, the spatial arrangement of the "*frontal filaments*" and of the associated structures described in the developmental studies on *B. improvisus* performed by Semmler et al. (2008), with the use of the same techniques, does not correspond to the one described herein. The "*frontal filaments*" in *B. improvisus* are connected with the antero-lateral part of the protocerebrum by several fibres which "*extend from the ring to the base of the frontal filaments resembling the spokes of a wheel*" (Semmler et al. 2008). There is no indication of any neural tract resembling the anlage of the frontal tract, since the presence of the medulla terminalis in the antero-dorsal region of the animal is completely missing (Fig. 82). On the basis of the data discussed in the present study, Semmler and co-workers' data (2008) need to be reviewed.

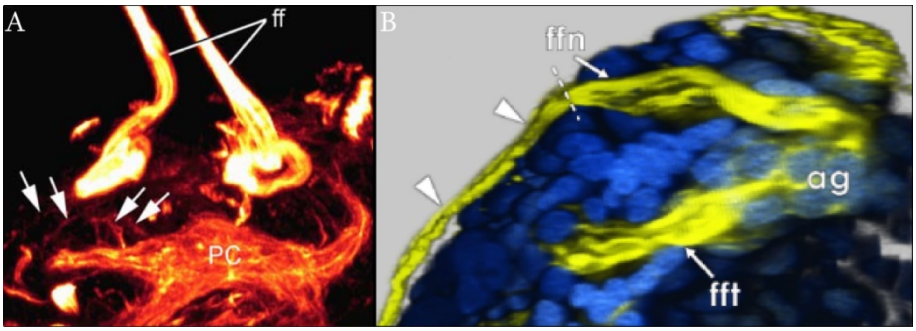

Fig. 82 – Comparison of developmental data on frontal filaments in cirripeds

A – The frontal filaments during the development of *B. improvisus* (ventral view) (modified from Semmler et al. 2008). Arrows point at the short nerves which are interpreted as connecting the protocerebrum to the frontal filament. **B -** The frontal filament during the development of *E. modestus* (lateral view) (modified from Ponomarenko 2014). Arrowheads point at the ventral extension of the frontal filament. The stippled line marks the border between the frontal filament nerve and the frontal filament.

The former study on the development of the frontal filaments in cirripeds by Semmler et al. (2008) shows the neural connection of the frontal filaments consisting of feeble short neurites spanning between the protocerebrum and the frontal filament (arrows in **A**). Recent data, however, show the frontal filament being connected to a dorsal ganglion (called "*anterior ganglion*" in **B**) via an oblique nerve with a dorso-ventral course which identifies the frontal filament nerve. As the frontal filament center within the medulla terminalis is connected to the protocerebrum via the fontal tract, the "*anterior ganglion*" is connected to the protocerebrum via a thick tract which is called the "*frontal filament tract*".

ag: anterior ganglion; ff: frontal filament; ffn: frontal filament nerve; fft: frontal filament tract; PC: protocerebrum.

In summary, despite the difference in external morphology, I propose that the "*frontal filaments*" of cirripeds and the frontal organs of malacostracans (as described in this study) are homologous structures. This confirms the strong morphological similarity between the brain of cirripeds and the brain of malacostracans already claimed in the past (e.g. Harrison and Sandeman 1999), including the morphology of the compound eyes and of the endocrine organs associated with them (Kauri 1966, 1969).

The frontal filament in Branchiopoda in the light of the present study

It is known that representatives of branchiopods have apical sensory/endocrine organs: we find *cavity receptor organs* (Elofsson and Lake 1971), also called *secretory X-organs* (Rasmussen 1971) in representatives of the Anostraca, *dorso-apical sensory organs* in representatives of the Cladocera (Claus 1876; Martin 1992), and, during development, "*frontal filaments*" have been recently detected in representatives of Anostraca (Frase and Richter 2016), Notostraca (Fritsch and Richter 2010) and Laevicaudata (Fritsch et al. 2013b). These organs are generally considered homologous structures (Elofsson and Lake 1971; Aramant and Elofsson 1976; Frase and Richter 2016), although the matter is still under debate (e.g. Weiss et al. 2012). Moreover, recent developmental data have advanced the hypothesis of the homology of these organs to the "*frontal filaments*" of cirripeds based on the evidence that they occur in the nauplius larva and are connected to the medulla terminalis (Fritsch and Richter 2010; Fritsch et al. 2013b; Frase and Richter 2016).

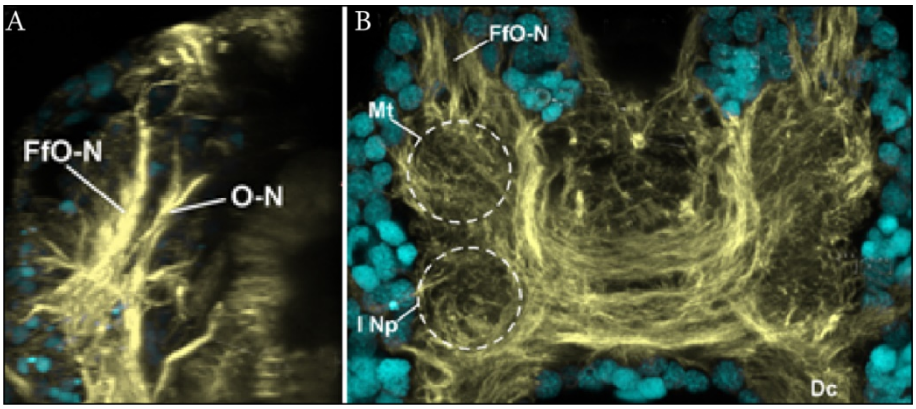

Fig. 83 – Development of the frontal filaments in branchiopods

Branchinella sp. (Branchiopoda, Anostraca), L4 stage in **A**, L10 in **B** (ventral view) (modified from Frase 2012). **A -** The optic nerve and the frontal filament-organ nerve run separately. The optic lobe does not include the frontal filament-organ. **B -** The medulla terminalis is indicated as part of the antero-lateral portion of the protocerebrum and connects the frontal filament-organ via the "*frontal filament-organ nerve*". The "*optic nerve*" connects the brain to the medulla+lamina separately.
Dc: deutocerebrum; FfO-N: frontal filament organ nerve; Mt: medulla terminalis; I Np: antenna 1 neuropil; O-N: optic nerve.

In the light of the present study, however, a fundamental difference emerges between the development of the "*frontal filaments*" of branchiopods and the development of the frontal organs of malacostracans/cirripeds. In fact, although in branchiopods, as in malacostracans/cirripeds, the "*frontal filaments*" are connected to the medulla terminalis (through a nerve called the "*frontal filament nerve*"), the optic lobe in branchiopods includes exclusively the medulla and the lamina which are connected to the medulla terminalis via a neurite bundle, named the "*optic nerve*", with a separate course from the "*frontal filament nerve*". The medulla terminalis is attached to the brain and, therefore, there is no nerve corresponding to the frontal tract. Although we do not have data which show their further development and eventual transformation in an adult structure, we could assume, given the stated homology of these organs (see above), that the final position of the "*frontal filaments*" should correspond, for instance, to the position of the "*cavity receptor organ*" as observed in the adult of *A. salina*, i.e. included within the medulla terminalis ("*lateral protocerebrum*") anterior to the brain (e.g. Elofsson and Lake 1971). As a consequence, the homology among the "*frontal filaments*" of branchiopods and the frontal organs of malacostracans and cirripeds could be questioned, or, alternatively, a different evolutionary developmental scenario could be followed based on the evidence, as advanced by the present study, that the medulla terminalis in fact represents a peripheral ganglion independent from the brain.

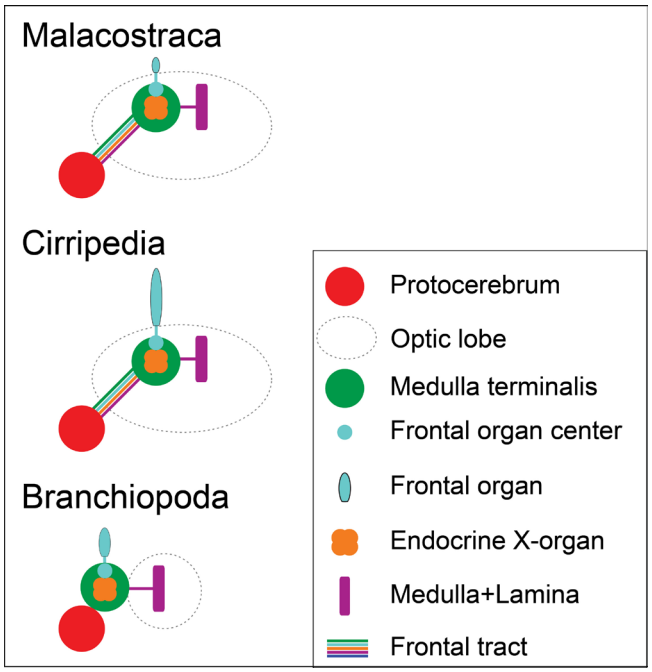

Fig. 84 – Comparison of the architecture of the medulla terminalis and its connections during development of malacostracans, cirripeds and branchiopods

The compared developmental stage corresponds to the time in which the medulla+lamina anlage have formed. In malacostracans, the optic lobe is still within the 'head' shield (e.g. protozoea1 stage). The frontal organ is small and the endocrine organ-X-organ anlage has formed but not the hemi-ellipsoid body, yet. The medulla terminalis includes the frontal organ center and the endocrine organ X-organ (also called the *cavity receptor organ* in branchiopods, see text). The frontal organ in cirripeds is particularly well developed. In branchiopods, the medulla terminalis is attached to the brain (protocerebrum) the frontal tract is absent, and the optic lobe includes only the medulla+lamina.

Unfortunately, there is no data on the development of the "*frontal filaments*" and of the medulla terminalis in the early embryonic stages of branchiopods which would have allowed a comparison with the present data. This would reveal whether the medulla terminalis anlage in branchiopods forms attached to the brain or its position is the consequence of a reduction of the distance between the medulla terminalis and the brain, as, for example, observed in some decapod and peracarid malacostracans, suggesting a developmental process linked to the compound eye reduction (see above). Following this scenario, we could speculate that the condition of branchiopods with the medulla terminalis attached to the brain represents a derived condition in the evolution of this group rather than a plesiomorphic condition for the Crustacea. This would reinforce the more recent studies which consider the branchiopods compound eye as a simplified/derived condition (e.g. Strausfeld 2005; Kress et al. 2016), against the former assumptions that a "simple" eye must have represented the common ancestral compound eye in crustaceans (e.g. Elofsson and Dahl 1970; Wildt and Harzsch 2002). Nevertheless, the presence of a complex stalked malacostracan-like eye in the common

ancestor of crustaceans is also suggested by paleontological data and neurophylogenetic analysis (e.g. the presence of stalked eyes in fossils (Castellani et al. 2012; Ma et al. 2012; Strausfeld 2012; Zhang and Pratt 2012). These data would also support the Branchiopoda as the sister group of the more derived Hexapoda within the Pancrustacea as proposed by recent analyses of molecular data (Meusemann et al. 2010).

Further studies, however, have to be conducted in order to clarify the exact location of the medulla terminalis during the development of this crustaceans' group. In particular, it would be of great interest to understand the actual early development of the medulla terminalis anlage and verify its connection with the brain in those early stages of development.

The medulla terminalis in the ground pattern of the Pancrustacea: evolutionary considerations

In the light of the present data we could attempt to reconstruct the condition of the medulla terminalis and its associated structures in the ground pattern of the Pancrustacea mapping their occurrence among the various pancrustacean groups (Fig. 85) on the consensus of the Pancrustacea phylogeny according to the trees proposed by Giribet and Edgecombe (2010) (on the left in Fig. 86) and by Regier et al. (2010) (on the right in Fig. 86). While the first tree is based on a combination of anatomical, paleontological and molecular data, the second tree is based exclusively on molecular data.

The mapped characters include: 1) the position of the medulla terminalis compared to the protocerebrum and thus, the occurrence of the frontal tract; 2) the presence of the frontal organ-frontal organ center; 3) the occurrence of the hemi-ellipsoid body; 4) the presence of the visual neuropils (i.e. lobula (lobula plates in malacostracans and hexapods), medulla+lamina); 5) the presence of the endocrine organ (i.e. X-organ/ Bellonci organ, see above for homology of these organs).

1_The frontal tract and the position of the medulla terminalis

The frontal tract as described in the present study corresponds to the neural tract which connects the medulla terminalis to the brain (i.e. the protocerebrum). The anlage of the frontal tract is composed only by the few neurites spanned between the brain and the frontal organ center (*frontal organ bundle*) and becomes more and more voluminous with the development of the compound eye (*optic bundle*) and of the hemi-ellipsoid body and the olfactory system (*olfactory bundle*). In adult malacostracans, the presence of distinct neurite bundles called

"*protocerebral tract*" and "*olfactory globular tract*" (Kenning et al. 2013), corresponds to the condition described here.

The frontal tract occurs in representatives of the major clades of Malacostraca which are equipped with prominent stalked compound eyes (e.g. Leptostraca: Kenning et al. 2013; Stomatopoda: Marshall et al. 1991; Decapoda: Sandeman et al. 1993; Sandeman and Scholtz 1995; Euphausiacea: Elofsson and Dahl 1970) and during development in cirripeds (see above). Furthermore, recent data on the nervous system development of some copepod larval stages using antibody staining techniques against α-tubulin, show a thick neurite bundle leaving the protocerebrum with an antero-dorsal course: "*Vom Protocerebrum führen stark angefärbte Nervenfasern nach anterolateral*" (transl: "Strongly stained neural fibers lead from the protocerebrum into antero-lateral direction") (Klann 2008). This resembles in my opinion the course of the frontal tract anlage as described in the present study. The presence of a distinct neurite bundle between the brain and the medulla terminalis is also reported in adult specimens (Andrew et al. 2012).

Since there is no report of the occurrence of the frontal tract in other taxa outside the Multicrustacea, we could assume the presence of the frontal tract to represent an apomorphy of the taxon. However, as already discussed above for branchiopods, the absence of developmental data leave the question open: if the primitive condition in the Pancrustacea corresponds to having the medulla terminalis close to the brain, and thus having no frontal tract, is this condition derived from a developmental process which brings the medulla terminalis closer to the brain and leads to the reduction of the frontal tract?

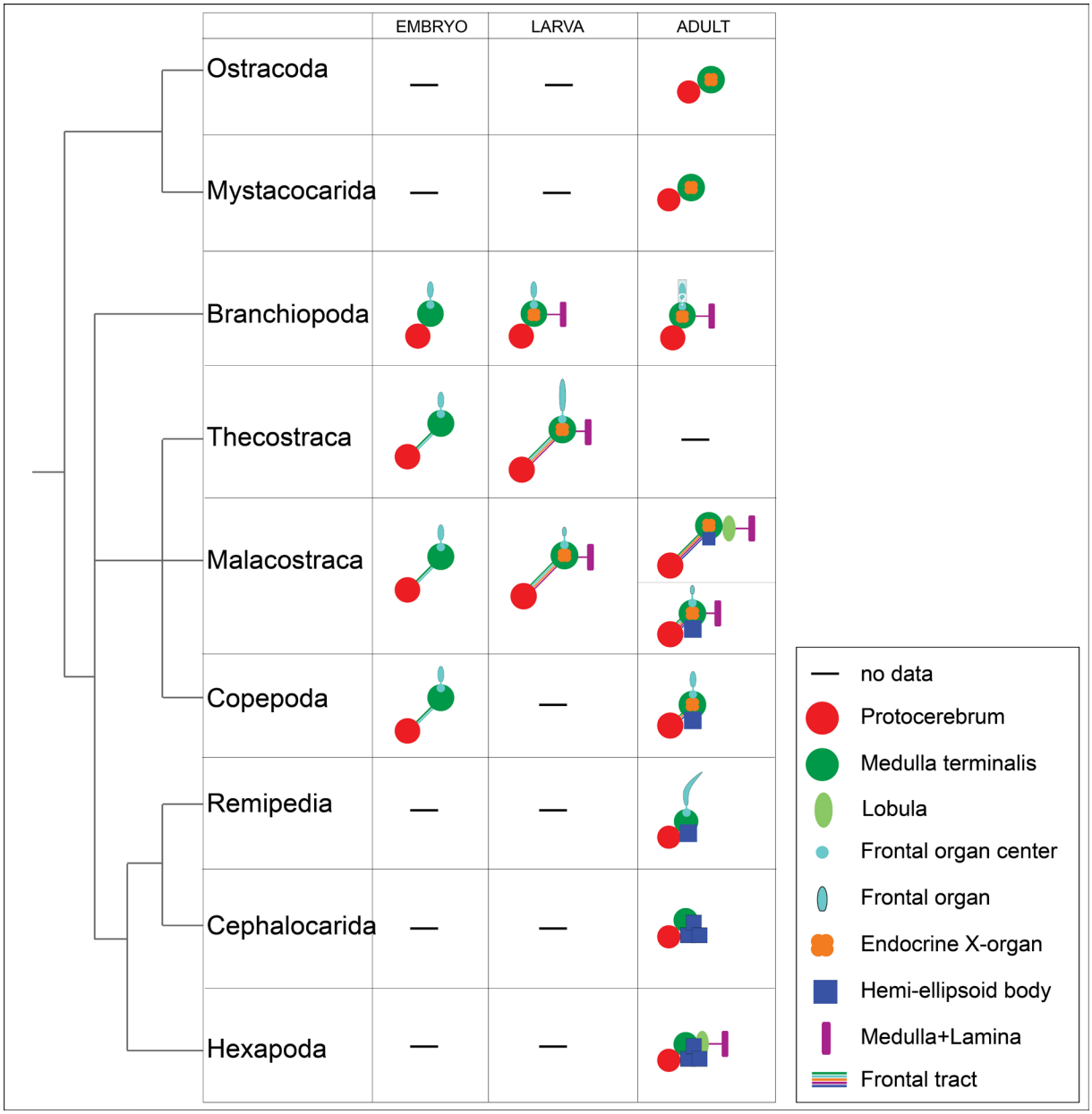

Fig. 85 – Distribution of the characters associated with the medulla terminalis in Pancrustacea

The taxa are ordered following the phylogeny of the Pancrustacea according to the tree proposed by Giribet and Edgecombe (2010) (on the left). In the columns, the architecture of the structures is schematized as it occurs during development (embryonic and larval stages) and in the adult.

The variability in the external morphology of the frontal organ is indicated by a different size of the light blue shape. The different composition of the frontal tract is indicated by the different coloured lines included in the scheme (colour code in agreement with the associated structures).

The hemi-ellipsoid body is represented in cephalocarids by multiple blue-squares to indicate the complex multilobed system described in this group (e.g. Stegner and Richter 2011). In hexapods, the same representation (multiple blue-squares) is used to identify the entity of the mushroom body. The medulla terminalis and the hemi-ellipsoid body of crustaceans are considered as homologous to the lateral horn and the mushroom body of hexapods, respectively (see for discussion e.g. Strausfeld 2009; Stegner and Richter 2011; Sandeman et al. 2014; Kress et al. 2016). The lobula of malacostracans and hexapods is homologous (e.g. Strausfeld and Nässel 1981; Harzsch 2002b; Sinakevitch et al. 2003).

2_The frontal organ and the frontal organ center

As reported above, the frontal organs of malacostracans and cirripeds are homologous structures which occur at different stages of development and, sometimes, in the adult of different species. Moreover, the present study suggests the presence of the frontal organ in the ground pattern of the Copepoda which is suggested by a closer analysis of some developmental data (see above). Moreover, adult copepods have a number of different apical sensory organs (e.g. Dudley 1972; Piasecki and MacKinnon 1993, Klann 2008) which correspondence and homology is not clear, however, the homology between specific part of an adult copepod's apical organ and the cirriped's frontal organ ("*frontal filaments*") (Hanström 1924b; Hanström 1928; Dahl 1953; Elofsson and Lake 1971). If we assume that the "*frontal filaments*" of branchiopods and of remipeds are homologous to the frontal organs described here we could trace back the presence of these organs to the Altocrustacea, claiming the convergent loss of the character in cephalocarids and hexapods.

Moreover, the present study shows that the anlage of the medulla terminalis is represented by a small cluster of cells, the frontal organ center. How did the medulla terminalis developed in the common ancestor of the Pancrustacea? Again we can only speculate a hypothetical appealing scenario of a nauplius larva common ancestor equipped with a simple sensory frontal organ associated to its sensory center (the frontal organ center), i.e. the anlage of the medulla terminalis connected to the protocerebrum. The frontal organ might have got lost during development while the medulla terminalis differentiated, for instance, into an endocrine organ, like it is the case in the Mystacocarida which presumably carry plesiomorphic features.

3_The hemi-ellipsoid body

The hemi-ellipsoid body is a secondary center integrating olfactory inputs and it occurs in representative of all the Altocrustacea (e.g. Copepoda: Andrew et al. 2012; Malacostraca: Sullivan and Beltz 2004; Remipedia: Fanenbruck and Harzsch 2005; Cephalocarida: Stegner and Richter 2011). The crustacean hemi-ellipsoid body have been proposed as homologous to a certain extent to the mushroom body of hexapods (see for discussion e.g. Strausfeld 1998; Stegner and Richter 2011). In this scenario, the Thecostraca and the Branchiopoda may have lost the hemi-ellipsoid body convergently.

Interestingly, in the evolution of Decapoda, the medulla terminalis is the most important neuropil in integrating second olfactory input in lower decapods, and its importance is

gradually lowered in favour of the hemi-ellipsoid bodies in higher decapods (Mynard and Yager 1968; Blaustein et al. 1988; Sullivan and Beltz 2004). Moreover, in species with highly reduced visual systems, the medulla terminalis takes over the function of a second order olfactory center completely and, the loss of visual input is compensated by a notable enhancement of the olfactory or mechano-sensory pathways or other part of the nervous system (Fanenbruck and Harzsch 2005; Aramant and Elofsson 1976; Stegner et and Richter 2011, 2015). If we include the presence of the frontal organs in species with reduced vision (see above) we may think of a mutual exclusive mechanism of centers connected to the medulla terminalis regulated by genetic switch on/off systems.

4_The visual neuropils

The plesiomorphic type of the eye in crustaceans and hexapods has been extensively discussed in the past (e.g. Hessler and Newman 1975; Bowman 1984; Elofsson 1992; Melzer et al. 1997, 2000; Harzsch and Waloszek 2001; Harzsch 2002b; Wildt and Harzsch 2002; Strausfeld 2005; Kress et al. 2016) and is still under debate (see e.g. Oakley 2003 for multiple origin (phylogenetic homoplasie) of the compound eyes in Crustacea). If we consider the occurrence of the medulla+lamina we can trace back their presence in the common ancestor of the Altocrustacea with the convergent loss in copepods and xenocarids. In this view we accept the absence of a compound eye in the ground pattern of ostracods as strongly advocated by some authors (e.g. Oakley and Cunningham 2002; Oakley 2003).

5_The endocrine organs

The presence of an endocrine organ associated to the medulla terminalis is part of the ground pattern of the Pancrustacea and looks like being a plesiomorphic character lost during evolution in the more derived taxon including the Xenocarida and the Hexapoda (i.e. the Miracrustacea). Ostracods and mystacocarids have a distinguished apical organ known as organ of Bellonci (e.g. Kauri 1962; Andersson 1977; Brenneis and Richter 2010). In particular, mystacocarids bear a massive organ of Bellonci, which resembles in its histology the same as described for decapods (they have so called “onion bodies”). The homology of this organ with the organ of Bellonci of malacostracans has been doubted since no clear innervation has been detected connecting the organ to the brain (Brenneis and Richter 2010). However, we know that in decapod brachyurans the corresponding neuro-secretory organ is an integral part of the ganglionic cell layer (Pyle 1943). The reduction of the axonal tract

between the brain and the organ of Bellonci in mystacocarids could have happened in development as the consequence of the increased mass of the endocrine organ (as observed in amphipods, see above).

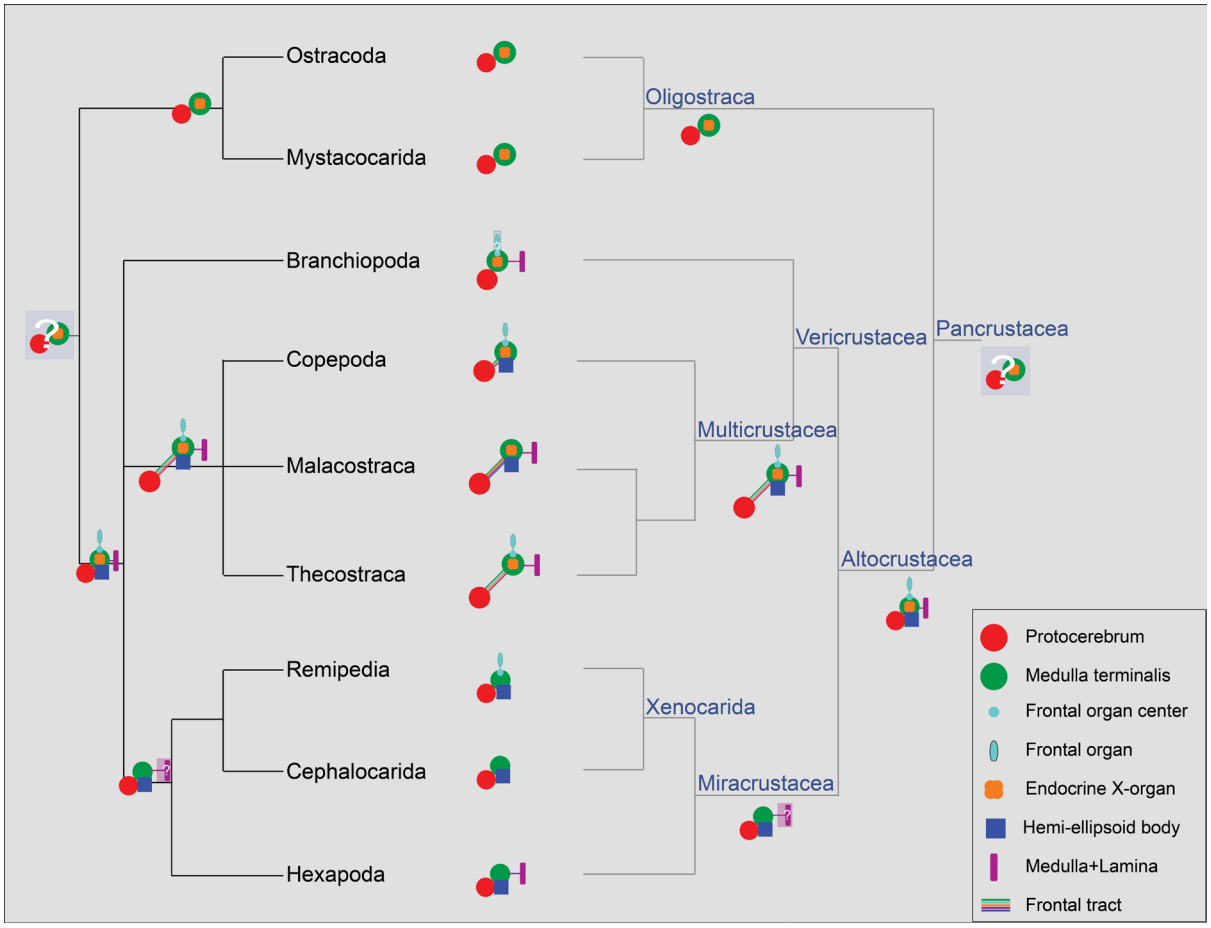

Fig. 86 – Evolutionary scenarios based on the distribution of the structures associated with the medulla terminalis (simplified)

The distribution of the elements associated with the medulla terminalis of the various crustacean groups is mapped on the consensus of arthropod phylogenetic relationships adopted from Giribet and Edgecombe (2010) (tree on the left) and from Regier et al. (2010) (tree on the right).

4.3 The development of the Stomatogastric Nervous System (SNS) and its connection to the brain: new insights from a simple developmental pattern

4.3.1 The morphology of the stomatogastric nervous system of crustaceans

The stomatogastric nervous system is probably the crustacean motor system which has been most widely studied (for a review see Harzsch et al. 2012). In particular, adult morphology of the stomatogastric nervous system in malacostracan crustaceans has been extensively documented by descriptions of the synaptic circuits (e.g. Maynard 1972; Selverston et al. 1976; Mulloney 1977; Böhm et al. 2001; Heinzel et al. 2002) and localization of identified neurons (e.g. Kushner and Maynard 1977; Kushner 1979; Claiborne and Selverston 1984; Tirney et al. 1999). Surprisingly, however, the developmental data of such well-known system are scattered, performed with the use of different techniques, and often presented with the adoption of an inconsistent nomenclature. Developmental studies have been performed mainly in representatives of decapods (e.g. Casasnovas and Meyrand 1995; Fenelon et al. 1998; Kilman et al. 1999; Vilpoux et al. 2006); we also have some data on stomatopods (Fischer 2006) and peracarids (Ungerer et al. 2011). Recently, with the advance of immunohistochemical techniques, morphological studies on the nervous system of non-malacostracans have refreshed our knowledge of the SNS architecture of this group, both in adult and developmental stages in different representatives (Branchiopoda; Harzsch and Glötzner 2002; Kirsch and Richter 2007; Fritsch and Richter 2010; Cephalocarida: Stegner and Richter: 2011; 2015; Mystacocarida: Brenneis and Richter 2010; Remipedia: Fanenbruck et al. 2004; Fanenbruck and Harzsch 2005), and some have attempted to determine homologies with the malacostracans (e.g. Kirsch and Richter 2007; Brenneis and Richter 2010; Stegner and Richter 2011, 2015).

The morphology of the stomatogastric nervous system of malacostracans

Despite some differences in the use of terminology, there is a certain agreement in the identification of the main components of the stomatogastric nervous system in adult malacostracans. The same lay-out as in adults is reached pretty early in development (Casasnovas and Meyrand 1995; Fenelon et al. 1998; Vilpoux et al. 2006), in concomitance with the formation of the foregut (Helluy and Beltz 1991). This architecture consists of four

main neurite bundles, and three ganglia. The neurite bundles include two unpaired median nerves: the inferior ventricular nerve, and the stomatogastric nerve, also called the recurrent nerve (e.g. Henry 1948; Sandeman et al. 1992); and two paired transversal nerves: the inferior esophageal nerve, also called the frontal commissure (Chaudonneret 1978) or alternatively, labral commissure due to its connection with the labral nerves (e.g. Henry 1948; Sandeman et al. 1992), and the superior esophageal nerve, also called the stomodeal nerve (e.g. Henry 1948). The ganglia include two median unpaired ganglia: the esophageal ganglion, also called "*primary stomodeal ganglion*" or "*frontal ganglion*" (Chaudonneret 1978), and the stomatogastric ganglion; and one paired lateral commissural ganglion. The inferior ventricular nerve connects the esophageal ganglion anteriorly to various regions of the brain (e.g. Böhm et al. 2001). The stomatogastric nerve runs along the dorsal wall of the stomodeum spanned between the stomatogastric ganglion, on the dorsal side of the stomodeum, and the esophageal ganglion above the entrance of the mouth. The inferior and superior esophageal nerves run out from the lateral commissural ganglion towards the midline. However, some studies describe these neurites both meeting their contralateral counterpart at the esophageal ganglion (e.g. Maynard and Dando 1974; Selverston et al. 1976) while others recognize only the inferior esophageal nerve as being medially connected to the esophageal nerve, while the superior esophageal nerve intersects the stomatogastric nerve separately (e.g. Böhm et al. 2001; Heinzel et al. 2002; Skiebe 2003). In this case, there is a short median nerve interposed between the inferior and the superior esophageal nerves, generically called by some authors the "*oesophageal nerve*" (e.g. Skiebe 2003). Moreover, some authors recognize two different portions, or units, of the esophageal ganglion, one anterior at the intersection of the inferior ventricular nerve with the inferior esophageal nerve, and one posterior at the intersection of the stomatogastric nerve and the superior esophageal nerve (Henry 1948; Chaudonneret 1978; Kushner 1979). Eventually, the esophageal ganglion was defined as the region of median cell bodies between the superior and inferior esophageal nerves and the variability observed among different species is interpreted as the different the degree of condensation and different location of the neural units (Maynard and Dando 1974).

For the first time, the present study shows a continuous sequence of development of the main components building the anlage of the SNS in three malacostracan species, and identifies single ontogenetic units which are possibly homologous among the species, offering a consistent nomenclature for a comparison with the former studies and shedding some new light on our understanding of the SNS architecture.

4.3.2 The developmental pattern of the stomatogastric nervous system in the three investigated species

In line with previous studies, the anlage of the SNS forms early in development in the three investigated species. Moreover, the present study underlines that the formation of its axonal scaffold happens in concomitance with the protrusion of the labrum, on one hand, and with the invagination of the stomodeum, on the other. The observation of the gradual addition of neural elements leads to the identification of a developmental pattern common to the three investigated species, with minor variation. This consists of two phases: firstly, the formation of the axonal scaffold obtained with the branching of the first axons, and their pioneer neurons which are referred to here as the primary axonal scaffold; secondly, the addition of neural elements, axons and neurons: the first reinforce the primary scaffold and connect the SNS to the brain, while the second lead to the formation of the ganglia.

The development of the primary axonal scaffold

The primary axonal scaffold is constituted by the branching pattern of two parallel systems of neurites which develop quite simultaneously: one, more ventral and associated with the labrum, includes the anlage of the inferior ventricular nerve and of the labral commissure; the other, more dorsal and associated with the stomodeum, includes the anlage of the stomatogastric nerve and of the stomodeal commissure. Only few neural cell somata are observable at this time. These correspond to: 1) the pioneer neurons of the inferior ventricular nerve, underneath the pre-oral commissure, which form the protocerebral median cell cluster; 2) the pioneer neurons of the stomatogastric nerve on the dorsal wall of the stomodeum, which constitute the anlage of the stomatogastric ganglion; 3) the lateral pioneer neurons of the labral commissure and of the stomodeal commissure at the ventro-lateral side of the stomodeum, which represent the anlage of the commissural ganglion (Fig. 87).

The development of the nervous system associated with the labrum

The inferior ventricular nerve anlage forms as a median neurite bundle spanned between the protocerebral median cell cluster and the proximal margin of the labrum. Distally it branches laterally along the proximal rim of the labrum and contributes to the formation of the labral commissure. The labral commissure anlage is thus composed of the lateral branches of the inferior ventricular nerve, and of the paired neurite bundle running from the commissural ganglion to the midline, into the inferior ventricular nerve (Fig. 87). The commissural

ganglion anlage is composed of a small number of neurons ventrally flanking the stomodeum. The labral commissure thus arises as a transversal neurite bundle running along the proximal edge of the labrum between the contra-lateral commissural ganglia, medially intersecting the inferior ventricular nerve without the interposition of any cell soma.

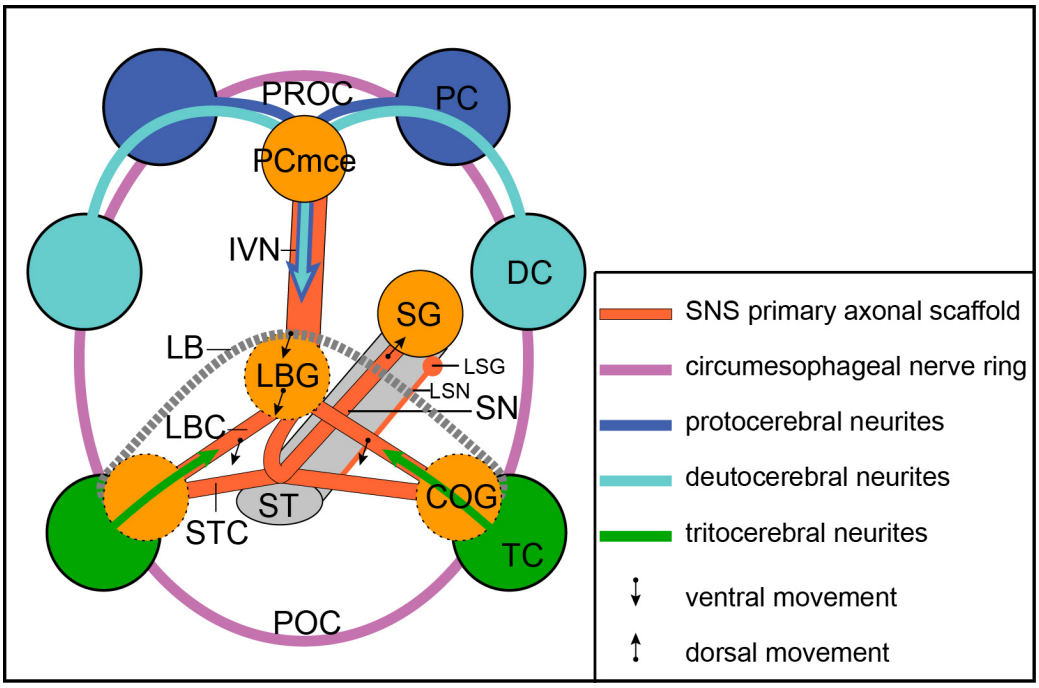

Fig. 87 – Schematic representation of the SNS developmental pattern and of the connection of the SNS to the brain

Overiew of the main components of the brain (ventral view) and of the stomatogastric nervous system (ventro-lateral view). The grey cylinder represents the anlage of the digestive tube. The grey line marks the distal margin of the labrum anlage. The coloured circles represent the brain neuromeres (i.e. blue: the protocerebrum; light blue: the deutocerebrum; green: the tritocerebrum). The orange circles represent the anlage of the ganglia of the SNS. The circles marking the LBG and the COG are surrounded by a broken line to indicate their relative delay in development. Only one of the two LSN is included in the scheme. The primary axonal scaffold of the SNS is composed of two median unpaired nerves, i.e. the IVN and the SN, and two transversal neurite bundles, i.e. the LBC and the STC. The SN runs from the SG on the dorsal wall of the digestive tube to the ventral stomodeal opening. Here, it turns to the anterior to meet the IVN. The LSN runs in parallel to the SN on the lateral side of the digestive tube and ventrally intersects the STC. The LBG is visible in the proximal margin of the labrum, at the intersection of the IVN, the SN and the LBC in a relative later time of development. In the same way, the COG is recognized as flanking the TC at a relatively later time of development of the SNS. The axons from the brain, indicated by the coloured arrows, enter the circuit only after the establishment of the primary axonal scaffold of the SNS. As a consequence of the ventral protrusion of the LB, the LBG moves into a more postero-ventral position than the one represented by the scheme. It follows, on one hand that the IVN elongates and, on the other hand that the LBC also moves postero-ventrally resulting, from a ventral view, in a more inferior position than the STC. As a consequence of the elongation of the digestive tube (invagination of the stomodeum), the SG and the LSG get into a more postero-dorsal position than the one represented in the scheme. It follows that the SN and the LSN elongate.

COG: commissural ganglion; DC: deutocerebrum; IVN: inferior ventricular nerve; LB: labrum; LBC: labral commissure; LBG: labral ganglion; LSG: lateral stomatogastric ganglion; LSN: lateral stomatogastric nerve; PC: protocerebrum; PCmce: protocerebral median cell cluster; POC: post-oral commissure; PROC: pre-oral commissure; SG: stomatogastric ganglion; SN: stomatogastric nerve; ST stomodeum; STC: stomodeal commissure; TC: tritocerebrum.

The development of the nervous system associated with the stomodeum

The stomatogastric nerve anlage is a median neurite bundle spanning between the stomatogastric ganglion anlage and the anterior margin of the stomodeum running along the dorsal midline of the digestive tube. Here, it branches laterally and contributes to the formation of the stomodeal commissure. The stomatogastric nerve runs further ventrally and turns anteriorly to connect the distal tip of the inferior ventricular nerve (Fig. 87), without the interposition of any neural soma. The stomatogastric ganglion anlage is represented by a small number of pioneer neurons at the distal dorso-medial margin of the digestive tube. Hence, the stomodeal commissure anlage is composed of the lateral branches of the stomatogastric nerve and of the paired neurite bundle running from the commissural ganglion to the midline into the stomatogastric nerve. Eventually, the stomodeal commissure emerges as a transversal neurite bundle, which ventrally surrounds the antero-dorsal margin of the stomodeum and medially intersects the stomatogastric nerve without the interposition of any cell soma.

The connection of SNS with the brain and the formation of the ganglia

Two developmental events characterize the second developmental phase of the SNS: on one hand, the labrum protrudes ventro-posteriorly; on the other hand, the stomodeum invaginates dorsally and folds posteriorly. As a consequence: the labral commissure moves postero-ventrally and the inferior ventricular nerve stretches ventrally, while the stomatogastric ganglion shifts postero-dorsally and the stomatogastric elongated dorsally. At this time, the increasing number of neurites reinforces the neurite bundles while the increasing number of neurons enriches the ganglion anlagen. Neurites from the brain now also contribute to the SNS scaffold: anteriorly via the inferior ventricular nerve through the protocerebral median cell cluster, and posteriorly via the labral and stomodeal commissures through the commissural ganglion (Fig. 87). Moreover, in the distal portion of the growing labrum, the sensory centers start to send the labral nerves into the labral commissure, while, on the dorsal wall of the stomodeum, laterally to the stomatogastric ganglion, a small paired lateral cluster of neurons send ventrally the lateral stomatogastric nerve which runs in parallel to the stomatogastric nerve and join the stomodeal commissure. Finally, the volume of the commissural ganglion visibly increases while new cell somata are recognized at the intersection of the inferior ventricular nerve with the stomatogastric nerve and the labral

commissure, medially at the proximal edge of the labrum, forming the anlage of the labral ganglion (Fig. 87).

4.3.3 Some clarification on the nomenclature and the identification of developmental units

In the light of the developmental pattern described here, the nomenclature in use for some structures has been revisited in an attempt to clarify their identification and to simplify comparisons among different species (see the *Glossary* below). The former nomenclature was mainly based on the identification of the stomatogastric motor neurons by reference to the muscles they innervate in the adult specimens (e.g. Maynard and Dando 1974) or by reference to a generic relative position among the sub-structures (e.g. Chaudonneret 1978). However, this leads to the incomplete identification of some structures and these may also be sometimes inconsistent in the light of the ontogenetic evidence underlined by the present study. These include: the actual location of those neural elements in relation to the associated structures (i.e. the anatomy) during development, the mixed composition of the neurite bundles and their variable mutual position during development. For instance, the labral commissure identifies the transversal neurite bundle, which intersects the inferior ventricular nerve, connects the commissural ganglion to the labral ganglion and receives the labral nerves. The labral commissure identifies the former "*inferior esophageal nerve*" or "*frontal commissure*". The stomodeal commissure identifies the neurite bundle which connects the stomatogastric nerve to the commissural ganglion and, in some cases, receives the lateral stomatogastric nerves. The stomodeal commissure was identified by the former term "*superior esophageal nerves*". The labral ganglion is that cluster of cells which grows at the intersection of the inferior ventricular nerve, the stomatogastric nerve and the labral commissure and is preferred to the terms "*esophageal ganglion*" or "*frontal ganglion*".

As the present study demonstrates, those three structures have a specific anatomical topology during development: the stomodeal commissure is associated with the stomodeum, while the labral commissure and the labral ganglion are associated with the labrum. Thus, the generic nomenclature referring to the esophagus as it appears in adulthood is discouraged for being inconsistent and creating confusion in the identification of these structures. Moreover, the identification of the mixed composition of the two transversal neurite bundles as underlined by the present study reveals that the former nomenclature only partially describes the actual composition of the two transversal neurite bundles. The labral commissure and the stomodeal

commissure are, in fact, composed of neurites not only coming from the lateral commissural ganglion to the midline, which alone would describe the former paired nerves (i.e. "*inferior*" and "*superior*" "*esophageal nerve*"), but also of the lateral branches of the inferior ventricular nerve and of the stomatogastric nerve to the commissural ganglion, and, later in development, of the neurites projecting from the brain. In this respect, to refer to these structures as lateral paired nerves as in the former studies, only partially describes the actual composition of the neurite bundles considered here and it is once more discouraged by the present study. Finally, for the first time in the present study it is observed that the position of the labral commissure relative to the position of the stomodeal commissure changes during development: after all, the choice of a nomenclature which refers to the position of the neurite bundles relative to one another, i.e. "*inferior*" and the "*superior*" is revealed semantically incomplete.

Comparison with the study by Vilpoux et al. (2006)

For a better understanding of the developing scaffold of the stomatogastric nervous system a comparison between the data on the crayfish *P. fallax* offered by Vilpoux et al. (2006) and the present study is provided here (Fig. 88; Table 9).

At Vilpoux et al.'s 60% stage which corresponds to stage 5 in the present study, the main structures of the axonal scaffold of the SNS have already reached the adult position. From a ventral view, the labral commissure ("*inferior esophageal nerve*") is located in a more posterior position relative to the stomodeal commissure ("*superior esophageal nerve*") (Fig. 88). However, the present study reveals that the labral commissure is clearly more ventrally positioned than the stomodeal commissure (which lies dorsally on the stomodeum) and, as discussed above, it is more posterior (or more inferior) relative to the stomodeal commissure (thus, more superior) (Fig. 88) as the result of the protrusion and posterior bending of the labrum at this stage of development. This is visible thanks to the 3-dimensional reconstruction of the neural structure arrangement in consecutive developmental sequences as offered by the render images offered by present study, while the 2-dimentional visualization of one single stage as shown in the former study (Vilpoux et al. 2005) could not resolve the issue. In fact, at the earlier stage of its development, the labral commissure ("*inferior esophageal nerve*") actually has a more anterior position than the stomodeal commissure ("*superior esophageal nerve*"). Thus, from a ventral view, the labral commissure has a location 'superior to' the stomodeal commissure, and the stomodeal commissure has a location 'inferior to' the labral commissure, which is manifestly incongruent with the former nomenclature. The present

study shows that, in the later stages of development, the labral commissure moves ventro-posteriorly following the protrusion of the labrum while the stomodeal commissure remains in loco above the ventral margin of the prospective mouth (while the stomodeum invaginates dorsally). Therefore, the labral commissure acquires a more 'inferior' location relatively to the stomodeal commissure only at a later stage of development. This is the final position of the two transversal neurite bundles. Such an arrangement is the only one which has been observed in the past and justifies the use of the former nomenclature, which becomes obsolete in the light of the present data.

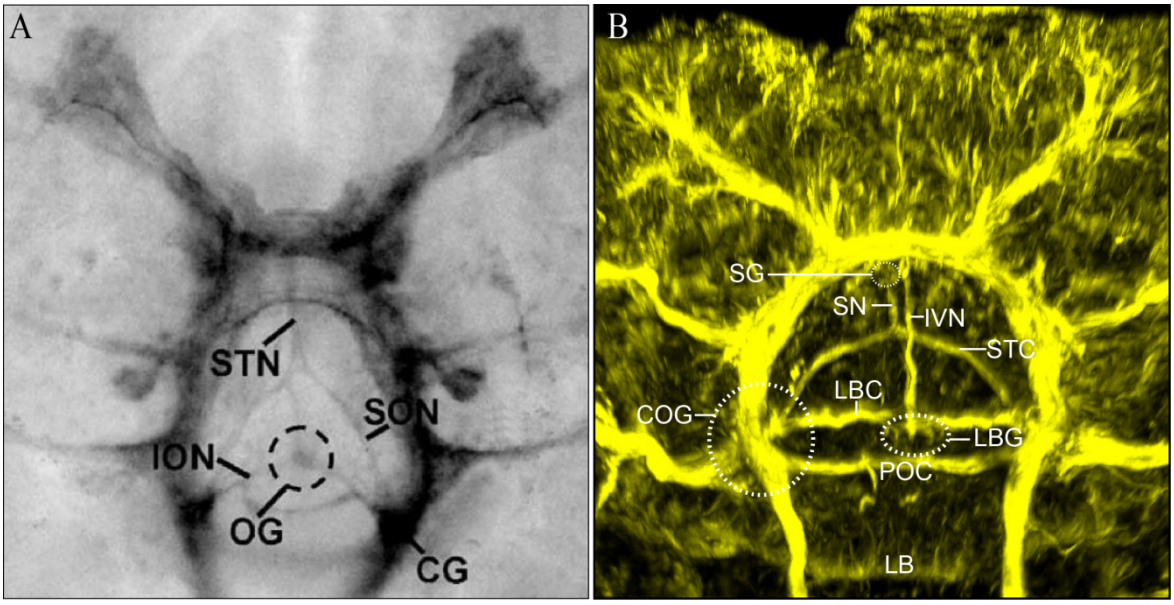

Fig. 88 – Comparison of SNS architecture in the marbled crayfish *P. fallax* stained with use of different techniques at a comparable developmental stage

A - Ventral view of the SNS (modified from Vilpoux et al. 2006). The Synapsin-labelling shows the commissural ganglion giving rise to the inferior and the "*superior oesophageal nerves*". The two branches of the "*inferior oesophageal nerve*" meet medially and target the "*oesophageal ganglion*". The two branches of the "*superior oesophageal nerves*" meet medially and form the stomatogastric nerve (Vilpoux et al. 2006). **B -** Present study. The α-tubulin labelling shows that the labral commissure is spanned between the commissural ganglion at the proximal margin of the labrum. The labral commissure intersects medially the inferior ventricular nerve where the anlage of the labral ganglion is forming. The stomodeal commissure is spanned between the commissural ganglion on the dorsal surface of the stomodeum and meets medially the stomatogastric nerve. The stomatogastric nerve runs on the dorsal wall of the digestive tube, from the dorsal stomatogastric ganglion. Following the perspective of the picture, the labral commissure and the inferior ventricular nerve, associated with the labrum (LB), are located in a more ventral position than the stomodeal commissure and the stomatogastric nerve. The post-oral commissure (POC) is located in a more dorsal position than the labral commissure and the labral ganglion. See **Table 9** for a review on the nomenclature.

In summary, the present study shows that the anlage of the SNS arises as a composition of the branching pattern of axons, which firstly form an axonal scaffold, i.e. the primary axonal scaffold, while the formation of the ganglia and the connection to the brain is a subsequent

event. In this way, the labral commissure ("*inferior esophageal nerve*") and the stomodeal commissure ("*superior esophageal nerve*") do not meet each other. In further development, the labral commissure alone meets the labral ganglion. The differences described in some adult samples may be due to variability among different species. Alternatively, if we considered the developmental pattern described here as a putative part of the ground pattern of malacostracans, these might be interpreted as the consequence of the following developmental changes which are not included in the present study.

Vilpoux et al. 2006	Present study
CG: commissural ganglion	COG: commissural ganglion
X	IVN: inferior ventricular nerve
ION: inferior oesophageal nerve	LBC: labral commissure
OG:oesophageal ganglion	LBG: labral ganglion
X	SG: stomtogastric ganglion
STN: stomatogastric nerve	SN: stomatogastric nerve
SON: superior oesophageal nerve	STC: stomodeal commissure

Table 10 – Comparison between the nomenclature adopted in the development of the SNS of *P. fallax* in the previous study by Vilpoux et al. (2006) and the present study

Moreover, the primary axonal scaffold as described in the present study includes direct synapses between axons i.e. between the inferior ventricular nerve and the stomatogastric nerve without the interposition of cell somata. This might correspond to the two "*ivn through fibers*" described in adult decapods, through which the inferior ventricular nerve regulates the inputs both of the gastric mill and of the pyloric apparatus (Dando and Selverston 1972; Russell and Hartline 1981; Sigvardt and Mulloney 1982; Harris-Warrick and Nagy 1992; Heinzel et al. 2002). These show a branching pattern with axons running into the labral into the commissural ganglion via the labral commissure ("*inferior esophageal nerve*") and the stomodeal commissure ("*superior esophageal nerve*"), and to the stomatogastric ganglion via the stomatogastric nerve (Kushner 1979; Hedrick et al. 2011) and have integrative regions in the labral ganglion (Selverston et al. 1976). Eventually, in this respect, there is no additional nerve connecting the labral commissure to the stomodeal commissure such as the

"*oesophageal nerve*", *sensu* e.g. Skiebe (2003), which is actually shown to be the antero-ventral prolongation of the stomatogastric nerve.

Glossary

The definitions of the main components forming the anlage of the SNS are listed below in alphabetical order.

Commissural Ganglion (COG). A pair of lateral cell clusters formed on the stomodeum wall. It includes the pioneer neurons of the stomodeal commissure and of the labral commissure. It fuses with the tritocerebral ganglion during development. Other terms: none.

Inferior Ventricular Nerve (IVN). A median neurite bundle spanned between the protocerebral median cell cluster and the labral ganglion. It has lateral branches which connect the commissural ganglion. It connects the labral ganglion to the anterior brain (proto- and deutocerebrum). It is formed by neurites from the protocerebral median cell cluster and by proto- and deutocerebral neurites running into the labrum and the stomodeum. It collects the lateral projections of the labral commissure from the commissural ganglion. It extends following the protrusion of the labrum. Other terms: nervus connectivus.

Labral Commissure (LBC). A transversal neurite bundle spanning between the commissural ganglion and the labral ganglion. It is associated with the labrum. It connects the labral ganglion to the tritocerebrum. It is formed by the ventrolateral branches of the inferior ventricular nerve and by neurites from the commissural ganglion. It connects the labral nerves. It moves ventro-posteriorly following protrusion of the labrum during development. Other terms: inferior esophageal nerve, esophageal commissure; frontal connective; frontal commissure; visceral commissure.

Labral Nerve (LBN). It is a paired lateral neurite bundle in the labrum. It spans between the sensory cell cluster of the labrum and the labral commissure. It is putatively a sensory nerve. Other terms: none.

Labral Ganglion (LBG). A medio-ventral cell cluster. It is associated with the labrum and is the main site of intersection of the SNS with the CNS. It receives the inferior ventricular nerve, the stomatogastric nerve, and the labral commissure. It moves ventrally following the protrusion of the labrum during development. Other terms: esophageal ganglion; labral ganglion; labral neuropil.

Lateral Stomatogastric Ganglion (LSG). A lateral paired cell cluster on the dorsal wall of the digestive tube. It is located laterally to the stomatogastric ganglion and moves posteriorly following the elongation of the digestive tube during development. It contains the pionner neurons of the lateral stomatogastric nerve. Other terms: none.

Lateral Stomatogastric Nerve (LSN). A lateral paired neurite bundle spanning between the lateral stomatogastric ganglion and the stomodeal commissure. It runs along the dorso-lateral wall of the digestive tube and elongates during development due to the extention of the digestive tube during development.

Protocerebral median cell cluster (PCmce). A median cluster of cells located below the pre-oral commissure. It includes the pioneer neurons of the inferior ventricular nerve. Other terms: median cell cluster.

Stomatogastric Ganglion (SG). A medio-dorsal cell cluster on the wall of the digestive tube. It includes the pioneer neurons of the stomatogastric nerve. It moves posteriorly following the elongation of the digestive tube during development. Other terms: none.

Stomatogastric Nerve (SN). A median neurite bundle spanning between the stomatogastric ganglion and the labral ganglion running along the dorsal wall of the digestive tube. It has lateral branches which connect the commissural ganglion. It is formed by neurites of the stomatogastric ganglion and collects the lateral projections of the stomodeal commissure from the commissural ganglion. It extends following the elongation of the digestive tube. Other terms: stomatogastric neurite bundle; dorsal fiber bundle; recurrent nerve.

Stomodeal Commissure (STC). A transversal neurite bundle spanned between the commissural ganglion and the stomatogastric nerve. It is associated with the stomodeum. It is formed by the ventrolateral branches of the stomatogastric nerve and neurites from the commissural ganglion. It receives the lateral stomatogastric nerves. Other terms: esophageal nerve; superior esophageal nerve.

4.3.4 The development of the inferior ventricular nerve in the ground pattern of crustaceans

The inferior ventricular nerve in adult crustaceans connects the SNS to different areas of the brain (e.g. Böhm et al. 2001; Bitsch and Bitsch 2010; Harzsch et al. 2012) and is responsible for the regulation of the inputs both from the gastric mill and the pyloric apparatus (see above). The occurrence of this delicate structure running from the anterior brain into the SNS

has been recently acknowledged to be more widespread among Crustacea then it was supposed in the past (e.g. Brenneis and Richter 2010). The present study shows that, together with the stomatogastric nerve, the inferior ventricular nerve is the first axonal projection of the SNS to develop. This is a novelty if we compare with former studies on other malacostracans. Those performed with stainings different from α-tubulin do not document the presence of the inferior ventricular nerve in the early developmental stages. In the lobster *H. gammarus*, for instance, the inferior ventricular nerve is not stained by the neurotransmitters FRF-amide and proctolin in the early embryonic stages, but it is stained in the hatched larva (Fenelon et al. 1998). The expression of specific neurotransmitters such as FLRF-amide and proctolin might not been expressed by a certain neural structure at the given time of development but this does not exclude the presence of the structure itself. The inferior ventricular nerve may already be formed in the *H. gammarus* embryo but may not express the given neurotransmitters. Moreover, the inferior ventricular nerve is not detected by synapsin in the marbled crayfish at the embryonic stage described by Vilpoux et al. (2006) (Fig. 88). As documented by the present study, the inferior ventricular nerve is brightly stained at this stage (Fig.87) and the expression of synaptic proteins at this point is expected. I would suggest two possible reasons for this. 1) A perspective based reason: the absence of the inferior ventricular nerve in the study of Vilpoux et al. (2006) might be explained as the consequence of an optical overlapping of the inferior ventricular nerve and the stomatogastric nerve which lie in parallel one above the other and in close proximity, as documented by the present study, and from a ventral view, as shown in the picture by Vilpoux et al. (2006), could not be distinctively recognized (Fig. 88). Instead, the two nerves are clearly observable as two separate structures in the 3-dimensional visualization offered in the present study, where with a slight turn to the lateral side of the render image the two structures are easily identified (Fig. 88). 2) An artefact-related reason: the *P. fallax* embryos are constituted by thin layers of relatively few cells. The labrum and the stomodeum develop simultaneously and, from the same ventral point of observation, they protrude in opposite directions (i.e. the labrum ventrally, the stomodeum dorsally). The thin axons forming the axonal scaffold of the SNS are delicate structures which can easily be damaged during the preparation of the objects, for example by excessive pressure on the cover glass, which would squeeze the structures one over the other, or by an accidental removal of the protruding labral tissue, which would remove the inferior ventricular nerve.

Interestingly, the inferior ventricular nerve is visibly stained by α-tubulin in the early developmental stages of the amphipod *O. cavimana* (Ungerer at al. 2011) and is clearly one of the first structures to be detected in the development of the SNS of the stomatopod *G. falcatus* (Fischer 2006). Here, however, the author calls it "*stomatogastric nerve*", creating some confusion in the identification of the structure. The "*stomatogastric nerve*", *sensu* Fisher (2006) is a median neurite which runs from the protocerebral commissure postero-ventrally, early in development - i.e. intermediate egg-nauplius - *Stadium des mittleren Einauplius* - Fig. 4A p. 21 in Fischer (2006). This pathway corresponds exactly to the course of the anlage of the inferior ventricular nerve. Moreover, in the following embryonic stage - i.e. late egg-nauplius - *Stadium des späten Einauplius* - Fig.5B p.24 in Fischer (2006), the "*stomatogastric nerve*", *sensu* Fischer (2006), meets a "*triangle shaped structure*", which in my opinion, clearly corresponds to the branching pattern described by the inferior ventricular nerve meeting the labral commissure as shown in the present study. The correspondence of the "*stomatogastric nerve*", *sensu* Fischer (2006), with the inferior ventricular nerve becomes more obvious in the later stages of development of the embryo - i.e. pleopod 3 stage - *Stadium Pleopod 3* - Fig. 13D pp. 42-43 in Fischer (2006), when this nerve intersects ventrally the labral commissure ("*inferior esophageal nerve*").

Outside the Malacostraca, the anlage of the inferior ventricular nerve detected by means of α-tubulin has also been observed in the early developmental stages of copepods (Klann 2008) and cirripeds (Schulz van Endert 2009; Ponomarenko 2014). Moreover, the labral ganglion nerves (lb-GN) described by Fritsch and Richter (2010) very likely represent the anlage of the inferior ventricular nerve (Fritsch, personal communication). These are among the first SNS structures detected by α-tubulin in the early development of the branchiopod *T. cancriformis* (Fritsch and Richter 2010) Although the absence of the inferior ventricular nerve in this taxon has been claimed (Stegner et al. 2014), in my opinion the inferior ventricular nerve is also visibly stained by α-tubulin in the early development of the cephalocarid (Stegner et al. 2015) as shown in Fig. 89.

The present study suggests that the inferior ventricular nerve anlage forms at the very early stages of development of the SNS in a branching pattern which, together with the stomatogastric nerve, forms the primary axonal scaffold. Such priority in development is probably a way of ensuring the connection of the labrum and of the stomatogastric ganglion to the brain, through the inferior ventricular nerve and the stomatogastric nerve, respectively.

4.3.5 The connection of the SNS to the brain

The interpretation of the SNS in relation to the brain plays a crucial role in the "*endless dispute*" (Rempel 1975) on the arthropod head segmentation (e.g. Harzsch 2004; Scholtz and Edgecombe 2006; Bitsch and Bitsch 2010) since the SNS and the labral innervation are assumed to originate in the tritocerebrum (Hanström 1928; Bullock and Horridge 1965; Harzsch 2004). Developmental data on crustaceans have provided some hints as to how to address the subject (Harzsch et al. 1997; Harzsch et al. 1998; Böhm et al. 2001; Harzsch and Glötzner 2002; Vilpoux et al. 2006). In the present study, the connection of the SNS to the brain follows the construction of the primary axonal scaffold. This means that the SNS constitutes a neural network which is autonomous from the brain and, as a whole connects the CNS. This assumption is based on the observation of the development of two fundamental neural centres: the protocerebral median cell cluster and the commissural ganglion. As seen above, the first gives rise to the inferior ventricular nerve, the second collects the lateral branches of the labral commissure and of the stomodeal commissure; and both represent the connection centres of the SNS to the brain.

The protocerebral median cell cluster

The protocerebral median cell cluster is observed in the two representatives of decapods in the present study and contains the pioneer neurons of the inferior ventricular nerve. The presence of a small median cell cluster visibly stained by α-tubulin underneath the pre-oral commissure, pioneering the inferior ventricular nerve in the early stages of development, has been observed in the amphipod *O. cavimana*. This is called the "*median cell cluster*" (Ungerer et al. 2011) and is proposed as homologous to the protocerebral median cell cluster described in the present study. The presence of two interneurons specific to "*ivn through fibers*" has previously been identified in adult malacostracans (Dando and Selverston 1972; Sigvardt and Mulloney 1982; Claiborne and Selverston 1984; Cazalets et al. 1987; Böhm et al. 2001; Christie et al. 2004). These neurons have been identified as part cluster 17 (*sensu* Sandeman et al. 1992) (e.g. Dando and Selverston 1972). The protocerebral median cell cluster described here might correspond to those neurons as they first appear during neurogenesis.

Interestingly, Rieger and Harzsch (2008) investigated the embryonic development of the histaminergic system of the marbled crayfish and demonstrated the presence of a stained median pair of cell somata posterior to the pre-oral commissure which is connected to a median neurite (in their Fig. 1D and G p. 114 and Fig. 2 p.115) (Fig. 89). Although the

authors do not describe these structures, I would claim they resemble the anlage of the protocerebral median cell cluster and of the inferior ventricular nerve. The protocerebral neuron associated with the "*ivn through fibers*" also expresses histamine in the spiny lobster (Claiborne and Selverston 1984). Moreover, the presence of median protocerebral neurons associated with the development of the inferior ventricular nerve also occurs in cephalocarids. Looking carefully into the data recently provided by Stegner and Richter (2015) on the development of the nervous system of representatives of cephalocarids, the presence of a median nerve connected to a median cell cluster identified by the authors as *s9* (Stegner and Richter 2015) is visibly stained by serotonin (marked by yellow arrows in Fig. 89A) and may be homologous to the inferior ventricular nerve herein described. Unfortunately, the authors do not mention its presence in the text and a careful revision of that data is required in order to confirm my suggestion.

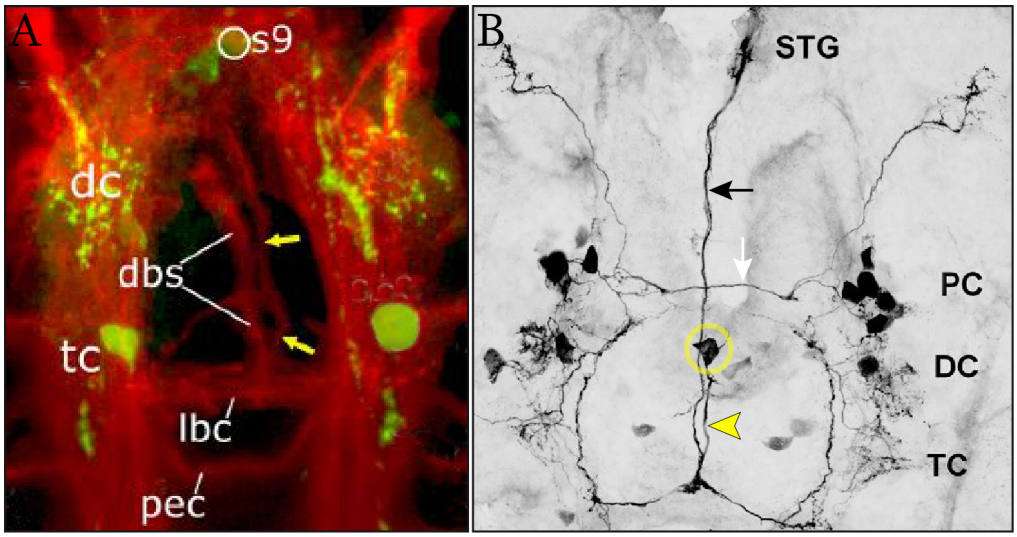

Fig. 89 – The anlage of the SNS stained in a cephalocarid representative and in the marmorkrebs

A – CLSM image stack of the embryonic nervous system in *H. macracantha* (ventral view) (modified from Stegner and Richter 2015 – Fig. 3H). The nervous system is stained by α-tubulin (in red) and by serotonin-like (in green). The "*dorsomedian neurite bundle*" is proposed to be homologous to the stomatogastric nerve in malacostracans. The yellow arrows point to a neurite bundle spanning between the pre-oral commissure and the labral commissure which is suggested to be homologous to the inferior ventricular nerve as described in the present study. The SL-ir neuron 9 might correspond to the protocerebral median cell cluster as described in the present study. **B** – Immunolocalization of histamine in the brain of the Marmorkrebs embryo at 60% of development (ventral view) (modified from Rieger and Harzsch 2008 – Fig. 1D). The yellow circle marks a median histaminergic neuron posterior to the pre-oral commissure (white arrow) which might be part of the protocerebral median cell cluster as observed in the present study. The yellow arrowhead indicates the putative anlage of the inferior ventricular nerve as observed in the present study. The black arrow points at the stomatogastric nerve.

dbs: dorsomedian neurite bundle; DC/dc deutocerebrum; lbc: labral commissure; PC: protocerebrum; pec:post-esophageal commissure; STG: stomatogastric ganglion; s9: SL-ir neuron 9; TC/tc tritocerebrum.

The anlage of the commissural ganglion

The commissural ganglion is considered as a derivative of the tritocerebrum (e.g. Harzsch et al. 1997; Fenelon et al. 1998; Vilpoux et al. 2006) but it has also been proposed that this structure represents the anterior part of the mandibular neuromere (Harzsch et al. 1997; 1998; Harzsch 2004). The very first anlage of the commissural ganglion is observed in the early stages only in *P. fallax*. This is composed of a small number of cells clustered at the lateral side of the stomodeum and its neural projections contribute, firstly to the anlage of the labral commissure, and secondly to the anlage of the stomodeal commissure. In later stages, the commissural ganglion becomes more voluminous and is recognized at the ventral-inner side of the tritocerebral neuromere, dorso-laterally to the proximal margin of the labrum not only in *P. fallax* but also in *P. monodon*. Instead, in *M. norvegica*, the lateral end of both the labral commissure and of the stomodeal commissure seem to fuse together with the connectives of the nerve ring at the level of the tritocerebrum, without the interposition of cell somata. However, the anlage of the commissural ganglion is shown as a small cluster of cells lateral to the stomodeum forming the labral commissure ("*frontal commissure*") also in the amphipod *O. cavimana* (Ungerer et al. 2011), which resembles the early developmental condition observed in *P. fallax* in the present study.

The commissural ganglion, in this respect, would represent an intrinsic ganglion of the SNS independent from the tritocerebrum or from any other central neuromeres, probably arising from the epithelium of the stomodeum and would erase any doubt about a possible dual nature to the tritocerebrum (see Bitsch and Bitsch 2010 for further discussion).

The innervation of the labrum

The anlage of the labrum is innervated by the labral commissure anlage, which is composed of axons of the commissural ganglion and by the lateral branches of the inferior ventricular nerve. Only in a second phase of development does the labral commissure receive projections from the brain and sensory axons from the ventral sensory centers of the labrum. The fact that the commissural ganglion is not a derivative of the tritocerebrum and that the brain contributes to the innervation of the labrum equally with projection from the proto-, deuto- and tritocerebrum, set the anlage of the labrum as a non-segmental appendage (probably sensory) associated with the stomodeum, independent from brain (segments).

In line with previous studies, the present study would offer ontogenetic evidence that the labrum in arthropods is not a pair of appendages of the tritocerebral segment nor the

appendage of a pre-antennal segment (see Scholtz and Edgecombe 2006 for further discussion), but represents an anterior non-segmental outgrowth intimately associated with the foregut and its specific nervous system (Waloszek and Müller 1998; Waloszeck et al. 2005; Scholtz and Edgecombe 2006; Bitsch and Bitsch 2010). The SNS together with the labrum is a morphologically autonomous unit that is not fundamentally affected by head metamerization.

4.4 An overview of the basic scaffold of the nervous system: connectivity among different systems

From the description of the development of the nervous system provided in the present study, it emerges that the nervous system arises as a basic scaffold formed by the interaction of the anlage of three systems: the central nervous system (CNS), the peripheral nervous system (PNS) and the enteric nervous system (ENS) (Fig. 90). The CNS anlage is constituted by the three brain neuromeres, the mandibular and the post-naupliar neuromeres, which are all organized in a metameric arrangement and send their projections (efferents) to the periphery, both to the PNS and to the ENS. The PNS anlage is represented by the peripheral sensory centres and their projections (afferents) sent towards the CNS and the ENS (neuro-muscular PNS is not considered in the present study). The ENS anlage includes the anlage of the stomatogastric nervous system (SNS), associated with the stomodeum, and the anlage of the intestinal nervous system (INS) associated with the proctodeum. These form an intrinsic neural network among the enteric ganglia and are connected to the CNS via specific neural centres. In the earliest developmental stages, the neural projections of those systems form a relatively simple network called the primary axonal scaffold, as represented in Fig. 90.

The CNS, the PNS and the ENS develop in parallel and build the primary axonal scaffold. The SNS and the INS build up their own axonal scaffold (intrinsic) and establish their connection to the CNS. The intrinsic axonal scaffold of the ENS includes the formation of the main neurites involved in the coordination of reflexes to control the gastro-intestinal system, and the afferences from the associated sensory PNS. This is represented by the sensory centres of the labrum in the SNS and by the terminal sensory centres of the telson in the INS. In this view, both the anlagen of the CNS and of the ENS represent two autonomous nervous systems, connected to each other, each equipped by its own sensory apparatus. The sensory PNS develops in parallel by conducting in concert the establishment of the primary axonal scaffold.

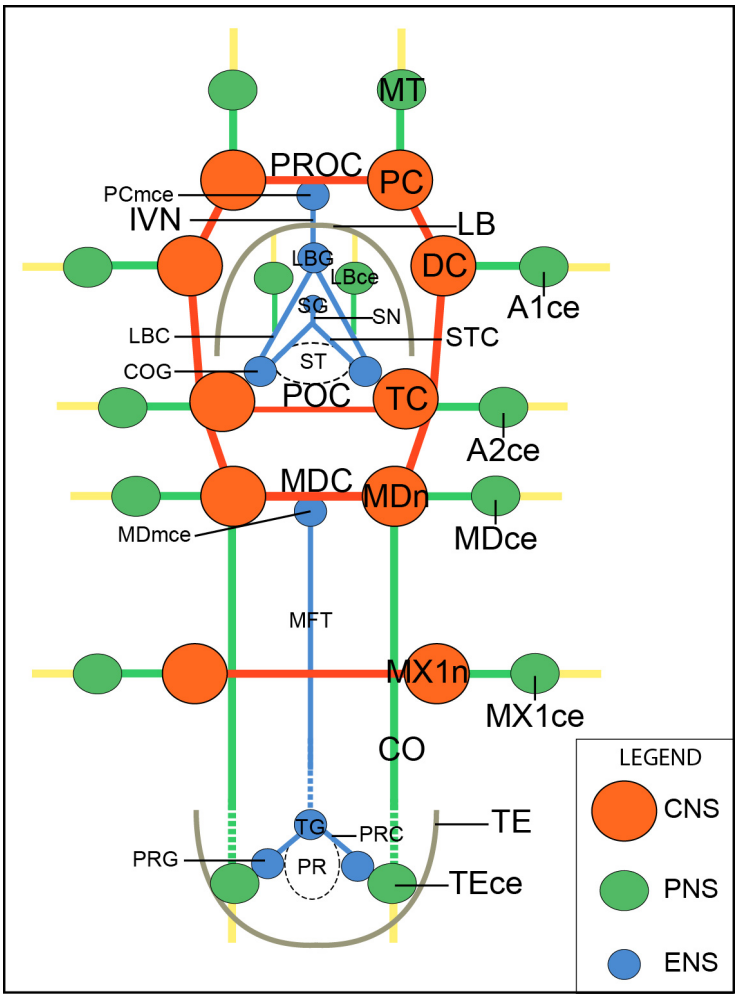

Fig. 90 – Schematic representation of the anlage of the nervous system in malacostracans

Overview of the nervous system during development (ventral view). The fundamental nervous system includes the anlage of the CNS (in orange), composed of the brain, the mandibular and the post-naupliar neuromeres; the ENS (in blue), which in turns includes the SNS and the INS; the sensory PNS (in green) which groups the sensory ganglia associated with both the CNS and the ENS. The medulla terminalis, the limbs peripheral cell clusters, the labral and telsonic peripheral cell clusters are considered part of the PNS. Note that the maxilla 1 is taken as being representative of all the post-naupliar neuromeres. The red lines mark the commissures and the connectives of the CNS which form the primary axonal scaffold. The blue lines represent the axons of the intrinsic ENS nervous system. The green lines indicate the peripheral nerves, including the afferences (green) and the sensory terminal neurites, i.e. the receptors (yellow).

A1ce: antenna 1 peripheral cell cluster; A2ce: antenna 2 peripheral cell cluster; DC: deutocerebrum; CO: connectives; COG commissural ganglion; IVN: inferior ventricular nerve; LB: labrum; LBC: labral commissure; LBce: labral peripheral cell cluster; LBG: labral ganglion; MDC: mandibular commissure; MDce: mandibular peripheral cluster; MDn: mandibular neuromere; MDmce: mandibular median cell cluster; MTF: median fiber tract; MT: medulla terminalis; MX1n: maxilla 1 neuromere; MX1ce: maxilla 1 peripheral cell cluster; PC: protocerebrum; PCmce: protocerebral median cell cluster; POC: post-oral commissure; PR: proctodeum; PRC: proctodeal commissure ; PRG: proctodeal ganglion; PROC: pre-oral commissure; SG: stomatogastric ganglion; SN: stomatogastric nerve; ST: stomodeum; STC: stomodeal commissure; TC: tritocerebrum; TE: telson; TEce: telsonic peripheral cell cluster; TG: terminal ganglion.

Serial homology in the peripheral sensory centre anlage

The present study offers an example of how the sensory system develops progressively and fundamentally affects the complexity of the ganglionic neuropils as already observed (Bate 1978; Laverack 1987). The present study shows that the beginning of neural activity is detected at the same time in the central neuromeres and at the periphery, where the anlage of sensory centres form. The sensory centres are small clusters of bipolar neurons provided by one peripheral sensory receptor, and one axon connecting the central axonal scaffold (either of the CNS or of the ENS). Those occur at the periphery of each central neuromere, and in the distal portion of the labrum and of the telson. Each sensory centre grows in the number of constituting neurons and in complexity during development, differentiating at different degrees. In this respect, the medulla terminalis anlage is considered by the present study as part of this sensory PNS, and thus, the peripheral sensory centre associated with the protocerebrum. Moreover, given the correspondence of the morphology of these peripheral sensory centers in the early stages of development, the present study suggests serial homology among the anlagen of these sensory units, including the medulla terminalis and the peripheral sensory centres of each of the more posterior limb buds.

In summary, the development of the nervous system, as put forward by the present study, proceeds with the formation of a primary axonal scaffold which constitutes the main pathway for the development of a more complex system. The primary axonal scaffold is pioneered by three systems which form as three **independent units** and interconnect in concert. These are the CNS, the PNS and the ENS. The CNS includes the neuromeres of the naupliar and of the post-naupliar region. The PNS consists of sensory units, or sensory centres, each composed of a small cluster of sensory cells, which progressively increase in number or differentiate into more complex systems. In this respect, for instance, the medulla terminalis anlage is considered as a peripheral centre associated with the sensory frontal organ. The ENS anlage, which includes the SNS and the INS anlagen, is connected to the CNS via a median component of the nervous system. The primary axonal scaffold is eventually constituted by central projections to the periphery, sensory peripheral projections, projections from the ENS, and, medially, by the connection between the CNS and the ENS.

Summaries

English summary

The present study addresses the development of the nervous system in three malacostracans species: the euphausiacean *Meganyctiphanes norvegica*, and the two decapods *Penaeus monodon* (Dendrobranchiata) and *Procambarus fallax* f. *virginalis* (Astacida). Based on the use of antibody stainings and fluorescent dyes in combination with CLSM and 3D reconstruction, the observations cover the onset of axogenesis and follow the establishment of the axonal scaffold in a consistent and comprehensive sequence through the embryonic and the post-embryonic development.

The development of the nervous system reveals a general developmental pattern shared by the three investigated species. With a comparative approach, the observed pattern is discussed with respect to the segmental organization of the animals' body. In particular, the development of the peripheral and of the enteric nervous systems plays a crucial role in the process of guiding the main axonal scaffold. In this context, the medulla terminalis, which in the nauplius larvae of *M. norvegica* and *P. monodon* develops strictly associated to a pair of frontal sensory organs, is proposed as a separate unit and not part of the tripartite brain. The homology of these sensory organs with the "frontal filaments" of non-malacostracan crustaceans and a new interpretation of the so called "lateral protocerebrum" in the developmental ground pattern of the Crustacea are discussed against the current phylogenetic background. Moreover, the present study offers a precise identification of the single structures forming the stomatogastric nervous system and provides a review of the former nomenclature. The interpretation of the labrum as a non-segmental appendage associated to the stomatogastric nervous system is advanced.

Finally, the present study proposes the development of the nervous system as the result of the coordinated interaction of three independent nervous systems, i.e. the central, the enteric and the peripheral. As a consequence, the development of the axonal scaffold, i.e. the formation of the basal network of afferents and efferents necessary for the connection among these three systems, appears uncoupled from the segmentation process.

Deutsche Zusammenfassung

Die vorliegende Studie untersucht die Entwicklung des Nervensystems von drei Arten der Höheren Krebse (Malacostraca): Die Leuchtgarnele (Euphausiacea) *Meganyctiphanes norvegica* und die beiden Zehnfußkrebse (Decapoda) *Penaeus monodon* (Dendrobranchiata) und *Procambarus fallax* f. *virginalis* (Astacida). Auf Basis von Antikörper- und Fluoreszenzfärbungen in Verbindung mit Konfokaler Laser-Scanning Mikroskopie und 3D Rekonstruktionen, umfasst die Studie den Beginn der Axogenese und zeichnet die Entstehung eines axonalen Grundgerüstes in einer umfassenden Abfolge durch die Embryonal- wie auch die Postembryonalentwicklung nach.

Die Daten zeigen, dass die drei untersuchten Arten ein allgemeines Muster bei der Entwicklung des Nervensystems teilen. Mittels eines vergleichenden Zuganges wird das gefundene Muster in Hinblick auf die segmentale Körperorganisation der Tiere diskutiert. Insbesondere die Entwicklung des peripheren und des enteralen Nervensystems spielen eine Schlüsselrolle im Prozess der Führung des grundlegenden axonalen Grundgerüstes. Der Vergleich zeigt, dass die medulla terminalis, welche sich bei den Naupliuslarven von *M. norvegica* und *P. monodon* in enger Verbindung zu einem Paar sensorischer Frontalorgane entwickelt, eine separate ontogenetische Einheit darstellt, die keinen Teil des dreiteiligen Gehirns der Tiere repräsentiert. Auf Grundlage der phylogenetischen Verwandtschaftsbeziehungen wird die Frage einer möglichen Homologie zwischen diesen sensorischen Organen und den “Frontalfilamenten“ bei nicht-malakostrakten Krebsen, sowie eine neue Interpretation des sogenannten “lateralen Protocerebrums” im Grundmuster der Crustacea-Entwicklung diskutiert. Darüber hinaus liefert die Studie die Identifikation der einzelnen Strukturen des sich entwickelnden stomatogastrischen Nervensystems und enthält eine Zusammenfassung der bisherigen diesbezüglich verwendeten Nomenklatur.

Abschließend wird die Hypothese der Entwicklung des Nervensystems als Ergebnis der koordinierten Interaktion dreier unabhängiger Nervensysteme, namentlich dem Zentral-, dem Enteral- und dem peripheren Nervensystem, entwickelt. Die Entwicklung des axonalen Grundgerüstes, als grundlegendes Netzwerk afferenter und efferenter Neuronen für die Verbindungen zwischen diesen drei Systemen, erscheint daher entkoppelt vom Prozess der Segmentierung.

References

Ache B W (1982) Chemoreception and thermoreception. The Biology of Crustacea 3: 369-398

Alwes F (2008) Cell lineage studies in Crustacea - Aspects of the early development and germ layer formation in *Meganyctiphanes norvegica* (Malacostraca, Euphausiacea) and *Bythotrephes longimanus* (Cladocera, Branchiopoda). Dissertation, Humboldt-Universität zu Berlin

Alwes F and Scholtz G (2004) Cleavage and gastrulation of the euphausiacean *Meganyctiphanes norvegica* (Crustacea, Malacostraca). Zoomorphology 123: 125-137

Alwes F and Scholtz G (2006) Stages and other aspects of the embryology of the parthenogentic marmorkrebs (Decapoda, Reptantia; Astacida). Development Genes and Evolution 216: 169-184

Andersson A (1977) The organ of Bellonci in ostracodes: an ultrastructural study of the rod-shaped, or frontal, organ. Acta Zoologica 58: 197-204

Andrew D R, Brown S M and Strausfeld N J (2012) The minute brain of the copepod *Tigriopus californicus* supports a complex ancestral ground pattern of the tetraconate cerebral nervous systems. Journal of Comparative Neurology 520: 3446-3470

Aramant R and Elofsson R (1976) Distribution of monoaminergic neurons in the nervous system of non-malacostracan crustaceans. Cell and Tissue Research 166: 1-24

Bate C S (1851) On the development of the Cirripedia. Annals and Magazine of Natural History 8: 324-332

Bellon-Humbert C and Van Herp F (1988) Localization of serotonin-like immunoreactivity in the eyestalk of the prawn *Palaemon serratus* (Crustacea, Decapoda, Natantia). Journal of Morphology 196: 307-320

Beltz B S and Kravitz E A (1987) Physiological identification, morphological analysis, and development of identified serotonin-proctolin containing neurons in the lobster ventral nerve cord. The Journal of Neuroscience 7: 533-546

Beltz B S and Kravitz E A (2002) Serotonin in crustacean systems: more than a half century of fundamental discoveries. In: Wiese K (ed.) Crustacean Experimental Systems in Neurobiology. Springer, Berlin: 141-163

Beltz B S, Helluy S M, Ruchhoeft M L and Gammill L S (1992) Aspects of the embryology and neural development of the american lobster. The Journal of Experimental Zoology 261: 288-297

Beltz B S, Pontes M, Helluy S M and Kravitz E A (1990) Patterns of appearance of serotonin and proctolin immunoreactivities in the developing nervous system of the american lobster. Journal of Neurobiology 21: 521-542

Bentley D and Keshishian H (1982) Pioneer neurons and pathways in insect appendages. Trends in Neurosciences 5: 354-358

Biffis C, Alwes F and Scholtz G (2009) Cleavage and gastrulation of the dendrobranchiate shrimp *Penaeus monodon* (Crustacea, Malacostraca, Decapoda). Arthropod Structure & Development 38: 527-540

Bitsch J and Bitsch C (2007) The segmental organization of the head region in Chelicerata: a critical review of recent studies and hypotheses. Acta Zoologica 88: 317-335

Bitsch J and Bitsch C (2010) The tritocerebrum and the clypeolabrum in mandibulate arthropods: segmental interpretations. Acta Zoologica 91: 249-266

Blanchard C E (1986) Early development of the thorax and the nervous system of the brine shrimp *Artemia*. Dissertation, University of Leicester

Blaustein D N, Derby C D, Simmons R B and Beall A C (1988) Structure of the brain and medulla terminalis of the spiny lobster *Panulirus argus* and the crayfish *Procambarus clarkii*, with an emphasis on olfactory centers. Journal of Crustacean Biology 8: 493-519

Böhm H, Dybek E and Heinzel H G (2001) Anatomy and in vivo activity of neurons connecting the crustacean stomatogastric nervous system to the brain. Journal of Comparative Physiology A 187: 393-403

Boyan G and Ehrhardt E (2015) Pioneer neurons of the antennal nervous system project to protocerebral pioneers in the grasshopper *Schistocerca gregaria*. Development Genes and Evolution 225: 377-382

Boyan G, Reichert H and Hirth F (2003) Commissure formation in the embryonic insect brain. Arthropod Structure & Development 32: 61-77

Boysen E and Buchholz F (1984) *Meganyctiphanes norvegica* in the Kattegat. Marine Biology 79: 195-207

Bowman T E (1984) Stalking the wild crustacean: the significance of sessile and stalked eyes in phylogeny. Journal of Crustacean Biology 4: 7-11

Brenneis G and Richter S (2010) Architecture of the nervous system in Mystacocarida (Arthropoda, Crustacea) - an immunohistochemical study and 3d reconstruction. Journal of Morphology 271: 169-189

Brenneis G, Ungerer P and Scholtz G (2008) The chelifores of sea spiders (Arthropoda, Pycnogonida) are the appendages of the deutocerebral segment. Evolution & Development 10: 717-724

Brinton E (1987) A new abyssal euphausiid, *Thysanopoda minyops*, with comparisons of eye size, photophores, and associated structures among deep-living species. Journal of Crustacean Biology 7: 636-666

Bullock T and Horridge G A (1965) Structure and function in the nervous systems of invertebrates. W. H. Freeman, San Francisco

Carlisle D B (1953) Studies on *Lysmata seticaudata* Risso (Crustacea Decapoda). VI Notes on the structure of the neurosecretory system of the eyestalk. Pubblicazioni della Stazione zoological di Napoli 24: 435-447

Carlisle D B (1959) On the sexual biology of *Pandalus borealis* (Crustacea Decapoda) II. The termination of the male phase. Journal of the Marine Biological Association of the United Kingdom 38: 481-491

Carlisle D B and Knowles F G W (1959) Endocrine control in crustaceans. In: Cambridge Monographs in Experimental Biology. Cambridge University Press, New York 10: 1–120

Carstam S P (1942) Weitere Beiträge zur Farbwechselphysiologie der Crustaceen. Journal of Comparative Physiology A: Neuroethology, Sensory, Neural, and Behavioral Physiology 29: 433-472

Casasnovas B and Meyrand P (1995) Functional differentiation of adult neural circuits from a single embryonic network. Journal of Neuroscience 15: 5703-5718

Castellani C, Haug J T, Haug C, Maas A, Schoenemann B and Waloszek D (2012) Exceptionally well-preserved isolated eyes from Cambrian 'Orsten' fossil assemblages of Sweden. Palaeontology 55: 553-566

Cazalets J R, Cournil I, Geffard M and Moulins M (1987) Suppression of oscillatory activity in crustacean pyloric neurons: implication of GABAergic inputs. Journal of Neuroscience 7: 2884-2893

Chaigneau J (1969) Étude ultrastructurale de l'organe de Bellonci de *Sphaeroma serratum* (Fabricius), crustacé isopode flabellifére. Comptes rendus hebdomadaires des séances de l'Académie des sciences Paris 268: 3177-3179

Chaigneau J (1971a) L'organe de Bellonci du crustacé isopode *Sphaeroma serratum* (Fabricius): ultrastructure et signification. Zeitschrift für Zellforschung und Mikroskopische Anatomie 112: 166-187

Chaigneau J (1971b) Etude préliminaire de l'ultrastructure des corps en bulbe d'oignon présents dans les organes de Bellonci de certains Crustacés, observations faites chez *Palaemon elegans*, Crustacé Décapode Natantia. Comptes Rendus de l'Académie des Sciences (Paris) 272: 303-306.

Chaigneau J (1973) Fine structure of the sensory pore present in the eyestalk of Crustacea Natantia. Zeitschrift für Zellforschung und Mikroskopische Anatomie 145: 213-227

Chaigneau J and Besse C (1994) The sensory tubercle on the eyestalk of the shrimp *Crangon crangon* (Linnaeus, 1758) (Decapoda, Caridea). Crustaceana 66: 78-89

Chaigneau J, Besse C, Jaros P P, Martin G, Wägele J W and Willig A (1991) Organ of Bellonci of an antarctic crustacean, the marine isopod *Glyptonotus antarcticus.* Journal of Morphology 207: 119-128

Chaigneau J and Chataigner J P (1977) The connections of the sensory organ of Bellonci with the brain in Isopoda (Crustacea). Cell and Tissue Research 182: 61-72

Chaigneau J and Juberthie-Jupeau L (1975) Ultrastructure de l'organe de Bellonci d'un Crustacé Dècapode Natantia vivant dans le milieu souterrain. Comptes Rendus de l'Académie des Sciences (Paris) 280: 1131-1134

Chaudonneret J (1957). Remarques sur le système nerveux des derniers segments thoraciques de la *Squille* (Crustacé Stomatopode). Annales des Sciences Naturelles, Zoologie 19: 225-232

Chaudonneret J (1978) La phylogenèse du système nerveux annélidoarthropodien. Bulletin de la Societé Zoologique de France 103: 69-95

Christie A E, Stein W, Quinlan J E, Beenhakker M P, Marder E and Nusbaum M P (2004) Actions of a histaminergic/peptidergic projection neuron on rhythmic motor patterns in the stomatogastric nervous system of the crab *Cancer borealis*. Journal of Comparative Neurology 469: 153-169

Claiborne B J and Selverston A I (1984) Histamine as a neurotransmitter in the stomatogastric nervous system of the spiny lobster. Journal of Neuroscience 4: 708-721

Claus C (1876) Untersuchungen zur Erforschung der genealogischen Grundlage des Crustaceen-Systems. Ein Beitrag zur Descendenzlehre. Carl Gerold's Sohn, Wien

Coman G J, Arnold S J, Peixoto S, Crocos P J, Coman F E and Preston N P (2006). Reproductive performance of reciprocally crossed wild-caught and tank-reared *Penaeus monodon* broodstock. Aquaculture 252: 372-384

Coman G J, Crocos P J, Arnold S J, Keys S I, Preston N P and Murphy B (2005) Growth, survival and reproductive performance of domesticated Australian stocks of the giant tiger prawn, *Penaeus monodon*, reared in tanks and raceways. Journal of the World Aquaculture Society 36: 464-479

Cooke I M and Sullivan R E (1982) Hormones and neurosecretion. The Biology of Crustacea 3: 205-290

Cuzin-Roudy J, Tarling G A and Strömberg J-O (2004) Life cycle strategies of northern krill (*Meganyctiphanes norvegica*) for regulating growth, moult, and reproductive activity in various environments: the case of fjordic populations. ICES Journal of Marine Science: 61: 721-737

Dahl E (1957) Embryology of X-organs in *Crangon allmanni*. Nature 179: 482

Dahl E (1965) Frontal organs and protocerebral neurosecretory systems in Crustacea and Insecta. General and Comparative Endocrinology 5: 614-617

Dahl E and Mecklenburg C V (1969) The sensory papilla X-organ in *Boreomysis arctica* (Krøyer) (Crustacea Malacostraca Mysidacea). Cell and Tissue Research 101: 88-97

Dando M R and Selverston A I (1972) Command fibres from the supra-oesophageal ganglion to the stomatogastric ganglion in *Panulirus argus*. Journal of Comparative Physiology 78: 138-175

Darwin C (1854) A monograph on the sub-class Cirripedia, with figures of all the species: the Balanidae (or sessile cirripedes), the Verrucidae, etc. Ray Society, London

Dobkin S (1961) Early developmental stages of pink shrimp, *Penaeus duorarum* from Florida waters. Fisheries 1: 23

Dudley P L (1972) The fine structure of a cephalic sensory receptor in the copepod *Doropygus seclusus* Illg (Crustacea: Copepoda: Notodelphyidae). Journal of Morphology 138: 407-431

Edwards J S (1977) Pathfinding by arthropod sensory nerves. In: Hoyle G (ed.) Identified Neurons and Behaviour of Arthropods. Plenum Press, New York 483-493

Eloffson R (1963) The nauplius eye and frontal organs in Decapoda (Crustacea). Sarsia 12: 1-68

Eloffson R (1965) The nauplius eye and frontal organs in Malacostraca (Crustacea). Sarsia 19: 1-54

Elofsson R (1966) The nauplius eye and frontal organs of the non-malacostraca (Crustacea). Sarsia 25: 1-128

Elofsson R (1969) The development of the compound eyes of *Penaeus duorarum* (Crustacea: Decapoda) with remarks on the nervous system. Zeitschrift für Zellforschung und mikroskopische Anatomie 97: 323-350

Elofsson R (1992) To the question of eyes in primitive crustaceans. Acta Zoologica 73: 369-372

Elofsson R and Dahl E (1970) The visual neuropiles and chiasmata of crustacea. Zeitschrift für Zellforschung und Mikroskopische Anatomie 107: 343-360

Elofsson R and Hallberg E H (1980) The juxtaposed compound eye and organ of Bellonci in *Haploops tubicola* (Crustacea: Amphipoda) **-** the fine structure of the organ of Bellonci. Zoomorphology 96: 255-262

Elofsson R and Hessler R R (1990) Central nervous system of *Hutchinsoniella macracantha* (Cephalocarida). Journal of Crustacean Biology 10: 423-439

Elofsson R and Hessler R R (2005) The tegumental sensory organ and nervous system of *Derocheilocaris typica* (Crustacea: Mystacocarida). Arthropod Structure & Development 34:139–152

Elofsson R and Klemm N (1972) Monamine containing neurons in the optic ganglia of crustaceans and insects. Cell and Tissue Research 133: 475-499

Elofsson R and Lake P S (1971) On the cavity receptor organ (X-organ or organ of Bellonci) of *Artemia salina* (Crustacea: Anostraca). Cell and Tissue Research 121: 319-326

Fanenbruck M and Harzsch S (2005) A brain atlas of *Godzilliognomus frondosus* Yager, 1989 (Remipedia, Godzilliidae) and comparison with the brain of *Speleonectes tulumensis* Yager, 1987 (Remipedia, Speleonectidae): implications for arthropod relationships. Arthropod Structure & Development 34: 343-378

Fanenbruck M, Harzsch S and Wägele J W (2004) The brain of the Remipedia (Crustacea) and an alternative hypothesis on their phylogenetic relationships. Proceedings of the National Academy of Sciences of the United States of America 101: 3868-3873

Fenelon V S, Casasnovas B, Faumont S and Meyrand P (1998) Ontogenetic alteration in peptidergic expression within a stable neuronal population in lobster stomatogastric nervous system. Journal of Comparative Neurology 399: 289-305

Fingerman M (1987) The endocrine mechanisms of crustaceans. Journal of Crustacean Biology 7: 1-24

Fischer A H L and Scholtz G (2010) Axogenesis in the stomatopod crustacean *Gonodactylaceus falcatus* (Malacostraca). Invertebrate Biology 129: 59-76

Frase T (2012) Entwicklung und Evolution des Nervensystems der Anostraca. Diploma-thesis. Universität Rostock

Frase T and Richter S (2013) The fate of the onychophoran antenna. Development Genes and Evolution 223: 247-251

Frase T and Richter S (2016) Nervous system development in the fairy shrimp *Branchinella* sp. (Crustacea: Branchiopoda: Anostraca): insights into the development and evolution of the branchiopod brain and its sensory organs. Journal of Morphology 277: 1423-1446

Fraser F C (1937) On the development and distribution of the young stages of krill (*Euphausia superba*). Cambridge University Press, London

Fritsch M and Richter S (2010) The formation of the nervous system during larval development in *Triops cancriformis* (Bosc) (Crustacea, Branchiopoda): an immunohistochemical survey. Journal of Morphology 271: 1457-1481

Fritsch M and Richter S (2012) Nervous system development in Spinicaudata and Cyclestherida (Crustacea, Branchiopoda) - comparing two different modes of indirect development by using an event pairing approach. Journal of Morphology 278: 672-695

Fritsch M, Bininda-Emonds O R and Richter S (2013a) Unraveling the origin of Cladocera by identifying heterochrony in the developmental sequences of Branchiopoda. Frontiers in Zoology 10: 35

Fritsch M, Kaji T, Olesen J and Richter S (2013b) The development of the nervous system in Laevicaudata (Crustacea, Branchiopoda): insights into the evolution and homologies of branchiopod limbs and 'frontal organs'. Zoomorphology 132: 163-181

Gabe M (1966) Neurosecretion. Vol. 28. Pergamon Press, Oxford

Gallus L, Ferrando S, Gambardella C, Diaspro A, Bianchini P, Piazza V and Tagliafierro G (2009) The GABAergic-like system in the cyprid of *Balanus amphitrite* (= *Amphibalanus amphitrite*) (Cirripedia, Crustacea). Biofouling 26: 155-165

Garzino V and Reichert H (1994) Early embryonic expression of a 60-kD glycoprotein in the developing nervous system of the lobster. Journal of Comparative Neurology 346: 572-582

Gerberding M and Scholtz G (1999) Cell lineage of the midline cells in the amphipod crustacean *Orchestia cavimana* (Crustacea, Malacostraca) during formation and separation of the germ band. Development Genes and Evolution 209: 91-102

Gerberding M and Scholtz G (2001) Neurons and glia in the midline of the higher crustacean *Orchestia cavimana* are generated via an invariant cell lineage that comprises a median neuroblast and glial progenitors. Developmental Biology 235: 397-409

Ghysen A (1980) The projection of sensory neurons in the central nervous system of Drosophila: choice of the appropriate pathway. Developmental Biology 78: 521-541

Giribet G and Edgecombe G D (2010) Revaluating the arthropod tree of life. Annual Review of Entomology 57: 167-186

Giribet G and Edgecombe G D (2013) The Arthropoda: a phylogenetic framework. In: Minelli A, Boxshall G and Fusco G (eds.) Arthropod biology and evolution **-** molecules, development, morphology. Springer, Berlin: 17-40

Hanström B (1924a) Untersuchungen über das Gehirn, insbesondere die Sehganglien der Crustaceen. Arkiv för zoologi 16:1–117

Hanström B (1924b) Beitrag zur Kenntnis des zentralen Nervensystems der Ostracoden und Copepoden. Zoologische Anziger, 61: 31-38

Hanström B (1925) The olfactory centers in crustaceans. The Journal of Comparative Neurology 38: 221-250

Hanström B (1928) Vergleichende Anatomie des Nervensystems der wirbellosen Tiere unter Berücksichtigung seiner Funktion. Springer, Berlin

Hanström B (1931) Neue Untersuchungen über Sinnesorgane und Nervensystem der Crustaceen, I. Zeitschrift für Morphologie und Ökologie der Tiere 23: 80-236

Hanström B (1934) Neue Untersuchungen über Sinnesorgane und Nervensystem der Crustaceen, IV. Arkiv för Zoologi 26: 1-66

Hanström B (1939) Hormones in invertebrates. Oxford University Press, London

Hanström B (1947) The brain, the sense organs, and the incretory organs of the head in the Crustacea Malacostraca. Kungliga Fysiografiska Sallskapets Handlingar N F 58:1–44

Harris-Warrick R M, Nagy F and Nusbaum M P (1992) Neuromodulation of stomatogastric networks by identified neurons and transmitters. In: Harris-Warrick R M, Marder E, Selverston A I and Moulins M (eds.) Dynamic biological networks: the stomatogastric nervous system. MIT Press, Cambridge: 87-137

Harrison R G (1910) The outgrowth of the nerve fiber as a mode of protoplasmic movement. Journal of Experimental Zoology 9: 787-846

Harrison P J H and Sandemann D C (1999) Morphology of the nervous system of the barnacle cypris larva (*Balanus amphitrite* Darwin) revealed by light and electron microscopy. Biological Bullentin 197: 144-158

Harzsch S (2001) Neurogenesis in the crustacean ventral nerve chord: homology of neuronal stem cells in Malacostraca and Branchiopoda? Evolution & Development 3: 154-169

Harzsch S (2002a) From stem cell to structure: neurogenesis in the CNS of decapod crustaceans. In: Wiese K (ed.) The crustacean nervous system. Springer, Berlin: 417-432

Harzsch S (2002b) The phylogenetic significance of crustacean visual neuropils and chiasmata: a re-examination. Journal of Comparative Neurology 453: 10-21

Harzsch S (2003a) Evolution of identified arthropod neurons: the serotonergic system in relation to engrailed-expressing cells in the embryonic ventral nerve cord of the american lobster *Homarus americanus* Milne Edwards, 1873 (Malacostraca, Pleocyemata, Homarida). Developmental Biology 258: 44-56

Harzsch S (2003b) Ontogeny of the ventral nerve cord in malacostracan crustaceans: a common plan for neuronal development in Crustacea, Hexapoda and other Arthropoda? Arthropod Structure & Development 32: 17-37

Harzsch S (2004) The tritocerebrum of Euarthropoda: a ‘‘non-drosophilocentric’’ perspective. Evolution & Development 6: 303-309

Harzsch S (2006) Neurophylogeny: architecture of the nervous system and a fresh view on arthropod phylogeny. Integrative and Comparative Biology 46: 162-194

Harzsch S and Dawirs R R (1993) On the morphology of the central nervous system in larval stages of *Carcinus maenas* (Decapoda, Brachyura). Helgoländer Meeresuntersuchungen 47: 61-79

Harzsch S and Dawirs R R (1994) Neurogenesis in the larval stages of the spider crab *Hyas araneus* (Decapoda. Brachyura): proliferation of neuroblasts in the ventral nerve cord. Roux's Archives of Developmental Biology 204: 93-100

Harzsch S and Dawirs R R (1995) A developmental study of serotonin-immunoreactive neurons in the larval central nervous system of the spider crab *Hyas araneus* (Decapoda, Brachyura). Invertebrate Neuroscience 1: 53-65

Harzsch S and Dawirs R R (1996a) Maturation of the compound eyes and eyestalk ganglia during larval development of the brachyuran crustaceans *Hyas araneus* L. (Decapoda, Majidae) and *Carcinus maenas* L. (Decapoda. Portunidae). Zoology 99: 189-204

Harzsch S and Dawirs R R (1996b) Development of neurons exhibiting FMRFamide-related immunoreactivity in the central nervous system of spider crab larvae (*Hyas araneus* L., Decapoda. Majidae). Journal of Crustacean Biology 16: 10-19

Harzsch S and Dawirs R R (1996c) Neurogenesis in the developing crab brain: postembryonic generation of neurons persists beyond metamorphosis. Journal of Neurobiology 29: 384-398

Harzsch S and Glötzner J (2002) An immunohistochemical study of structure and development of the nervous system in the brine shrimp *Artemia salina* Linnaeus, 1758 (Branchiopoda, Annostraca) with remarks of the arthropod brain. Arthropod Structure & Development 30: 251-270

Harzsch S and Hansson BS (2008) Brain architecture in the terrestrial hermit crab *Coenobita clypeatus* (Anomura, Coenobitidae), a crustacean with a good aerial sense of smell. BMC Neuroscience 9.1: 1

Harzsch S and Waloszek D (2000) Serotonin-immunoreactive neurons in the ventral nerve chord of Crustacea: a character to study aspects of arthropod phylogeny. Arthropod Structure & Development 29: 307-322

Harzsch S and Waloszek D (2001) Neurogenesis in the developing visual system of the branchiopod crustacean *Triops longicaudatus* (Leconte, 1846): corresponding patterns of compound-eye formation in Crustacea and Insecta? Development Genes and Evolution 211: 37-43

Harzsch S, Anger K and Dawirs R R (1997) Immunocytochemical detection of acetylated a-tubulin and *Drosophila* synapsin in the embryonic crustacean nervous system. International Journal for Developmental Biology 41: 477-484

Harzsch S, Benton J, Dawirs R R and Beltz B (1999) A new look at embryonic development of the visual system in decapod crustaceans: neuropil formation, neurogenesis, and apoptotic cell death. Journal of Neurobiology 39: 294-306

Harzsch S, Miller J, Benton J, Dawirs R R and Beltz B (1998) Neurogenesis in the thoracic neuromeres of two crustaceans with different types of metamorphic development. The Journal of Experimental Biology 201: 2465-2479

Harzsch S, Sandeman D and Chaigneau J (2012) Morphology and development of the central nervous system. In: Forest J and von Vaupel Klein J C (eds.) Treatise on Zoology - Anatomy, Taxonomy, Biology. The Crustacea. Vol. 3. Koninklijke Brill Academic Publishers, Leiden Boston: 9-236

Hedrich U B, Diehl F and Stein W (2011) Gastric and pyloric motor pattern control by a modulatory projection neuron in the intact crab *Cancer pagurus*. Journal of Neurophysiology 105: 1671-1680

Heinzel H-G, Dybek E, Böhm H and Sandeman D (2002) Connections of the head to networks of the stomatogastric system in crayfish. In: Wiese K (ed.) The crustacean nervous system. Springer, Berlin: 560-566

Helluy S M and Beltz B S (1991) Embryonic development of the American lobster (*Homarus americanus*): quantitative staging and characterization of an embryonic molt cycle. Biological Bulletin 180: 355-371

Helluy S M, Benton J L, Langworthy K A, Ruchhoeft M L and Beltz B S (1996) Glomerular organization in developing olfactory and accessory lobes of american lobsters: stabilization of numbers and increase in size after metamorphosis. Journal of Neurobiology 29: 459-472

Helluy S M, Ruchhoeft M L and Beltz B S (1995) Development of the olfactory and accessory lobes in the american lobster: an allometric analysis and its implications for deutocerebral structure of decapods. The Journal of Comparative Neurology 357: 433-445

Helluy S M, Sandemann R, Beltz B and Sandemann D (1993) Comparative brain ontogeny of the crayfish and clawed lobster: implications of direct and larval development. The Journal of Comparative Neurology 335: 343-354

Helm F (1928) Vergleichend-anatomische Untersuchungen über das Gehirn, insbesondere das „Antennalganglion" der Dekapoden. Zeitschrift für Morphologie und Ökologie der Tiere 12: 70-134

Henry L M (1948) The nervous system and the segmentation of the head in Annulata. IV. Arthropoda. Microentomology 13: 1-26

Herring P (2002) The biology of the deep ocean. Oxford University Press, Oxford

Hertzler P L (2015) "Crustacea": Decapoda (Dendrobranchiata). In: Wanninger A (ed.) Evolutionary Developmental Biology of Invertebrates 4. Springer, Vienna: 63-100

Hessler R R and Newman W A (1975) A trilobitomorph origin for the Crustacea. Fossils and Strata 4: 437-459

Ho R K and Goodman C S (1982) Peripheral pathways are pioneered by an array of central and peripheral neurones in grasshopper embryos. Nature 297: 404

Hubschman J H (1963) Development and function of neurosecretory sites in the eyestalks of larval *Palaemonetes* (Decapoda: Natantia). Biological Bulletin 125: 96-113

Huvard A (1990) Ultrastructural study of the naupliar eye of the *Ostracodevargula graminicola* (Crustacea, Ostracoda). Zoomorphology 110: 47-51

Jarman S N (2001) The evolutionary history of krill inferred from nuclear large subunit rDNA sequence analysis. Biological Journal of the Linnean Society 73: 199-212

Jimenez S A and Faulkes Z (2010) Establishment and care of a colony of parthenogenetic marbled crayfish, Marmorkrebs. Invertebrate Rearing 1: 10-18

Jirikowski G, Kreissl S, Richter S and Wolff C (2010) Muscle development in the marbled crayfish - insights from an emerging model organism (Crustacea, Malacostraca, Decapoda). Development Genes and Evolution 220: 89-105

Jirikowski G J, Richter S and Wolff C (2013) Myogenesis of Malacostraca: the egg-nauplius concept revisited. Frontiers in Zoology 10: 1

Jirikowski G J, Wolff C and Richter S (2015) Evolution of eumalacostracan development: new insights into loss and reacquisition of larval stages revealed by heterochrony analysis. EvoDevo 6: 1

Kauri T (1962) On the frontal filaments and nauplius eye in *Balanus*. Crustaceana 4: 131-142

Kauri T (1966) On the sensory papilla x organ in cirriped larvae. Crustaceana 11: 115-122

Kauri T and Dahl E (1975) Fine structure of the organ of Bellonci (SPX) in *Boreomysis arctica* (Krøyer) (Crustacea, Mysidacea). Zoologica Scripta 4: 41-47

Kauri T and Lake P S (1972) The structure of the organ of Bellonci of the syncarid crustacean, *Anaspides tasmaniae* (Thomson). Zeitschrift für Zellforschung 132: 431-450

Kenning M and Harzsch S (2013) Brain anatomy of the marine isopod *Saduria entomon* Linnaeus, 1758 (Valvifera, Isopoda) with special emphasis on the olfactory pathway. Frontiers in Neuroanatomy 7: 32

Kenning M, Müller C, Wirkner C S and Harzsch S (2013) The Malacostraca (Crustacea) from a neurophylogenetic perspective: new insights from brain architecture in *Nebalia herbstii* Leach, 1814 (Leptostraca, Phyllocarida). Zoologischer Anzeiger - A Journal of Comparative Zoology 252: 319-336

Keshishian H (1980) The origin and morphogenesis of pioneer neurons in the grasshopper metathoracic leg. Developmental Biology 80: 388-397

Kilman V, Fenelon V S, Richards K S, Thirumalai V, Meyrand P and Marder E (1999) Sequential developmental acquisition of cotransmitters in identified sensory neurons of the stomatogastric nervous system of the lobsters, *Homarus americanus* and *Homarus gammarus*. Journal of Comparative Neurology 408: 318-334.

Kirsch R and Richter S (2007) The nervous system of *Leptodora kindtii* (Branchiopoda, Cladocera) surveyed with confocal scanning microscopy (CLSM), including general remarks on the branchiopod neuromorphological ground pattern. Arthropod Structure & Development 36: 143-156

Klann M (2008) Aspekte der Neurogenese bei Hüpferlingen (Crustacea, Copepoda). Bachelor Thesis, Humboldt-Universität zu Berlin

Knight M D (1980) Larval development of *Euphausia eximia* (Crustacea, Euphausiacea) with notes on its vertical-distribution and morphological divergence between populations. Fishery Bulletin 78: 313-335

Knowles F G W and Carlisle D B (1956) Endocrine control in Crustacea. Biological Reviews 31: 396-473

Koenemann S, Olesen J, Alwes F, Iliffe T M, Hoenemann M, Ungerer P, Wolff C and Scholtz G (2009) The post-embryonic development of Remipedia (Crustacea) **-** additional results and new insights. Development Genes and Evolution 219: 131-145

Komaki Y (1966) Technical notes on keeping euphausiids live in the laboratory, with a review of experimental studies on euphausiids. Information Bulletin of Planktology in Japan 13: 95-105

Korschelt E and Heider K (1891) Lehrbuch der vergleichenden Entwicklungsgeschichte der wirbellosen Thiere. Gustav Fischer, Jena

Kress T, Harzsch S and Dircksen H (2016) Neuroanatomy of the optic ganglia and central brain of the water flea *Daphnia magna* (Crustacea, Cladocera). Cell and tissue research 363: 649-677

Krieger J, Sandeman R E, Sandeman D C, Hansson B S and Harzsch S (2010) Brain architecture of the largest living land arthropod, the giant robber crab *Birgus latro* (Crustacea, Anomura, Coenobitidae): evidence for a prominent central olfactory pathway? Frontiers in Zoology 7: 1

Kushner P D (1979) Location of interganglionic neurons in the stomatogastric system of the spiny lobster. Journal of Neurocytology 8: 81-94

Kushner P D and Maynard E A (1977) Localization of monoamine fluroscence in the stomatogastric nervous system of lobsters. Brain Research 129: 13-28

Lake P S and Ong J E (1970) Ultrastructure of the 'onion bodies' of the sensory pore X-organ of *Paratya tasmaniensis*, Reik (Crustacea, Decapoda). Experientia 26: 1129-1130

Lake P S and Ong J E (1972) Observations of the organ of Bellonci of the shrimp *Paratya rasmaniensis*, Riek (Crustacea: Decapoda: Atyidae) with particular reference to the structure of the onion body cells. Australian Journal of Zoology 20: 215-234

Lass S, Tarling G A, Virtue P, Matthews J B L, Mayzaud P and Buchholz F (2001) On the food of northern krill *Meganyctiphanes norvegica* in relation to its vertical distribution. Marine Ecology Progress Series 214: 177-200

Laverack M S (1987) The nervous system of the Crustacea, with special reference of the sensory system. In: Ali M A (ed.) Nervous Systems in Invertebrates. Springer, US 141: 323-351

Laverack M S (1988) Larval locomotion, sensors, growth and their implication for the nervous system. In: Fincham A M and Rainbow P S (eds.) Aspects of Decapod Crustacean Biology. Symposia of the Zoological Society of London. Clarendon Press, Oxford 59: 103-122

Lichtneckert R and Reichert H (2005) Insights into the urbilaterian brain: conserved genetic patterning mechanisms in insect and vertebrate brain development. Heredity 94: 465-477

Loesel R (2011) Neurophylogeny: retracing early metazoan brain evolution. In: Pontarotti P (ed.) Evolutionary biology - concepts, biodiversity, macroevolution and genome evolution. Springer, Berlin: 169-191

Ma X, Hou X, Edgecombe G D and Strausfeld N J (2012) Complex brain and optic lobes in an early cambrian arthropod. Nature 490: 258-261

Marshall N J, Land M F, King C A and Cronin T W (1991) The compound eyes of mantis shrimps (Crustacea, Hoplocarida, Stomatopoda). II. Colour pigments in the eyes of stomatopod crustaceans: polychromatic vision by serial and lateral filtering. Philosophical Transactions of the Royal Society of London B: Biological Sciences 334: 57-84

Martin G (1976) Mise en évidence et étude ultrastructurale des ocelles médians chez les crustacés isopodes. Annales des Sciences Naturelles Zoologie Paris 18: 405-436

Martin J W (1992) Branchiopoda. Microscopic Anatomy of Invertebrates 9: 25-224

Martin P and Scholtz G (2012) A case of intersexuality in the parthenogenetic marmorkrebs (Decapoda: Astacida: Cambaridae). Journal of Crustacean Biology 32: 345-350

Martin P, Dorn N J, Kawai T, van der Heiden C and Scholtz G (2010) The enigmatic marmorkrebs (marbled crayfish) is the parthenogenetic form of *Procambarus fallax* (Hagen, 1870). Contributions to Zoology 79: 107-118

Maynard D M (1972) Simpler networks. Annals of the New York Academy of Sciences 193: 59-72

Maynard D M and Dando M R (1974) The structure of the stomatogastric neuromuscular system in *Callinectes sapidus*, *Homarus americanus* and *Panulirus argus* (Decapoda Crustacea). Philosophical Transactions of the Royal Society of London B: Biological Sciences 268: 161-220

Maynard D and Yager J (1968) Function of an eyestalk ganglion, the medulla terminalis, in olfactory integration in the lobster, *Panulirus argus*. Zeitschrift für Vergleichende Physiologie 59: 241-249

Meier T and Reichert H (1990) Neuronal development in the crustacean nervous system studied by neuron-specific antibody labelling. In: Frontiers in crustacean neurobiology. Birkhäuser, Basel: 523-529

Melzer R R, Diersch R, Nicastro D and Smola U (1997) Compound eye evolution: highly conserved retinula and cone cell patterns indicate a common origin of the insect and crustacean ommatidium. Naturwissenschaften 84: 542-544

Melzer R R, Michalke C and Smola U (2000) Walking on insect paths? Early ommatidial development in the compound eye of the ancestral crustacean, *Triops cancriformis*. Naturwissenschaften 87: 308-311

Meusemann K, von Reumont B M, Simon S, Roeding F, Strauss S, Kück P and Achter V (2010) A phylogenomic approach to resolve the arthropod tree of life. Molecular biology and Evolution 27: 2451-2464

Mittmann B and Scholtz G (2003) Development of the nervous system in the "head" of *Limulus polyphemus* (Chelicerata: Xiphosura): morphological evidence for a correspondence between the segments of the chelicerae and of the (first) antennae of Mandibulata. Development Genes and Evolution 213: 9-17

Motoh H (1981) Studies on the fisheries biology of the giant tiger prawn, *Penaeus monodon* in the Philippines (Technical Report No. 7). Aquaculture Department, Southeast Asian Fisheries Development Center, Tigbauan

Müller F (1864) Für Darwin. Wilhelm Engelmann, Leipzig

Müller F (1878) Über die Naupliusbrut der Garneelen. Zeitschrift für wissenschaftliche Zoologie, Leipzig 30: 163-166

Nilsson D-E and Osorio D (1998) Homology and parallelism in arthropod sensory processing. In: Fortey R A and Thomas R H (eds.) Arthropod relationships. Springer, Dordrecht: 333-347

Oakley T H (2003) On homology of arthropod compound eyes. Integrative and Comparative Biology 43: 522-530

Oakley T H and Cunningham C W (2002) Molecular phylogenetic evidence for the independent evolutionary origin of an arthropod compound eye. Proceedings of the National Academy of Sciences of the United States of America 99: 1426-1430

Pabst T (2004) Zur Beinentwicklung eines leptostraken Krebses. Diploma-thesis, Humboldt-Universität zu Berlin

Patel N H, Martin-Blanco E, Coleman K G, Poole S J, Ellis M C, Kornberg T B and Goodman C S (1989) Expression of engrailed proteins in arthropods, annelids, and chordates. Cell 58: 955-968

Piasecki W and MacKinnon B M (1993) Changes in structure of the frontal filament in sequential developmental stages of *Caligus elongatus* von Nordmann, 1832 (Crustacea, Copepoda, Siphonostomatoida). Canadian Journal of Zoology 71: 889-895

Ponomarenko E A (2014) The embryonic development of *Elminius modestus* Darwin, 1854 (Thecostraca: Cirripedia). Dissertation, Humboldt-Universität zu Berlin

Pyle R W (1943) The histogenesis and cyclic phenomena of the sinus gland and X-organ in Crustacea. Biological Bulletin 85: 87-102

Rasmussen S (1971) Die Feinstruktur des Mittelauges und des ventralen Frontalorgans von *Artemia salina* L. (Crustacea: Anostraca). Zeitschrift für Zellforschung und Mikroskopische Anatomie 117: 576-596

Regier J C, Shultz, J W, Zwick A, Hussey A, Ball B, Wetzer R and Cunningham C W (2010) Arthropod relationships revealed by phylogenomic analysis of nuclear protein-coding sequences. Nature 463: 1079-1083

Reichert H and Boyan G (1997) Building a brain: developmental insights in insects. Trends in Neurosciences 20: 258-264

Rempel J G (1975) Evolution of the insect head: the endless dispute. Quaestiones Entomologicae 11: 7-25

Richter S and Scholtz G (2001) Phylogenetic analysis of the Malacostraca (Crustacea). Journal of Zoological Systematics and Evolutionary Research 39: 113-136

Richter S, Loesel R, Purschke G, Schmidt-Rhaesa A, Scholtz G, Stach T, Vogt L, Wanninger A, Brenneis G, Döring C, Faller S, Fritsch M, Grobe P, Heuer C, Kaul S, Møller O, Müller C, Rieger V, Rothe B, Stegner M and Harzsch S (2010) Invertebrate neurophylogeny: suggested terms and definitions for a neuoanatomical glossary. Frontiers in Zoology 7: 1-49

Richter S, Stein M, Frase T and Szucsich N U (2013) The arthropod head. In: Minelli A, Boxshall G and Fusco G (eds.) Arthropod biology and evolution **-** molecules, development, morphology. Springer, Berlin: 223-240

Rieger V and Harzsch S (2008) Embryonic development of the histaminergic system in the ventral nerve cord of the marbled crayfish (marmorkrebs). Tissue and Cell 40: 113-126

Rotllant G, De Kleijn D, Charmantier-Daures M, Charmantier G and Van Herp F (1993) Localization of crustacean hyperglycemic hormone (CHH) and gonad-inhibiting hormone (GIH) in the eyestalk of *Homarus gammarus* larvae by immunocytochemistry and in situ hybridization. Cell and Tissue Research 271: 507-512

Rotllant G, Charmantier-Daures M, Trilles J P and Charmantier G (1994) Ontogeny of the sinus gland and of the organ of Bellonci in larvae and postlarvae of the European lobster *Homarus gammarus*. Invertebrate Reproduction & Development 26: 13-22

Rotllant G, Charmantier-Daures M, De Kleijn D, Charmantier G and Van Herp F (1995) Ontogeny of neuroendocrine centers in the eyestalk of *Homarus gammarus* embryos: an anatomical and hormonal approach. Invertebrate Reproduction & Development 27: 233-245

Russell D F and Hartline D K (1981) A multiaction synapse evoking both EPSPs and enhancement of endogenous bursting. Brain Research 223: 19-38

Sandeman D C (1982) Organisation of the central nervous system. In: Atwood H L and Sandeman D C (eds.) The biology of Crustacea, Vol 3. Neurobiology: structure and function. Academic Press, New York: 1-61

Sandeman R E and Sandeman D C (1990) Development and identified neural systems in the crayfish brain. In: Wiese K, Krenz W-D, Tautz J, Reichert H and Mulloney B (eds.) Frontiers in crustacean neurobiology. Springer, Basel: 498-508

Sandeman R E and Sandeman D C(2003) Development, growth, and plasticity in the crayfish olfactory system. Microscopy Research and Technique 60: 266-277

Sandeman D C and Scholtz G (1995) Ground plans, evolutionary changes and homologies in decapod crustacean brains. In: Breidbach O and Kutsch W (eds.) The nervous systems of invertebrates: an evolutionary and comparative approach. Birkhäuser, Basel: 329-347

Sandeman D C, Sandeman R, Derby C and Schmidt M (1992) Morphology of the brain of crayfish, crabs, and spiny lobsters: a common nomenclature foe homologues structures. Biological Bulletin 183: 304-326

Sandeman D C, Scholtz G and Sandeman R E (1993) Brain evolution in decapod Crustacea. Journal of Experimental Zoology Part A: Ecological Genetics and Physiology 265: 112-133

Schneider H, Budhiraja P, Walter I, Beltz B S, Pecko L E and Kravitz E A (1996) Developmental expression of the octopamine phenotype in lobsters*, Homarus americanus*. The Journal of Comparative Neurology 371: 3-14

Scholtz G (1992) Cell lineage studies in the crayfish *Cherax destructor* (Crustacea, Decapoda): germ band formation, segmentation, and early neurogenesis. Roux's Archives of Developmental Biology 202: 36-48

Scholtz G (1995a) Head segmentation in Crustacea **-** an immunocytochemical study. Zoology **-** Analysis of Complex Systems 98: 104-114

Scholtz G (1995b) Expression of the engrailed gene reveals nine putative segment-anlagen in the embryonic pleon of the freshwater crayfish *Cherax destructor* (Crustacea, Malacostraca, Decapoda). Biological Bulletin 188: 157-165

Scholtz G (2000) Evolution of the nauplius stage in malacostracan crustaceans. Journal of Zoological Systematics and Evolutionary Research 38: 175-187

Scholtz G and Edgecombe G D (2006) The evolution of arthropod heads: reconciling morphological, developmental and palaeontological evidence. Development Genes and Evolution 216: 395-415

Schram F R and Hof C H J (1998) Fossils and the interrelationships of major crustacean groups. In: Edgecombe G D (ed.) Arthropod fossils and phylogeny. Columbia University Press, New York: 233-302

Schulz van Endert S (2009) Axogenesis in the barnacle, *Balanus* spec. (Arthropoda, Cirripedia). Bachelor Thesis, Humboldt-Universität zu Berlin

Selverston A I, Russell D F, Miller J P and King D G (1976) The stomatogastric nervous system: structure and function of a small neural network. Progress in Neurobiology 7: 215-289

Selverston A I and Moulins M (eds.) (2012) The crustacean stomatogastric system: a model for the study of central nervous systems. Springer-Verlag, Berlin

Semmler H, Wanninger A, Høeg J T and Scholtz G (2008) Immunocytochemical studies on the naupliar nervous system of *Balanus improvisus* (Crustacea, Cirripedia, Thecostraca). Arthropod Structure & Development 37: 383-395

Siewing R (1963) Studies in malacostracan morphology: results and problems. Phylogeny and Evolution of Crustacea, Museum of Comparative Zoology Special Publications 13: 85-103

Sigvardt K A and Mulloney B (1982) Properties of synapses made by IVN command-interneurones in the stomatogastric ganglion of the spiny lobster *Panulirus interruptus*. Journal of Experimental Biology 97: 153-168

Sintoni S, Fabritius-Vilpoux K and Harzsch S (2007) The engrailed-expressing secondary head spots in the embryonic crayfish brain: examples for a group of homologous neurons in Crustacea and Hexapoda? Development Genes and Evolution 217: 791-799

Skiebe P (2003) Neuropeptides in the crayfish stomatogastric nervous system. Microscopy Research and Technique 60: 302-312

Smith G (1974) The ultrastructure of the organ of Bellonci of *Carcinus maenas* (Crustacea: Decapoda). Cell and Tissue Research 155: 127-134

Spiridonov V and Casanova B (2010) Order Euphausiacea Dana, 1852. In: Schram F R and von Vaupel Klein J C (eds.) Treatise on Zoology - Anatomy, Taxonomy, Biology. The Crustacea, complementary to the volumes of the Traité de Zoologie. Vol. 9, Part A. Koninklijke Brill Academic Publishers, Leiden: 5-82

Steele V J (1984) Morphology and ultrastructure of the organ of Bellonci in the marine amphipod *Gammarus setosus*. Journal of Morphology 181: 97-131

Steele V J and Oshel P E (1989) Ultrastructure of the attachment cells of the organ of Bellonci in *Gammarus setosus* (Crustacea, Amphipoda). Journal of Morphology 200: 93-119

Stegner M E J and Richter S (2011) Morphology of the brain in *Hutchinsoniella macracantha* (Cephalocarida, Crustacea). Arthropod Structure & Development 40: 221-243

Stegner M E J and Richter S (2015) Development of the nervous system in Cephalocarida (Crustacea): early neuronal differentiation and successive patterning. Zoomorphology 134: 183-209

Stegner M E J, Brenneis G and Richter S (2014) The ventral nerve cord in Cephalocarida (Crustacea): new insights into the ground pattern of Tetraconata. Journal of Morphology 275: 269-294

Stegner M E, Stemme T, Iliffe T M, Richter S and Wirkner C S (2015) The brain in three crustaceans from cavernous darkness. BMC Neuroscience 16: 1

Strausfeld N J (1998) Crustacean–insect relationships: the use of brain characters to derive phylogeny amongst segmented invertebrates. Brain, Behavior and Evolution 52: 186-206

Strausfeld N J (2005) The evolution of crustacean and insect optic lobes and the origins of chiasmata. Arthropod Structure & Development 34: 235-256

Strausfeld N J (2012) Arthropod brains: evolution, functional elegance, and historical significance. Harvard University Press, Cambridge

Strausfeld N J and Andrew D R (2011) A new view of insect-crustacean relationships I. Inferences from neural cladistics and comparative neuroanatomy. Arthropod Structure & Development 40: 276-288

Strausfeld N J and Hildebrand J G (1999) Olfactory systems: common design, uncommon origins? Current Opinion in Neurobiology 9: 634-639

Strausfeld N J and Nassel D R (1981) Neuroarchitecture of brain regions that subserve the compound eyes of Crustacea and insects. In: Autrum H (ed.) Vision in invertebrates (Handbook of sensory physiology, Vol VII/6 B) Springer, Berlin 1-134

Sullivan J M and Beltz B S (2001a) Neural pathways connecting the deutocerebrum and the lateral protocerebrum in the brains of decapod crustaceans. Journal of Comparative Neurology 441: 9-22

Sullivan J M and Beltz B S (2001b) Development and connectivity of olfactory pathways in the brain of the lobster *Homarus americanus*. Journal of Comparative Neurology 441: 23-43

Sullivan J M and Beltz B S (2004) Evolutionary changes in the olfactory projection neuron pathways of eumalacostracan crustaceans. The Journal of Comparative Neurology 470: 25-38

Sullivan J M and Macmillan D L (2001) Embryonic and postembryonic neurogenesis in the ventral nerve cord of the freshwater crayfish *Cherax destructor*. Journal of Experimental Zoology 290: 49-60

Tarling G A, Cuzin-Roudy J and Buchholz F (1999) Vertical migration behaviour in the northern krill *Meganyctiphanes norvegica* is influenced by moult and reproductive processes. Marine Ecology Progress Series 190: 253-262

Thomasson M A, Johnson M L, Strömberg J-O and Gaten E (2003) Swimming capacity and pleopod beat rate as a function of sex, size and moult stage in Northern krill *Meganyctiphanes norvegica*. Marine Ecology Progress Series 250: 205-213

Tierney A J, Godleski M S and Rattananont P (1999) Serotonin-like immunoreactivity in the stomatogastric nervous systems of crayfishes from four genera. Cell and Tissue Research 295: 537-551

Ungerer P and Scholtz G (2008) Filling the gap between identified neuroblasts and neurons in crustaceans adds new support for Tetraconata. Proceedings of the Royal Society of London B: Biological Sciences 275: 369-376

Ungerer P, Geppert M and Wolff C (2011) Axogenesis in the central and peripheral nervous system of the amphipod crustacean *Orchestia cavimana*. Integrative Zoology 6: 28-44

Vilpoux K, Bisch-Knaden S and Harzsch S (2008) Engrailed-like immunoreactivity in the embryonic ventral nerve cord of the marbled crayfish (marmorkrebs). Invertebrate Neuroscience 8: 177-197

Vilpoux K, Sandeman R and Harzsch S (2006) Early embryonic development of the central nervous system in the australian crayfish and the marbled crayfish (marmorkrebs). Development Genes and Evolution 216: 209-223

Vogt G (2008) The marbled crayfish: a new model organism for research on development, epigenetics and evolutionary biology. Journal of Zoology 276: 1-13

Vogt G (2011) Marmorkrebs: natural crayfish clone as emerging model for various biological disciplines. Journal of Biosciences 36: 377-382

Vogt G, Tolley L and Scholtz G (2004) Life stages and reproductive components of the marmorkrebs (marbled crayfish), the first parthenogenetic decapod crustacean. Journal of Morphology 261: 286-311

Walker G (1974) The fine structure of the frontal filament complex of barnacle larvae (Crustacea: Cirripedia). Cell Tissue Research 152: 449-465

Walker G (1992) Cirripedia, Crustacea. In: Harrison F W and Humes A G (eds.) Microscopic anatomy of invertebrates. Wiley-Liss, New York 9: 249-312

Walley L J and Rees E I S (1969) Studies on the larval structure and metamorphosis of *Balanus balanoides* (L.). Philosophical Transactions of the Royal Society of London B: Biological Sciences 256: 237-280

Waloszek D (2003) Cambrian 'Orsten'-type preserved arthropods and the phylogeny of Crustacea. In: Legakis A, Sfenthourakis, S, Polymeni R and Thessalou-Legaki M (eds.) Proceedings of the 18th International Congress of Zoology, Athens 2000:69–87

Waloszek D and Müller K J (1997) Cambrian 'Orsten'-type arthropods and the phylogeny of Crustacea. In: Fortey R R and Thomas R (eds.) Arthropod relationships, Systematics Association. Chapman & Hall, London 55: 139-153

Waloszek D, Chen J, Maas A and Wang X (2005) Early cambrian arthropods **-** new insights into arthropod head and structural evolution. Arthropod Structure & Development 34: 189-205

Webster S G. and Dircksen H (1991) Putative molt-inhibiting hormone in larvae of the shore crab *Carcinus maenas* L.: an immunocytochemical approach. Biological Bulletin 180: 65-71

Weiss L C, Tollrian R, Herbert Z and Laforsch C (2012) Morphology of the daphnia nervous system: a comparative study on *Daphnia pulex*, *Daphnia lumholtzi*, and *Daphnia longicephala*. Journal of Morphology 273: 1392-1405

Weygoldt P (1958) Die Embryonalentwicklung des Amphipoden *Gammarus pulex pulex* L. Zoologische Jahrbücher, Abteilung für Anatomie und Ontogenie der Tiere 77: 51--110

Whitington P M (2004) The development of the crustacean nervous system. In: Scholtz G (ed.) Evolutionary developmental biology of Crustacea. Balkema Publishers: Lisse: 135-167

Whitington P M, Leach D and Sandeman R (1993) Evolutionary change in neural development within the arthropods: axogenesis in the embryos of two crustaceans. Development 118: 449-461

Wildt M and Harzsch S (2002) A new look at an old visual system: structure and development of the compound eyes and optic ganglia of the brine shrimp *Artemia salina* Linnaeus, 1758 (Branchiopoda, Anostraca). Journal of Neurobiology 52: 117-132

Wolff G, Harzsch S, Hansson B S, Brown S and Strausfeld N (2012) Neuronal organization of the hemineurpsoid body of the land hermit crab, *Coenobita clypeatus*: correspondence with the mushroom body ground pattern. Journal of Comparative Neurology 520: 2824-2846

Zhang X G and Pratt B R (2012) The first stalk-eyed phosphatocopine crustacean from the Lower Cambrian of China. Current Biology 22: 2149-2154

Zieger E, Bräunig P and Harzsch S (2013) A developmental study of serotonin-immunoreactive neurons in the embryonic brain of the marbled crayfish and the migratory locust: evidence for a homologous protocerebral group of neurons. Arthropod Structure & Development 42: 507-520

Acknowledgments

I am very grateful to Prof. Gerhard Scholtz for welcoming me in his lab and giving me the opportunity to start my doctoral studies under his supervision. I would also like to thank him for introducing me to the vibrant world of scientific debates, and for giving me a second chance when the first project did not take off as expected. My gratitude goes also to Dr. Carsten Wolff for his constant support and availability to answer my questions, and for his encouragement to find my way around unexpected bumps in the road and keep going.

Frederike Alwes, Georg Brenneis, Ines Drescher, Markus Pennerstorfer, Ekaterina Ponomarenko and Petra Ungerer are heartily thanked for their support, valuable feedback, chats, laughs, hugs and kicks, and for persistently cheering me on. Thank you to Markus Pennerstorfer, in particular, for his patience in reading the first draft of the manuscript discussion, always listening and helping to find a way to clarify my thoughts. Thank you very much to Georg Brenneis for his bravery in reading all the results of the manuscript and for his sharp observations (da G forever!). And I will not forget in my thanks all the words of encouragement and smiles of Chiara Anselmi, Franziska Caspari, Anke Braband, Maria Geppert, Hendrikje Hein, Vera Hunnekuhl, Günther Jirikowski, Marleen Klann, Kai Lindemann, Tino Pabst, Andre Reimann, Hong Shen, nor the spirit of the AG Vergleichende Zoologie, Berlin. We rock!!!

A special thanks goes to Prof. Alessandro Minelli who opened me the doors to science and never stops feeding my passion for it with his own. I will be eternally thankful to Pia and Sandro who always welcomed me in their wonderful garden house and have kept my motivation high in all these years, being my guides through the beauty of Nature.

Prof. Steffen Harzsch is thanked for his insightful observations and clear thoughts, which have helped on many occasions to better order my ideas and maintain a thread through the complex skein of the nervous system.

I am very grateful to Prof. Giuseppe Fusco for hosting me in Padua when it was needed, for his constructive critical views, and his strength and dedication, which helped me to maintain my own passion for science.

Greg Coman and Melony Sellars are thanked for helping me to collect the samples of the *Penaues monodon*'s nauplius larvae at the CSIRO marine station of Cleveland (Qeensland, Australia), and for having revealed a bit of their huge continent to me. The valorous captain of the marine station of Kristineberg (Sweden), Andreas Hejnol, and Mark Martindale are

thanked for having supported me in the enterprise of fishing samples of *Meganyctiphanes norvegica* in the remote Gullmar fiord, and rearing them under the harsh conditions of the freezing cellars of the station. In Sweden I'd like to thank also Prof. Rolf Elofsson for providing me his original papers, I hope to soon return the favour…

Special thanks go to my friends Andreas, Carola, Petra, Rebecca and Ulpiana, who have been constantly close to me during my years in Berlin, regardless of the distance, the weather, the stars, the mood, or the moon.

Anche alle ragazze ed i ragazzi della Magica e dei Monelli: grazie!

A particular thank you goes to Dr. Tobias Krier (Doktor Tobi!) for sharing the pains of the final rush, for his precious help in managing the formatting of the manuscript, and in training my organizational skills (…from 0 to 1…). Alun Philips is kindly thanked for his precious help on proof reading most of the manuscript and pushing me towards the end. Thank you very much to Joachim Maier for guiding me towards the paths of growth and development.

And an endless thank you goes to my sister Mariaelisabetta, Bob and the rest of my family for teaching me the joy of sharing.

Selbstständigkeitserklärung

Hiermit versichere ich, dass ich die vorliegende Dissertation selbstständig und nur unter Verwendung der angegebenen Quellen und Hilfsmittel erarbeitet und verfasst habe. Diese Arbeit wurde keiner anderen Prüfungsbehörde vorgelegt.

Berlin, den